

Effective Width of Concrete Slab Bridges in Delaware

By

BRIAN P. JONES

HARRY W. SHENTON, III

**Department of Civil and Environmental Engineering
College of Engineering
University of Delaware**

January 2012

**Delaware Center for Transportation
University of Delaware
355 DuPont Hall
Newark, Delaware 19716
(302) 831-1446**



The Delaware Center for Transportation is a university-wide multi-disciplinary research unit reporting to the Chair of the Department of Civil and Environmental Engineering, and is co-sponsored by the University of Delaware and the Delaware Department of Transportation.

DCT Staff

Ardeshir Faghri
Director

Jerome Lewis
Associate Director

Ellen Pletz
Assistant to the Director

Earl "Rusty" Lee
T² Program Coordinator

Matheu Carter
T² Engineer

Sandra Wolfe
Event Coordinator

DCT Policy Council

Natalie Barnhart, Co-Chair
Chief Engineer, Delaware Department of Transportation

Babatunde Ogunnaike, Co-Chair
Dean, College of Engineering

Delaware General Assembly Member
Chair, Senate Highways & Transportation Committee

Delaware General Assembly Member
Chair, House of Representatives Transportation/Land Use & Infrastructure Committee

Ajay Prasad
Professor, Department of Mechanical Engineering

Harry Shenton
Chair, Civil and Environmental Engineering

Michael Strange
Director of Planning, Delaware Department of Transportation

Ralph Reeb
Planning Division, Delaware Department of Transportation

Stephen Kingsberry
Executive Director, Delaware Transit Corporation

Shannon Marchman
Representative of the Director of the Delaware Development Office

James Johnson
Executive Director, Delaware River & Bay Authority

Holly Rybinski
Project Manager-Transportation, AECOM

*Delaware Center for Transportation
University of Delaware
Newark, DE 19716
(302) 831-1446*

Effective Width of Concrete Slab Bridges in Delaware

By

Brian P. Jones

Harry W. Shenton III, Ph.D.

Version #3

January 24, 2012

Executive Summary

The University of Delaware Center for Innovative Bridge Engineering (CIBrE) was contracted by the Delaware Department of Transportation to conduct load tests of several concrete slab bridges in Delaware, for the purpose of evaluating the slab effective width of the bridges and to develop an improved formula for calculating slab effective width that is specific to Delaware slab bridges. This report documents the results of the tests and the development of the improved effective width equations.

Diagnostic load tests were conducted on six slab bridges. This included bridges 1-442, 1-352W, 1-384, 2-101B, 3-318, and 3-316. The bridges were built between 1923 and 1932; widths ranged from 26 to 47 ft; span lengths ranged from 8 to 19.5 ft. Four of the six bridges (1-442, 1-352W, 3-318 and 3-316) were originally narrower in width and were at some time widened to increase the width of the roadway.

A typical diagnostic load test involved mounting strain transducers across the transverse centerline of the bridge, at a spacing of approximately every two feet. Loaded dump trucks then made passes across the bridge while the strains were recorded. Load passes were made with a single truck in different transverse positions on the bridge (e.g., left shoulder, left lane, center of the bridge, etc), and also with two trucks side-by-side in different transverse positions. From the measured strains, plots of the longitudinal strain versus transverse position of the sensor were generated for every truck load pass. From these plots the actual slab effective width was determined. The effective width was calculated for all single truck passes and all side-by-side truck passes (i.e., each load test

yielded multiple estimates of the effective width, for both single and side-by-side truck passes). The single truck pass effective widths ranged from a low of 9.9 ft to a high of 21.3. The side-by-side truck effective widths ranged from a low of 9.0 ft to a high of 12.4 ft.

Comparing the measured effective widths to the widths given by the AASHTO LRFD equation shows that the AASHTO formula is in general conservative. For single truck passes, the measured effective width was up to 116% greater than the LRFD code result. For the side-by-side truck passes, the measured effective width was up to 33% greater than the LRFD code result.

New formulas were developed for estimating the slab effective width based on the measured effective width of the six bridges. This was done by fitting an equation of the form of the AASHTO LRFD equation to the measured effective widths, using a least squares approach. Because of the variability of the test data, new formulas were developed for the average effective width of each bridge, and the lowest effective width of each bridge (the lowest being the most conservative). This was done for both the single truck passes and side-by-side truck (multiple presence) truck passes. The recommended new formulas are:

$$\text{Single-lane loaded: } E = 10 + 5.8\sqrt{L_1W_1}$$

$$\text{Multi-lane loaded: } E = 84 + 2.06\sqrt{L_1W_1} \leq \frac{12W}{N_L}$$

These are based on the lowest measured effective width, thus they are the most conservative. The equations based on the average measured effective width are included in the report.

TABLE OF CONTENTS

LIST OF TABLES	iii
LIST OF FIGURES	v
ABSTRACT.....	viii
1 INTRODUCTION	1
1.1 Motivation.....	1
1.2 AASHTO Slab Effective Width.....	1
1.3 Objectives of Research	5
1.4 Approach.....	6
1.5 Organization of Report	9
2 LITERATURE REVIEW	11
2.1 Zokie, et al (1991).....	12
2.2 Amer, et al (1999).....	19
2.3 Mabsout et al. (2004).....	26
3 TEST PROCEDURE, ANALYSIS OF DATA, AND RESULTS	29
3.1 Bridge Test Procedure	29
3.1.1 Test Preparation	29
3.1.2 On Site Procedure	30
3.2 Data Analysis.....	32
3.2.1 Sensor Data Corrections	33
3.2.2 Calculation of Effective Width	38
3.3 Summary of Bridge tests and Results	41
3.3.1 Bridge 1-442	42
3.3.2 Bridge 2-101B	44
3.3.3 Bridge 1-352W	47
3.3.4 Bridge 1-384	50
3.3.5 Bridge 3-318	53
3.3.6 Bridge 3-316	56
4 ANALYSIS.....	60

4.1	Introduction.....	60
4.2	Methodology	60
4.2.1	Determination of New Effective Width Equation	64
4.2.2	New Equation based on Low Measured Values	69
4.2.3	New Equation Based on Average Measured Values	74
4.3	Recommendations.....	77
5	CONCLUSIONS.....	81
	REFERENCES	83

Appendix

A	Bridge Test Report 1-442
B	Bridge Test Report 2-101
C	Bridge Test Report 1-352W
D	Bridge Test Report 1-384
E	Bridge Test Report 3-318
F	Bridge Test Report 3-316

LIST OF TABLES

Table 1.1:	Bridges Selected for Testing.....	9
Table 2.1:	Comparison of interior girder moment distribution factors by varying levels of accuracy using the “average bridge” for each bridge type (Zokaie, et al 1991).....	18
Table 2.2:	Solid Slab Bridge Field Tests (Amer 1999).....	25
Table 2.3:	Equivalent Width E for Solid Slab Bridges (Amer 1999)	26
Table 3.1:	Comparison of AASHTO Effective Width and Measured Effective Width (ft) Bridge 1-442	43
Table 3.2:	Comparison of AASHTO Effective Width and Measured Effective Width (ft) Bridge 2-101	46
Table 3.3:	Comparison of AASHTO and measured effective width (ft) for Bridge 1-352	49
Table 3.4:	Comparison of AASHTO and measured effective width (ft) for Bridge 1-384	52
Table 3.5:	Comparison of AASHTO and Measured Effective Width (ft) for Bridge 3-318	55
Table 3.6:	Comparison of AASHTO and Measured Effective Width (ft) for Bridge 3-316	58
Table 4.1:	Effective Width Values for Single Truck Passes.....	63
Table 4.2:	Effective Width Values for Multilane Truck Passes	64
Table 4.3:	Normalized Measured Effective Width Values for Single Truck Passes	66
Table 4.4:	Normalized Measured Effective Width Values for Multi Truck Passes	66
Table 4.5:	Fitted Equations based on Measured Low Effective Width	70

Table 4.6: Fitted Equations based on Measured Average Effective Width74

LIST OF FIGURES

Figure 1.1: Idealized Strain Distribution for a Concrete Slab Bridge	3
Figure 1.2: Aspect Ratio (L/W) Histogram	7
Figure 1.3: Scatter Plot of Aspect Ratio to Slab Thickness (Red dots donate bridges selected)	8
Figure 2.1: Effect of parameter variation on slab bridges (Zokaie, et al 1991).....	15
Figure 2.2: Effect of parameter variation on multi-box beam bridges (Zokaie, et al 1991).....	16
Figure 2.3: Effective Width Variation with Span Length for Solid Slab Bridges (Amer et al 1999).....	21
Figure 2.4: Effective Width Variation with Bridge Width for Solid Slab Bridges (Amer et al, 1999).....	22
Figure 2.5: Effective Width Variation for Different Edge Beam Depths and Widths (Amer et al 1999).....	23
Figure 2.6: Bending Moment Intensities Based on Field Test and Grillage Analogy (Field Test 3 – Nassau County Bridge) (Amer et al, 1999).....	25
Figure 3.1: Typical Excel Sheet for Raw Data Analysis	33
Figure 3.2: Raw Strain Data with “Drift” (Br. 318, Sensor 318, Run 1).....	34
Figure 3.3: Corrected Strain Data with “Drift”.....	35
Figure 3.4: Raw Data for Sensor Exhibiting “Noise” (Br. 318, Sens. 298, Run 5).....	36
Figure 3.5: Corrected Data for Sensor Exhibiting “Noise”	37
Figure 3.6: Typical Transverse Distribution Plot (Br. 384, Pass 3)	39
Figure 3.7 Idealized Strain Distribution and Effective Width Representation	40
Figure 3.8: Calculating Effective Width from Transverse Distribution Plots	41

Figure 3.9: Bridge 1-442 Looking West.....	43
Figure 3.10: Bridge 1-442 Sensor Layout	44
Figure 3.11: Bridge 2-101 Looking East	46
Figure 3.12: Bridge 2-101 Sensor Layout	47
Figure 3.13: Bridge 1-352W Looking East	49
Figure 3.14: Bridge 3-352W Sensor Layout.....	50
Figure 3.15: Bridge 1-384 Looking South West.....	52
Figure 3.16: Sensor Layout Bridge 1-384	53
Figure 3.17: Picture of Bridge 3-318 Looking South	55
Figure 3.18: Sensor Layout for Bridge 3-318.....	56
Figure 3.19: Picture of Bridge 3-316 Looking South	58
Figure 3.20: Sensor Layout for Bridge 3-316.....	59
Figure 4.1: Comparison of Effective Width Code Values to Measured Values (Single Truck Pass, Controlling Parameter: Width).....	61
Figure 4.2: Comparison of Effective Width Code Values to Measured Values (Single Truck Pass, Controlling Parameter: Aspect Ratio)	61
Figure 4.3: Comparison of Effective Width Code Values to Measured Values (Multiple Truck Pass, Controlling Parameter: Aspect Ratio).....	62
Figure 4.4: Normalized LRFD: Equations (4.5) and (4.7).....	67
Figure 4.5: Measured (low) Effective Widths for Single Lane Truck Passes in comparison to normalized LRFD code values.....	678
Figure 4.6: Measured (low) Effective Widths for Multilane Truck Passes in comparison to normalized LRFD code values.....	678
Figure 4.7: Normalized effective width versus aspect ratio	72

Figure 4.8: Proposed New Effective Width Equation vs. AASHTO LRFD equation (Single)	73
Figure 4.9: Proposed New Effective Width Equation vs. AASHTO LRFD equation (Multi).....	73
Figure 4.10: Comparing the two derived equations for Average Multi-lane Effective Width.....	75
Figure 4.11: Proposed New Effective Width Equation vs. LRFD equation (Single)...	76
Figure 4.12: Proposed New Effective Width Equations vs. LRFD equation (Multi)...	76
Figure 4.13: Proposed new equations for effective width, single truck pass.....	78
Figure 4.14: Proposed new equation for effective width, multi-truck pass	78

ABSTRACT

In recent years the need to reevaluate the integrity of Delaware's concrete slab bridges has become a high priority. The load rating of a bridge is very dependent on the value of the slab effective width. The effective width value is calculated from the American Association of State Highway and Transportation Officials code equation. Research has suggested that the AASHTO code effective width may be conservative. Strain gauge tests were conducted on six concrete slab bridges of varying geometry and design to determine the actual slab effective width. The resulting measured effective widths were compared to the AASHTO LRFD code width. For single truck passes, the effective width was up to 116% greater than the code. For multiple truck passes, the measured effective width was up to 33% greater than the code. A new formula was derived based on the measured data, for single and multiple truck passes, which more accurately reflects the true slab effective width.

Chapter 1

INTRODUCTION

1.1 Motivation

In recent years the need to reevaluate the integrity of Delaware's concrete slab bridges has become a high priority. Some of the concern has arisen due to the fact that of the approximately 250 slab bridges in Delaware, most were built between 1920 and 1950 and need to be evaluated for new load ratings. The load rating of a bridge is very dependent on the value of the slab effective width. The effective width value is calculated from the American Association of State Highway and Transportation Officials (AASHTO) code equation; research has suggested that the AASHTO code effective width may be conservative (Amer, et al, 1999; Zokaie, et al 1995). Therefore, the Delaware Department of Transportation saw the benefit in developing a more accurate effective width equation specific to Delaware's bridges.

The University of Delaware conducted strain gage testing on six bridges in Delaware. The purpose of these tests was to measure the effective slab width of the bridges and compare it to current AASHTO specifications. The goal of this study is to ultimately derive an equation that more accurately represents the actual effective width in concrete slab bridges.

1.2 AASHTO Slab Effective Width

The methodology chosen was a parametric study of the effective width in each bridge. The hypothesis of this project is that the equations governed by AASHTO

Standard Specifications and AASHTO LRFD for the effective width calculation are too conservative. According to Zokaie et al. (1992) “The formulas currently presented in the AASHTO specifications do not present the degree of accuracy demanded by today’s bridge engineers. (NCHRP Paper) In some cases, these formulas can result in highly conservative results of up to 50%. On the other hand, there have been documented cases of the AASHTO formulas giving highly unconservative results, up to 40%.” This variation in the accuracy of the effective width is causing a discrepancy in the evaluation of the bridges under study. By comparing the effective width measured in the field versus the values dictated by code, an accurate portrayal of the bridge’s structural capacity can be determined. By implementing on-site strain measuring technologies, these effective widths can be compared against other bridges that were similarly constructed. In this regard, a collective dataset of experimental versus theoretical effective widths can be utilized to rate each bridge’s performance.

The equations governed by the code will be the controlling factor throughout this paper. As our main objective is evaluating the accuracy of this code as it pertains to reinforced concrete slab bridges in Delaware, we will need a thorough understanding of the concept of effective width and how the code was implemented. Looking at the idealized strain distribution in Figure 1.1, it can be seen that given a point load on a slab, the strain has a peak at that point load and dissipates as the distance from the load increases.

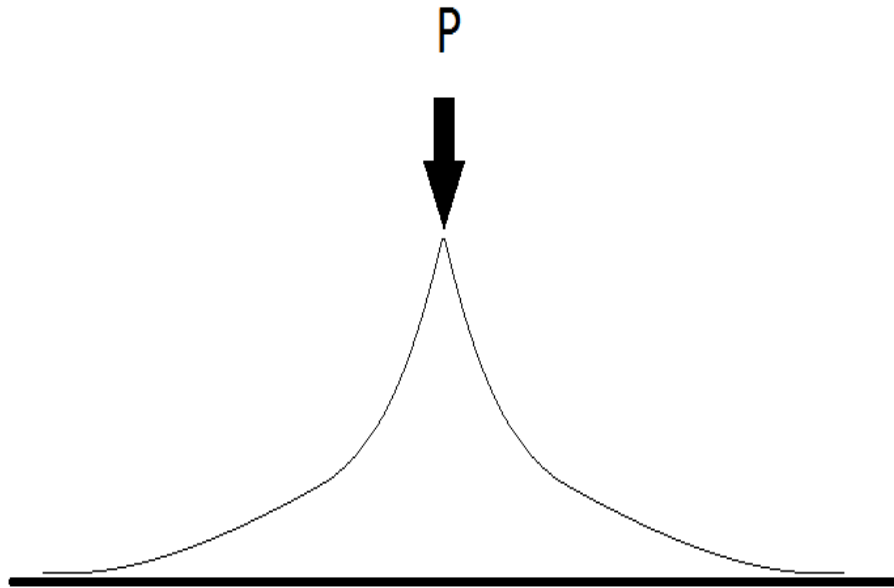


Figure 1.1: Idealized Strain Distribution for a Concrete Slab Bridge

This is a result of shear-lag in the areas of the slab experiencing tension. The concept of shear-lag implies that the area that is effective in resisting tension may be less than the calculated net area. The effective width design parameter was developed to calculate the area of a slab that is effectively experiencing tension. It is an equation aimed at simplifying how strain is distributed in a slab. “The widely accepted definition of the effective width is the width that would have a uniform strain equal to the maximum strain but creates the same total effect as that caused by the actual strain distribution” (Chiewanichakorn et al., 2004).

The equation for effective width of a slab, per AASHTO LRFD, is

$$E = 10 + 5\sqrt{L_1 W_1} \tag{1.1}$$

for a single lane loaded, and

$$E = 84.0 + 1.44\sqrt{L_1 W_1} < \frac{12W}{N_L} \quad (1.2)$$

for multilane loading, where as defined by AASHTO:

E = Equivalent width (in.)

L_1 = Modified span length taken equal to the lesser of the actual span or 60.0 (ft.)

W_1 = Modified edge-to-edge width of bridge taken to be equal to the lesser of the actual width or 60.0 for multilane loading, or 30.0 for single-lane loading (ft.)

W = Physical edge-to-edge width of bridge

N_L = Number of design lanes

For comparison, the formula for effective width per the AASHTO Standard Specification is

$$b_{eff} = 4.0 + 0.06S \quad (1.3)$$

where S is the span (ft.). Note that b_{eff} is for a single wheel line and must be multiplied by 2 for direct comparison with E , which is for two wheel lines.

To measure the actual effective width of a bridge, the University of Delaware implemented on-site strain gage technology. As a truck (which is treated as a two-point load, separated by typically 7' wheel space) drives across the bridge, the longitudinal strain at mid-span is recorded. Using this data a final effective width value is calculated. This process is discussed in detail in Chapter 3: Project Application. Finally, in the analysis section, the comparisons between code and measured value will be discussed.

By observation, it can be seen that these formulas seem rather simple compared to the concept they represent. This is due to the fact that the derivations for this

code were based on an “average” bridge which may not be representative of the bridges in Delaware of this type. Another issue is that of the structure of the bridges being tested. This formula treats these bridges as simple slab bridges. However, the construction of these bridges is similar to that of a frame. This frame-like behavior would theoretically result in less strain on the bridge exhibited by the live truck load. This would result in further inaccuracies in the AASHTO code for effective width.

Additionally, as stated in the objectives, a formula is intended to be derived specific to Delaware slab concrete bridges of this nature. This paper examines six bridges that will be used to represent the bridges that are currently under consideration for rehabilitation. One limitation of this study is that the formula to be derived will only be applicable to bridges within the range of parameters of these six bridges. This will lead to an effective width formula that may not be accurate for every bridge in Delaware.

Other limitations lie in the selection of bridges tested. Much consideration went into the bridges which we selected for strain gage testing and evaluation. However there will be variations in any particular formula derived based on the bridges selected for testing. This variance would exist with any selection of bridges. The goal was to select the bridges so that the variance in the developed formula was minimized.

Further theoretical limitations of the effective width concept for load ratings will be discussed in the Literature Review Chapter, wherein others’ research will be compared qualitatively to this paper.

1.3 Objectives of Research

The objective of this research is to create a more accurate formula for the effective width of concrete slab bridges in Delaware. This formula is intended to be used by the Delaware Department of Transportation in calculating the load ratings of these

bridges. This information will help in determining the remaining life of the structure and whether rehabilitation is needed.

1.4 Approach

The first challenge of this project was to select a number of bridges that represents the concrete slab bridges in Delaware. A method was needed to identify which bridges needed renovation. However, as testing over 250 bridges is impractical, a more efficient means of evaluating a large number of bridges becomes necessary. After a sample size and particular bridges have been chosen, an accurate methodology must be used to evaluate each bridge to determine its structural performance.

It was determined that due to the large number of bridges, many of which were constructed around the same time period, a case study of a select number of bridges could represent the majority of them. The University of Delaware, in collaboration with the Delaware Department of Transportation, selected six bridges for testing and evaluation. These bridges were selected based on their span length, aspect ratio, cover depth thickness, and slab thickness. Aspect ratio is the ratio of a bridge's length to its width. This parameter was considered because both the width and length of the bridge are used in the current LRFD effective width equation. Some consideration was also given to age, location, and construction. Bridges with extensive repairs were avoided. Correlations were drawn between parameters to determine which bridges would most accurately represent the majority of the concrete slab bridges in the state. A subset of 28 bridges was chosen with varying parameters that were determined to be representative of the slab bridges in Delaware. Histograms were created to find the highest frequency of particular properties of a bridge to determine which bridges were the most representative. Figure 1.2 shows an example of one of the histogram used to assess the 28 bridges.

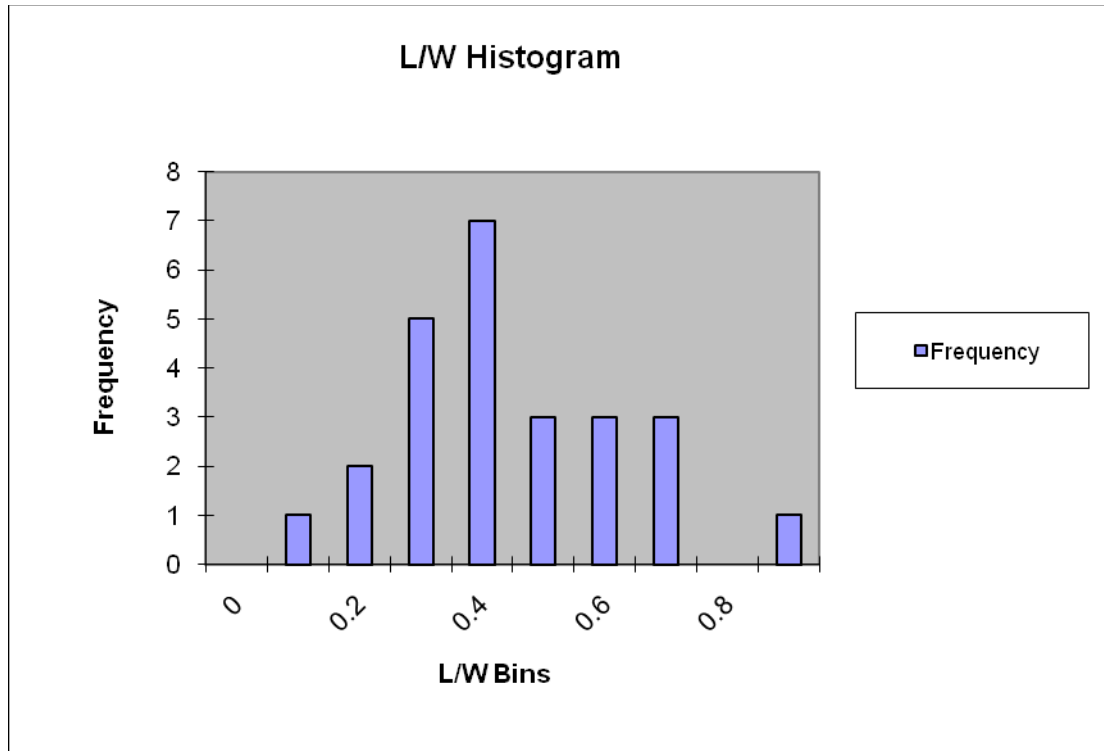


Figure 1.2: Aspect Ratio (L/W) Histogram of 28 Candidate Test Bridges

However, ‘typical’ bridges were not simply chosen, bridges with a varying range of parameters was also important to achieve an accurate representation. For example, the aspect ratios (L/W) of the tested bridges from smallest to largest are 0.17, 0.21, 0.32, 0.37, 0.46, and 0.67. This method allows the selection of bridges to be diversified.

It also seemed apparent that comparing the occurrence of multiple parameters was important in bridge selection. Simply comparing the frequency of individual parameters in histograms may result in bridges that are statistically representative of only one parameter. It is the object of this project to consider all parameters in the comparison to the effective width. As such, bridges were put into scatter plots comparing the two parameters. Figure 1.3 shows slab thickness versus aspect ratio. The 28 bridges from the

first screening were compared in the graph. The red dots highlight the bridges that were selected for testing. This method was not used as the primary selection method. It was a consideration to ensure an accurate spread of parameters was being displayed.

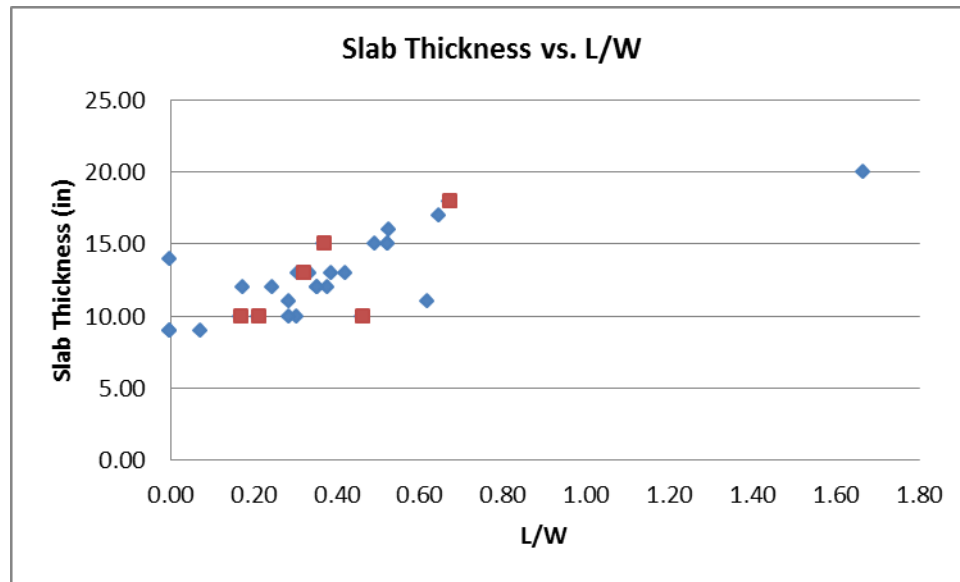


Figure 1.3: Scatter Plot of Aspect Ratio to Slab Thickness (Red dots donate bridges selected)

Cover depth was considered to be an important parameter due to the fact that cover can reduce the stain experienced by the slab as a load travels across it. However it was determined that such dissipation is considered negligible for bridges with less than two feet of cover depth. All bridges selected had less than two feet of cover. There were some bridges that had a cover depth over two feet but these were not selected for testing. There were also bridges that were avoided because of unique construction or renovations. It was determined that the analysis of such bridges may yield inconsistent results which

could impair the data. Table 1.1 shows the list of the bridges that were selected for testing.

Table 1.1: Bridges Selected for Testing

Bridge	Facility Carried	Span Length (ft)	Slab Thickness (in)	Width (ft)	L/W	Year Built	Structure Rating (NBI)
1-442	Money Rd	13.08	13.00	41	0.32	1923	6
2-101B	Pearsons Corner Rd.	19.50	18.00	28.53	0.68	1931	6
1-352W	US 40	8.0	10.00	47	0.17	1932	6
1-384	Dutch Neck Rd	12.0	10.00	26	0.46	1931	7
3-318	SR 24	8.0	10.00	37.8	0.21	1924	7
3-316	SR 24	14.0	15.00	38.3	0.37	1924	5 (scour)

1.5 Organization of Report

This report contains five Chapters. The first chapter is the Introduction which discusses the general background of the paper, the need for this research, and the objectives of this project.

Chapter two is the Literature Review. This chapter discusses previous work in this area of bridge engineering. It compares various other works to this one and aids in the understanding of the effective width concept. It also provides insight into the methodology of developing an empirical formula.

Chapter three discusses the methodology of the bridge tests and collection of the data. It begins by outlining the procedure used followed by the interpretation of data.

Finally, the chapter concludes with summaries of each bridge test and the data specific to each one.

Chapter four is the Data Analysis chapter. This chapter uses the data gathered throughout the project to develop a new equation for effective width of concrete slab bridges in Delaware.

Chapter five is the conclusion of the report. This summarizes the work done throughout the project. Recommendations for further research are also stated.

Chapter 2

LITERATURE REVIEW

There has been an increased interest in field testing bridges in recent years due to a high demand to reassess the condition of many of this nation's older bridges. Some field tests are done to estimate the remaining life of older bridges, if any. Other bridges are tested because the posted weight limits shown are lower than that of legal truck weights. In addition, more concern over the structural integrity of our bridges has been fueled by the U.S. Federal Highway Administration's 2010 National Bridge Inventory's report that about 23.3 percent of the nation's 600,513 bridges are structural deficient or functionally obsolete in *Better Roads* magazine (Barbaccia 2010). These deficiencies lead to the need to repair or replace a considerable number of bridges. In order to evaluate which ones, field testing and interpretation of code values for weight-limit posting, strength and serviceability are required.

The theoretical evaluation of the effective width is dependent on the distribution of loads across a bridge. It can be seen, therefore, that in order to accurately compute the effective width of a given bridge an understanding of how wheel loads behave throughout a bridge is necessary. The first factor that determines how a bridge behaves under such loading is the location of the loads and their magnitude. These are controllable parameters which can be simply measured and located prior to testing. For this research specifically, truck wheel locations and weights were recorded prior to all field testing. The second factor requires more analytical attention as it is the response of the bridge to these given loads. It is the objective of this report to evaluate how a bridge

reacts to our known loads at their given locations in order to assess its condition.

Therefore it seems imperative to detail research which pertains to that course of study.

2.1 Zokie, et al (1991)

Zokaie et al. (1991) focuses on this second factor, the response of a bridge to a predefined set of wheel loads. Their intention was to better understand the response of highway bridges to vehicular live loads in order to better analyze the strength and serviceability of existing bridges and to aid in the design of new bridges. AASHTO Standard Specifications for Highway Bridges implemented wheel load distribution factors which allowed engineers to treat transverse and longitudinal effects of wheel loads as uncoupled phenomena. However these distribution factors have been available in AASHTO's Standard Specifications since 1931 with minor changes. The formulas currently presented therein do not present the degree of accuracy needed by today's engineers. It was because of a lack of research in this area that the National Cooperative Highway Research Program (NCHRP) initiated Project 12-26 in the mid 1980's to develop comprehensive specification provisions for the distribution of wheel loads in bridges.

The objective of Project 12-26 was to evaluate the available methods for wheel load distribution in various bridge types. Although the current AASHTO regulations provided simplified methods of analysis for beam and slab, box girder, slab, multi-box beam and spread box beam bridge superstructures, they found certain shortcomings. They give inconsistent consideration of a reduction in load intensity for multiple lane loadings. There were also inconsistent changes in distribution factors to reflect the changes in design lane width and inconsistent verification of accuracy of wheel load distribution factors for various bridge types. The current specifications were

also solely developed for nonskewed, simply-supported bridges, limiting their practical application. In fact they found that in "...many cases these formulae resulted in highly unconservative results (up to 40%); and in other cases they may be highly conservative (more than 50%)."

Bridges were analyzed on three different levels. Level one methods are the simplified formulas which predict lateral load distribution. This is the majority of Zokaie's work due to ease of application and the strong correlation achieved in their application to the majority of bridges. Level two methods include graphical methods, nomographs, influence surfaces or simple computer programs. Level three, the most accurate analysis, involves detailed modeling of the bridges deck. This level involves the use of finite element or grillage analysis computer technologies to obtain extremely accurate results. Due to its high accuracy, this method was used as the standard for which to compare the results from level one and level two analyses.

Level three analysis used all suitable computer programs specializing in finite element analysis. Programs were for the most part specific to the bridge type being tested. For slab bridges, computer programs MUPDI, FINITE, SAP and GENDEK were used. To confirm their validity, results were compared to field and laboratory tests. "The results were compared in three ways: (1) by visual comparison of the results plotted on the same figure, (2) by comparison of the averages and standard deviations of the ratios of analytical to experimental results and (3) by comparison of statistical differences of analytical and experimental results." MUPDI was found to be the most accurate and practical program for nonskewed prismatic bridges.

Level two methods use graphical and simple computer based analysis. This particular study used influence surface methods and grillage analysis using plane grid models. For slab bridges, the programs used were OHBDC, SALOD, and MSI. MSI was

found to be the most accurate method and, thus, was used in the evaluation of level one methods.

Level one methods encompass the simplified formulas currently recommended by AASHTO specifications. This is the level directly related to this paper's research. Although there have been other studies which reevaluate the AASHTO effective width, most of these studies are for moment distributions of beam and slab bridges subjected to multilane loading. This study pertains to various types of bridges mentioned earlier, including the slab bridge. In order to ensure that common values of various bridge types were considered, a database of actual bridges was compiled. They randomly selected bridges from various states in order to achieve national representation. For the slab bridge type, 130 bridges were selected throughout the United States. They then studied the different parameters of these bridges such as span length and slab thickness to identify the common values. A hypothetical slab bridge was created as an average of each of these values.

The evaluation of these simplified formulae requires an understanding of how these parameters affect the behavior of the bridge. Bridge parameters in the average bridge were varied one at a time as shear and moment distribution were obtained. As the wheel load distribution varies a certain amount of each parameter varies, the quantitative influence of a given parameter can be found for the purposes of deriving a formula. As part of their level one study, they also evaluated the sensitivity of wheel load distribution factors to various bridge parameters. Span length, longitudinal stiffness and transverse stiffness are the major contributors to the effective width criteria.

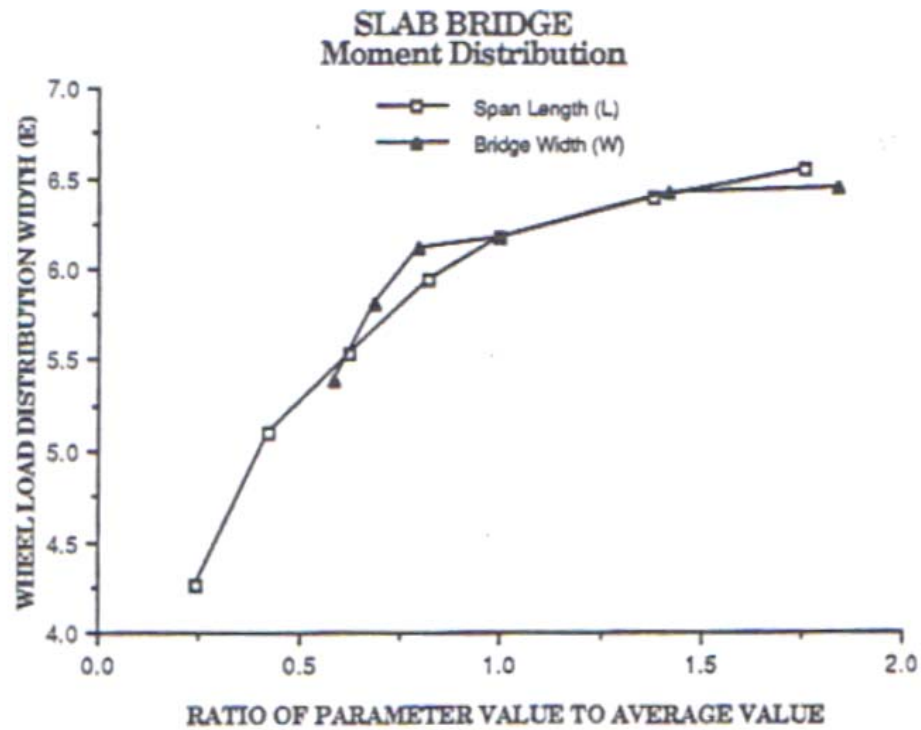


Figure 2.1: Effect of parameter variation on slab bridges (Zokaie, et al 1991)

Figure 2.1 demonstrates how extreme values of bridge span or width can affect the wheel load distribution. Although this research only pertains to slab bridges, it is interesting to note how the distribution factors are affected by the bridge parameters in a multi-box beam bridge (Refer to Figure 2.2).

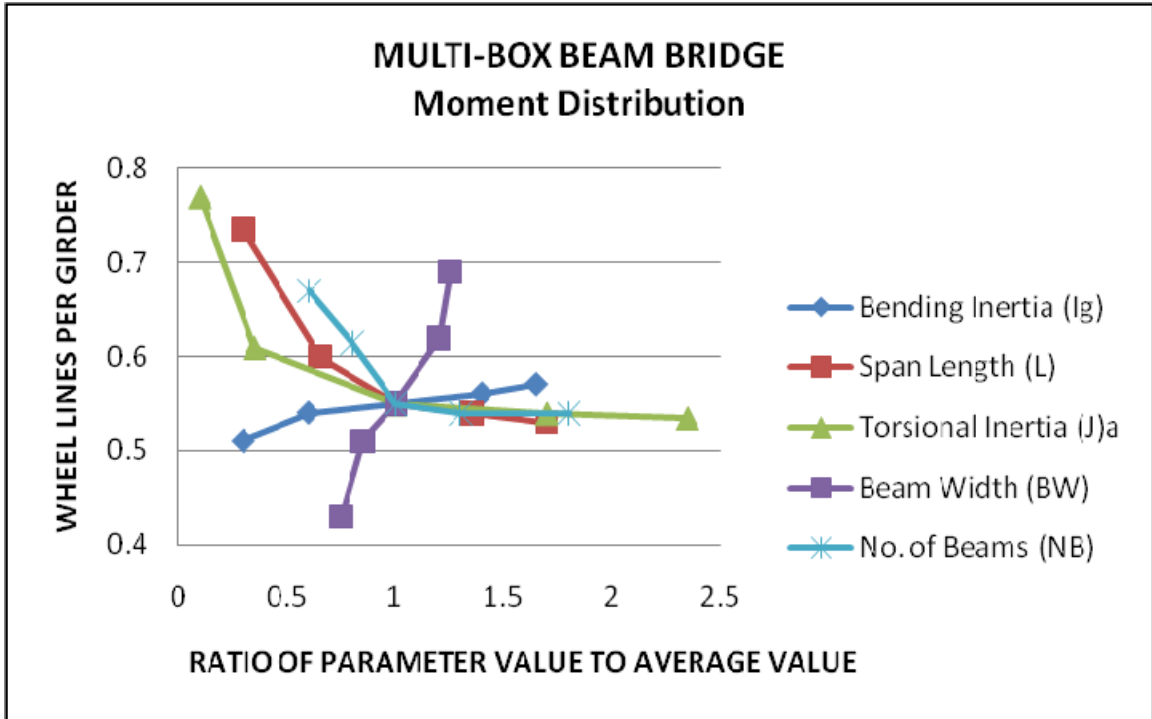


Figure 2.2: Effect of parameter variation on multi-box beam bridges (Zokaie, et al 1991)

Note the conflicting affects of various parameters on the effective width. This graph helps reaffirm how the formulas presented by AASHTO fail to recognize how variable the distribution factor can be given which parameters are used in its evaluation.

The following is an excerpt of Zokaie et al. (1991) explaining the methodology used in developing the formula for effective width and moment distribution. “First, it is assumed that the effect of each parameter can be modeled by an exponential function in the form ax^b , where x is the value of the given parameter, and a and b are coefficients to be determined based on the variation of x . Second, it is assumed that the effects of different parameters are independent of each other, which allows each parameter to be considered separately. The final distribution factor will be modeled by an exponential formula of the form: $g = (a)(S^{b1})(L^{b2})(t^{b3})(\dots)$ where g is the wheel load

distribution factor; S , L , and t are the parameters included in the formula; a is the scale factor; and b_1 , b_2 , b_3 are determined from the variation of S , L , and t , respectively.

Assuming that for the two cases all bridge parameters are the same except for S , then:

$$g^1 = (a)(S_1^{b_1})(L^{b_2})(t^{b_3})(\dots) \quad (1.4)$$

$$g^2 = (a)(S_2^{b_1})(L^{b_2})(t^{b_3})(\dots) \quad (1.5)$$

Therefore:

$$\frac{g_1}{g_2} = \left(\frac{S_1}{S_2} \right)^{b_1} \quad (1.6)$$

If n different values of S are examined and successive pairs are used to determine the value of b_1 , $n-1$ different values of b_1 can be obtained. If these b_1 values are close to each other, an exponential curve may be used to accurately model the variation of the distribution factor with S . In that case the average of $n-1$ values of b_1 is used to achieve the best match. Once all the power factors (i.e., b_1 , b_2 , and so on) are determined, the value of a can be obtained from the average bridge, i.e.,

$$a = g_o \div \left[(S_o^{b_1})(L_o^{b_2})(t_o^{b_3})(\dots) \right] \quad (1.7)$$

This procedure was followed during the entire course of the study to develop new formulas as needed.”

It is important to compare the results obtained from these formulas with real bridge data. This is due to the fact that certain assumptions were made in the derivations, and some bridge parameters were not included in the equations. To verify the accuracy, the formulas were applied to the database of bridges used in developing the “average” bridge. The wheel load distribution factors obtained from the accurate analysis were

compared to the results of the simplified method. The standard deviation, average, and maximum/minimum percentage difference were evaluated for each comparison and the simplified formula with the smallest standard deviation is considered to be the most accurate.

Table 2.1: Comparison of interior girder moment distribution factors by varying levels of accuracy using the “average bridge” for each bridge type (Zokaie, et al 1991)

Bridge Type	AASHTO	NCHRP 12-26 (Level 1)	Grillage (Level 2)	Finite Element (Level 3)
Beam-and-slab ^a	1.413 (S/5.5)	1.458	1.368	1.378
Box girder ^a	1.144	1.143	0.970	1.005
Slab ^b	5.980	5.625	6.242	6.204
Multi-box beam ^a	0.646	0.597	0.540	0.552
Spread box beam ^a	1.564	1.282	1.248	1.241

^a Number of wheel lines per girder, ^b Wheel line distribution width in, feet

The researchers were able to evaluate and develop formulae for all bridge types listed earlier, however it is of this paper’s interest to explore the work done on slab bridges. The formulas developed here are repeated from the introduction in different units.

The formula developed for the effective width for moment distribution of a single lane loaded bridge is:

$$E = 3.5' + .06\sqrt{(L_1 \times W_1)} \quad (1.8)$$

The formula for effective width for moment distribution on a bridge with a multilane loading is:

$$E = \frac{2 + \sqrt{(L_1 \times W_1)}}{4} \quad (1.9)$$

Zokaie also explored the effects of skew. This formula accounts for the reduction of moment in skewed bridges:

$$r = 1.05 - 0.25(\tan \theta) \leq 1.0 \quad (1.10)$$

Where r = the reduction factor to be applied to the distribution factor (E) obtained and θ = the skew angle between the centerline of a support and a line normal to the roadway centerline.

In general, these formulas are within 5 percent of the results obtained from an accurate analysis. Although these formulas are for the most part accurate and easy to use, they do hold some limitations which engineers need to be aware of. For one, the multilane loading condition includes multiple presence reduction factors. If other reduction factors conditional to a specific bridge are present, then the formulas needs to be reevaluated. For example, if a bridge type falls outside the bridges used in this study or has a unique type of design or construction process. Secondly, the formulas presented here are developed for a specific truck, typically the AASHTO HS design truck. The effects of other truck configurations should be considered. A limited study did show that if a trucks weight or longitudinal axis were different, but the gauge widths remain the same then the formulas accuracy is not greatly affected. However, in the condition where multiple different trucks are being considered simultaneously, then the formulas are not applicable.

2.2 Amer, et al (1999)

Amer et al. (1999) explores the fact that the load capacity of a bridge based on field tests is typically greater than the load capacity determined from standard rating calculations. They attempt to show through a grillage analogy that the equivalent

width values governed by the AASHTO Standard Specifications and LRFD are conservative estimates. As stated by Amer et al (1999) “Warren and Malvar (1993) investigated the lateral distribution of the wheel loads in a navy pier deck. Analyses and test results confirmed that the equivalent widths for reinforced concrete slabs in the navy pier decks can often be doubled over current AASHTO allowable values. This led to the introduction of the load and Resistance Factor Design (LRFD) specifications (AASHTO 1994).” As outlined in this report, the LRFD code is similar to the AASHTO Standard Specifications, but considers more parameters, namely width and number of lanes. Amer’s research is focused on highway bridges whose span is less than 45 ft, which is ideal for short span slab concrete bridges. Similar to the research being presented in this paper, they focused on slab bridges. Their objectives was to identify the main parameters affecting the equivalent width using the grillage analogy, compare the code values with that of field testing, and finally propose simple design formulas for effective width values.

The grillage analogy is a method of implementing loads onto a series of one dimensional beams in order to create a stiffness matrix. This matrix is used as a blueprint to construct the properties of the structure being evaluated. Twenty seven bridges were investigated using the grillage method in an attempt to identify the parameters that were most applicable to the effective width. Span length, bridge width, slab thickness, edge beam, and number of lanes were the main parameters chosen in this study. Over the twenty seven bridges, the average width was 30 ft, the average span was 21 ft, and the average thickness was 12 inches. The range of span lengths was 15 feet to 40 feet. The range of bridge widths was between 26 feet and 38 feet. The range of the aspect ratio (span length to width) was 0.5 to 1.6. Figure 2.3 and 2.4 show how the effective width varies with span length and bridge width.

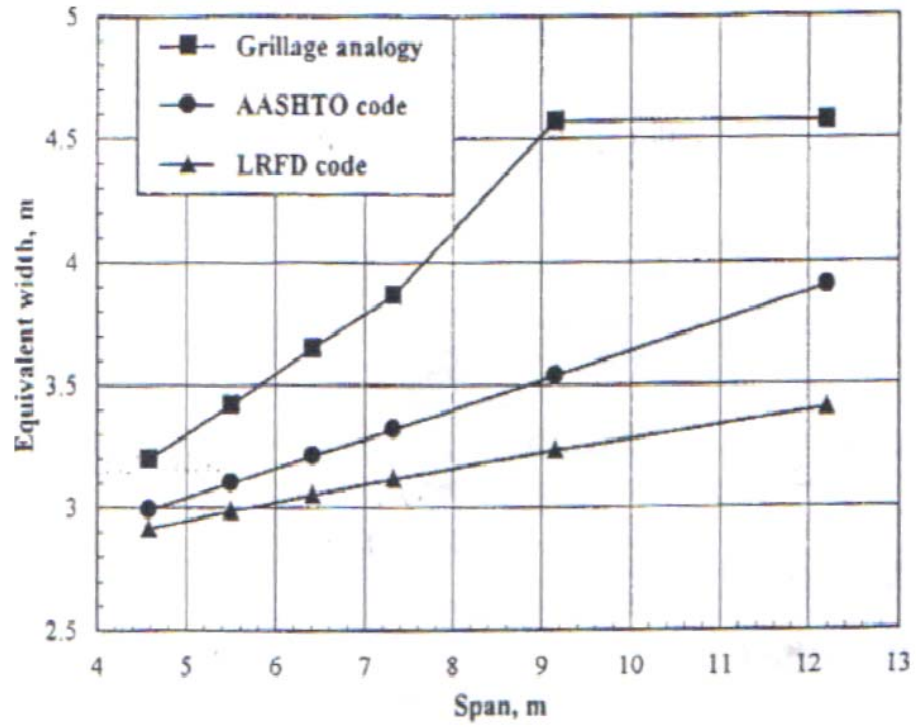


Figure 2.3: Effective Width Variation with Span Length for Solid Slab Bridges (Amer et al 1999)

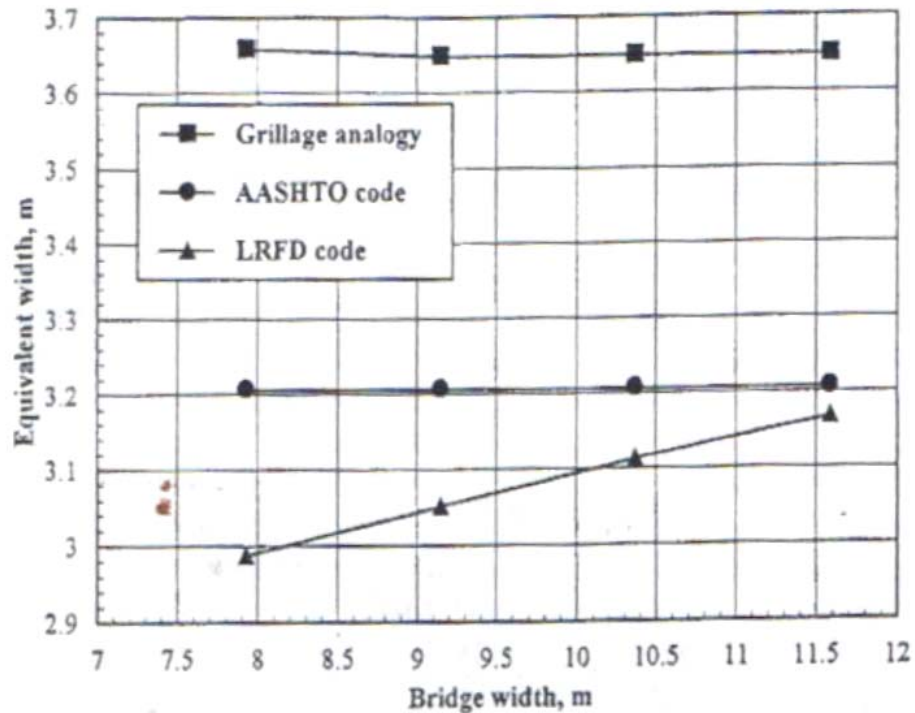


Figure 2.4: Effective Width Variation with Bridge Width for Solid Slab Bridges (Amer et al, 1999)

As a side note, it is of interest to see that the AASHTO Standard Specifications do not use width as a criteria in their formula for effective width, whereas the LRFD code does. Figure 2.4 shows equivalent width calculations for bridges with the same span and different widths. It seems to appear that the changes in the effective width are insignificant as the width varies. This limited study done by Amer showed that although LRFD code uses width as a parameter in its equation, it may not have a large impact. However, this conclusion was drawn on a small data set and only for two-lane slab bridges.

This research goes on to assess the affect of different edge beams on the slab equivalent width. “The AASHTO code requires that an edge beam should be

provided for longitudinally reinforced concrete slabs (main reinforcement parallel to traffic). The edge beam can be one the following three types: (1) a slab section additionally reinforced; (2) a beam integral with the slab and deeper than the slab; and (3) a reinforced section of the slab integral with the curb.” Figure 2.5 shows the equivalent width variation for various edge beam dimensions.

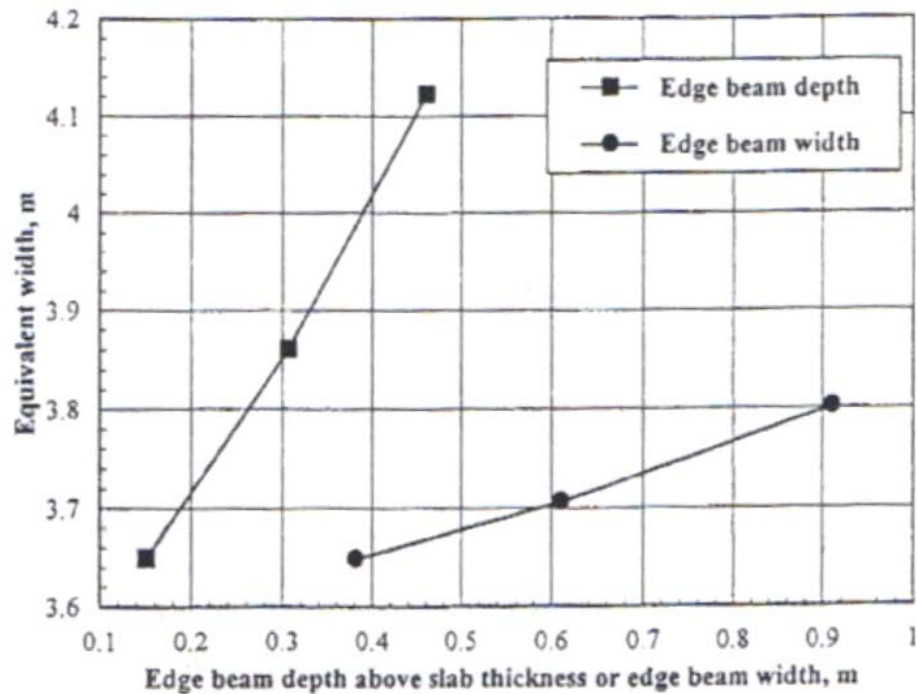


Figure 2.5: Effective Width Variation for Different Edge Beam Depths and Widths (Amer et al 1999)

As edge beam depth or width increases, so does the moment of inertia. It seems apparent that as the edge beam moment increases, so does the equivalent width, making a more efficiently loaded bridge. Slab bridges without edge beams would have a greater maximum moment intensity, thus decreasing the equivalent width. This suggests

that edge beam width may need to be taken into account for wheel load distribution factor calculation.

Based on this entire study, the span length and edge beam depth have the greatest impact on equivalent width. An equation was determined based on the least square fit of the results. Given the range of bridges tested, this equation can be used for spans of up to 40 feet.

$$E = 2.10 + 0.23L \leq \frac{W}{N_L} \quad (1.11)$$

Where E = the equivalent width (in feet) over which truck load is assumed to be uniformly distributed, L = the span length (feet), W = width (feet) and N_L = number of design lanes. The effect of edge beam depth can be used as scalar modifier on the previous equation.

$$C_{edge} = 1.0 + 0.5(d_1 - 0.15) \geq 1.0 \quad (1.12)$$

Where d_1 = edge beam depth (feet) above the slab thickness.

Three field tests were performed by Amer et al. (1999). Table 2.2 shows the data for each bridge test, while Figure 2.6 shows the resulting moment intensities based on the third field test and grillage analogy. Finally, a summary of the equivalent width measured in each of the studies is listed in Table 2.3.

Table 2.2: Solid Slab Bridge Field Tests (Amer 1999)

Field test (1)	Location (Florida) (2)	Span length [m (ft)] (3)	Total width [m (ft)] (4)	Width curb to curb [m (ft)] (5)	Slab thickness [m (in.)] (6)	Bridge conditions before testing (7)
1	Palm Beach County	4.57 (15.0)	7.92 (26.0)	7.32 (24.0)	0.30 (12.0)	Bridge elements appeared in good conditions
2	Taylor County	4.65 (15.3)	10.67 (35.0)	9.14 (30.0)	0.30 (12.0)	Bridge elements appeared in good conditions
3	Nassau County	6.10 (20.0)	10.36 (34.0)	8.53 (28.0)	0.30 (12.0)	Some longitudinal cracks were observed at bottom and top of the slab

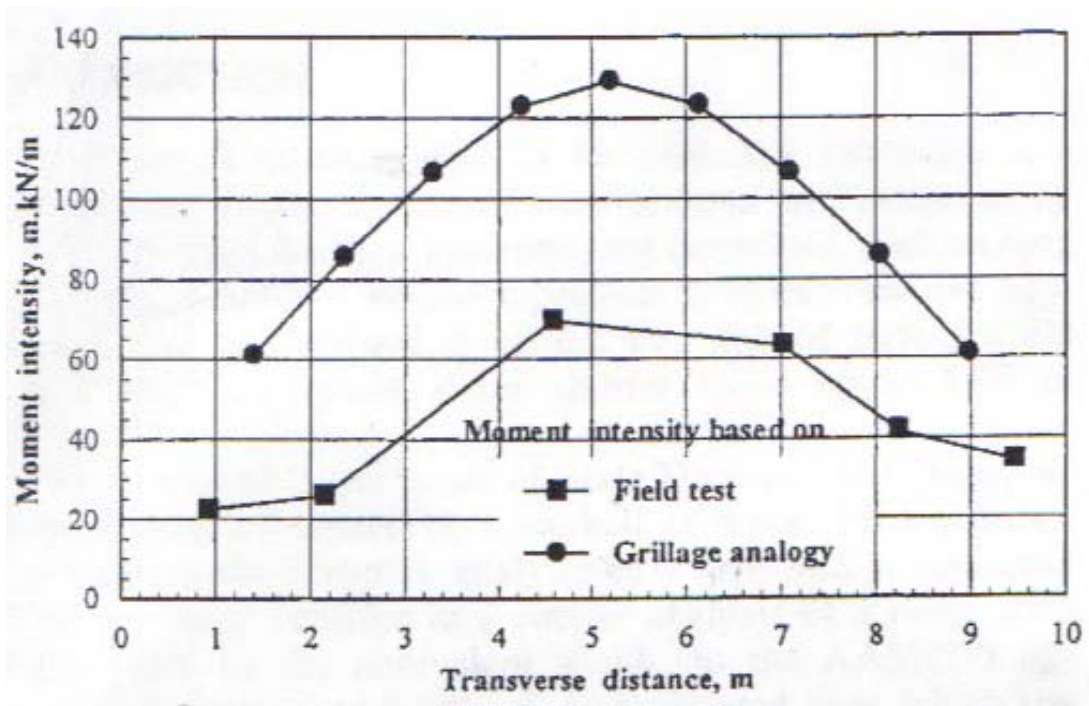


Figure 2.6: Bending Moment Intensities Based on Field Test and Grillage Analogy (Field Test 3 – Nassau County Bridge) (Amer et al, 1999)

Table 2.3: Equivalent Width E for Solid Slab Bridges (Amer 1999)

Field test (1)	Measured strains [m (ft)] (2)	Grillage analogy [m (ft)] (3)	AASHTO [m (ft)] (4)	LRFD [m (ft)] (5)	Proposed simplified equation [m (ft)] (6)
1	3.09 (10.14)	3.37 (11.06)	2.99 (9.80)	2.83 (9.36)	3.27 (10.73)
2	4.54 (14.89)	3.25 (10.67)	2.99 (9.80)	2.97 (9.75)	3.29 (10.79)
3	5.18 (17.00)	3.79 (12.44)	3.17 (10.4)	3.09 (10.13)	3.63 (11.92)

The values obtained from the grillage analogy are very close to that of the proposed formula for said bridges. It can also be observed that both the grillage analogy and proposed simplified formulas are more accurate in estimating the equivalent width of bridges of this type.

2.3 Mabsout et al. (2004)

Other research in finite element analysis has been done in order to reassess the formula for effective width. Mabsout (2004) reviewed the work of Frederick who presented the results of an experimental and finite-element investigation of load distribution in a single concrete slab bridge. He used a 28 ft span, simply supported slab bridge with a three-lane 34 ft width. The design live-load bending moments were calculated using AASHTO standard specification provisions. The FEA was performed using rectangular plate bending element. A one-fifteenth size scale model was constructed and tested in the laboratory. Design trucks were positioned one at a time along the center of each of the three lanes. The FEA results correlated well with the test data and were less than AASHTO empirical equations. The results for the multi-lane loading indicated that the slab behaved essentially as a wide beam with minor variations in the longitudinal bending moment across the width. It was also shown that there is no need for edge beam provisions in the specifications. Note how two separate research

projects done independently can reach differing conclusions. Amer's research led him to believe that edge beam depth and width influenced the effective width quite significantly while the FEA models presented by Frederick concluded otherwise. However, it should be noted that Frederick's work was based on a single slab bridge geometry that did not include integral edge beams, whereas Amer's study included 27 different bridge geometries, 6 of which included integral edge beams. It is important to consider methodology and initial data for just this reason as the conclusions drawn are always subject to them.

Mabsout et al. (2004) continued on Frederick's research findings and developed a total of 112 one-span, simply supported, nonskew, reinforced concrete slab bridge case studies in a finite element analysis. The bridges were varied from one lane to four total lanes. Four widths were considered (12, 24, 36, and 48 feet) and four spans were considered (24, 36, 46, and 54 feet). Two truck locations were considered: (1) each truck centered in own lane, (2) each truck placed close to one another near the edge, such that the closest wheel is one foot from the edge. The finite element program SAP2000 was used for 3D model analysis. The three main parameters compared between the FEA model and AASHTO (Standard Specifications and LRFD) were maximum longitudinal bending moment, edge beam moment, and maximum deflection. Bridges with shoulders and without shoulders were considered and the results of each were compared.

Regarding longitudinal bending moments: For slabs without shoulders in the case where the edge loaded condition is the greatest, and for one-lane bridges, AASHTO Standard Specifications overestimates the FEA moments found in this study by 30 percent for short spans (up to 25 feet). For longer spans of this condition, the current code is accurate. For bridges with more than one lane, AASHTO is accurate for short spans but underestimates the FEA model for longer spans by 15 to 30 percent. "Reinforced

concrete bridges with shoulders on both sides tend to increase in load carrying capacity. Therefore, it was found that the edge loading condition was found to be critical for bridges with shoulders on both free edges.”

Regarding edge beam moments and slabs without shoulders and short spans, AASHTO overestimates the FEA by 20 percent for one-lane bridges. For bridges with more than one lane, AASHTO agrees with the FEA. For longer spans, AASHTO agrees with the FEA for one-lane bridges and underestimates the FEA for more than one lane by 15 to 20 percent. For slabs with shoulders, AASHTO agrees with the FEA for short span bridges but underestimates the maximum FEA moment by 20 to 30 percent for longer spans.

Chapter 3

TEST PROCEDURE, ANALYSIS OF DATA, AND RESULTS

3.1 Bridge Test Procedure

3.1.1 Test Preparation

Upon the confirmation of a bridge being approved for testing, location maps, plans, and inspection reports for the bridge were obtained from the Delaware Department of Transportation. Bridges were visited within a few weeks of the test date where measurements and photographs were taken. Access was evaluated to determine if a johnboat or ladder was needed to mount the transducers. The condition of the concrete was also recorded in order to determine which strain mounting technique was best. Weather was also a factor in this decision. The adhesive used has an effective temperature range of -65° to 225° F however during application of the adhesive it is not effective to bond in temperatures lower than freezing. The trip also confirmed bridge plans, directions, and roadway layout to minimize the time lost on the day of the test. On several site visits, concrete strength was measured using a Schmidt hammer. The hammer was used several times at one location, averaging the results. Typically, measurements were taken at each end of the slab, the center of the slab, and each wall at the center.

A day to test the bridge was scheduled with the Delaware Department of Transportation, considering weather and logistics. Using the information from the inspection reports, location maps, and plans, the number of transducers needed was determined and a sensor layout drawing was created in AutoCAD.

The tests were conducted using Bridge Diagnostics Structural Testing System (STS). The STS system consists of strain transducers and a networked system of data acquisition junction boxes that are connected to a main power supply and control unit.

The strain transducers were prepared by attaching aluminum extensions and mounting tabs. The extensions are thin aluminum channels with a series of drilled holes. These holes allow the user to select the length of extension needed for the strain transducer. The selected length for our transducer was 12 inches (the long gage length is used when testing concrete to average out the effects of microcracks in the concrete). As will be described later, this 12 inch extension requires the strain measured in the field to be divided by 4 for the actual strain experienced in the bridge. Typically, two or three additional transducers were brought to the testing site.

3.1.2 On Site Procedure

Actual testing of the bridges took part in 3 stages. The initial stage was the test setup which included confirming the bridge geometry and marking strain gage locations. The location of the centerline of the slab transversely and longitudinally was determined using a measuring tape and marked with a chalk line. Transducer locations were marked on the slab, and walls if applicable. Roadway measurements given in the plans and inspection report were confirmed. Finally, bridge access equipment was prepared and preparations were made to mount the strain gages.

The second stage of the field test was the test preparation. Strain gages were mounted using a quick setting two part epoxy manufactured by Loctite, or in one case screws (this case is discussed in the summary of bridge 2-101B). Within seconds of the adhesive and accelerator spray being applied, the transducer was held in its

predetermined mounting location for about one minute until the adhesive set. Although there were preset mounting locations for each transducer, there was some variation in their exact placement. First, transducers were intended to be mounted longitudinally and typically 2' from each other. As they were mounted by hand visually, human error will tend to produce small variations in their actual placement. Secondly, the concrete surface of the slab was not always smooth and flush. There were occasionally cracks, joints, sealant, and excess concrete protruding slightly throughout the slab. To ensure a flat surface and a strong bond, wire brushes were used to remove protrusions and roughen the concrete surface. Transducers need a flat surface to adhere to, and because of these factors, slight adjustments were made longitudinally to the transducers location as needed. However, this instance was rare, and no transducer was relocated more than a few inches longitudinally from its intended location.

If necessary, a rope was tied transversely along the slab wall to mount the STS junction boxes and keep them out of the water. All transducers were connected to the junction boxes which in turn were connected to the STS power supply and control unit. All transducers were balanced, i.e., “zeroed,” before the test was conducted. In most instances the gages balanced; however, in some tests one or two gages would not balance or could not be identified by the STS system. The particular bridge cases, gage number and their location can be found in the test report section of the appendix.

The third stage of the field test was the truck passes. The test trucks were first weighed using Intercomp portable truck scales which are accurate to within ± 10 pounds. The wheel spacings were measured and recorded. The truck passes then commenced, starting with the single truck passes and ending with the multiple (side-by-side) truck passes. Typically, two identical runs were done for each pass for comparison and to account for any faults that may occur. If two different trucks were available for

testing, this also allowed for differing weights to be analyzed. For single passes, trucks were instructed to do a pass for each shoulder and each lane. For multiple truck passes, trucks were aligned side by side with a center to center wheel spacing of around 3 feet. Multiple truck passes were instructed to do a pass for each adjacent two-lane combination. For example, a 2-lane, 2-shoulder bridge would have 3 multiple truck passes (left shoulder/left lane, left lane/right lane, right lane/right shoulder). Information on each specific pass for each test can be found in the Appendix. Trucks were instructed to drive across the bridge at a “crawl” speed, i.e. around 5 to 10 mph. After each pass, the strains were collected and saved to a data file specific to each pass. As the trucks drove across the bridge, the data acquisition system recorded the microstrain. Photographs were taken for each unique truck pass.

When the test was completed, all transducers were removed by unscrewing the gage from the extension, then removing the mounting tabs from the concrete using pliers. All tools and data management software were removed and safely stored. Back at the bridge lab, all materials were cleaned, organized and replaced.

3.2 Data Analysis

Data was saved by the STS system as a text file, specific to each pass. Files were imported into Microsoft Excel and translated into a recognizable format that could be used to analyze the data. The raw data was given in microstrain, measured at 20 samples-per-second; therefore, the time interval between data point was 1/20 of a second. The data was recorded over the time in which the truck traveled across the bridge. Presented in Figure 3.1 is a screen shot of an Excel file with the data and a sample plot (microstrain versus time) of one of the sensors.

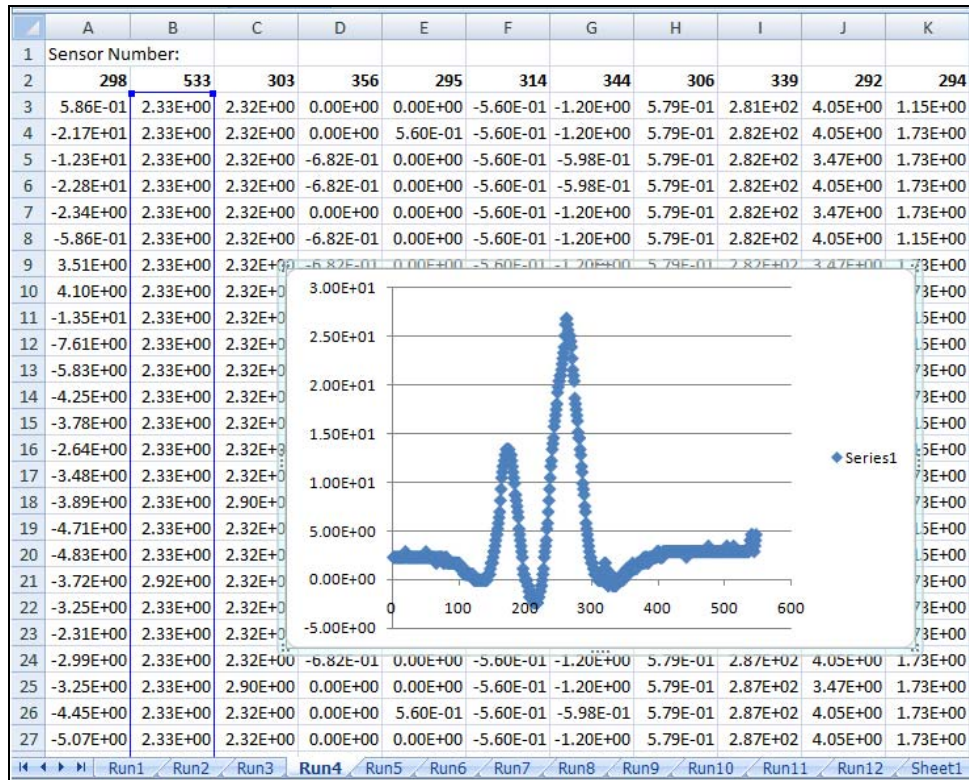


Figure 3.1: Typical Excel Sheet for Raw Data Analysis

Figure 3.1 shows how the strain increases and drops for the first truck wheel and does so once again at a greater magnitude for the second truck wheel. This kind of behavior was not observed for every sensor; sensors located farther from the transverse truck location recorded much lower strains with much higher variation in readings. This will be discussed more later.

3.2.1 Sensor Data Corrections

With each particular bridge and truck pass there were some issues that had to be addressed. The most common issue was sensor “drift”. Some sensors which were zeroed before a truck pass would have a non-zero constant reading after the truck had crossed (See Figure 3.2). Although the measured strain is still accurate the data must be

corrected for the drift. To correct for the drift the following process was used. The slope of the drift trend line was found by taking the average of the first ten points and subtracting the average of the last ten points, then dividing by the time, giving a value for the slope of the drift. The drift was then removed by subtracting the trend line from the raw data. Although typically very small, every sensor experienced some amount of “drift”. To remain consistent, every sensor was treated for “drift” using the method discussed above. A sample graph of the corrected “drift” sensors is shown in Figure 3.3.

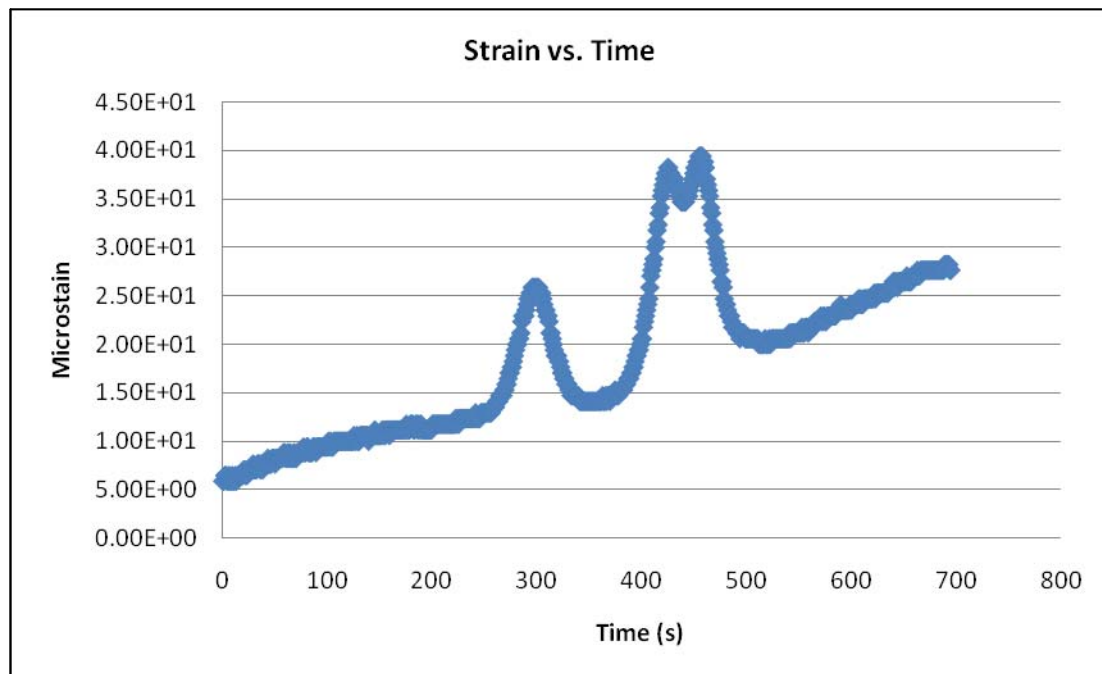


Figure 3.2: Raw Strain Data with “Drift” (Br. 318, Sensor 318, Run 1)

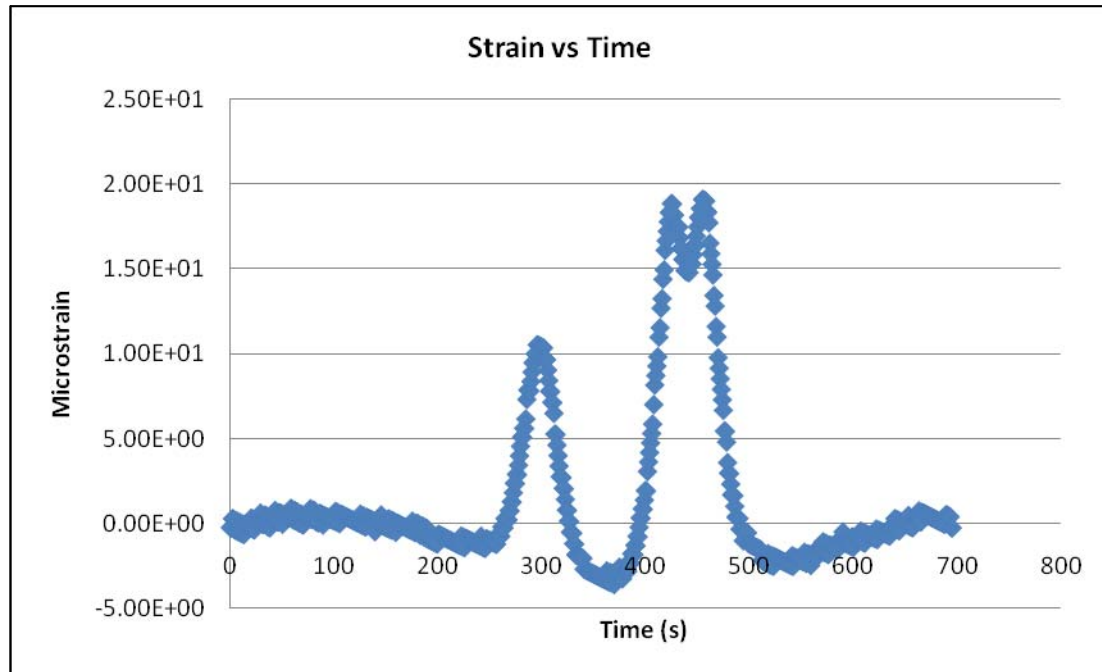


Figure 3.3: Corrected Strain Data with “Drift”

The other problem that was encountered was that of “noise”: strain values scattered about the expected strain path but with a large variation. Shown in Figure 3.4 is an example of a sensor that exhibited excessive “noise”. To correct for the noise, a running average procedure was used. Since the data followed a typical strain history, it was determined that by averaging each point by surrounding data points, an accurate graph was created. As such, each data point recorded was adjusted by averaging the 10 points preceding it and the 10 points following it, for a total of 21 strain values averaged. This method was used on each strain data point to complete the running average. Subsequently, the first and last 10 points were not averaged for lack of data. A corrected strain graph using the running average is shown in Figure 3.5. Only sensors showing signs of “noise” were treated for it.

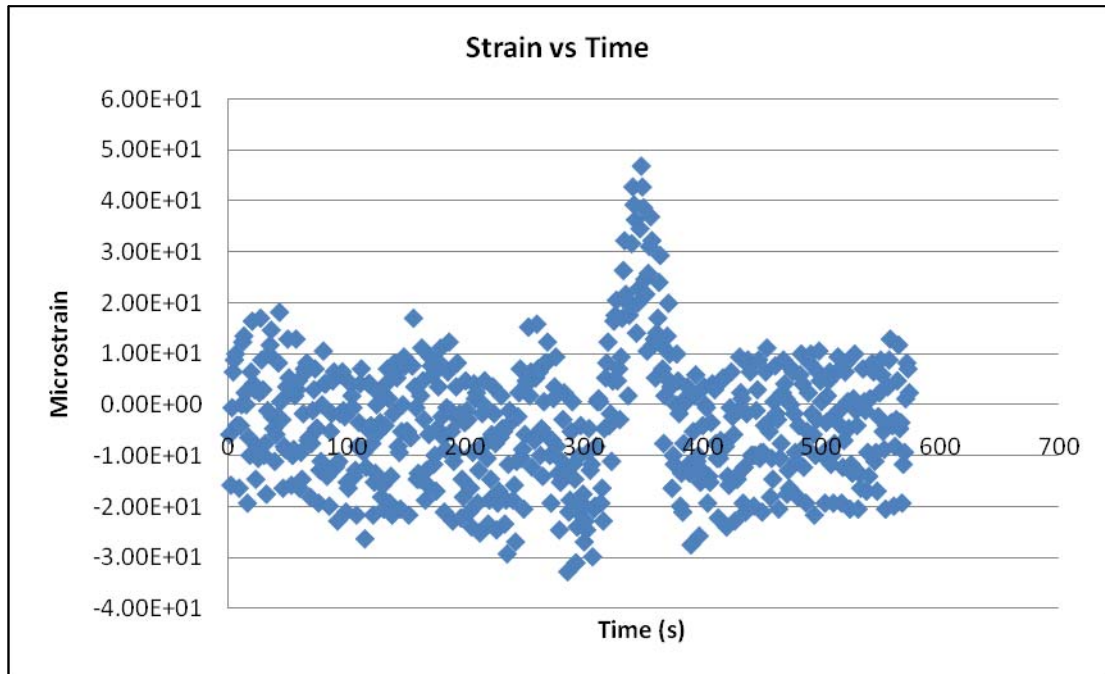


Figure 3.4: Raw Data for Sensor Exhibiting “Noise” (Br. 318, Sens. 298, Run 5)

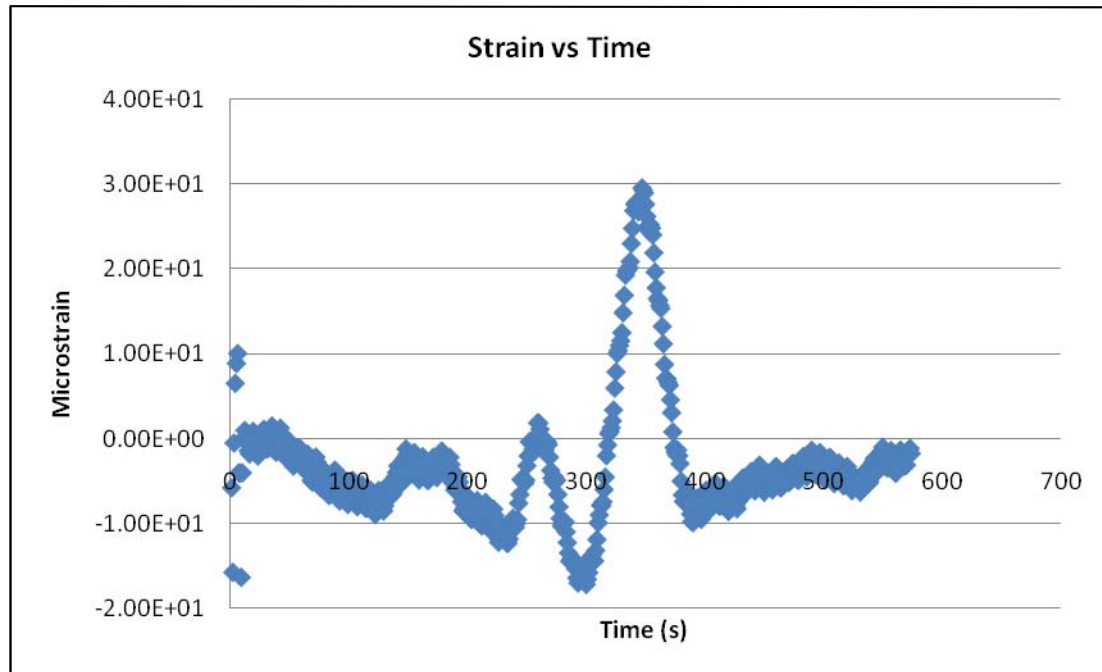


Figure 3.5: Corrected Data for Sensor Exhibiting “Noise”

“Drift” and “noise” were the most common problems encountered during data analysis. Although every sensor experienced some amount of each, there were typically two to five sensors on each bridge test that experienced a large amount. Figures 3.2 and 3.4 are extreme examples of each problem. The problems were usually a function of the sensor itself, meaning that a specific sensor would consistently display signs of “drift” and/or “noise”. Sensors that exhibited this behavior more typically experienced “drift” rather than “noise”. However the placement of the sensor relative to the truck pass was also a cause of some data inaccuracies. For example, if the sensor was on the opposite side of a truck pass, or located on a separate joint opposite a truck pass, “noise” was seen often. Occasionally the data would appear to “jump” to larger values which resulted in a graph with discontinuous strain measurements. However, these results were not significant due to their relatively small strain measurements and the data required for

analysis was taken from the graphs experiencing the maximum strain. Other problems with the strain measurement are specific to each bridge and can also be found in the test report section of the appendix.

3.2.2 Calculation of Effective Width

The recorded strain data was used to create a plot of the longitudinal strain versus transverse location, from which the effective slab width was determined. This plot is used to show the distribution of strain in the slab at mid span, in the transverse direction. To be conservative, the peak strain values measured were taken over the entire truck pass. The absolute maximum strain experienced at any given time in the corrected data was used as our time data point. Although there may be an instant in time where a larger summation of all the strains was larger, the calculation for effective width is dependent upon the peak strain of the distribution graph. Also these instances were rare and when they occurred the increased strain values were insignificant; therefore, the maximum strain at any given instant was used. The strain values at this instant for each sensor were then organized into the distribution plot. A typical strain distribution plot is shown in Figure 3.6. A plot was created for each truck pass.

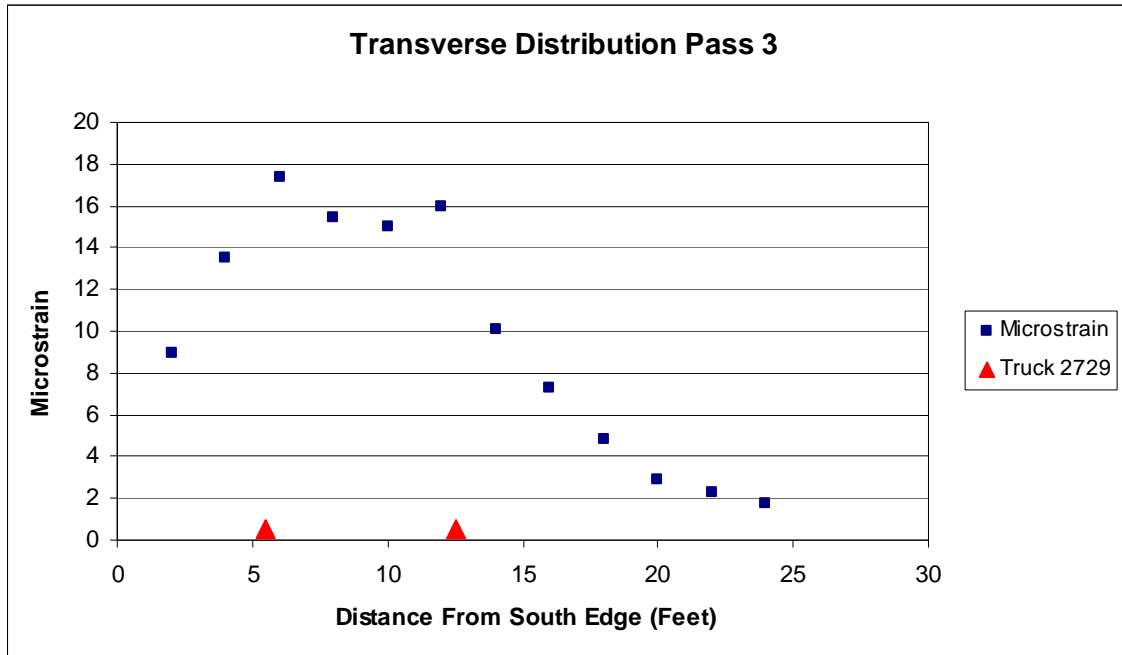


Figure 3.6: Typical Transverse Distribution Plot (Br. 384, Pass 3)

An idealized strain distribution would have a relatively constant peak value (strain max.) between the truck wheels, and would decrease to zero as one moves away from the wheels. This non-uniform strain (or stress) is a result of shear-lag. In order to simplify the evaluation of slabs that exhibit shear lag, the concept of effective width was developed. The effective width section has a constant strain (or stress) across its width. The widely accepted definition of the effective width is “the width that would have a uniform strain equal to the maximum strain but creates the same total effect as that caused by the actual strain distribution” (Chiewanichakorn et al., 2004). To turn the plot having a varying strain into one having a uniform strain, one must transform the area under the strain distribution into an area of a rectangle with the same maximum strain (height).

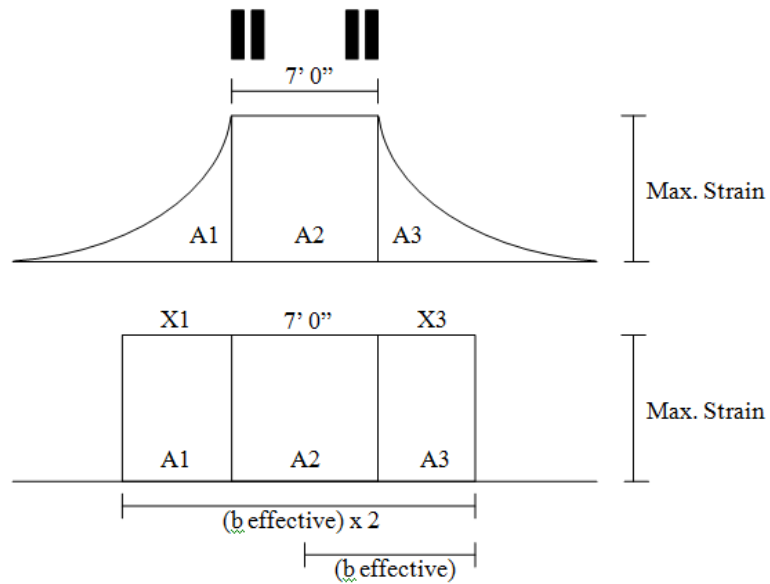


Figure 3.7 Idealized Strain Distribution and Effective Width Representation

Figure 3.7 visually illustrates how the transformed areas are found. Calculating the areas outside the wheel spacing results in two values for effective width. If the areas were too small or there were not enough data points for an accurate calculation, only one area was used. However, in the case of two usable areas, the conservative area was taken which resulted in the smaller effective width. Figure 3.8 shows an example of an actual bridge distribution and how the areas outside the wheel locations were calculated. The final values at each end of the bridge were taken as equal to the strain measured in the last sensor. This is a conservative estimate used due to the lack of data at the endpoints of the bridge (typically 2 feet or less from the last sensor).

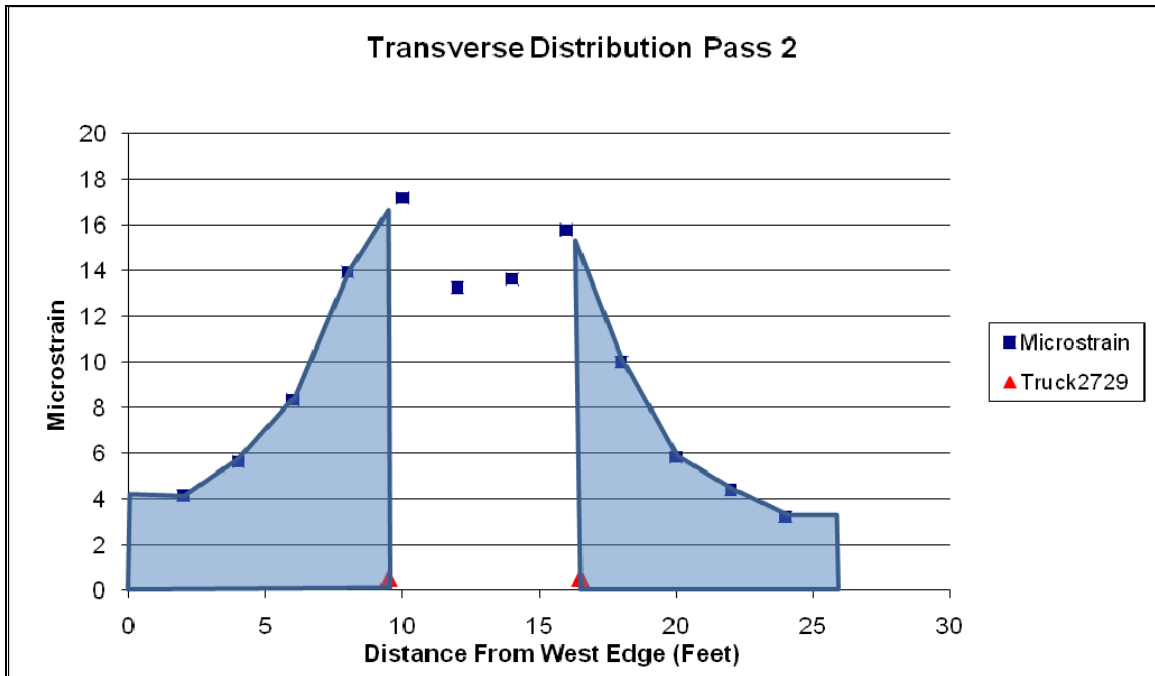


Figure 3.8: Calculating Effective Width from Transverse Distribution Plots

3.3 Summary of Bridge tests and Results

Presented in this section are summaries of the six bridges tests and the test results. Detailed reports for each are presented in the Appendix. At the conclusion of each bridge summary, a picture of the bridge, a sensor layout, and a summary of results is shown. The summary includes a table showing two times the AASHTO Standard Specification effective width and the AASHTO LRFD effective width calculated using the existing bridge properties (note that for easy direct comparison of all the results, any reference to the AASHTO Standard Specification effective width in the discussion is actually two times the Standard Specification width)Next to these values is the measured effective width value that was gathered during bridge testing. For the measured values, occasionally a minimum or average value is given. The minimum value is the smallest

effective width measured when evaluating each truck pass. This is the most conservative estimate for a bridge's effective width. The average effective width value was obtained by averaging the effective width values gathered from every truck pass. Some bridge runs do not have an average value due to lack of data, i.e., if there were not enough truck passes for a given bridge, an average value was not calculated.

3.3.1 Bridge 1-442

Bridge 1-442 is located on Money Road in New Castle, County and was tested on November 13, 2006. It is a concrete slab bridge with a 12 foot clear span, 13.08 foot effective span, which crosses a tributary to the Noxontown Pond. It was originally constructed in 1923, and was widened in 1964 to its current out-to-out width of 41 feet. The slab was instrumented with fourteen strain transducers placed on the underside of the concrete slab (six on the old section of the slab, and 8 on the newer slab section).

A fully loaded 6-wheel dump truck was used as a controlled live load for the test. The total weight of the loaded truck was 41.66 kips, with a combined rear axle weight of 30.49 kips. The maximum recorded concrete tensile stain at any time during the test was 22.8 $\mu\epsilon$ on the newer slab, and 14.5 $\mu\epsilon$ on the older slab. Based on evaluation of the observed transverse load distribution for both the new and old slab, a conservative estimate for the effective slab width of 6.5 feet for the older slab and 7.0 feet for the newer slab is recommended. Both of these are greater than the recommended AASHTO Standard Specification value of 4.78 ft, and the AASHTO LRFD recommended 4.03 ft. No multiple truck passes were done.



Figure 3.9: Bridge 1-442 Looking West

Table 3.1: Comparison of AASHTO Effective Width and Measured Effective Width (ft) Bridge 1-442

Lane loading	AASHTO LRFD (E)	AASHTO STANDARD SPECIFICATION $2b_{eff}$	Measured E_m
Single Truck	4.03	4.78	6.5

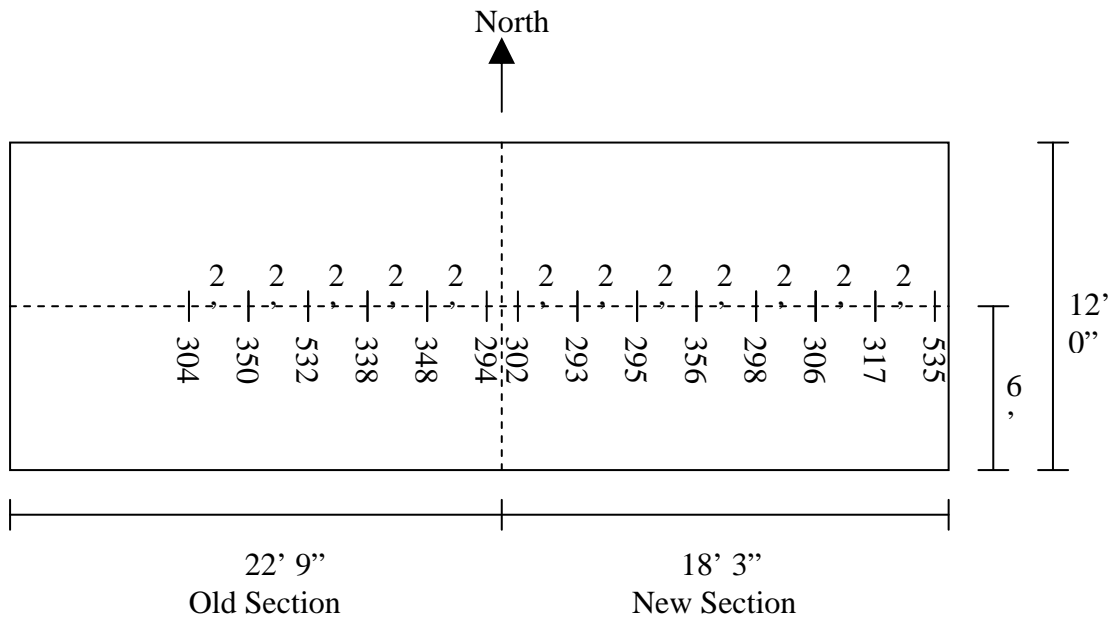


Figure 3.10: Bridge 1-442 Sensor Layout

3.3.2 Bridge 2-101B

Bridge 2-101B is located on Pearson's Corner Road and was tested on August 12, 2008. It is a concrete slab bridge with an 18 foot clear span and a 19.5 foot effective span. The slab bridge was originally constructed in 1931. The slab was instrumented with twelve strain transducers placed on the underside of the concrete slab.

Two fully loaded 6-wheel dump trucks were used as a controlled live load for the test. The gross weight of truck #2553 was 38.4 kips, with a combined rear axle weight of 27.8 kips. The gross weight of truck #2547 was 35.2 kips, with a combined rear axle weight of 24.4 kips. The test utilized eight load passes. The maximum recorded concrete

tensile stain at any time during the test was $14 \mu\epsilon$. For a single pass, the conservative measurement for the effective width value was 15.7 ft, which is 51.8% greater than the AASHTO Standard Specification value of 10.34 ft. For multiple trucks, the conservative effective width value measured was 10.6 ft, which is 2.5% greater than the AASHTO Standard Specification value of 10.34 ft. In comparison to the AASHTO LRFD code, the conservative measured value for a single lane was 46% greater than the LRFD effective width of 10.74 ft. The conservative measured value for multilane loaded was 7.6% greater than the AASHTO LRFD effective width of 9.85 ft.

Finally, the maximum strains in gages 294, 350, and 293 are consistently lower than the other gages, and are lower than one would expect for a theoretical distribution of strain. These were the three gages that were attached to the slab using concrete screws. In the plots they are data points between 9 ft. and 14 ft. These gages read lower than the others that were bonded to the slab. This is most likely due to “play” in between the mounting screw and the mounting bracket, or perhaps micro-cracking caused by the drilling and screwing operations.



Figure 3.11: Bridge 2-101 Looking East

Table 3.2: Comparison of AASHTO Effective Width and Measured Effective Width (ft) Bridge 2-101

Lane loading	AASHTO LRFD (E)	AASHTO Standard Specification ($2b_{eff}$)	Measured E_m
Single Truck	10.74	10.34	15.7
Multilane Truck	9.85	10.34	10.6

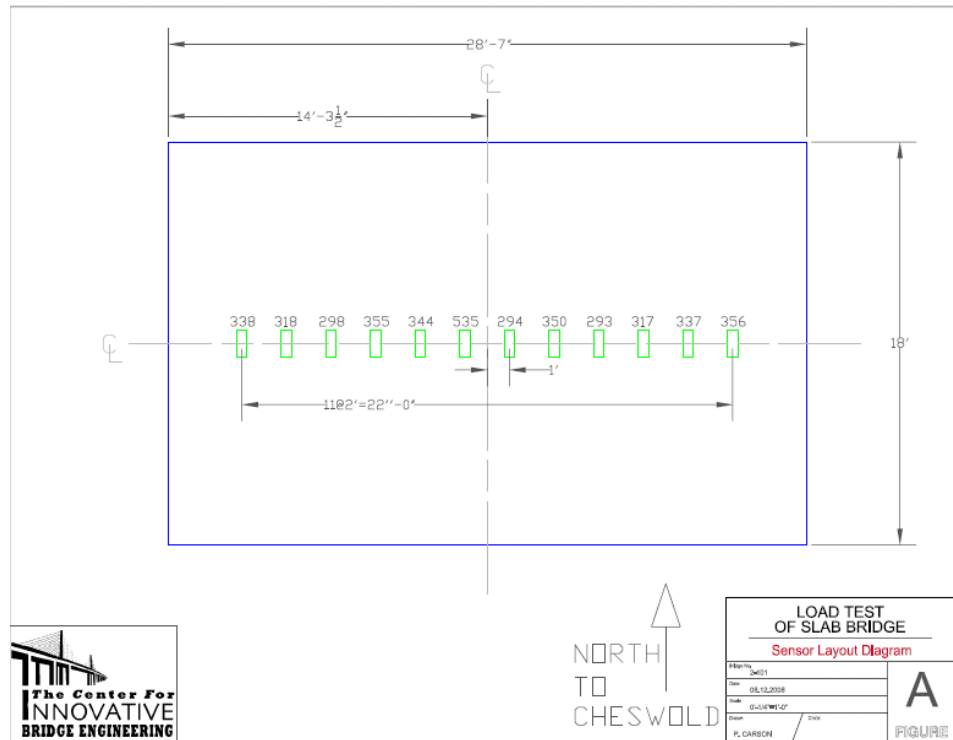


Figure 3.12: Bridge 2-101 Sensor Layout

3.3.3 Bridge 1-352W

Bridge 1-352W is located on Route 40 in Glasgow, Delaware and was tested on November 19, 2008. It is a concrete slab bridge/culvert with an 8 foot span and an out-to-out deck width of 47 ft. It was originally constructed in 1932. The slab was instrumented with sixteen strain transducers placed on the underside of the concrete slab.

Two fully loaded 6-wheel dump trucks were used as a controlled live load for the test. The gross weight of truck #2729 was 35.5 kips, with a combined rear axle weight of 24.1 kips. The gross weight of truck #2571 was 36.9 kips, with a combined rear axle weight of 25.7 kips. The test utilized nine load passes. The maximum recorded concrete tensile stain at any time during the test was 12 $\mu\epsilon$. For a single pass, the conservative

measurement for the effective width value was 12.00 ft, which is 34% greater than the AASHTO Standard Specification value of 8.96 ft. The average value is almost 50% higher than the AASHTO Standard Specification width. For multiple trucks, the conservative effective width value measured was 10.52 ft, which is 17% greater than the AASHTO Standard Specification value. The average value is 29% higher than the AASHTO Standard Specification width. In comparison to the AASHTO LRFD code, the conservative measured value for a single lane was 64% greater than the AASHTO LRFD effective width of 7.3 ft. The conservative measured value for multilane loaded was 13% greater than the AASHTO LRFD effective width of 9.3 ft.

The strains recorded for bridge 1-352W were atypically low. The very low strains can be attributed to a number of reasons. First is possible frame action provided by the abutments. Although the bridge was not designed as a rigid frame, there is some continuity between the slab and walls which will tend to reduce the strain at mid-span. Second, there appears to be about a foot of fill between the top of the slab and the bottom of the roadway. The fill will distribute the load out in all directions and therefore reduces the effective load acting on the slab. This can be particularly significant in short span bridges. Finally, the concrete strength may be greater than the design specified strength, which will also tend to reduce the strain at mid-span. The output of gage 317 was consistently very low for all the truck passes and is believed to have not been operating properly during the test, therefore, the results for that gage are not included in the tables or the plots.



Figure 3.13: Bridge 1-352W Looking East

Table 3.3: Comparison of AASHTO and measured effective width (ft) for Bridge 1-352

Lane loading	AASHTO LRFD (E)	AASHTO Standard Specification ($2b_{eff}$)	Measured E_m	
			Min	Average
Single	7.3	8.96	12.00	13.1
Multilane	9.3	8.96	10.52	11.58

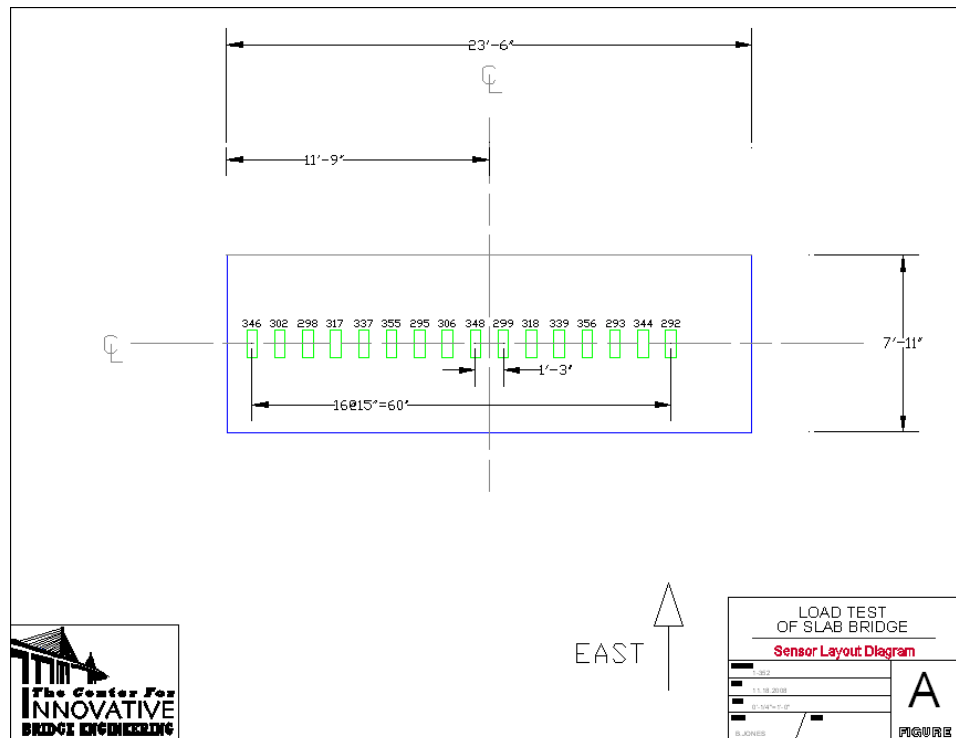


Figure 3.14: Bridge 1-352W Sensor Layout

3.3.4 Bridge 1-384

Bridge 1-384 is located on Dutch Neck Road, New Castle County, Delaware and was tested on December 22, 2008. It is a concrete slab bridge/culvert with a 12 foot span and an out-to out deck width of 26 foot. The bridge crosses a small creek and was originally constructed in 1931. The slab was instrumented with twelve strain transducers placed on the underside of the concrete slab.

Two fully loaded 6-wheel dump trucks and a utility vehicle were used as a controlled live load for the test. The gross weight of truck #2729 was 37.5 kips, with a combined rear axle weight of 26.4 kips. The gross weight of truck #2741 was 34.2 kips, with a combined rear axle weight of 23.8 kips. The gross weight of truck #2719 was 15.8

kips. The test utilized 14 load passes in which the maximum recorded concrete tensile stain at any time during the test was 26 $\mu\epsilon$. The conservative measured effective width value for a single lane was 13.2 ft, which was 40% greater than the AASHTO Standard Specifications code effective width of 9.44 ft. The conservative measured value for multilane loaded was 11.1 ft, which was 18% greater than the code effective width of 9.44 ft. In comparison, for a single truck a conservative effective width was 61% greater than the AASHTO LRFD width of 8.2 ft for single lane loading. For multiple truck passes, the conservative estimate for the effective slab width of the bridge was 22% greater than the AASHTO LRFD width of 9.1 ft for multi-lane loading. The test also provided a “proof” safe load limit relative to the current 7 ton load posting: a total of 36 tons was placed on the bridge without any measurable or visual distress to the bridge.

During the installation it was noted that a crack exists in the bottom of the slab that runs longitudinally from one abutment to the other. It is to the west of the centerline of the bridge. It appears to have been filled as sometime with a type of polymer material. Strain gage 314 was located to the east of the crack and gage 302 was located to the west of the crack.

The effective widths for passes 1 and 1a are significantly higher than the corresponding values for passes 2, 2a, 3, and 3a, for truck #2729. Likewise, the effective widths for passes 6 and 6a are significantly higher than the corresponding values for passes 7, 7a, 8, and 8a, for truck #2719. This is most likely due to the longitudinal crack in the bottom of the slab. The effects of the crack are accounted for in the calculation and details can be seen in the final report, shown in the Appendix.



Figure 3.15: Bridge 1-384 Looking South West

Table 3.4: Comparison of AASHTO and measured effective width (ft) for Bridge 1-384

Lane loading	AASHTO LRFD (E)	AASHTO Standard Specification ($2b_{eff}$)	Measured E_m	
			Min	Average
Single	8.2	9.44	13.2	16.3
Multilane	9.1	9.44	11.14	11.29

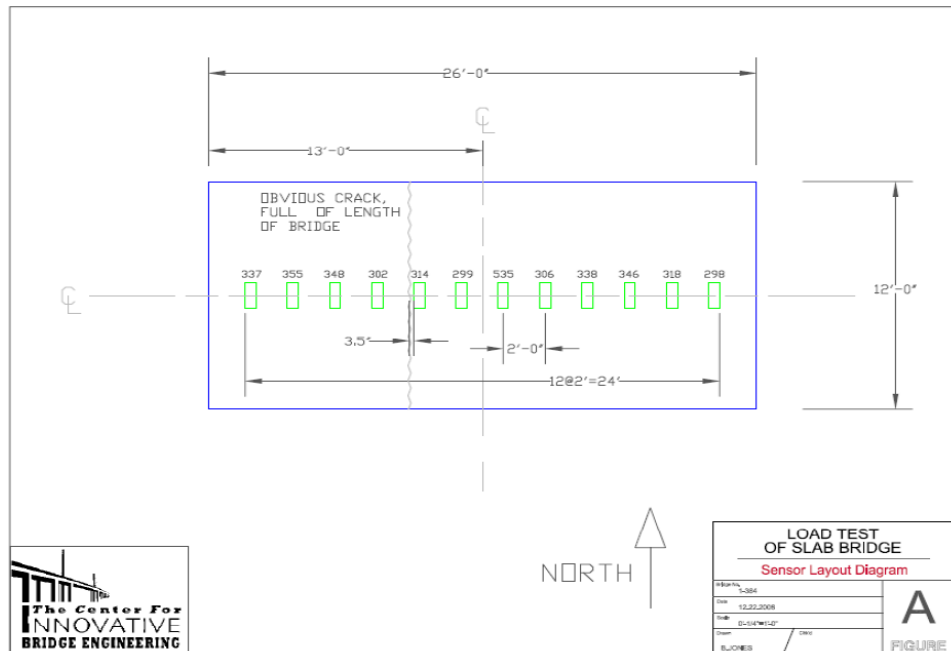


Figure 3.16: Sensor Layout Bridge 1-384

3.3.5 Bridge 3-318

Bridge 3-318 is located on Laurel Road, Sussex County, Delaware and was tested October 29, 2009. It is a concrete slab bridge/culvert with an 8 foot span and a current out-to-out deck width of 37.8 foot. The bridge was originally constructed in 1924 and renovated in 1949 when an additional 6 foot 6 inches of roadway was added. The joint is north of the centerline of the bridge and runs longitudinally from one abutment to the other. The slab was instrumented with nineteen strain transducers placed on the underside of the concrete slab. Transducers were mounted 6 inches to each side of the joint. Strain gage 1476 was located to the south of the joint and gage 1477 was located to the north of the joint.

Two fully loaded 10-wheel dump trucks were used as a controlled live load for the test. The gross weight of truck #2826 was 59.7 kips, with a combined rear axle weight of 45.2 kips. The gross weight of truck #2939 was 62.1 kips, with a combined rear axle weight of 45.7 kips. The test utilized 12 load passes. The maximum recorded concrete tensile stain at any time during the test was 14 $\mu\epsilon$. Based on evaluation of the observed transverse load distribution, a conservative estimate for the effective slab width of the bridge for two vehicles is 9.0 ft. This is approximately equal to the AASHTO LRFD width of 9.1 ft for multi-lane loading. For a single truck the conservative effective width was 9.9 ft, which is 36% greater than the AASHTO LRFD width of 7.29 ft for single lane loading and 10% greater than the AASHTO Standard Specification of 8.96 ft.

The strains recorded for bridge 3-318 were atypically low. The very low strains can be attributed to two factors. First is possible frame action provided by the abutments. Although the bridge was not designed as a rigid frame, there is some continuity between the slab and walls which will tend to reduce the strain at mid-span. Second, the concrete strength may be greater than the design specified strength, which will also tend to reduce the strain at mid-span.

There were a few sensors which gave atypical data. Sensors 350 and 1478 did not function and thus there was no data read for those two sensors. Sensor 298 had a large amount of “noise” in the data. Sensor 339 showed a large amount of “drift” in the data. The data for sensor 346 was on average about 30% larger than what might be expected data, based on the transverse distribution plot. Adjustments were made on these sensors and full details can be seen in the final report, seen in the Appendix.



Figure 3.17: Picture of Bridge 3-318 Looking South

Table 3.5: Comparison of AASHTO and Measured Effective Width (ft) for Bridge 3-318

Lane loading	AASHTO LRFD (E)	AASHTO Standard Specification ($2b_{eff}$)	Measured E_m	
			Min	Average
Single	7.29	8.96	9.9	13.2
Multilane	9.09	8.96	9.0	10.1

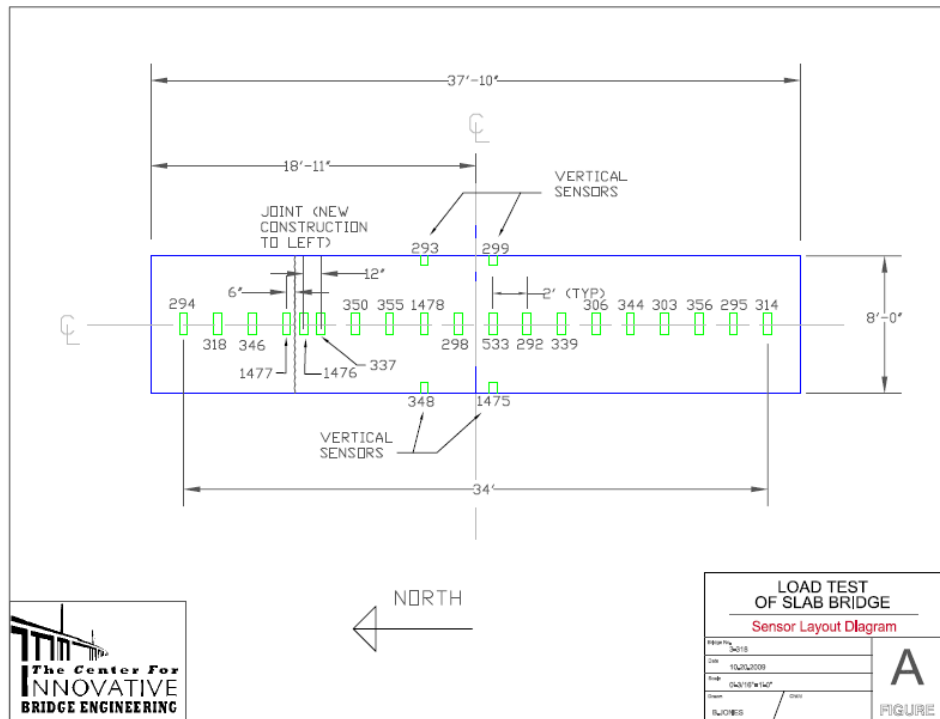


Figure 3.18: Sensor Layout for Bridge 3-318

3.3.6 Bridge 3-316

Bridge 3-316 is located on Laurel Road, Sussex County, Delaware and was tested April 19, 2010. It is a concrete slab bridge/culvert with a 14 foot span and a current out-to-out deck width of 38.25 foot. The bridge was originally constructed in 1924 and renovated in 1949 when an additional 9 foot 6 inches of roadway was added. The joint is south of the centerline of the bridge and runs longitudinally from one abutment to the other. The slab was instrumented with eighteen strain transducers placed on the underside of the concrete slab. Strain gage 355 was located to the south of the joint and gage 295 was located to the north of the joint.

Two fully loaded 10-wheel dump trucks were used as a controlled live load for the test. The gross weight of truck #2818 was 59.7 kips, with a combined rear axle weight of 44.9

kips. The gross weight of truck #2939 was 65.1 kips, with a combined rear axle weight of 50.8 kips. The test utilized 13 load passes. The maximum recorded concrete tensile stain at any time during the test was 17.4 $\mu\epsilon$. Based on evaluation of the observed transverse load distribution, a conservative estimate for the effective slab width of the bridge for two vehicles is 11.7 ft. This is 18% greater than the AASHTO LRFD width of 9.91 ft for multi-lane loading. For a single truck a conservative effective width is 14.5 ft, which is 48% greater than the AASHTO LRFD width of 9.77 ft. The AASHTO Standard Specifications approximations for these effective widths are nearly the same as the LRFD approximations. As such, the percentages are the same for the Standard Specifications.

The strains recorded for bridge 3-316 were low. The very low strains can be attributed to two factors. First is possible frame action provided by the abutments. Although the bridge was not designed as a rigid frame, there is some continuity between the slab and walls which will tend to reduce the strain at mid-span. Second, the concrete strength may be greater than the design specified strength, which will also tend to reduce the strain at mid-span. A photo of Bridge 3-316 and pertinent data can be seen in the following figures.



Figure 3.19: Picture of Bridge 3-316 Looking South

Table 3.6: Comparison of AASHTO and Measured Effective Width (ft) for Bridge 3-316

Lane loading	AASHTO LRFD (E)	AASHTO Standard Specification ($2b_{eff}$)	Measured E_m	
			Min	Average
Single	9.77	9.84	14.5	17.4
Multilane	9.91	9.84	11.7	12.0

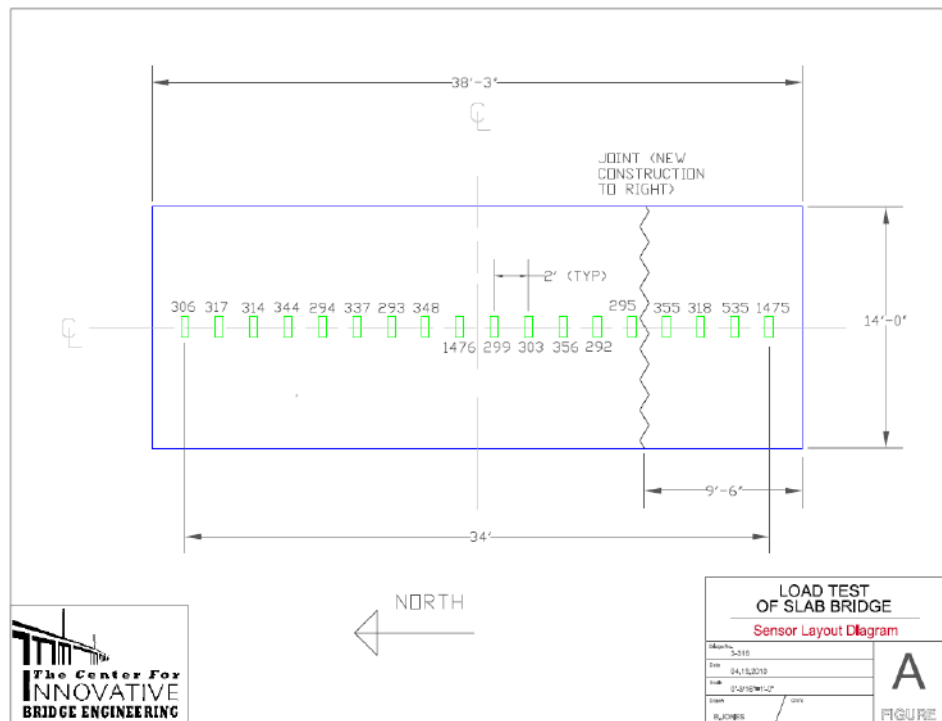


Figure 3.20: Sensor Layout for Bridge 3-316

Chapter 4

ANALYSIS

4.1 Introduction

Using the test results presented earlier, a new, more accurate equation for effective width of concrete slab bridges in Delaware is developed in this chapter. The new formula is obtained using a regression line analysis of the test results. Results are compared to existing AASHTO Standard Specifications and LRFD values. The main comparison was made to the LRFD code as it is used now by the Delaware Department of Transportation for evaluating its bridges. The results are obtained using a power regression line for single truck passes and multiple truck passes. Details on the calculations and theory are presented below.

4.2 Methodology

Initially, graphs were created comparing all effective width values for single passes and multiple passes. These graphs included measured values, AASHTO Standard Specification, and LRFD values. The controlling parameters used were width, span length, and aspect ratio. Figure 4.1 and 4.2 show single truck pass graphs of each effective width value versus width and aspect ratio (L/W), respectively. The measured low, average, and max effective widths are marked by the green lines and triangles. A range of measured effective width values was not obtained for Bridge 1-

442, therefore no average or maximum values are given. For this bridge, the measured effective width value is taken as the low (conservative) value.

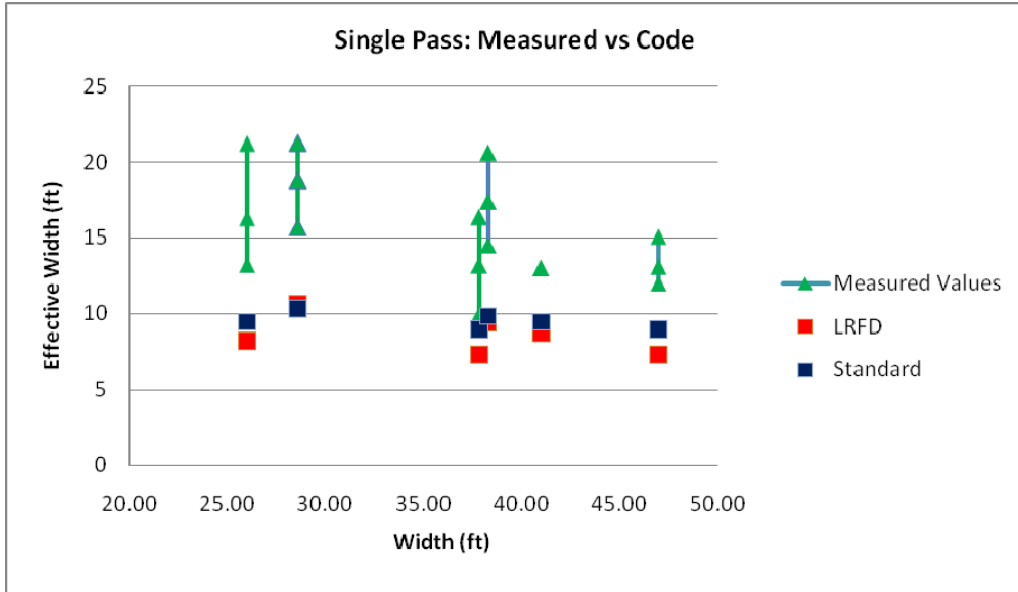


Figure 4.1: Comparison of Effective Width Code Values to Measured Values (Single Truck Pass, Controlling Parameter: Width)

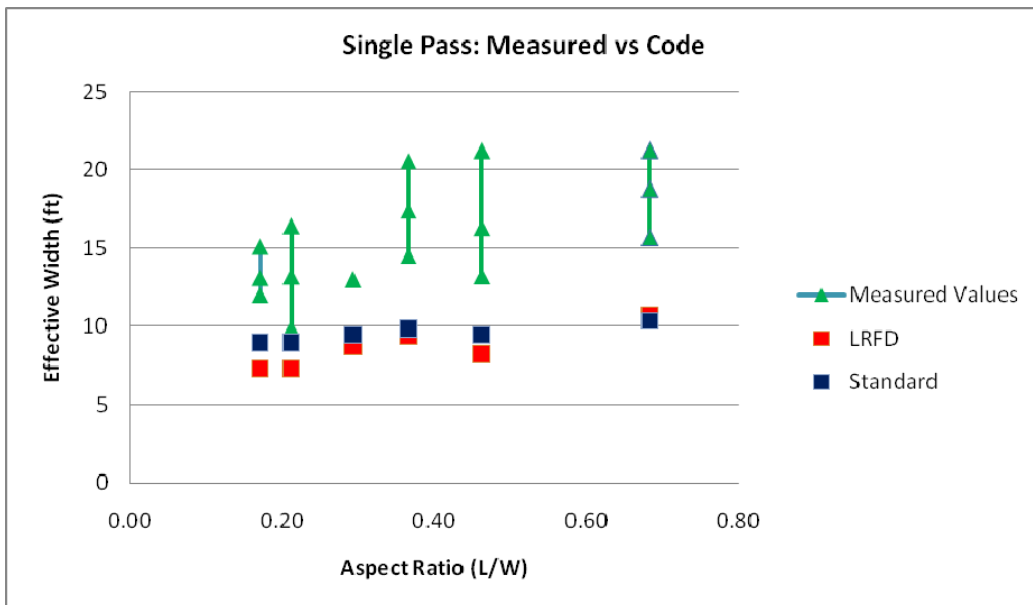


Figure 4.2: Comparison of Effective Width Code Values to Measured Values (Single Truck Pass, Controlling Parameter: Aspect Ratio)

Figure 4.3 shows a multiple truck pass graph comparing effective width values versus aspect ratio. In Chapter 3 it was explained that for bridge 2-101 a different method for measuring side-by-side truck passes was used. Trucks were placed statically at mid span as opposed to crossing at a “crawl” speed. Due to the method used and the low sample size of multiple truck passes (2), an average and maximum value were not found. The measured effective width value for bridge 2-101 is taken as the low (conservative) value. For other bridges, the measured low, average, and max effective widths are marked by the green lines and triangles. A multiple truck pass for bridge 1-442 was not performed, so only five of the bridge test values are shown.

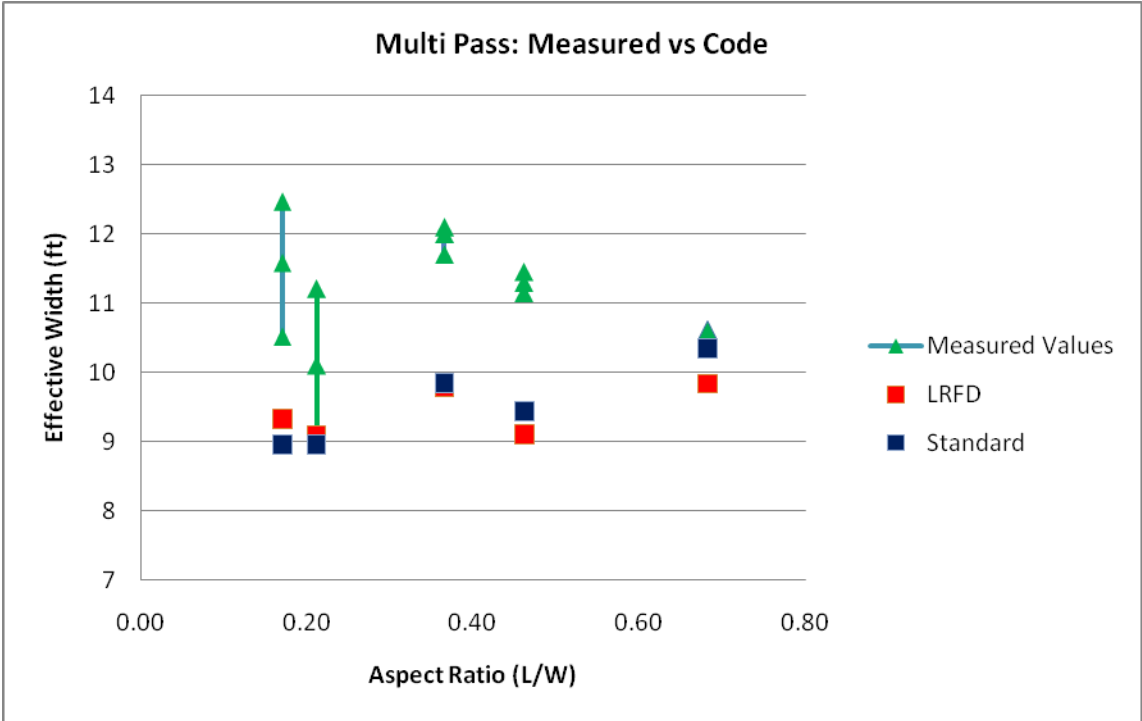


Figure 4.3: Comparison of Effective Width Code Values to Measured Values (Multiple Truck Pass, Controlling Parameter: Aspect Ratio)

Table 4.1 shows the effective width value measured for each bridge versus the code for single passes. Table 4.2 shows the same for multilane passes. The results presented in the graphs and tables illustrate the conservative nature of the code equations.

Table 4.1: Effective Width Values for Single Truck Passes

BRIDGE		Effective Width, ft (Single)			% Increase (Standard)	% Increase (LRFD)
		Measured	Standard	LRFD*		
1-442	low	13	9.4	10.9**	37.7	19.3
	avg	-				
	high	-				
2-101B	low	15.7	10.3	12.8	51.8	22.7
	avg	18.8			81.8	46.9
	high	21.3			105.8	66.4
1-352W	low	12.0	9.0	8.7**	33.9	37.9
	avg	13.1			46.2	50.6
	high	15.1			68.5	73.6
1-384	low	13.2	9.4	9.8	39.8	34.7
	avg	16.3			72.7	66.3
	high	21.2			125.0	116.3
3-318	low	9.9	9.0	8.7**	10.5	13.8
	avg	13.2			47.3	51.7
	high	16.4			83.0	88.5
1-316	low	14.5	9.8	11.2**	47.4	29.5
	avg	17.4			76.8	55.4
	high	20.6			109.4	83.9

* LRFD single lane effective width formula, equation (1.1), includes a factor of 1.2 for multi-presence, thus must be multiplied by 1.2 for a direct comparison to the measured values; values listed are 1.2 times the code equation.

** $W_1=30$ ft in code equation since $W>30$ ft.

Table 4.2: Effective Width Values for Multilane Truck Passes

BRIDGE		Effective Width, ft (Multi)			% Increase (Standard)	% Increase (LRFD)
		Measured	Standard	LRFD		
2-101B	low	10.6	10.3	9.8	2.5	8.2
	avg	-				
	high	-				
1-352W	low	10.5	9.0	9.3	17.4	12.9
	avg	11.6			29.2	24.7
	high	12.4			39.1	33.3
1-384	low	11.1	9.4	9.1	18.0	22.0
	avg	11.3			19.6	24.2
	high	11.5			21.3	26.4
3-318	low	9.0	9.0	9.1	0.5	1.1
	avg	10.1			12.7	11.0
	high	11.2			25.0	23.1
1-316	low	11.7	9.8	9.8	18.9	19.4
	avg	12.0			22.0	22.4
	high	12.1			23.0	23.5

4.2.1 Determination of New Effective Width Equation

The basis for the proposed new equation will be the current LRFD equation. The equation for effective width of a slab, per AASHTO LRFD, is

$$E = 10.0 + 5.0\sqrt{L_1 W_1} \quad (4.1)$$

for a single lane loaded, and

$$E = 84.0 + 1.44\sqrt{L_1 W_1} \leq \frac{12W}{N_L} \quad (4.2)$$

for multilane loading (see Chapter 1 for variable definitions).

Multiplying the right hand side of equation (4.1) by 1.2, to remove the multiple presence factor yields

$$E = 12 + 6\sqrt{L_1 W_1} \quad (4.3)$$

For effective width in feet (E_f), equation (4.3) can be expressed as

$$12E_f = 12 + 6\sqrt{L_1W_1} \quad (4.4)$$

Rearranging, this can be expressed as:

$$\frac{12E_f - 12}{6W_1} = \sqrt{\frac{L_1}{W_1}} \quad (4.5)$$

Similarly, for multilane loading, except that there is no multiple presence factor for multi-lane loaded, equation (4.2) becomes:

$$12E_f = 84 + 1.44\sqrt{L_1W_1} \quad (4.6)$$

$$\frac{12E_f - 84}{1.44W_1} = \sqrt{\frac{L_1}{W_1}} \quad (4.7)$$

Note that in this form the code equations for effective width are basically proportional to the square root of the bridge aspect ratio. Presented in Tables 4.3 and 4.4 are the normalized measured effective widths for each bridge, for the measured low, average, and high values, for the single and multi-truck passes. These are computed by substituting the measured width into the left hand side of either equation (4.5) or (4.7), respectively.

Table 4.3: Normalized Measured Effective Width Values for Single Truck Passes

Bridge	Span Length (ft)	Width (ft)	L/W	Measured EW (ft)		$\frac{12E_f - 12}{6W}$
				Low	High	
1-442	13.08	41	0.32	Low	13	0.5854
				Ave	-	-
				High	-	-
2-101B	19.5	28.5	0.68	Low	15.7	1.0316
				Ave	18.8	1.2491
				High	21.3	1.4246
1-352W	8.0	47	0.17	Low	12.0	0.4681
				Ave	13.1	0.5149
				High	15.1	0.6000
1-384	12.0	26	0.46	Low	13.2	0.9385
				Ave	16.3	1.1769
				High	21.2	1.5538
3-318	8.0	37.8	0.21	Low	9.9	0.4709
				Ave	13.2	0.6455
				High	16.4	0.8148
3-316	14.0	38.3	0.37	Low	14.5	0.7050
				Ave	17.4	0.8564
				High	20.6	1.0235

Table 4.4: Normalized Measured Effective Width Values for Multi Truck Passes

Bridge	Span Length (ft)	Width (ft)	L/W	Measured EW (ft)		$\frac{12E_f - 84}{1.44W}$
				Low	High	
2-101B	19.5	28.5	0.68	Low	10.6	1.0526
				Ave	-	
				High	-	
1-352W	8.0	47	0.17	Low	10.5	0.6206
				Ave	11.6	0.8156
				High	12.4	0.9574
1-384	12.0	26	0.46	Low	11.1	1.3141
				Ave	11.3	1.3782
				High	11.5	1.4423
3-318	8.0	37.8	0.21	Low	9.0	0.4409
				Ave	10.1	0.6834
				High	11.2	0.9259
3-316	14.0	38.3	0.37	Low	11.7	1.0226
				Ave	12.0	1.0879
				High	12.1	1.1097

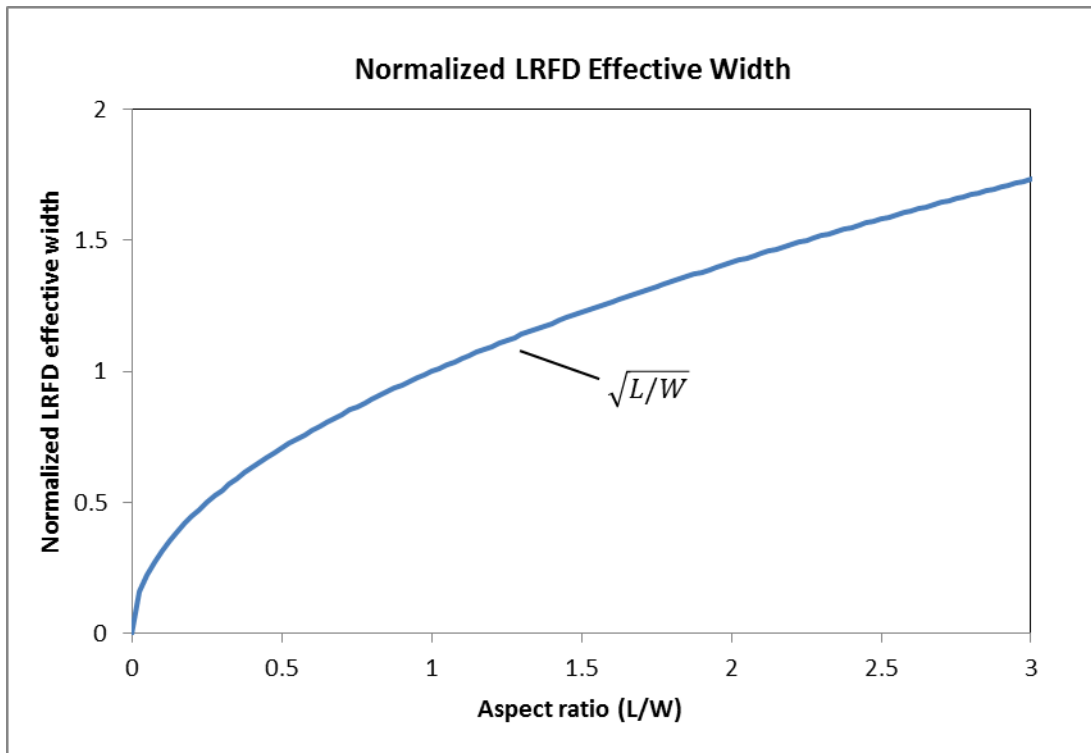


Figure 4.4: Normalized LRFD: Equations (4.5) and (4.7)

The right hand side of equation (4.5) and (4.7) is plotted in Figure 4.4. Plotted in Figure 4.5 is the right hand side of equation (4.5) and the normalized measured low effective widths for single truck passes (the last column on the right in Table 4.3). Figure 4.6 shows the same results for multi truck loading. These figures show, in another format, how the AASHTO equations provide conservative estimates of the effective width. In the following sections, new equations are derived based on the measured low and measured average effective widths of the six bridges tested, that are accurate but not as conservative as the AASHTO equations.

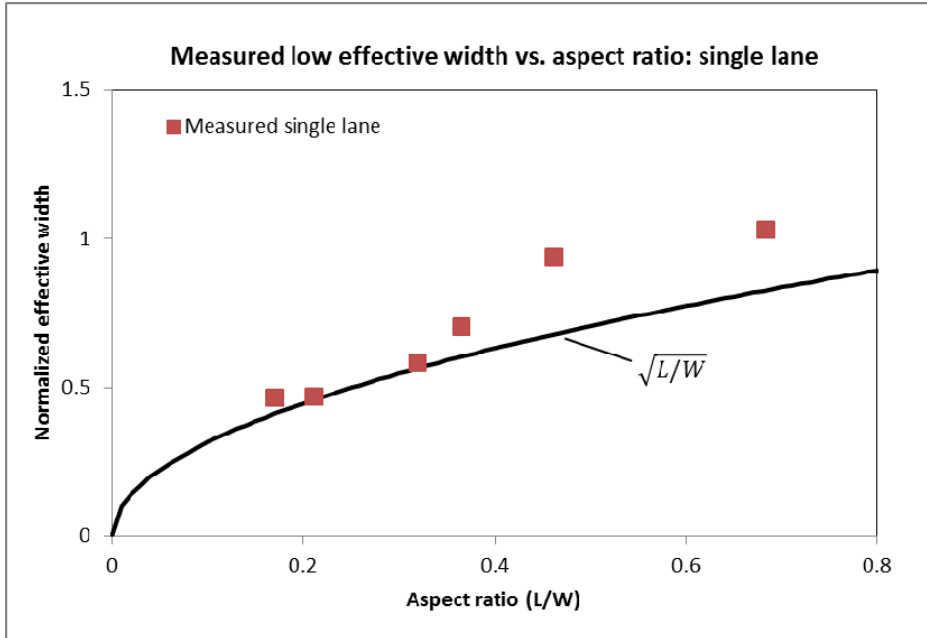


Figure 4.5: Measured (low) Effective Widths for Single Lane Truck Passes in comparison to normalized LRFD code values

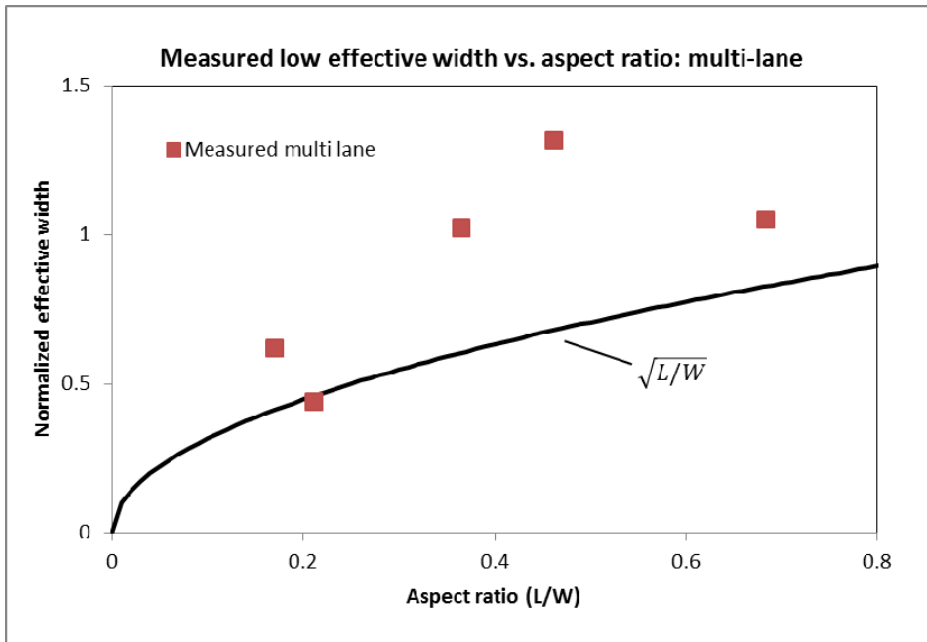


Figure 4.6: Measured (low) Effective Widths for Multilane Truck Passes in comparison to normalized LRFD code values

4.2.2 New Equation based on Low Measured Values

Two different power curves were fit to the measured low values of effective width using the data presented in Table 4.3. The low values were selected because they are the most conservative of the test results, i.e., will yield the lowest effective width. Noting that the normalized AASHTO code equations (4.5) and (4.7) are of the form $y = ax^b$, this was selected as the base form for both of the new equations. Values of a and b were first obtained using Microsoft Excel's power curve "trendline" function, which uses a least squares approach to determine the optimal values for the coefficients a and b . In this equation x corresponds to the aspect ratio of the bridge and y corresponds to the normalized effective width of the low measured value (the last column on the right in Table 4.3)

For the second curve fit the exponent b was set equal to 0.5, which makes it consistent in form with the LRFD equation shown in equation (4.1). Therefore, the equation would take the form $y = ax^{0.5}$. To determine the value of a , the method of linear least squares was used. The following calculation was then used to determine the value of a (McClave, 2008):

$$y = ax^{0.5} \quad (4.8)$$

$$\ln(y) = \ln(ax^{0.5}) = \ln(a) + 0.5 \ln(x) \quad (4.9)$$

Therefore,

$$\ln(a) = \ln(y) - 0.5 \ln(x) \quad (4.10)$$

Using the linear least squares approach to solve for $\ln(a)$ yields:

$$\ln(a) = \frac{1}{n} \sum_{i=1}^n [\ln(y_i) - 0.5 \ln(x_i)] = \bar{y} - 0.5 \bar{x} \quad (4.11)$$

We then obtain the value for a for the single pass data and the multiple pass data. To obtain the R^2 value, the following formula was used (McClave, 2008).

$$R^2 = \frac{\delta_{xy}^2}{\delta_{xx}\delta_{yy}} \quad (4.12)$$

The results of the curve fits for single and multilane truck passes along with the resulting equations are presented in Table 4.5. Their R^2 (coefficient of determination) values are listed.

Table 4.5: Fitted Equations Based on Measured Low Effective Width

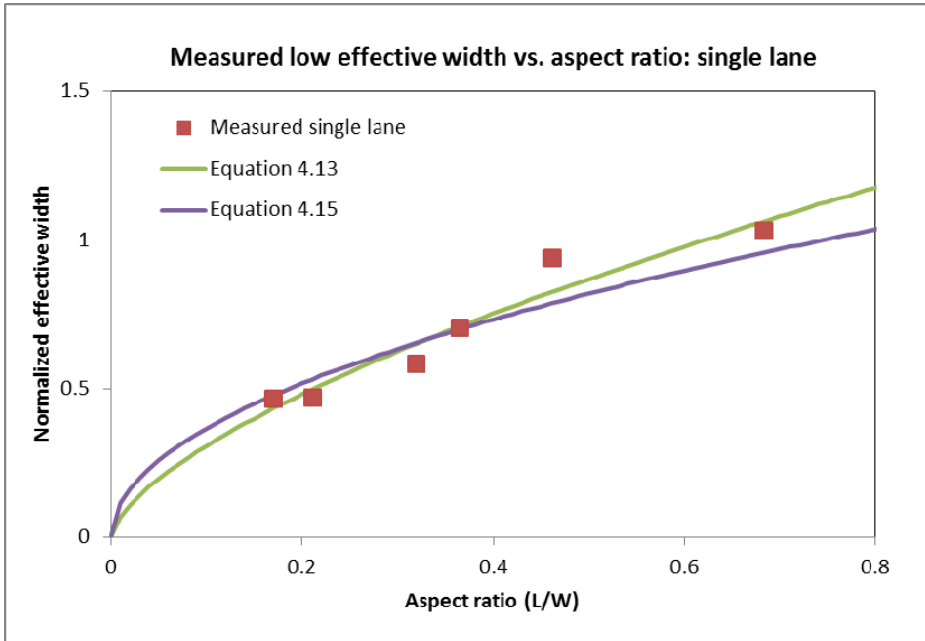
Case	a	b	R^2	Equation	Equation No.
Single truck S1	1.3578	0.6438	0.9295	$y = 1.3578x^{0.6438}$	(4.13)
Multi-truck M1	1.6643	0.6378	0.5722	$y = 1.6643x^{0.6378}$	(4.14)
Single truck S2	1.1583	0.5	0.8263	$y = 1.1583x^{0.5}$	(4.15)
Multi-truck M2	1.4309	0.5	0.5837	$y = 1.4309x^{0.5}$	(4.16)

Presented in Figure 4.7(a) are the measured results and curve fits for the single lane loaded, i.e., equations (4.13) and (4.15) from Table 4.5; presented in Figure 4.7(b) are the measured results and curve fits for the multi-lane lane loaded, i.e., equations (4.14) and (4.16) from Table 4.5.

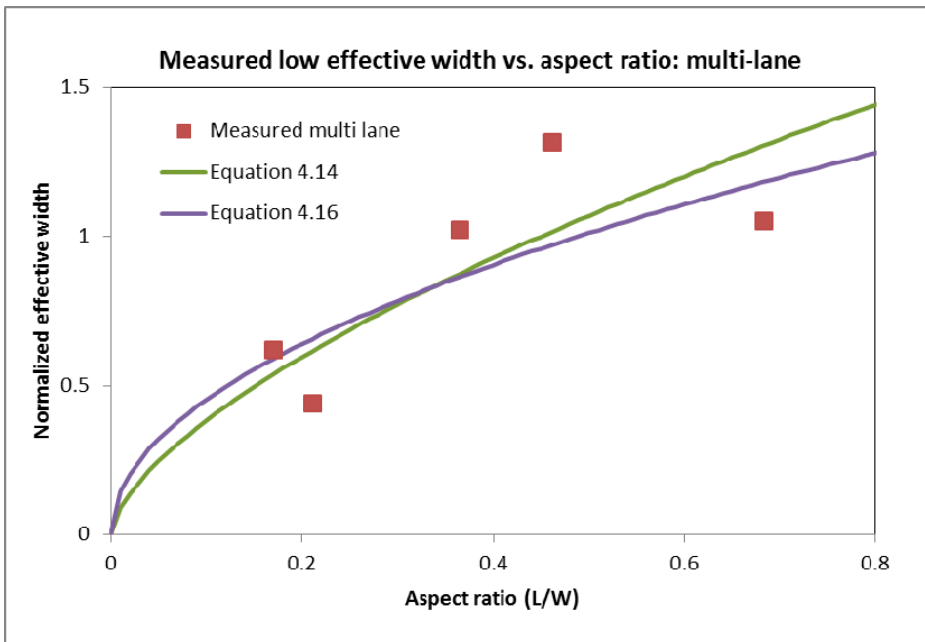
One will note that the resulting two equations for the single truck passes are very similar, both in terms of the final equations and the goodness of the fit, as noted by the R^2 value. Equation (4.13) is a slightly better fit than equation (4.15), but only marginally so. The same can be said for the two equations for the multi truck passes. Equation (4.14) fits the data better than equation (4.16), but only marginally so.

Since there is only a slight difference between the equations, it is recommended that equations (4.15) and (4.16) be adopted, since they are closer in form to the existing AASHTO LRFD equations, and would only involve a change in

one coefficient. Presented in Figures 4.8 and 4.9 are the proposed new equations for single lane loaded and multi lane loaded, respectively. Shown in the figure are the measured results and the current LRFD equation.



(a.) Single truck passes



(b.) Multi-truck passes

Figure 4.7 Normalized effective width versus aspect ratio

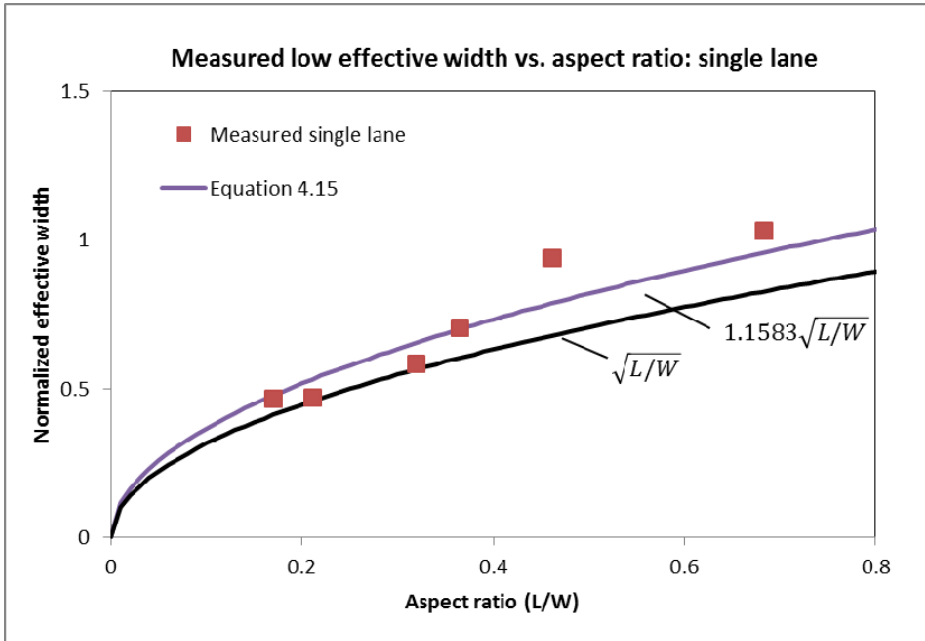


Figure 4.8: Proposed New Effective Width Equation vs. AASHTO LRFD equation (Single)

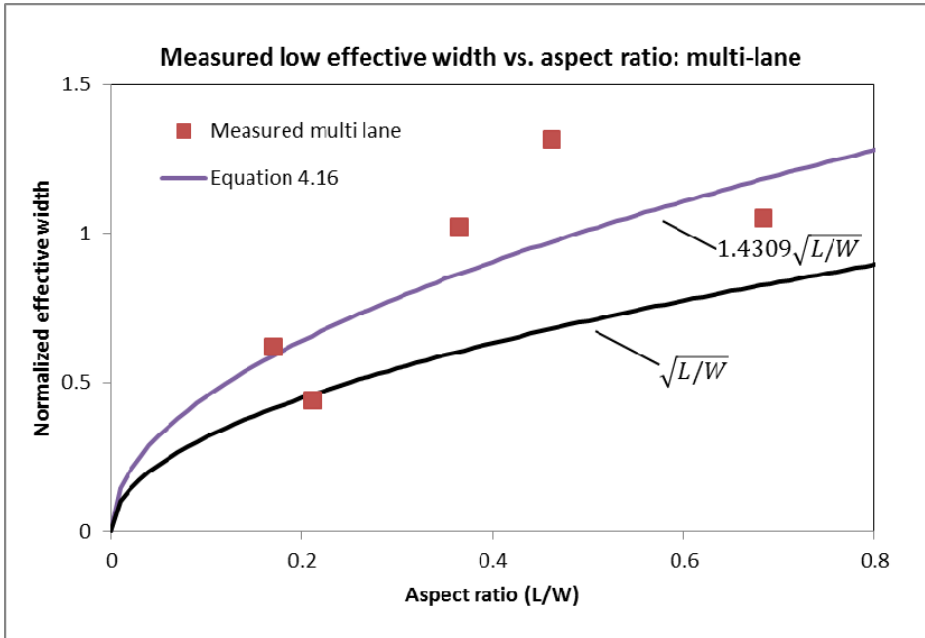


Figure 4.9: Proposed New Effective Width Equation vs. AASHTO LRFD equation (Multi)

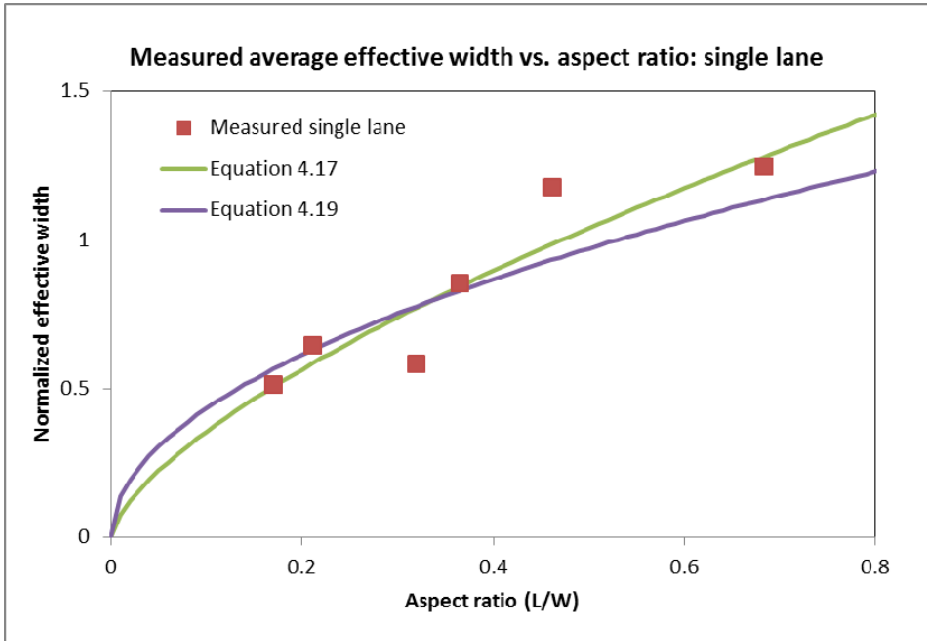
4.2.3 New Equation Based on Average Measured Values

In this section new equations are derived based on the average effective widths determined from the tests. For single passes, bridge 1-442 has no average value; therefore, the low conservative estimation was used instead. For multiple passes, bridge 2-101 has no average value; therefore, the low conservative value was used instead. Once again, two separate power curves were fit to the data using the same approach as for the low measured values. The resulting equations and the values for a and b are listed in Table 4.6.

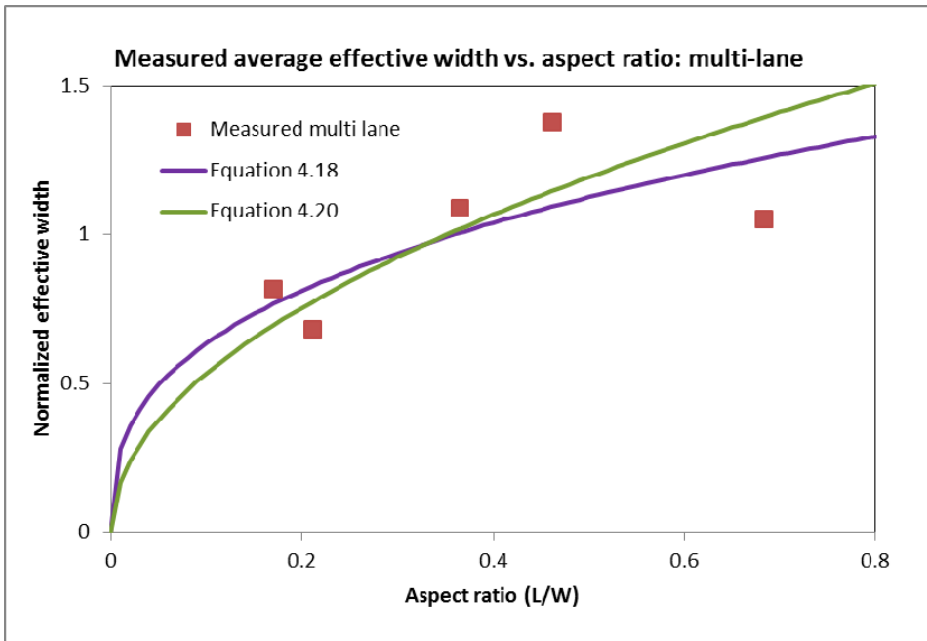
Table 4.6: Fitted Equations Based on Average Effective Width

Case	a	b	R ²	Equation	Equation No.
Single truck S1	1.6488	0.6652	0.8449	$y = 1.6488x^{0.6652}$	(4.17)
Multi-truck M1	1.4397	0.3558	0.4658	$y = 1.4397x^{0.3558}$	(4.18)
Single truck S2	1.3738	0.5	0.7711	$y = 1.3738x^{0.5}$	(4.19)
Multi-truck M2	1.6863	0.5	0.3077	$y = 1.6863x^{0.5}$	(4.20)

Once again, the equations for a single pass are very similar: presented in Figure 4.10(a) are the two equations and the measured data. Presented in Figure 4.10(b) are the results for multi lane loaded. Once again, since there is only minor differences between the equations with the fitted exponent and the equation with the exponent set to equal 0.5, the later is the recommended set. Presented in Figure 4.11 and 4.12 are the final equations for the single lane loaded and the multi lane loaded.



(a.) Single truck passes



(b.) Multi truck passes

Figure 4.10: Comparing the two derived equations for Average Multi-lane Effective Width

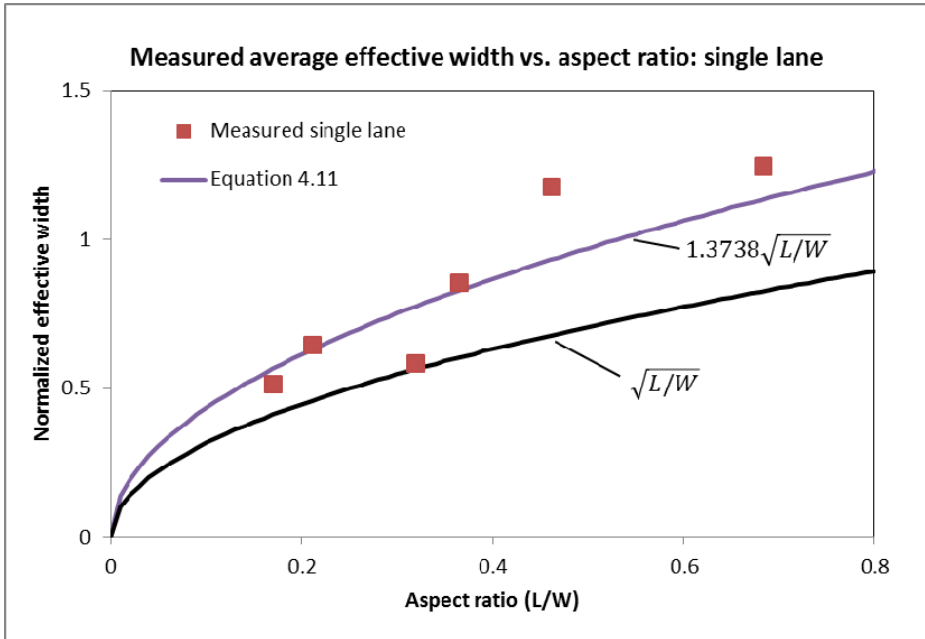


Figure 4.11: Proposed New Effective Width Equation vs. LRFD equation (Single)

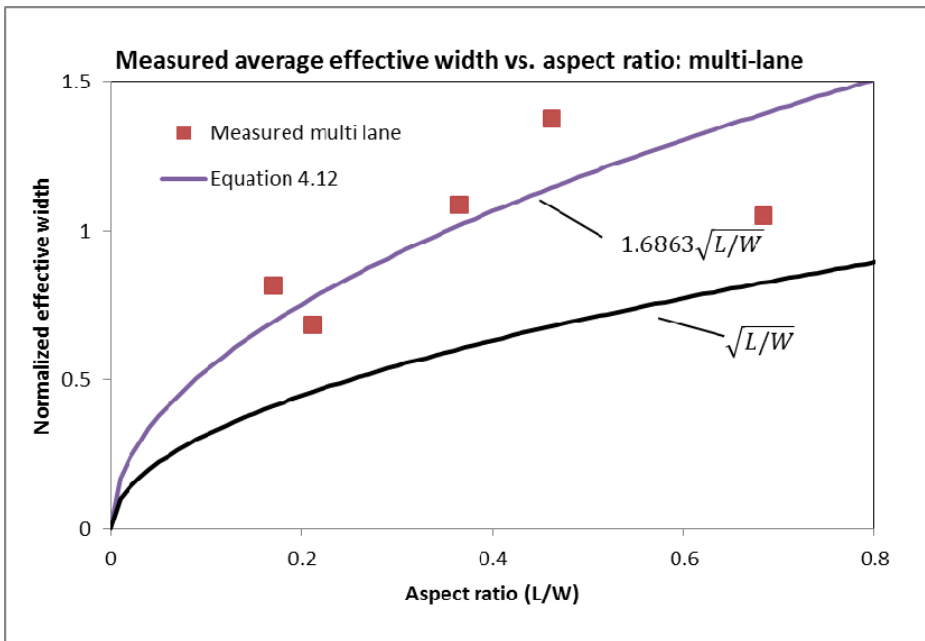


Figure 4.12: Proposed New Effective Width Equations vs. LRFD equation (Multi)

4.3 Recommendations

Based on the data that has been presented, the equations derived using $b = 0.5$ are recommended. The data is accurate and can be easily compared to LRFD code standards. The recommended equations for single pass are Equations (4.15) and (4.19). Equation (4.15) is derived from the lowest measured effective width value. Equation (4.19) is derived from the average measured effective width value. Figure 4.13 shows them both as compared to the current LRFD standard. Also presented in the figure are the measured average effective widths. It can be seen that the new equation based on the low values is still conservative with respect to all of the measured average values, except for one.

The recommended equations for multi lane loaded are (4.16) and (4.20). Equation (4.16) is derived from the lowest measured effective width. Equation (4.20) is derived from the average measured effective width. Figure 4.14 shows the two curves. Again, also presented in the figure are the measured average effective widths. The new equation for the low values is still conservative with respect to all of the measured average values, except for one.

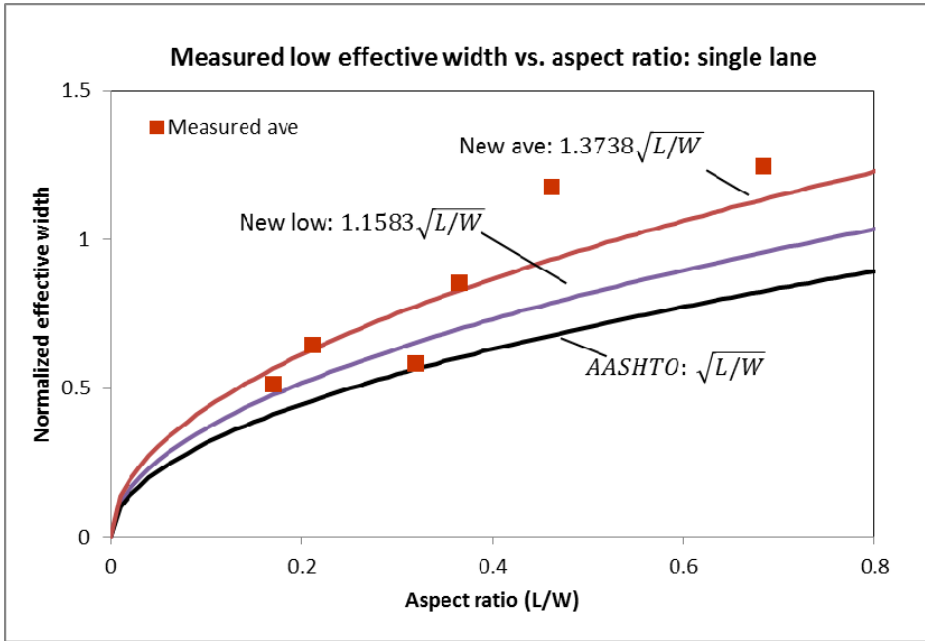


Figure 4.13: Proposed new equations for effective width, single truck pass

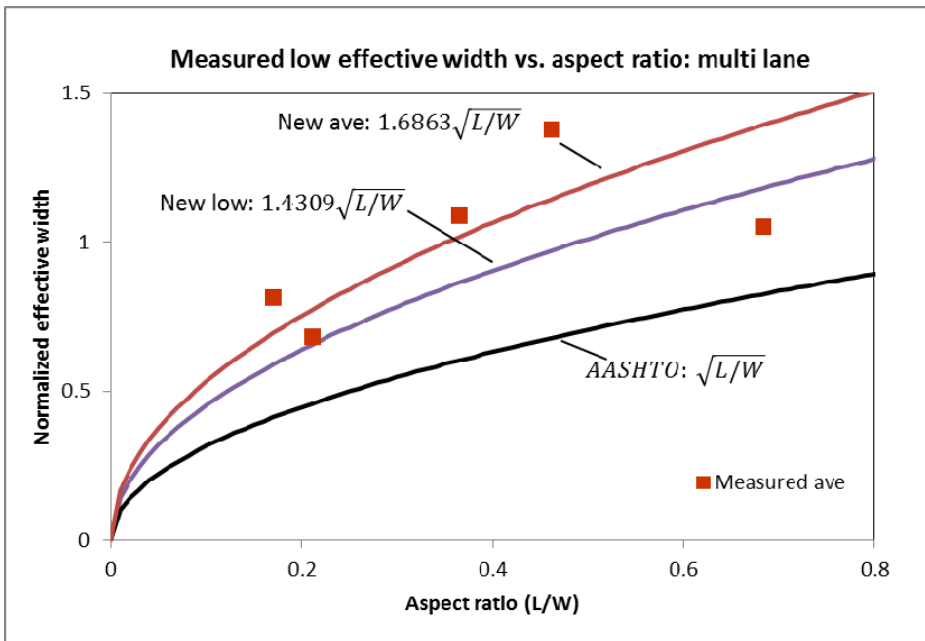


Figure 4.14: Proposed new equation for effective width, multi-truck pass

Finally, we can convert the new equations back into their original form to be consistent with the current LRFD equation. For single lane loading, we recommend equation (4.15); therefore, working backwards from equation (4.5) using the new normalized equation, the final equation becomes

$$\frac{12E_f - 12}{6W_1} = 1.1583 \sqrt{\frac{L_1}{W_1}} \quad (4.21)$$

$$12E_f - 12 = 6 * 1.1583 W_1 \sqrt{\frac{L_1}{W_1}} \quad (4.22)$$

$$12E_f = 12 + 6.95 \sqrt{L_1 W_1} \quad (4.23)$$

Converting back to inches

$$E = 12 + 6.95 \sqrt{L_1 W_1} \quad (4.24)$$

Finally, dividing by 1.2 to account for multiple presences, yields the final new equation

$$E = 10 + 5.8 \sqrt{L_1 W_1} \quad (4.25)$$

Similarly for multi-lane loaded we recommend using equation (4.16), working backwards from equation (4.7), using the new fitted equation

$$\frac{12E_f - 84}{1.44W_1} = 1.4309 \sqrt{\frac{L_1}{W_1}} \quad (4.26)$$

$$12E_f - 84 = 1.44 * 1.4309 W_1 \sqrt{\frac{L_1}{W_1}} \quad (4.27)$$

$$12E_f = 84 + 2.06 \sqrt{L_1 W_1} \quad (4.28)$$

Converting back to inches yields the final new equation

$$E = 84 + 2.06\sqrt{L_1W_1} < \frac{12.0W}{N_L} \quad (4.29)$$

Chapter 5

CONCLUSIONS

The field tests conducted were beneficial to understanding the behavior of the concrete slab bridges. The measured effective widths were all greater than the widths given by the AASHTO Standard Specification and the AASHTO LRFD specification. Based on the test results modified equations for the effective width of concrete slab bridges have been developed by fitting power curves, of a form similar to the code equations, to the experimental results.

For single lane loading, the new recommended formula for effective width of Delaware's slab bridges is

$$E = 10 + 5.8\sqrt{L_1W_1} \quad (5.1)$$

For multi lane loading, the new recommended formula for effective width of Delaware's slab bridges is

$$E = 84 + 2.06\sqrt{L_1W_1} < \frac{12.0W}{N_L} \quad (5.2)$$

Both of these equations have been derived based on the measured low effective widths obtained from the tests. Equations have also been derived that are based on the measured average effective widths that are somewhat less conservative than those presented above, but predict results that fall within the average of that measured in the field.

The study and results presented are based on field tests of six typical slab bridges in Delaware. The six bridges were selected as being typical based on their span length, width, aspect ratio, and slab thickness: spans ranged from a low of 8 ft to a high of almost 20 ft, widths from 26 to 47 ft, aspect ratios from 0.17 to 0.68, and slab thicknesses from 10 to 18 in. Caution should be used when applying the new equations to bridges that fall outside of these ranges, as any such bridge would be outside of the range of bridges that were tested and used to develop the new equations.

REFERENCES

- Amer, A., Arockiasamy, M., Shahawy, M., (1999). "Load Distribution of Existing Solid Slab Bridges Based on Field Tests", *Journal of Bridge Engineering*, ASCE, Volume 4, Number 3, P. 189-193
- American Association of State and Highway Transportation Officials, *AASHTO LRFD Bridge design specifications* (1994). 1st Ed., Washington, D.C.
- American Association of State Highway and Transportation Officials (1996). *AASHTO standard specifications for highway bridges*. 16th Ed., Washington, D.C.
- Barbaccia, T, (2010). "The State of Your Bridges", *Better Roads Magazine*, November 2010, P. 18 to 29
- Chiewanichakorn, M, Aref, A.J., Chen, S.S., and Ahn, I-S, (2004). "Effective Flange Width Definition for Steel-Concrete Composite Bridge Girder", *Journal of Structural Engineering*, ASCE, Volume 130, Number 12, P. 2016-2031.
- Mabsout, M., Jabakhanji, R., Tarhini, K., Awwad, E. (2004). "Wheel Load Distribution in Simply Supported Concrete Slab Bridges", *Journal of Bridge Engineering*, ASCE, Volume 9, Number 2, P. 147 to 155
- J.T. McClave, P.G. Benson, and T. Sincich, *Statistics for Business and Economics*, Pearson Prentice Hall, New Jersey, 2008
- Zokaie, T., Imbsen, R.A., and Osterkamp, T.A. (1991). "Distribution of wheel loads on highway bridges", *Transp. Res. Rec. 1290*, Vol. 1, Bridges and Structures, Transportation Research Board, Washington, D.C., 1191.
- Zokaie, T., Mish, K.D., and Imbsen, R.A. (1995). "Distribution of wheel loads on highway bridges, phase 3", NCHRP 12-26/2 Final Rep., National Cooperative Highway Research Program, Washington, D.C.

Appendix A

BRIDGE TEST REPORT 1-442

FIELD TEST OF BRIDGE 1-442

by

Michael Chajes and Tripp Shenton



Test Date:

November 13, 2006

Project:

Bridge 1-442 on Money Road over Tributary to Noxontown Pond
New Castle County, Delaware

Client:

Delaware Department of Transportation
P.O. Box 778
Dover, DE 19903

Executive Summary

The University of Delaware conducted a load test of Bridge 1-442 on Money Road over a tributary to Noxontown Pond on November 13, 2006 to evaluate its transverse load distribution. The slab bridge was originally constructed in 1923, and then widened in 1964. The slab was instrumented with fourteen strain transducers placed on the underside of the concrete slab (six on the old section of the slab, and 8 on the newer slab section). A fully loaded 6-wheel dump truck was used as a controlled live load for the test. The total weight of the loaded truck was 41.66 kips, with a combined rear axle weight of 30.49 kips. The test utilized two load cases in which the truck backed across the bridge, and then was brought to a stop with the rear axles centered over the midspan of the bridge. The maximum recorded concrete tensile strain at any time during the test was 22.8 $\mu\epsilon$ on the newer slab, and 14.5 $\mu\epsilon$ on the older slab. Based on evaluation of the observed transverse load distribution for both the new and old slab, a conservative estimate for the effective slab width of 6.5 feet for the older slab and 7.0 feet for the newer slab is recommended. Both of these are greater than the recommended AASHTO value of 4.6 feet.

Description of the Bridge

Bridge 1-442 is located on Money Road in New Castle, County (northeast of Townsend). It is a concrete slab bridge with a 12 foot clear span, 13.08 foot effective span, that crosses a tributary to the Noxontown Pond. It was originally constructed in 1923, and was widened in 1964 to its current out-to-out width of 41 feet. A picture of the bridge as well as the original name plate is shown in Figures 1 and 2.

The bridge carries local traffic and has a current ADT of 692 vehicles. The bridge was last inspected on May 31, 2006. The bridge is in relatively good condition, with no major signs of distress.

Test Purpose

The load test was performed at the request of DelDOT's Bridge Management section in order to assess the transverse load distribution of the slab. Based on the current AASHTO formula for effective slab width, $b_{eff} = 4 + (.06)S$, the effective slab width is 4.78 feet. The reinforcement details at the ends of the slab do not appear to be sufficient to transfer negative bending into the abutment walls. As such, the bridge must be rated as a slab as opposed to a rigid frame. DelDOT has found that the bridge is not predicted to be able to carry legal loads when an effective slab width of 4.78 feet, combined with the assumption that the bridge acts as a simply supported slab, are assumed. Since the bridge is over 90 years old, has never had any load postings, is on a rural road, and remains in good condition, the need for posting the bridge was questioned. It was determined that a load test would allow a more accurate assessment of the bridge's transverse load

distribution characteristics. The remainder of this report discussed how the bridge was tested and how the effective slab width was computed using load test data.

Test Setup

The bridge load test was conducted on November 13, 2006 using the Bridge Diagnostics Inc, Structural Testing System (STS) and a fully loaded 6-wheel dump truck. Fourteen strain transducers with 12 inch extensions were mounted to the underside of the concrete slab. All transducers were mounted at the midspan of the 12 foot clear span. The transducers were mounted with a transverse spacing of 2 feet per transducer. Figures 3 and 4 show transducers mounted to the slab. Two transducers were mounted adjacent to each other (8 inches apart) at the location where the old and new slab joined together (see Figure 5). Moving outward from that location, there were six transducers on the old section, and 8 transducers on the new section. Figure 6 shows the transducer layout with the associated three-digit transducer identification number. All of the strain transducers were connected to the STS data acquisition system and were read simultaneously, at an appropriate sampling rate during the test.

A fully loaded 6-wheel dump truck was used as a controlled live load for the test. The truck axles were weighed at the site using Intercomp portable truck scales which are accurate to within +/- 10 lbs. The gross weight of the loaded truck was 41.66 kips, with a combined rear axle weight of 30.49 kips. The spacing between the front and rear axle is 13' 8". As a result, when the rear axle was at midspan, the front axle was off of the bridge. Figure 7 shows the measured wheel spacings and wheel loads.

Two load passes were used to collect data. Each pass consisted of backing the rear axle of the truck across the bridge, and then pulling it forward and stopping it when the rear axle was over the midspan (i.e. 6 feet from either abutment). In Pass 1, the truck was positioned transversely so that it would be on the new section with the driver side wheels close to the joint between the old and new slab. This pass was used to see how loads distributed transversely in the old slab. In Pass 2, the truck was positioned transversely so that it would be on the old section with the passenger side wheels close to the joint between the old and new slab. This pass was used to see how loads distributed transversely in the new slab. The locations of the two passes are shown in Figure 8 and summarized below.

Pass 1: truck on new section of slab, loads distribute to old slab.

Pass 2: truck on old section of slab, loads distribute to new slab.

Results

Peak Strains and Transverse Strain Distribution

The maximum recorded concrete tensile stain at any time during the test was 22.8 $\mu\epsilon$ on the newer slab, and 14.5 $\mu\epsilon$ on the older slab. When the trucks were in a stationary position with the rear axle at midspan and straddling either the newer or older slab, the maximum recorded concrete tensile stain was 15.3 $\mu\epsilon$ on the new slab, and 14.5 $\mu\epsilon$ on the old slab. The recorded strains at this time for both the truck on the newer section of slab and for the truck on the older section of slab are given in Table 1. Plots of these strains to show the transverse distribution are shown in Figures 9 and 10.

Computation of Effective Slab Width (b_{eff})

Figure 11 shows an idealized transverse strain distribution that might result if a rear axle were sitting on an infinitely wide slab. The strain would have a relatively constant peak value (strain max.) between the truck wheels, and would decrease to zero as one moves away from the wheels. This non-uniform strain (or stress) is a result of shear-lag. In order to simplify the evaluation of slabs that exhibit shear lag, a concept of effective width has been developed. The effective width section has a constant strain (or stress) across its width. The widely accepted definition of the effective width (b_{eff}) is the width that would have a uniform strain equal to the maximum strain but creates the same total effect as that caused by the actual strain distribution (Chiewanichakorn et al., 2004). To turn the plot having a varying strain into one having a uniform strain, one must keep the areas A_1 and A_3 for the two distributions equal (see Figure 11). Since the strain in this case is caused by two wheel lines, the actual effective width used in evaluating a bridge for a single wheel line is one half of the distance $X_1 + 7.0' + X_3$. In other words, for a 7-foot wide test truck, the effective width is given by $b_{eff} = (X_1 \text{ or } X_3) + 3.5'$. Recall that the AASHTO formula is given by $b_{eff} = 4.0' + (0.6)S$. For Bridge 1-442, the AASHTO formula gives $b_{eff} = 4.78'$.

Using the data plotted in Figures 9 and 10, we can compute the area of the tails (A_1 or A_3). The areas used are indicated in the two figures, as well as the location of the truck. Dividing these areas by the maximum strain produced on the equivalent section of slab, we can find values for X_1 or X_3 . The area under the tail for the old section (Figure 9) is 46.0 while the area under the tail for the new section (Figure 10) is 55.4. The maximum strain produced for the truck on the old section is $14.5 \mu\epsilon$ (from Figure 10), while the maximum strain produced for the truck on the old section is $15.3 \mu\epsilon$ (from Figure 9). Using these values, we find that:

$$\begin{aligned} b_{eff \text{ old section}} &= (46.0/14.5) + 3.5' = 6.67 \text{ feet} \\ b_{eff \text{ new section}} &= (55.4/15.3) + 3.5' = 7.12 \text{ feet} \end{aligned}$$

One will notice that the strain is not constant beneath the truck (as it is in the idealized depiction). While it may be acceptable to use the average value from this region as opposed to the peak value, effective width calculations found using the peak value will be conservative.

Since we have only one set of test results, we may want to select conservative values. It is recommended that the following values be used for the final effective widths:

$$\begin{aligned} b_{eff \text{ old section}} &= 6.5 \text{ feet} \\ b_{eff \text{ new section}} &= 7.0 \text{ feet} \end{aligned}$$

These values are greater than the 4.78 feet recommended by the AASHTO code.

Consideration of Multiple Presence in the Effective Slab Width Calculation (b_{eff})

Since the tests were run with only one truck at a time, the above calculated widths do not incorporate the effect of side-by-side trucks. In essence, the above values are the effective width resulting from a single wheel load. If we want to account for side-by-side

trucks in the effective width computation, we should place two trucks on the bridge with their wheels as close together as permitted by the code (this would be 4 feet, 2 feet from the edge of each 12 foot lane). To see what this would do, we can superimpose the results shown in Figures 9 and 10. In doing so, we need to combine them such that the adjacent wheels of the two trucks are 4 feet apart. Figure 12 shows the result of the superposition. In the figure, the two outer areas A1 and A3 are labeled, as well as location of the trucks. The peak value is $19.4 \mu\epsilon$, and the areas A1 and A3 are 68.0 and 75.4 respectively). Using these values, we find that:

$$b_{\text{eff}} = [(68.0/19.4) + (75.4/19.4) + 7' + 4' + 7'] / 4 = 6.35 \text{ feet}$$

This value incorporates both the old and new section. Like the value for a single wheel, it is greater than the 4.78 feet recommended by the AASHTO code.

Since it is possible to have side-by-side trucks, it is recommended that the value for the effective width for bridge 1-442 be taken as:

$$b_{\text{eff}} = \mathbf{6.3 \text{ feet}}$$

In future tests, it is recommended that two trucks be used in order to directly evaluate the effects of multiple presence.

References

Chiewanichakorn, M, Aref, A.J., Chen, S.S., and Ahn, I-S, (2004). *Effective Flange Width Definition for Steel-Concrete Composite Bridge Girder*, Journal of Structural Engineering, ASCE, Volume 130, Number 12, P. 2016-2031.



Figure 1. Bridge 1-442 Looking West



Figure 2. Bridge 1-442 Name Plate from 1923



Figure 3. Strain Transducers Mounted to Bridge 1-442 (New Section)



Figure 4. Strain Transducers Mounted to Bridge 1-442 (Old Section)



Figure 5. Strain Transducers Mounted to Bridge 1-442 on Either Side of New (right) and Old (left) Slab

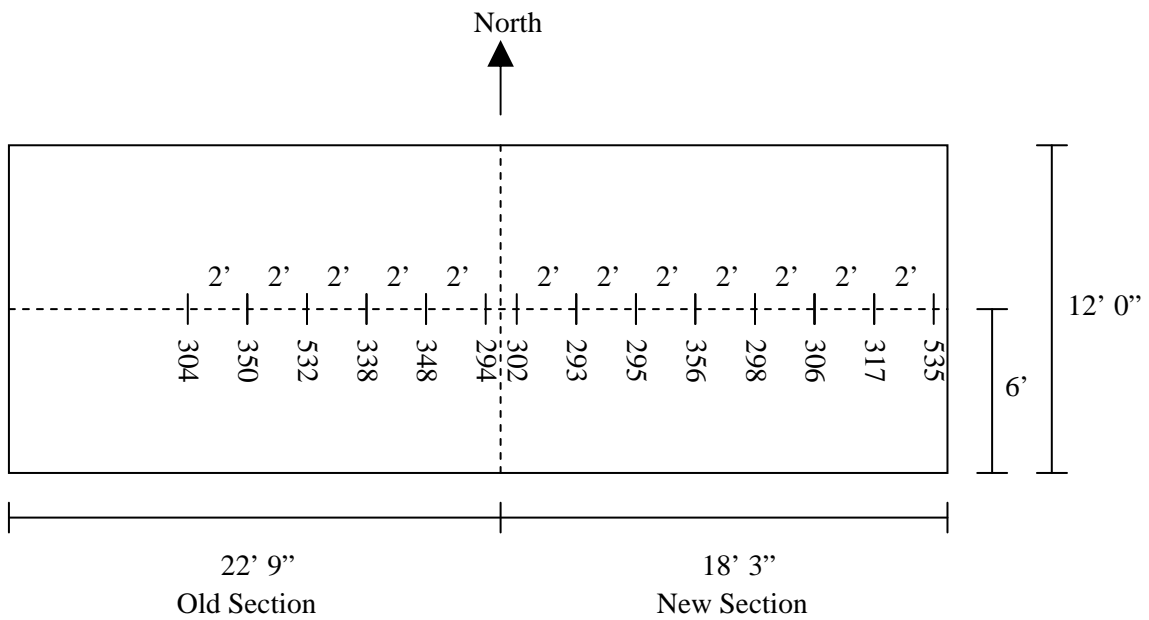


Figure 6. Layout of Transducers on Slab

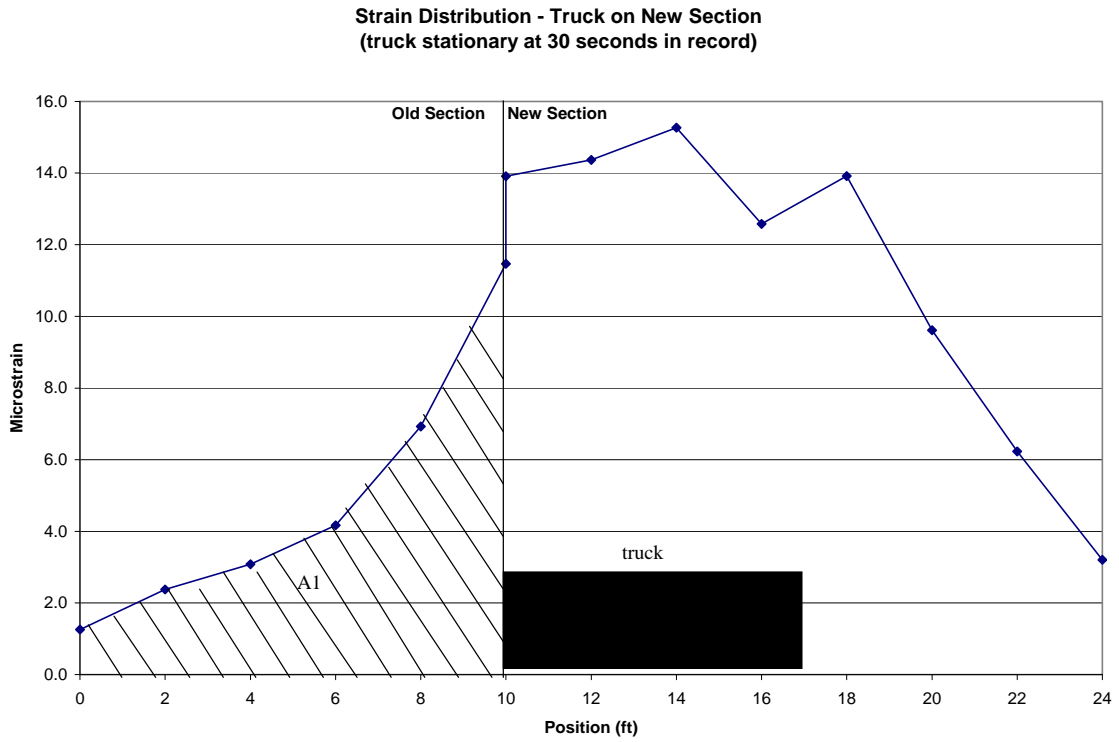


Figure 9. Strain Distribution – Truck on New Section (Pass 1)

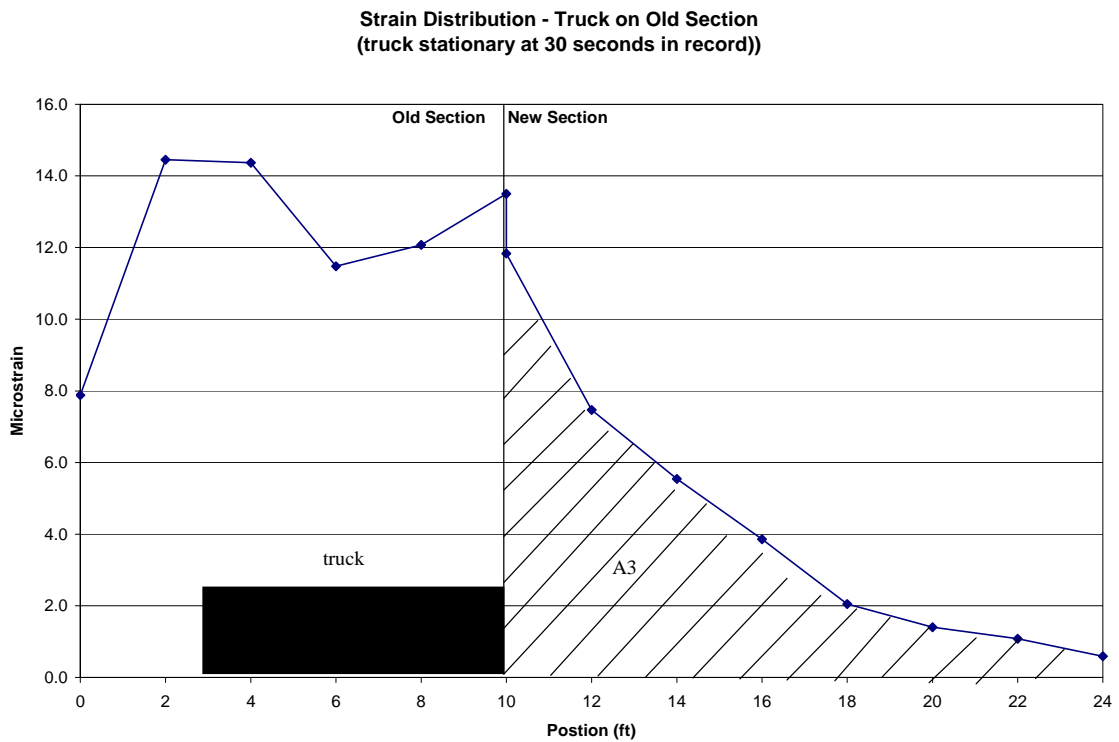


Figure 10. Strain Distribution – Truck on Old Section (Pass 2)

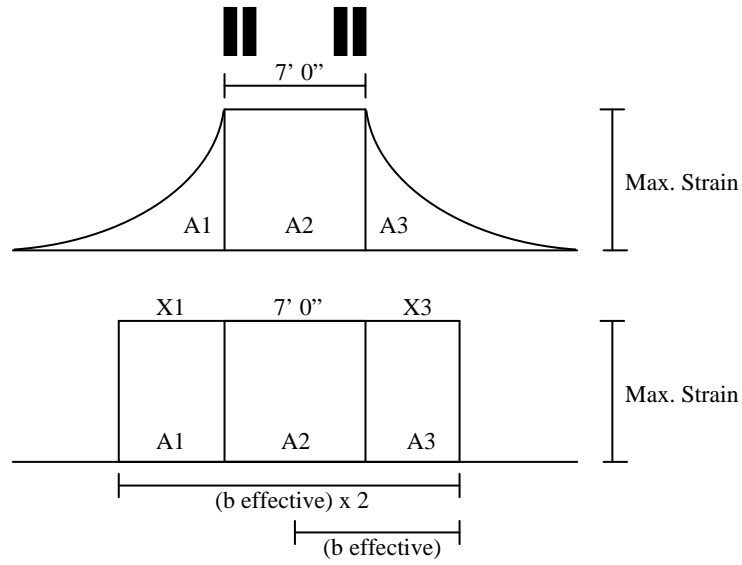


Figure 11. Idealized Strain Distribution and Effective Width Representation

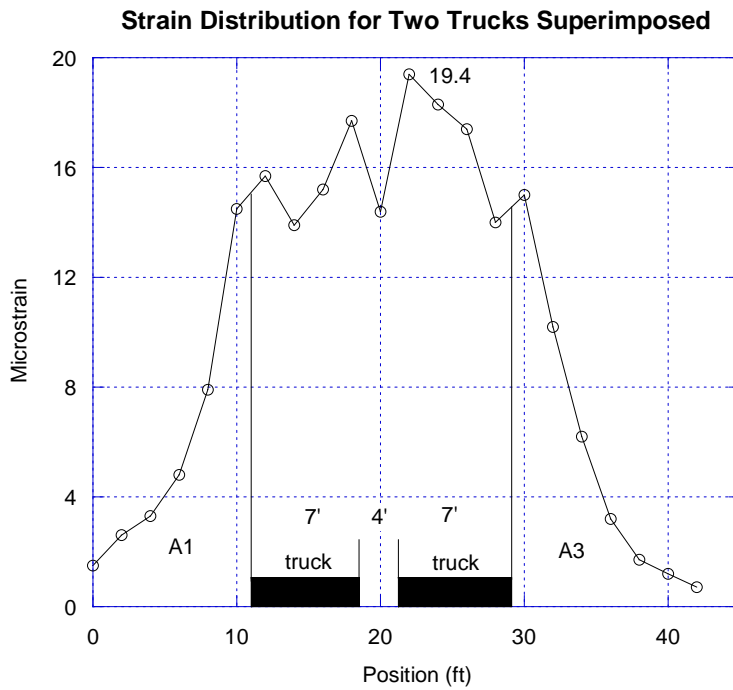


Figure 12. Superimposed Strain Distribution for Two Trucks Side-by-Side

Table 1. Recorded Tensile Strains when Truck was Stationary with Rear Axle at Midspan and over New Section (Pass 1) and Old Section (Pass 2). Note: all values are in microstrain (1×10^{-6} in./in.)

	Transducer #	Pass 1 ($\mu\epsilon$)	Pass 2 ($\mu\epsilon$)
Transverse Across Slab Centerline	304	1.3	7.9
	350	2.4	14.5
	532	3.1	14.4
	338	4.2	11.5
	348	6.9	12.1
	294	11.5	13.5
	302	13.9	11.8
	293	14.4	7.5
	295	15.3	5.5
	356	12.6	3.9
	298	13.9	2.1
	306	9.6	1.4
	317	6.2	1.1
	535	3.2	0.6

Appendix B

BRIDGE TEST REPORT 2-101

FIELD TEST OF BRIDGE 2-101B101

by

Harry W Shenton III, Ph.D.
Professor and Chair
Center for Innovative Bridge Engineering
University of Delaware
Newark, Delaware 19716



Test Date:

August 12, 2008

Project:

Bridge 2-101B101 on Pearsons Corner Road over Fork Branch
Kent County, Delaware

Client:

Delaware Department of Transportation
P.O. Box 778
Dover, DE 19903

Executive Summary

The University of Delaware conducted a load test of Bridge 2-101B101 on Pearsons Corner Road on August 12, 2008, to evaluate its transverse load distribution. The slab bridge was originally constructed in 1931. The slab was instrumented with twelve strain transducers placed on the underside of the concrete slab. Two fully loaded 6-wheel dump trucks were used as a controlled live load for the test. The gross weight of truck #2553 was 38.4 kips, with a combined rear axle weight of 27.8 kips. The gross weight of truck #2547 was 35.2 kips, with a combined rear axle weight of 24.4 kips. The test utilized eight load passes in which the truck moved across the bridge at a slow crawl. For the side-by-side truck pass, the vehicles were brought to a stop with their rear axles centered over the midspan of the bridge. The maximum recorded concrete tensile strain at any time during the test was 14 $\mu\epsilon$. Based on evaluation of the observed transverse load distribution, a conservative estimate for the effective slab width of the bridge is 5.30 ft. This is just slightly greater than that recommended by the AASHTO code, which is 5.17 ft.

Description of the Bridge

Bridge 2-101B101 is located on Pearsons Corner Road in Kent County (southwest of Smyrna) and crosses Fork Branch. It is a concrete slab bridge with an 18 foot clear span and a 19.5 foot effective span. It was originally constructed in 1931. Pictures of the bridge are shown in Figures 1 and 2.

The bridge carries local traffic and has an ADT of 1299 vehicles (as of 2006). The bridge was last inspected on September 4, 2007. The bridge is in relatively good condition, with no major signs of distress.

Test Purpose

The load test was performed at the request of DelDOT's Bridge Management section in order to assess the transverse load distribution of the slab. Based on the current AASHTO formula for effective slab width, $b_{eff} = 4.0 + 0.06S$, the effective slab width is 5.17 feet. The reinforcement details at the ends of the slab do not appear to be sufficient to transfer negative bending into the abutment walls. As such, the bridge must be rated as a slab as opposed to a rigid frame. It was determined that a load test would allow a more accurate assessment of the bridge's transverse load distribution characteristics. The remainder of this report discusses how the bridge was tested and how the effective slab width was computed using load test data.

Test Setup

The bridge load test was conducted on August 12, 2008 using the Bridge Diagnostics Inc, Structural Testing System (STS) and two fully loaded 2-axle, 6-wheel dump trucks. Twelve strain transducers with 12 inch extensions were

mounted to the underside of the concrete slab. All transducers were mounted at the midspan of the 18 foot clear span. The transducers were mounted with a transverse spacing of 2 feet per transducer. Access to the bottom of the slab was from a small boat. Figure 3 shows the crew mounting gages to the bottom of the slab. Figures 4 and 5 show the transducers mounted to the slab. Figure 6 shows the transducer layout with the associated three-digit transducer identification number. All of the strain transducers were connected to the STS data acquisition system and were read simultaneously, at an appropriate sampling rate during the test.

The bridge was originally scheduled for testing in the spring of 2008. At that time, an attempt was made to mount transducers on the bridge using a quick setting adhesive. However, the adhesive did not hold due to excessive moisture on the bottom of the slab: the water level in the creek was at least a foot higher and the ambient temperature was lower when the attempt was made to test the bridge in spring '08. Therefore, in the current setup, the transducers were to be mounted using 1 in. concrete screws. The first three transducers (gages 294, 350, and 293) were mounted using the screws; however, this proved to be very time consuming and difficult. The remaining transducers were therefore bonded to the slab using a quick setting adhesive manufactured by HILTI (HFX#284266 Adhesive mortar, the same one used in the earlier setup). Because of the higher temperature and low moisture on the slab, the gages bonded very well this time.

Two fully loaded 2-axle, 6-wheel dump trucks were used as a controlled live load for the test. The truck axles were weighed at the site using Intercomp portable truck scales which are accurate to within ± 10 lbs. The gross weight of truck #2553 was 38.4 kips, with a rear axle weight of 27.8 kips. The gross weight of truck #2547 was 35.2 kips, with a rear axle weight of 24.4 kips. The spacing between the front and rear axle was 13' 8". As a result, when the rear axle was at midspan, the front axle was off of the bridge. Figures 7 and 8 show the measured wheel spacings and wheel loads of the two vehicles.

Eight truck passes were completed and are listed in Table 1. In all cases the truck or trucks crossed the bridge in a northbound direction. All passes were conducted at a "crawl" speed, i.e., between 5 and 10 mph. The transverse position of the truck on the bridge is defined by "right", "center," and "left" lane, when looking in a northerly direction. Passes 1 through 6 involved only a single truck (#2553): passes 1 and 2 in the right lane, 3 and 4 in the center, and 5 and 6 in the left lane. For pass 7, truck #2553 traveled slowly across the bridge along the centerline until the rear axle was just past mid-span, then backed up and stopped with the rear axle at mid-span. For pass 8, the same procedure was repeated but with truck #2553 in the right lane and truck #2547 in the left lane.

Results

Peak Strains and Transverse Strain Distribution

The strains induced in the slab by the load vehicles were very small: the absolute maximum recorded concrete tensile strain at any time during the test was 14 $\mu\epsilon$. This occurred at gage 344, which was located 3 feet west of the longitudinal centerline, and occurred for pass 8 (both vehicles on the bridge at the same time). The absolute maximum strain recorded for a single truck pass was 9 $\mu\epsilon$ and that also occurred at gage 344, for passes 3 and 4 (truck in the center of the bridge). The absolute maximum recorded strains are listed for all gages in Table 2.

Plots of the transverse distribution of strain for the single truck passes are shown in Figures 9 through 11, and for the side-by-side truck pass in Figure 12. Clearly the strains are largest underneath the vehicle and tend to get smaller as you move away from the vehicle.

The maximum strains in gages 294, 350, and 293 are consistently lower than the other gages, and are lower than one would expect for a theoretical distribution of strain. These were the three gages that were attached to the slab using concrete screws. In the plots they are data points between 9 ft. and 14 ft. These gages read lower than the others that were bonded to the slab. This is most likely due to “play” in between the mounting screw and the mounting bracket, or perhaps micro-cracking caused by the drilling and screwing operations.

Computation of Effective Slab Width (b_{eff})

Figure 13 shows an idealized transverse strain distribution that might result if a rear axle were sitting on an infinitely wide slab. The strain would have a relatively constant peak value (strain max.) between the truck wheels, and would decrease to zero as one moves away from the wheels. This non-uniform strain (or stress) is a result of shear-lag. In order to simplify the evaluation of slabs that exhibit shear lag, the concept of effective width was developed. The effective width section has a constant strain (or stress) across its width. The widely accepted definition of the effective width (b_{eff}) is the width that would have a uniform strain equal to the maximum strain but creates the same total effect as that caused by the actual strain distribution (Chiewanichakorn et al., 2004). To turn the plot having a varying strain into one having a uniform strain, one must keep the areas A_1 and A_3 for the two distributions equal (see Figure 13). Since the strain in this case is caused by two wheel lines, the actual effective width used in evaluating a bridge for a single wheel line is one half of the distance $X_1 + 7.0' + X_3$. In other words, for a 7-foot wide test truck, the effective width is given by $b_{eff} = (X_1 \text{ or } X_3) + 3.5'$. Recall that the AASHTO formula is given by $b_{eff} = 4.0' + (0.06)S$. For Bridge 2-101B101, the AASHTO formula gives $b_{eff} = 5.17'$.

Using the data plotted in Figure 10 (vehicle in the center of the bridge), we can compute the area of the tails (A_1 and A_3). Because of the problem with mounting alluded to earlier with gages 294, 350, and 293, the strain at these gage locations have been taken to be equal to those of the gages symmetrically located about the centerline, i.e., gages 535, 344, and 355.

The areas used are indicated in the figure, as well as the location of the truck. Note that we do not know what the strain is at the edge of the bridge, but assume it is zero (a conservative assumption for calculating the effective width). Dividing these areas by the maximum strain produced on the equivalent section of slab, we can find the effective width. Area $A_1 = 40.0$, which yields an effective width of

$$b_{eff} = (40.0 / 9.2) + 3.5' = 7.85'$$

Area $A_3 = 46.2$, which yields an effective width of

$$b_{eff} = (46.2 / 9.2) + 3.5' = 8.52'$$

Taking the more conservative of the two, the effective width for the single truck is 7.85 ft. This value is greater than the 5.17 feet recommended by the AASHTO code.

One will notice that the strain is not constant beneath the truck (as it is in the idealized depiction). While it may be acceptable to use the average value from this region as opposed to the peak value, effective width calculations found using the peak value will be conservative.

Consideration of Multiple Presence in the Effective Slab Width Calculation (b_{eff})

The above calculated widths do not incorporate the effect of side-by-side trucks. In essence, the above values are the effective width resulting from a single wheel load. If we want to account for side-by-side trucks in the effective width computation, we should place two trucks on the bridge with their wheels as close together as permitted by the code (this would be 4 feet, 2 feet from the edge of each 12 foot lane). These correspond to the results for pass 8 (Figure 12). Here again, the strain for gages 294, 350, and 293 have been taken to be equal to those of the gages symmetrically located about the centerline, i.e., gages 535, 344, and 355 (although in this case it has no bearing on the effective width calculation).

The transverse distribution of strain for the side-by-side truck pass is shown in Figure 14 again, with the tail areas A_1 and A_3 indicated. The peak strain is 13.2 me. The areas are $A_1 = 17.0$ and $A_3 = 25.5$. Using these values, we find that:

$$b_{eff} = (17.0 / 13.2) + (25.5 / 13.2) + 7' + 7' + 4' / 4 = 5.30'$$

This is just slightly greater than the value given by the code.

Since it is possible to have side-by-side trucks, it is recommended that the value for the effective width for bridge 2-101B101 be taken as:

$$b_{eff} = 5.30'$$

References

Chiewanichakorn, M, Aref, A.J., Chen, S.S., and Ahn, I-S, (2004). *Effective Flange Width Definition for Steel-Concrete Composite Bridge Girder*, Journal of Structural Engineering, ASCE, Volume 130, Number 12, P. 2016-2031.

Table 1. Truck passes

Pass #	Description (All trucks traveling northbound)
1	Truck #2553 in Right Lane
2	Truck #2553 in Right Lane
3	Truck #2553 in Center
4	Truck #2553 in Center
5	Truck #2553 in Left Lane
6	Truck #2553 in Left Lane
7	Truck #2553 in Center, Traveled slow past midspan and backed up so rear axle was over midspan
8	2 Trucks (Truck #2553 in right lane, truck #2547 in left lane), Traveled slow past midspan and backed up so rear axle was over midspan

Table 2. Absolute maximum recorded strain

Pass #	Absolute max microstrain measured for given gage ID													
	350	294	535	344	298	338	318	355	293	317	356	337		
1	4	5	6	5	3	1	2	4	2	9	4	6		
2	4	5	7	6	3	2	2	4	2	9	4	6		
3	3	5	8	9	6	3	4	8	1	4	2	3		
4	3	5	8	9	6	3	4	8	1	4	2	3		
5	1	2	5	8	8	6	7	8	0	1	1	1		
6	1	2	5	7	8	7	7	8	1	1	1	1		
7	3	5	8	9	6	2	3	8	1	4	2	3		
8	6	7	13	14	11	8	9	11	3	11	5	8		



Figure 1. Bridge 2-101 looking east



Figure 2. Bridge 2-101 looking south



Figure 3. Crew mounting transducers



Figure 4. Strain transducers mounted to Bridge 2-101



Figure 5. Close up of strain transducer with concrete extension, mounted to Bridge 2-101

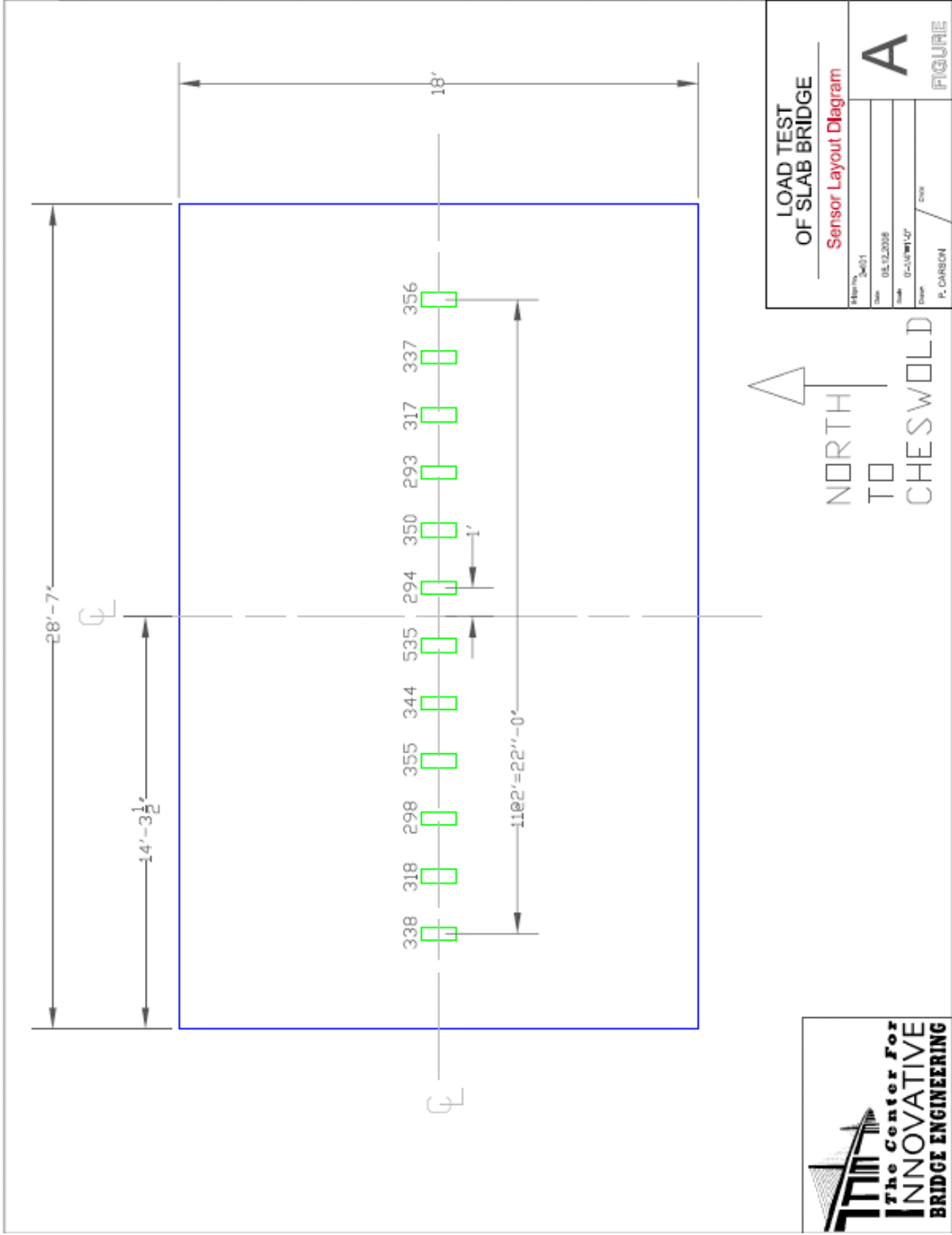


Figure 6. Sensor layout



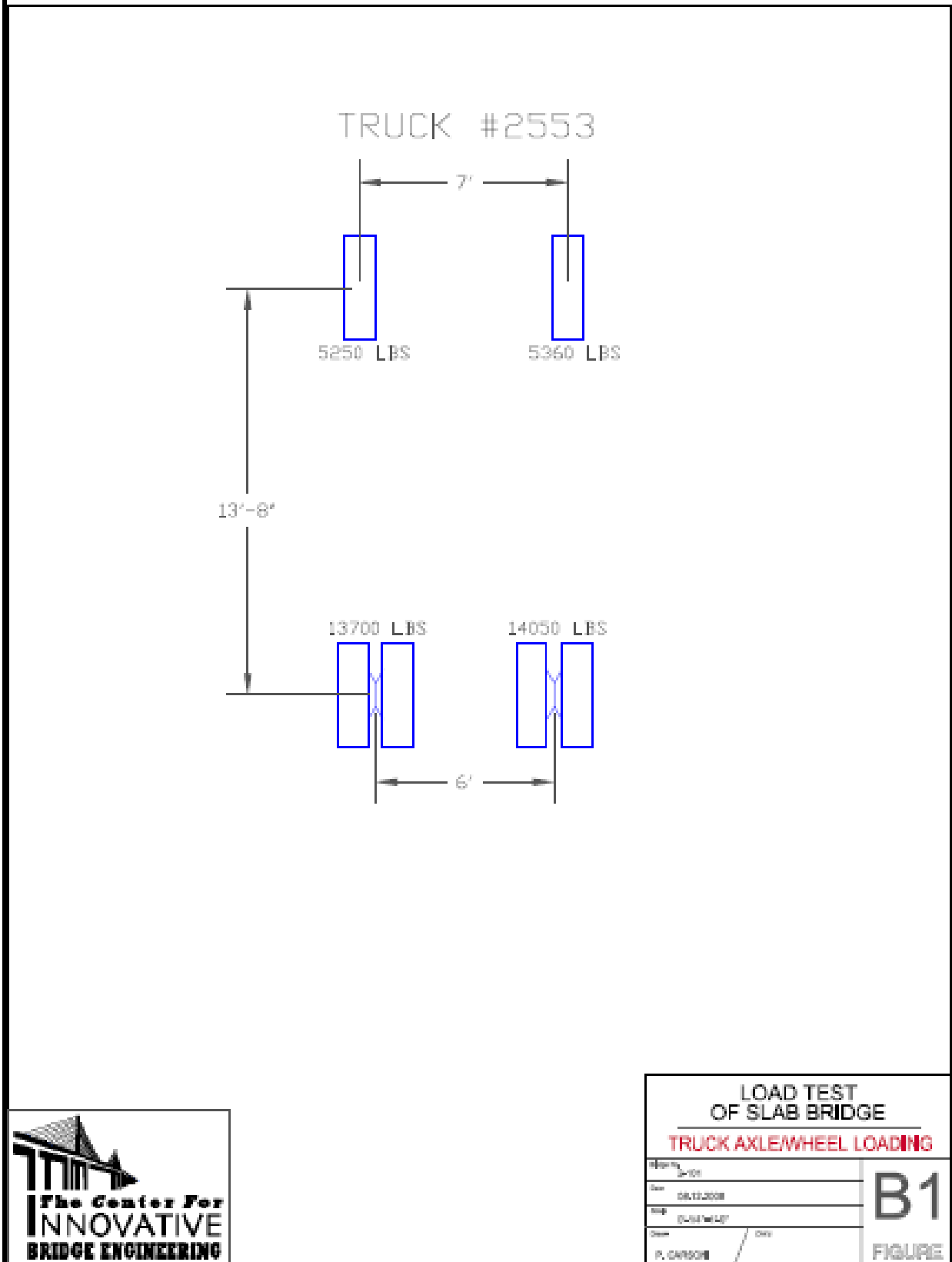


Figure 7. Wheel weights of truck #2553

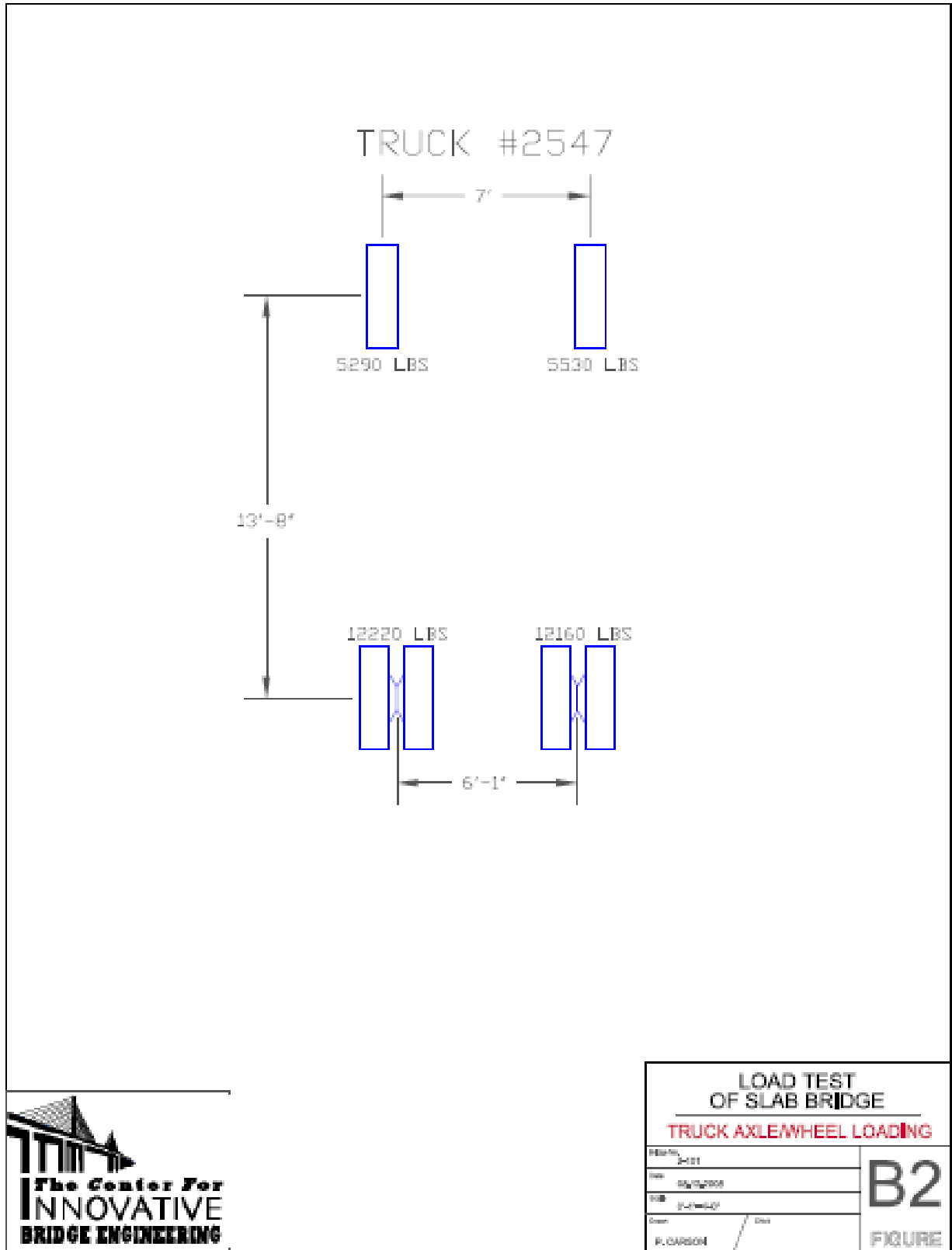


Figure 8. Wheel weights of truck #2547

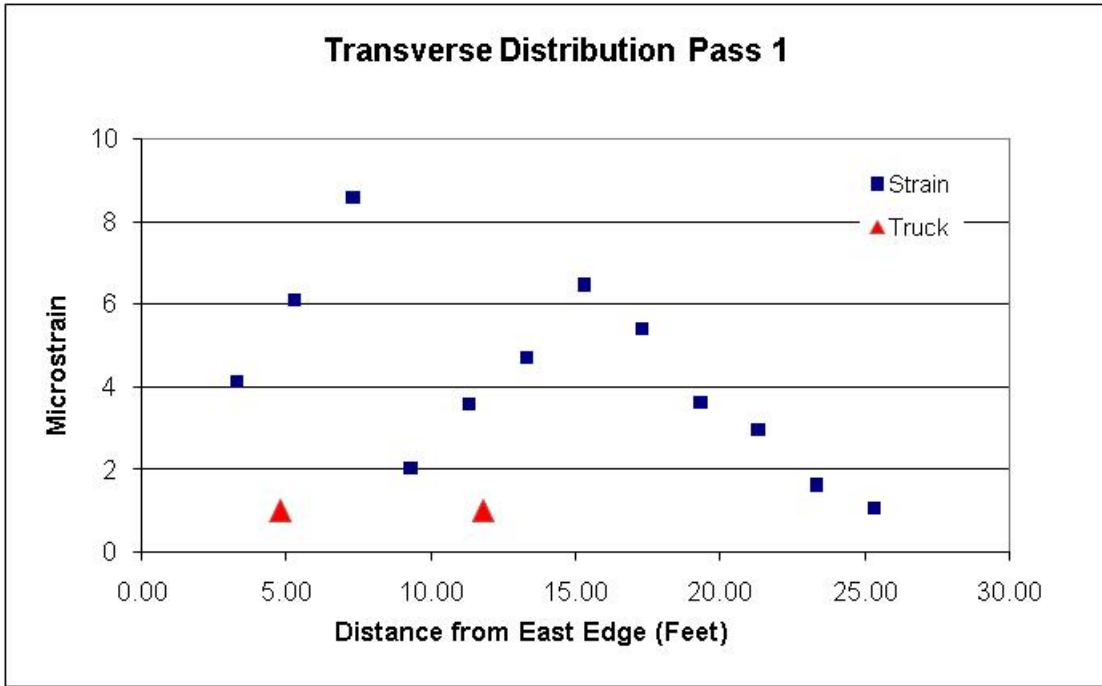


Figure 9. Transverse strain distribution Pass 1

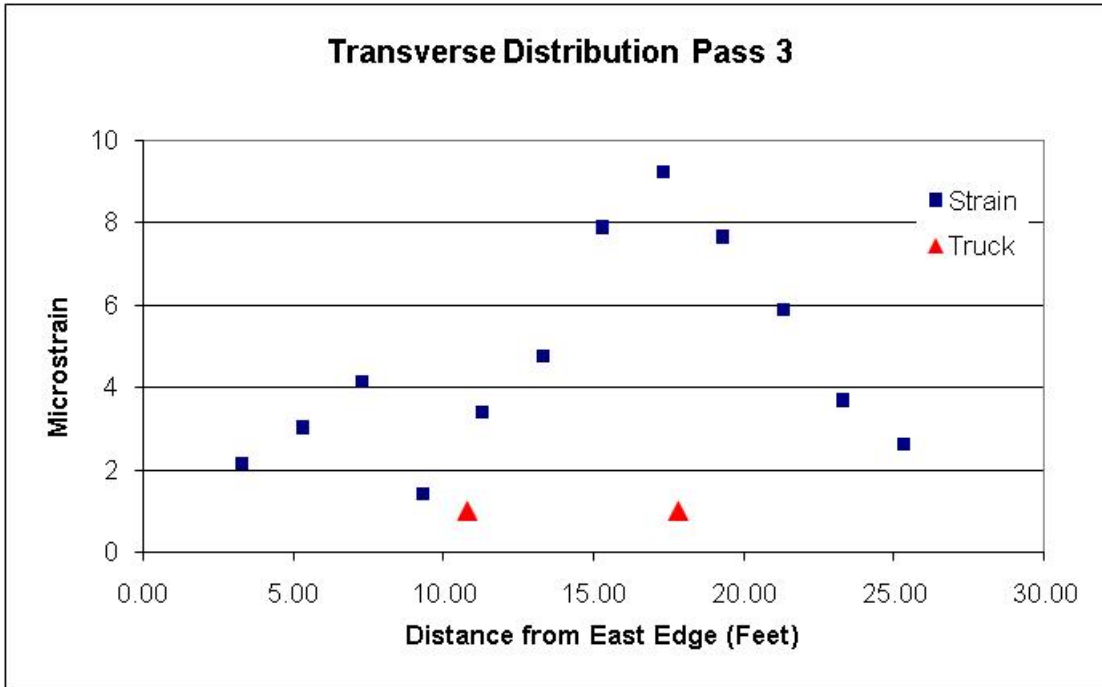


Figure 10. Transverse strain distribution Pass 3

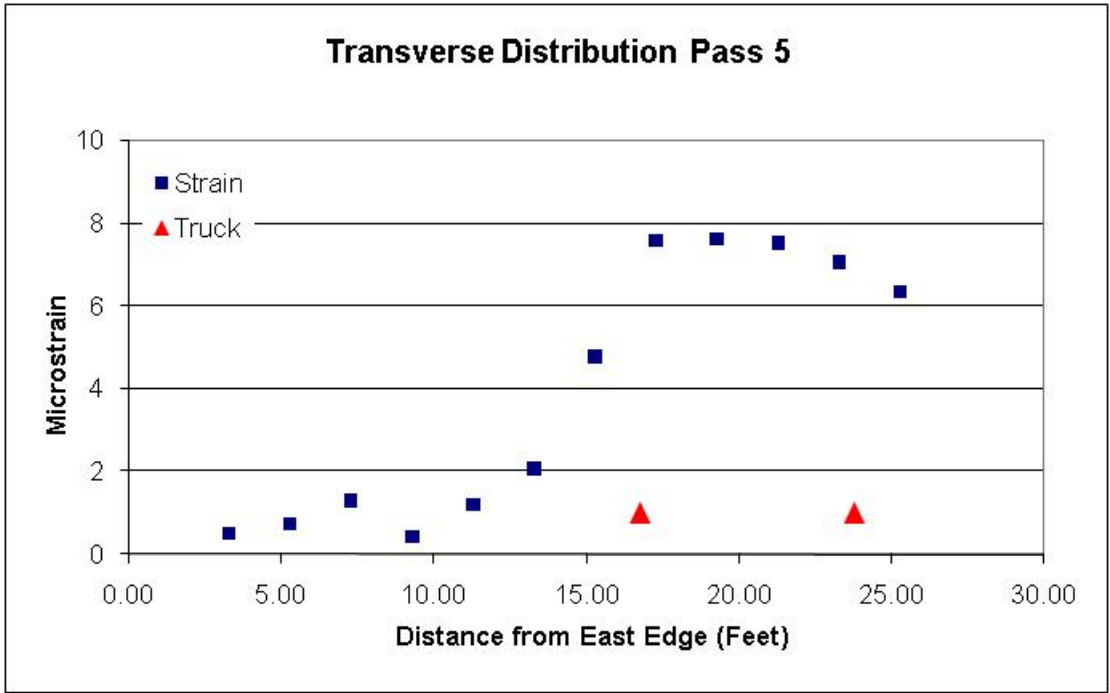


Figure 11. Transverse distribution of strain Pass 5

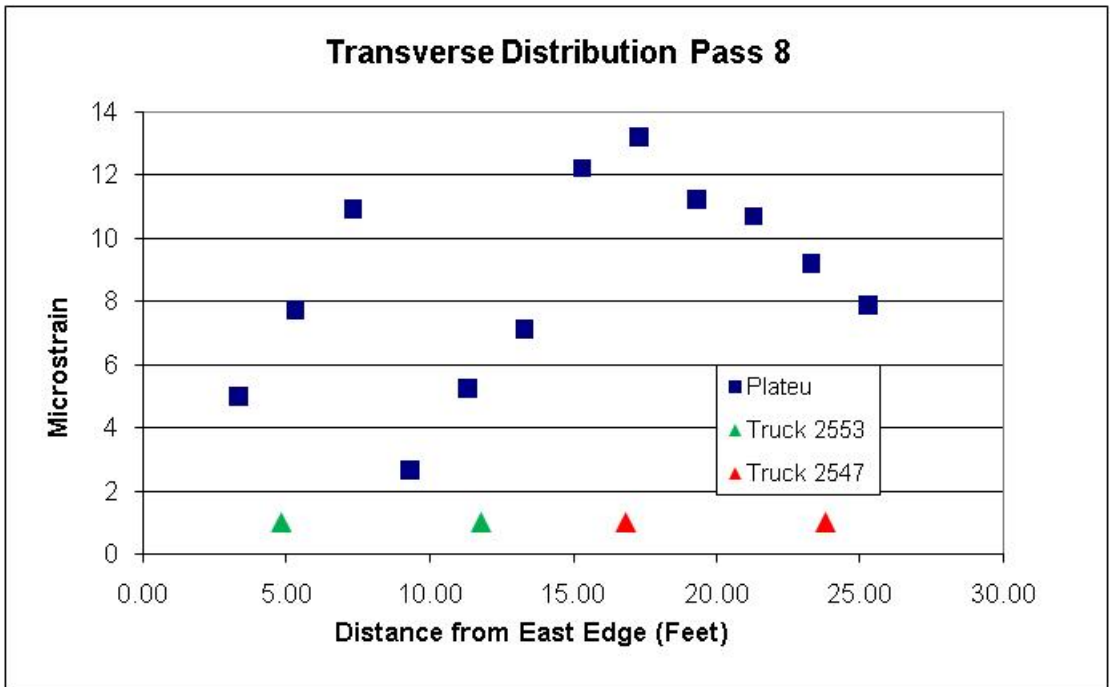


Figure 12. Transverse distribution of strain Pass 8 (two trucks side-by-side)

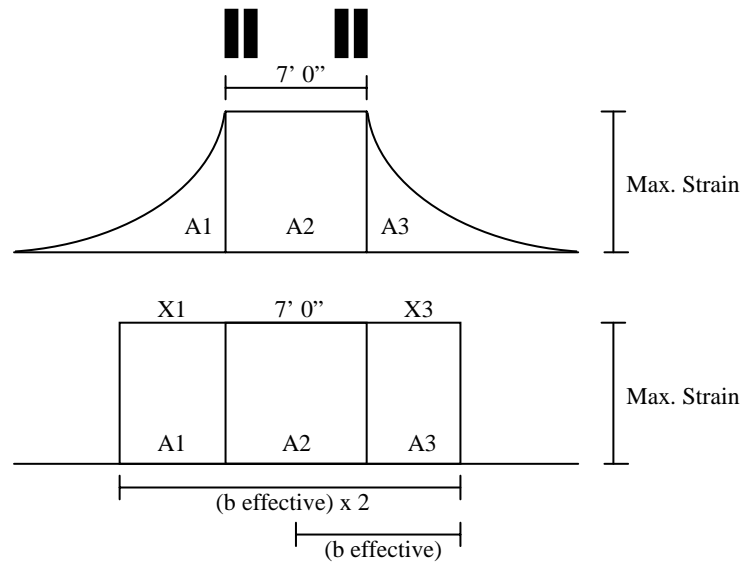


Figure 13. Idealized strain distribution and effective width representation

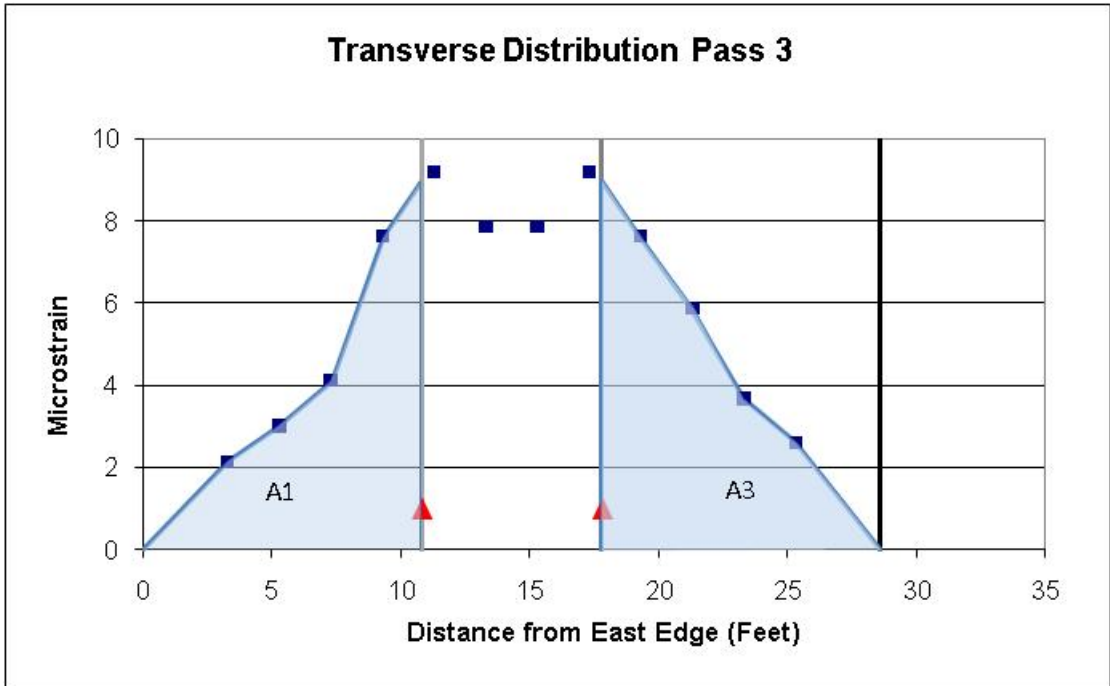


Figure 14. Determination of areas A1 and A3 for single truck

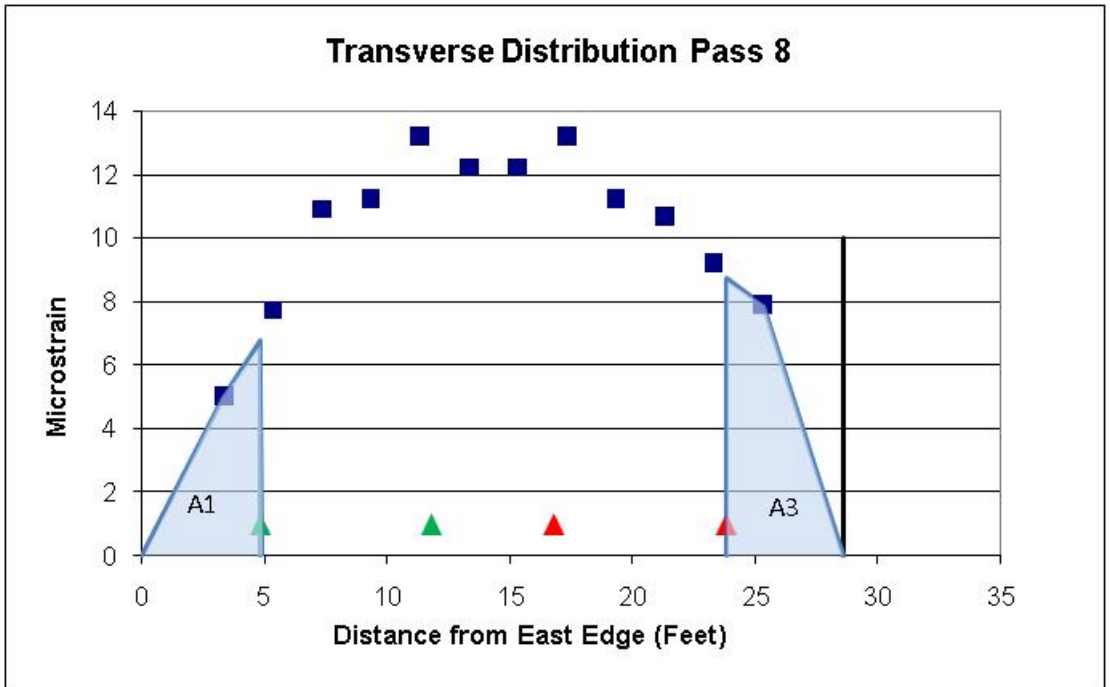


Figure 15. Determination of areas A1 and A3 for side-by-side trucks

Appendix C

BRIDGE TEST REPORT 1-352W

FIELD TEST OF BRIDGE 1-352W

by

Harry W Shenton III, Ph.D., Professor and Chair
&
Brian P Jones, Graduate Research Assistant

*Department of Civil and Environmental Engineering
Center for Innovative Bridge Engineering
University of Delaware
Newark, Delaware 19716*



July 15, 2009

Project:

Bridge 1-352W on Route 40
New Castle County, Delaware

Client:

Delaware Department of Transportation
P.O. Box 778
Dover, DE 19903

Executive Summary

The University of Delaware conducted a load test of Bridge 1-352W on Route 40 in Glasgow, Delaware on November 19, 2008, to evaluate its transverse load distribution. The slab bridge was originally constructed in 1932. The slab was instrumented with sixteen strain transducers placed on the underside of the concrete slab. Two fully loaded 6-wheel dump trucks were used as a controlled live load for the test. The gross weight of truck #2729 was 35.5 kips, with a combined rear axle weight of 24.1 kips. The gross weight of truck #2571 was 36.9 kips, with a combined rear axle weight of 25.7 kips. The test utilized nine load passes in which the truck moved across the bridge at a slow crawl. The maximum recorded concrete tensile stain at any time during the test was 12 $\mu\epsilon$. Based on evaluation of the observed transverse load distribution, a conservative estimate for the effective slab width of the bridge for two vehicles is 5.26 ft. This is 17% greater than the AASHTO Standard Specification code width of 4.48 ft, and 13% greater than the AASHTO LRFD width for multilane loading. For a single truck a conservative effective width is 6.00 ft, which is 34% greater than the AASHTO Standard Specification code width and 64% greater than the LRFD width for single lane loading.

Description of the Bridge

Bridge 1-352W is located on Pulaski Highway (Route 40) in Glasgow, Delaware, New Castle County and crosses a tributary to Muddy Run. It is a concrete slab bridge/culvert with an 8 foot span and an out-to-out deck width of 47 foot. It was originally constructed in 1932. Pictures of the bridge are shown in Figures 1 and 2.

The bridge has an ADT of 14956 vehicles (as of 2007), with 9% being trucks. The bridge was last inspected on July 23, 2008. The bridge is in relatively good condition, with no major signs of distress.

Test Purpose

The load test was performed at the request of DelDOT's Bridge Management section in order to assess the transverse load distribution of the slab. Based on the current AASHTO Standard Specification formula for effective slab width, $b_{eff} = 4.0 + 0.06S$, the effective slab width is 4.48 feet. The reinforcement details at the ends of the slab do not appear to be sufficient to transfer negative bending into the abutment walls. As such, the bridge must be rated as a slab as opposed to a rigid frame. It was determined that a load test would allow a more accurate assessment of the bridge's transverse load distribution characteristics. The remainder of this report discusses how the bridge was tested and how the effective slab width was computed using load test data.

Test Setup

The bridge load test was conducted on November 19, 2008 using the Bridge Diagnostics Inc, Structural Testing System (STS) and two fully loaded 6-wheel dump trucks. Sixteen strain transducers with 12 inch extensions were mounted to the underside of the concrete slab. All transducers were mounted at the midspan of the 8 foot clear span. The transducers were mounted with a transverse spacing of 2.5 feet per transducer. The transducers were mounted to the slab using a quick setting two-part epoxy manufactured by Loctite. No special equipment or ladders were needed to access the bottom of the slab. Figure 3 shows the crew mounting gages to the bottom of the slab. Figures 4 and 5 show the transducers mounted to the slab. Figure 6 shows the transducer layout with the associated three-digit transducer identification number. All of the strain transducers were connected to the STS data acquisition system and were read simultaneously, at an appropriate sampling rate during the test.

The two loaded dump trucks were used as a controlled live load for the test. The truck axles were weighed at the site using Intercomp portable truck scales which are accurate to within ± 10 lbs. The gross weight of truck #2729 was 35.5 kips, with a combined rear axle weight of 24.1 kips. The gross weight of truck #2571 was 36.9 kips, with a combined rear axle weight of 25.7 kips. The spacing between the front and rear axle was 13'-6". As a result, when the rear axle was at midspan, the front axle was off of the bridge. Figures 7 and 8 show the measured wheel spacings and wheel loads of the two vehicles.

Nine truck passes were completed and are listed in Table 1. In all cases the truck or trucks crossed the bridge in a westbound direction (toward Elkton, Maryland). All passes were conducted at a "crawl" speed, i.e., between 5 and 10 mph. The transverse position of the truck on the bridge is defined by "right shoulder", "right lane", "left lane", and "left shoulder" when looking in a westerly direction. Passes 1 through 4, and 6 through 7 involved only a single truck (#2571). Passes 8 through 10 were side-by-side truck passes with truck #2729 on the right and truck #2561 on the left (looking westerly) for all passes.

Results

Peak Strains and Transverse Strain Distribution

The strains induced in the slab by the load vehicles were very small: the absolute maximum recorded concrete tensile stain at any time during the test was $12 \mu\epsilon$. This occurred at gage 344, which was located close to the south edge of the bridge and occurred for pass 10 (both vehicles on the bridge at the same time). The absolute maximum strain recorded for a single truck pass was $8 \mu\epsilon$, which occurred at gage 298, for passes 1 and 2 (truck in the right shoulder). The absolute maximum recorded strains are listed for all gages in Table 2.

Although these strains are very low, good resolution was achieved in the measurements by using the concrete extensions. It should be noted, however, that these are average strains over the measurement range; the peak strain may be somewhat underestimated because of that.

The very low strains can be attributed to a number of reasons. First is possible frame action provided by the abutments. Although the bridge was not designed as a rigid frame, there is some continuity between the slab and walls which will tend to reduce the strain at mid-span. Second, there appears to be about a foot of fill between the top of the slab and the bottom of the roadway. The fill will distribute the load out in all directions and therefore reduces the effective load acting on the slab. This can be particularly significant in short span bridges. Finally, the concrete strength may be greater than the design specified strength, which will also tend to reduce the strain at mid-span.

Plots of the transverse distribution of strain for the single truck passes are shown in Figures 9 through 11, and for the side-by-side truck passes in Figures 12 through 14. Clearly the strains are largest underneath the vehicle and tend to get smaller as you move away from the vehicle.

The output of gage 317 was consistently very low for all the truck passes and is believed to have not been operating properly during the test, therefore, the results for that gage are not included in the tables or the plots.

Computation of Effective Slab Width (b_{eff})

Figure 15 shows an idealized transverse strain distribution that might result if a rear axle were sitting on an infinitely wide slab. The strain would have a relatively constant peak value (strain max.) between the truck wheels, and would decrease to zero as one moves away from the wheels. This non-uniform strain (or stress) is a result of shear-lag. In order to simplify the evaluation of slabs that exhibit shear lag, the concept of effective width was developed. The effective width section has a constant strain (or stress) across its width. The widely accepted definition of the effective width (b_{eff}) is the width that would have a uniform strain equal to the maximum strain but creates the same total effect as that caused by the actual strain distribution (Chiewanichakorn et al., 2004). To turn the plot having a varying strain into one having a uniform strain, one must keep the areas A_1 and A_3 for the two distributions equal (see Figure 13). Since the strain in this case is caused by two wheel lines, the actual effective width used in evaluating a bridge for a single wheel line is one half of the distance $X_1 + 7' + X_3$. Recall that the AASHTO formula is $b_{eff} = 4.0 + 0.06S$: for Bridge 1-352W, the AASHTO effective width is $b_{eff} = 4.48'$.

Figures 16 and 17 show examples of the areas used in calculating the effective width for the single truck passes. Effective widths have been calculated for all of the single truck passes and are summarized in Table 2.

The single truck effective widths vary from a low of 6.00 ft to a high of 7.55 ft. The average is 6.55 ft. The conservative value is the lowest, 6.00 ft, which is still 34% greater than the AASHTO value. The average value is almost 50% higher than the AASHTO width.

One will notice that the strain is not constant beneath the truck (as it is in the idealized depiction). While it may be acceptable to use the average value from this region as opposed to the peak value, effective width calculations found using the peak value will be conservative.

Consideration of Multiple Presence in the Effective Slab Width Calculation (b_{eff})

The above calculated widths do not incorporate the effect of side-by-side trucks. In essence, the above values are the effective width resulting from a single wheel load. If we want to account for side-by-side trucks in the effective width computation, we should place two trucks on the bridge with their wheels as close together as permitted by the code (this would be 4 feet; 2 feet from the edge of each 12 foot lane). These correspond to the results for passes 8 through 10.

Figure 18 shows an example of the areas used in calculating the effective width for the side-by-side trucks. The results are shown in Table 3.

The widths vary from a low of 5.26 ft to a high of 6.23 ft, with the average being 5.79 ft. The conservative value is the lowest, 5.26 ft, which is still 17% greater than the AASHTO value. The average value is 29% higher than the AASHTO width.

Since it is possible to have side-by-side trucks, it is recommended that the value for the effective width for bridge 1-352W be taken as:

$$b_{eff} = 5.26'$$

Comparison to AASHTO LRFD Effective Width

It is also worthwhile comparing the measured effective width to the AASHTO LRFD effective width. The equations for these are

$$E = 10.0 + 5.0\sqrt{L_1 W_1}$$

for a single lane loaded, and

$$E = 84.0 + 1.44\sqrt{L_1 W_1} \leq \frac{12.0W}{N_L}$$

for multilane loading, where:

- E = Equivalent width (in.)
- L_1 = Modified span length taken equal to the lesser of the actual span or 60.0 (ft.)
- W_1 = Modified edge-to-edge width of bridge taken to be equal to the lesser of the actual width or 60.0 for multilane loading, or 30.0 for single-lane loading (ft.)
- W = Physical edge-to-edge width of bridge (ft.)
- N_L = Number of design lanes

For bridge 1-352W

- L_1 = 8 ft
- W_1 = 30 ft for single lane
47 ft for multilane loading
- W = 47 ft
- N_L = 2

Substituting these values into the expressions above yields $E = 7.3$ ft for single lane loading and $E = 9.3$ ft for multilane loading. To compare these to the AASHTO Standard Specification values we must divide by 2, i.e., $b_{eff} = E / 2$.

Presented in Table 4 is a summary of the AASHTO Standard Specification effective width, the AASHTO LRFD effective width (divided by 2), and the measured values. The conservative, or lowest measured value for a single lane loaded is 64% greater than the LRFD effective width; the conservative measured value for multilane loaded is 13% greater than the LRFD effective width. The averaged measured effective width is even greater than the code values.

References

Chiewanichakorn, M, Aref, A.J., Chen, S.S., and Ahn, I-S, (2004). *Effective Flange Width Definition for Steel-Concrete Composite Bridge Girder*, Journal of Structural Engineering, ASCE, Volume 130, Number 12, P. 2016-2031.

Table 1. Truck passes

Pass #	Description (All trucks moving towards Elkton, West)
1	Truck 2571, Right Shoulder
2	Truck 2571, Right Shoulder
3	Truck 2571, Right Lane
4	Truck 2571, Right Lane
6	Truck 2571, Left Lane
7	Truck 2571, Left Lane
8	Trucks 2729 and 2571, Right Shoulder/Right Lane
9	Trucks 2729 and 2571, Right Lane/Left Lane
10	Trucks 2729 and 2571, Left Lane/Left Shoulder

Table 2. Effective width based on single truck passes

Pass #	Effective width (ft)
1	7.55
2	6.60
3	6.08
4	6.14
6	6.90
7	6.00
Average	6.55
St. Dev	0.603

Table 3. Effective width based on side-by-side truck passes

Pass #	Effective width (ft)
8	5.87
9	6.23
10	5.26
Average	5.79
St. Dev	0.490

Table 4. Comparison of AASHTO and measured effective width (ft)

Lane loading	AASHTO Standard Specification	AASHTO LRFD divided by 2 (E/2)	Measured	
			Low	Average
Single	4.48	3.65	6.00	6.55
Multilane	4.48	4.65	5.26	5.79

Table 2. Absolute maximum recorded strain

Absolute max microstrain measured for given gage ID															
Pass #	292	344	293	356	339	318	299	348	306	295	355	337	298	302	346
1	0	0	0	0.2	0.1	0	0	0.3	0.7	1.2	2.4	3.9	8.2	7.7	5.1
2	0.1	0.1	0	0.1	0	0.1	0	0	0	0.1	1.5	3.7	8.1	7.4	3.4
3	0	0.1	0	0.1	0	0.1	0.7	2.3	4.3	5.7	6.5	4.5	5.3	0	0.1
4	0	0.1	0.1	0	0.3	0.8	2	3.6	5.3	6.5	6.9	4.5	0.7	0.1	0
6	1.6	3.6	5.3	6.6	7	5.7	4.1	2.8	1.8	1	0.8	0.6	0.7	0.5	0.3
7	0.7	2.7	4.5	5.6	5.7	4.5	2.9	1.5	0.6	0	0.2	0.1	0.1	0	0.1
8	1.9	2.5	2.6	2.7	2.7	2.9	3.6	5.4	7.1	8.8	10	8.9	9.5	8.1	4.8
9	1.3	3.4	5.4	6.7	5.4	6.3	5.8	6.1	6.4	6.5	6.4	4	0.9	0.3	0.2
10	8.8	11.5	8.7	7.2	6.2	4.8	3.3	1.9	0.8	0.3	0	0	0.1	0.1	0.2



Figure 1. Bridge 1-352W looking north



Figure 2. Bridge 1-352W looking east



Figure 3. Crew mounting transducers



Figure 4. Strain transducers mounted to Bridge 1-352W



Figure 5. Close up of strain transducer with concrete extension, mounted to Bridge 1-35

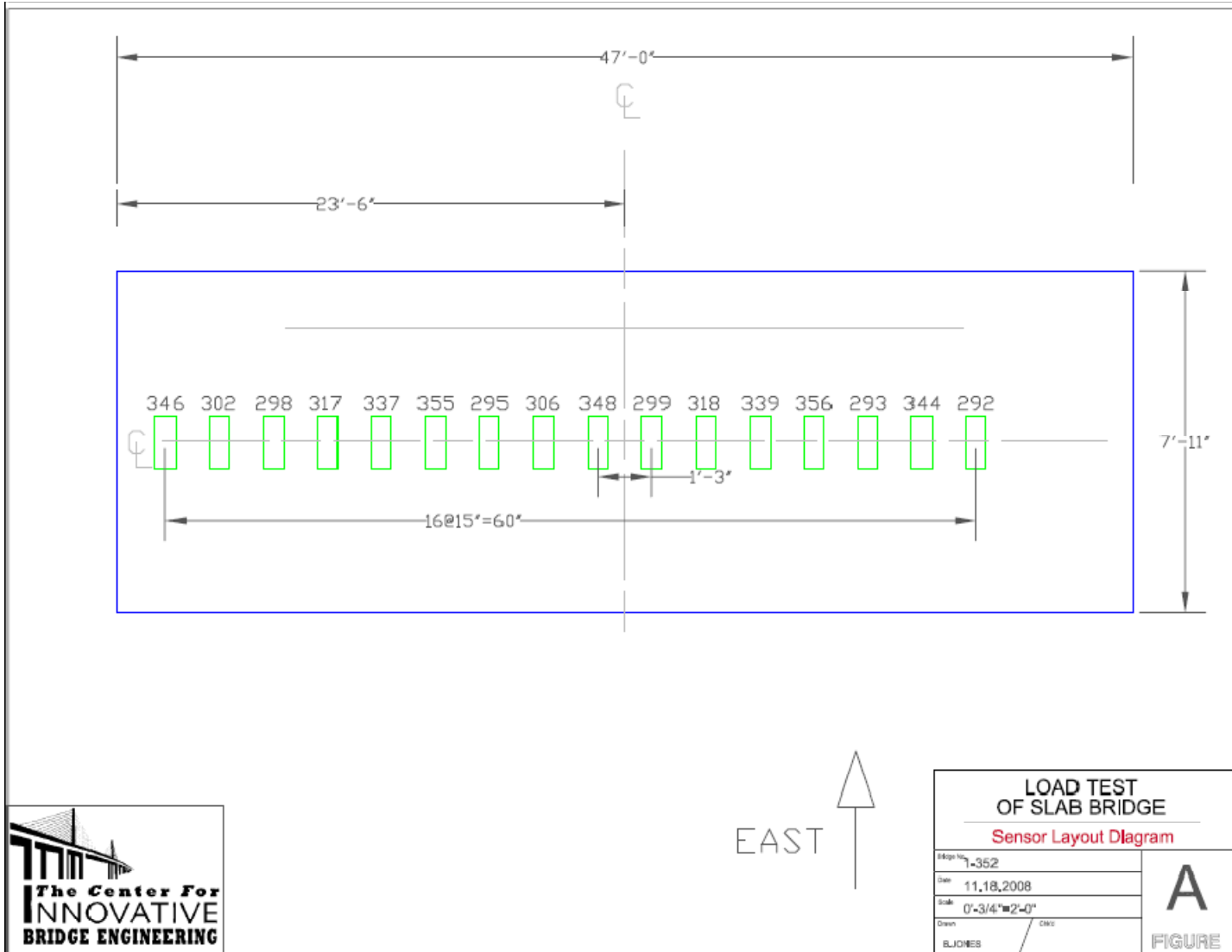
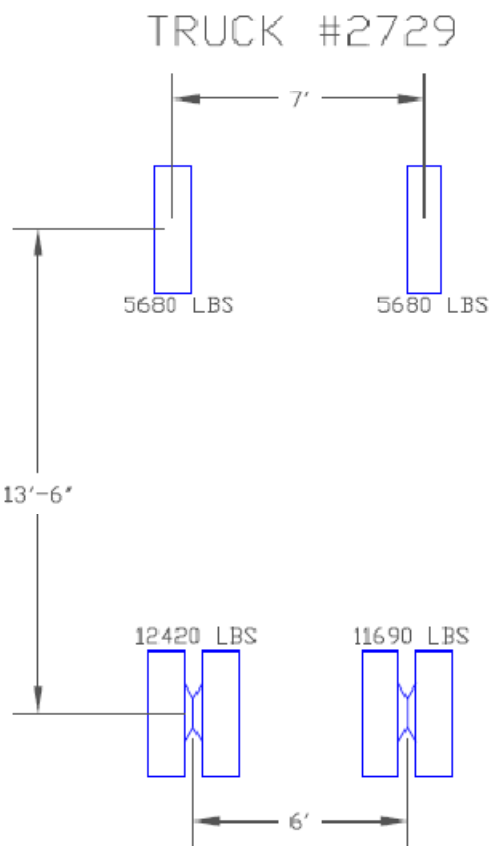


Figure 6. Sensor layout



LOAD TEST OF SLAB BRIDGE	
TRUCK AXLE/WHEEL LOADING	
Project No.	1-352
Date	11.18.2008
Scale	0'-1/4" = 1'-0"
Drawn	B. JONES

B1

FIGURE

Figure 7. Wheel weights of truck #2729

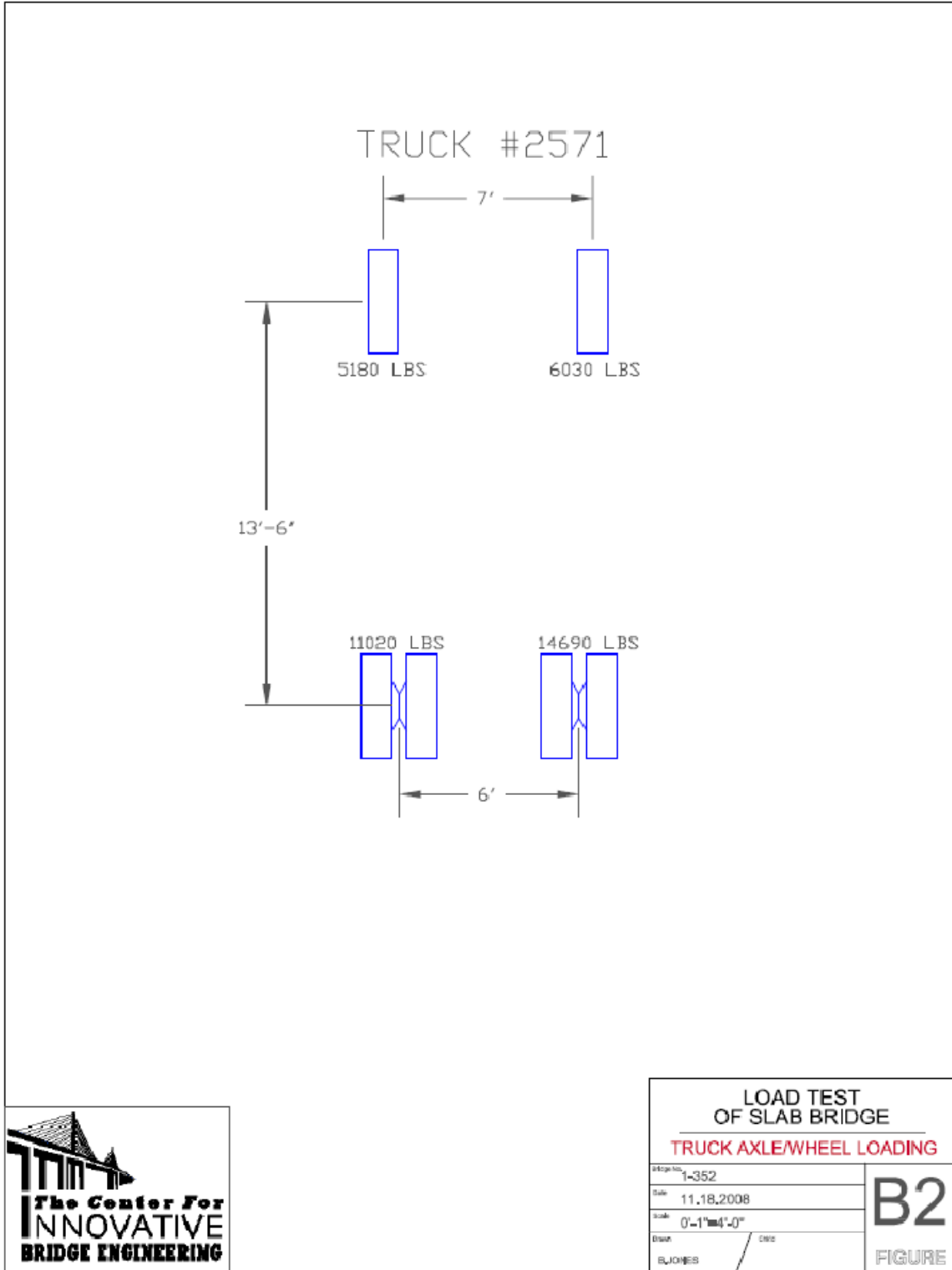


Figure 8. Wheel weights of truck #2571

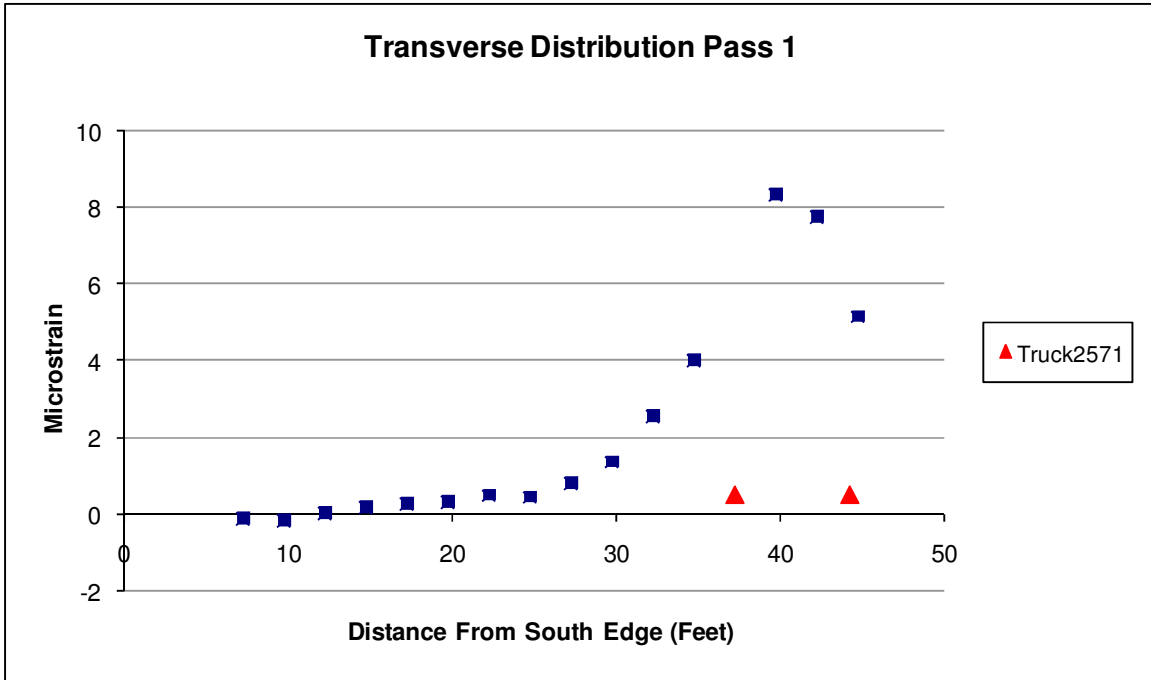


Figure 9. Transverse strain distribution Pass 1

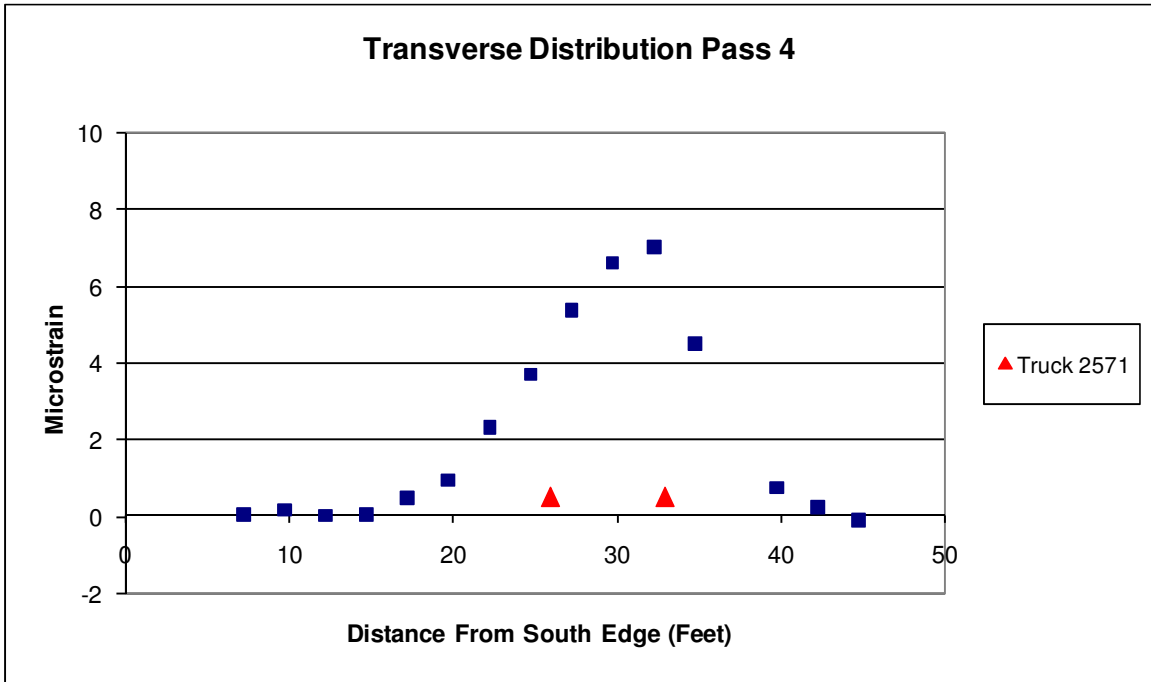


Figure 10. Transverse strain distribution Pass 4

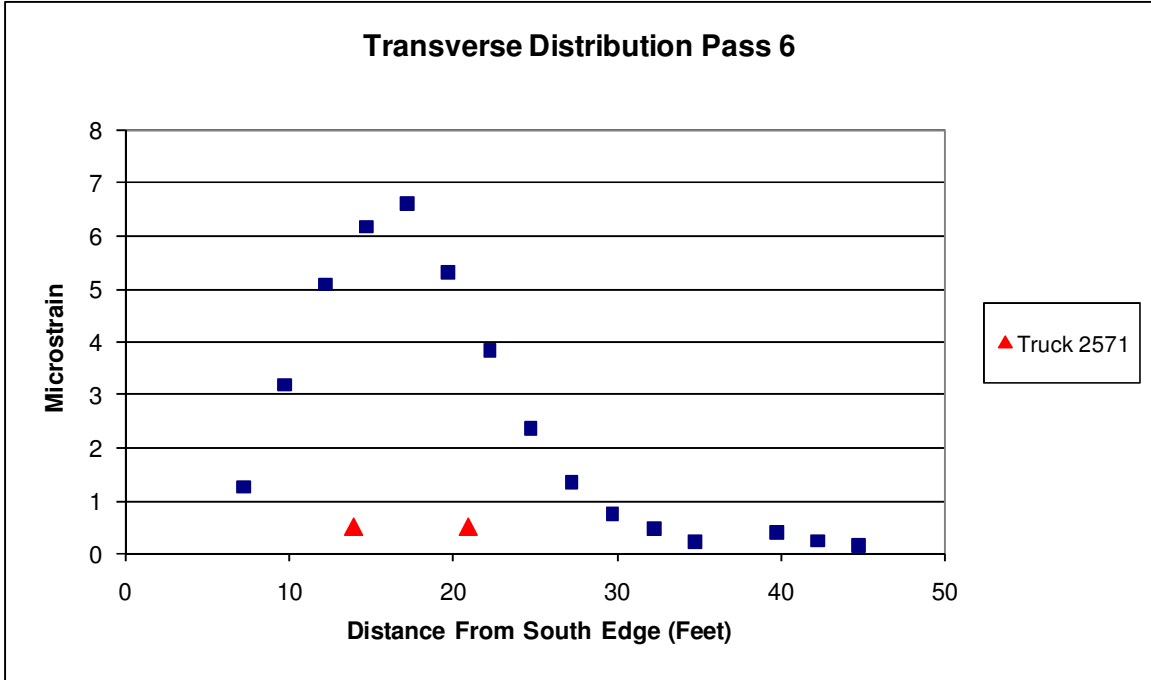


Figure 11. Transverse distribution of strain Pass 6

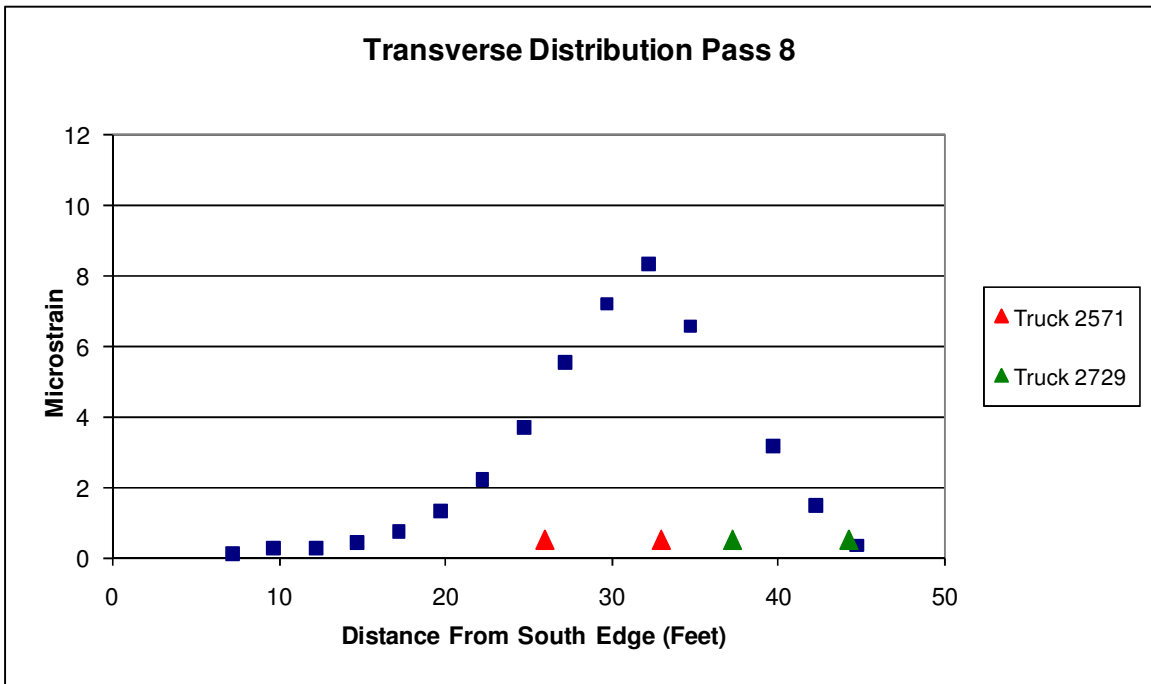


Figure 12. Transverse distribution of strain Pass 8 (two trucks side-by-side)

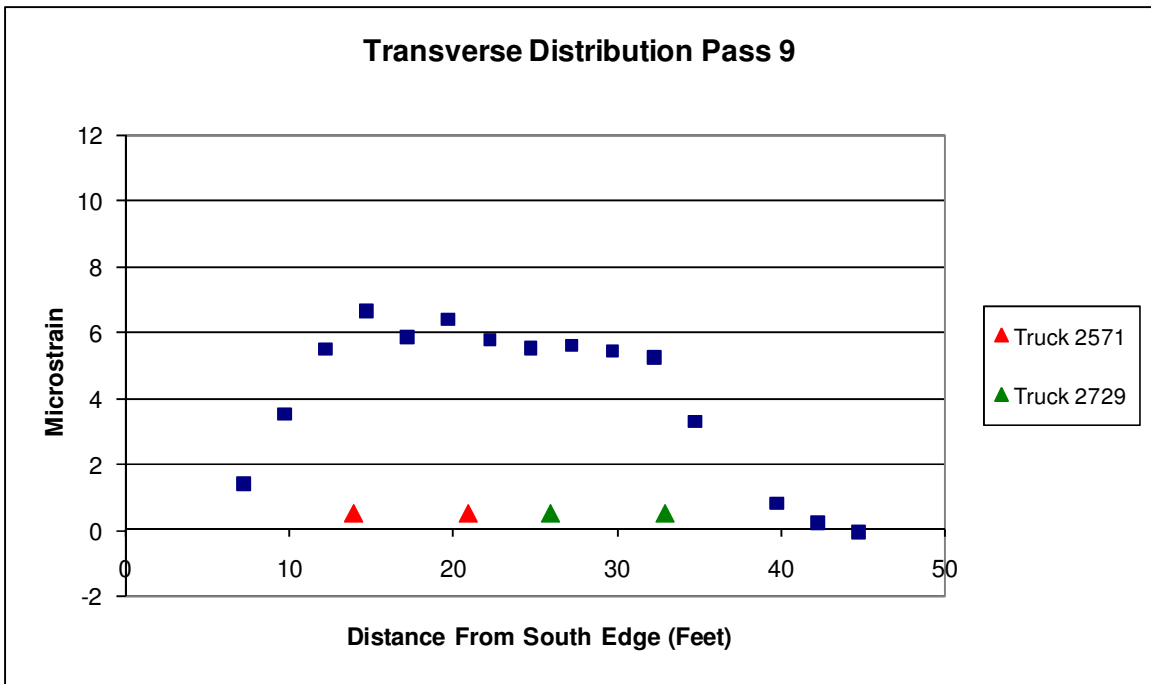


Figure 13. Transverse distribution of strain Pass 9 (two trucks side-by-side)

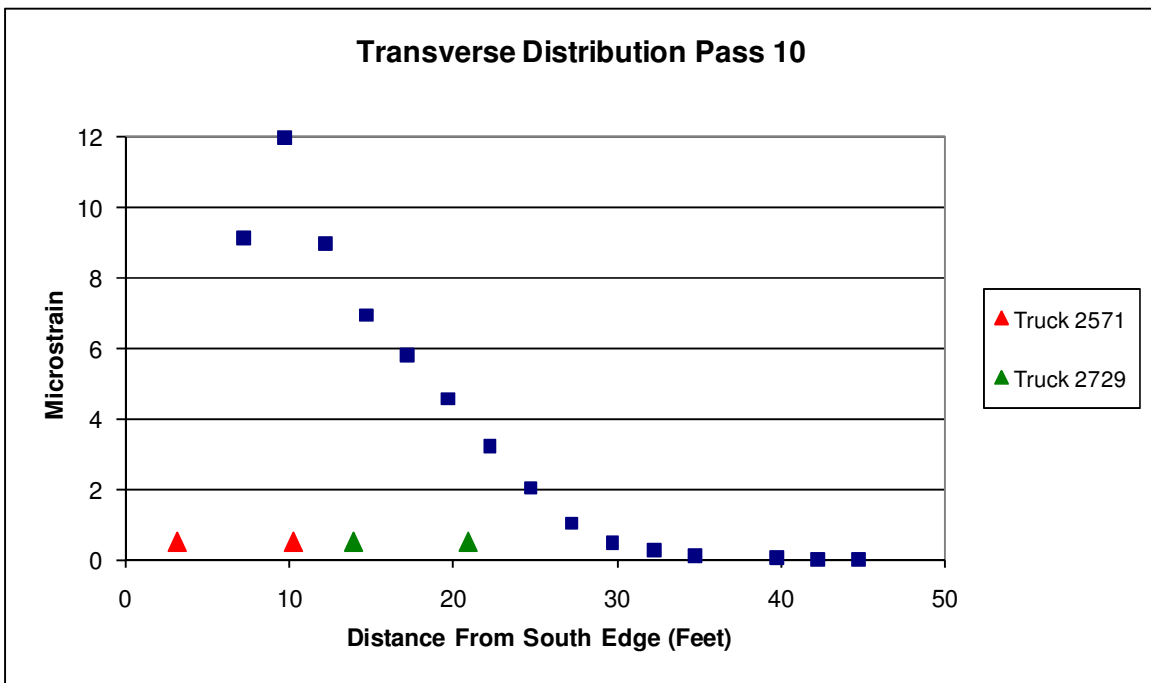


Figure 14. Transverse distribution of strain Pass 10 (two trucks side-by-side)

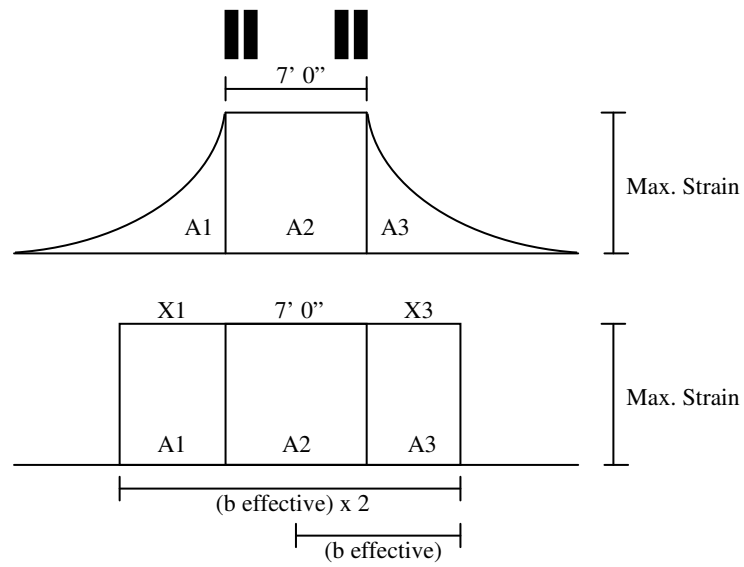


Figure 15. Idealized strain distribution and effective width representation

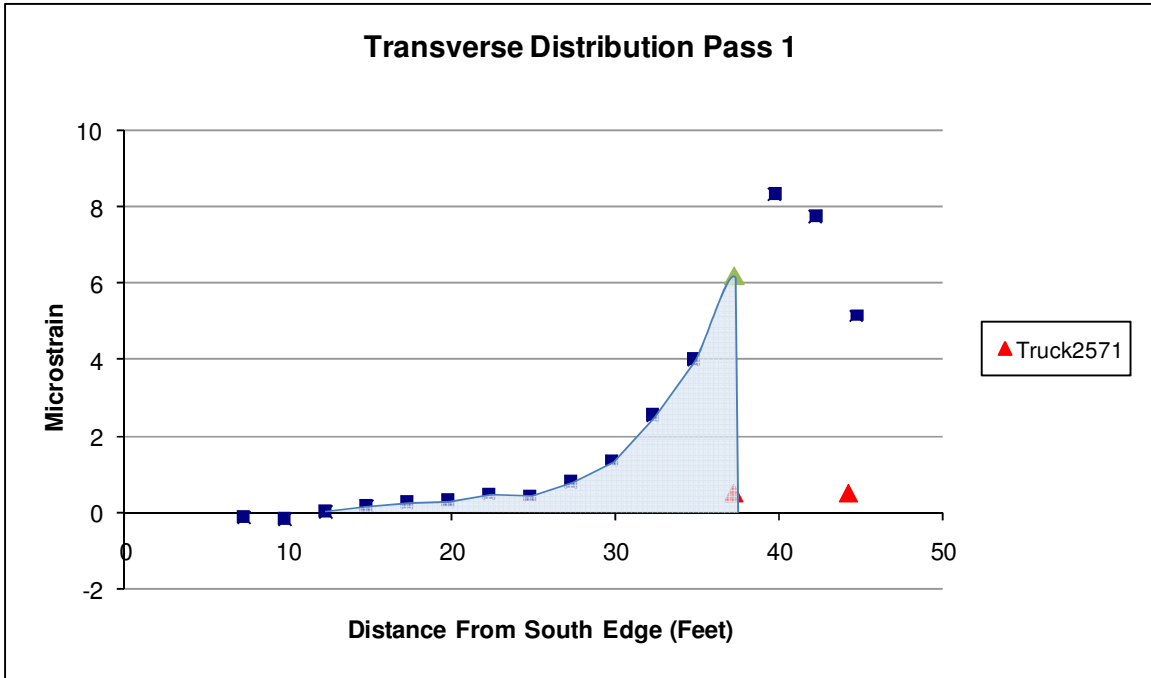


Figure 16. Determination of area A1 for single truck

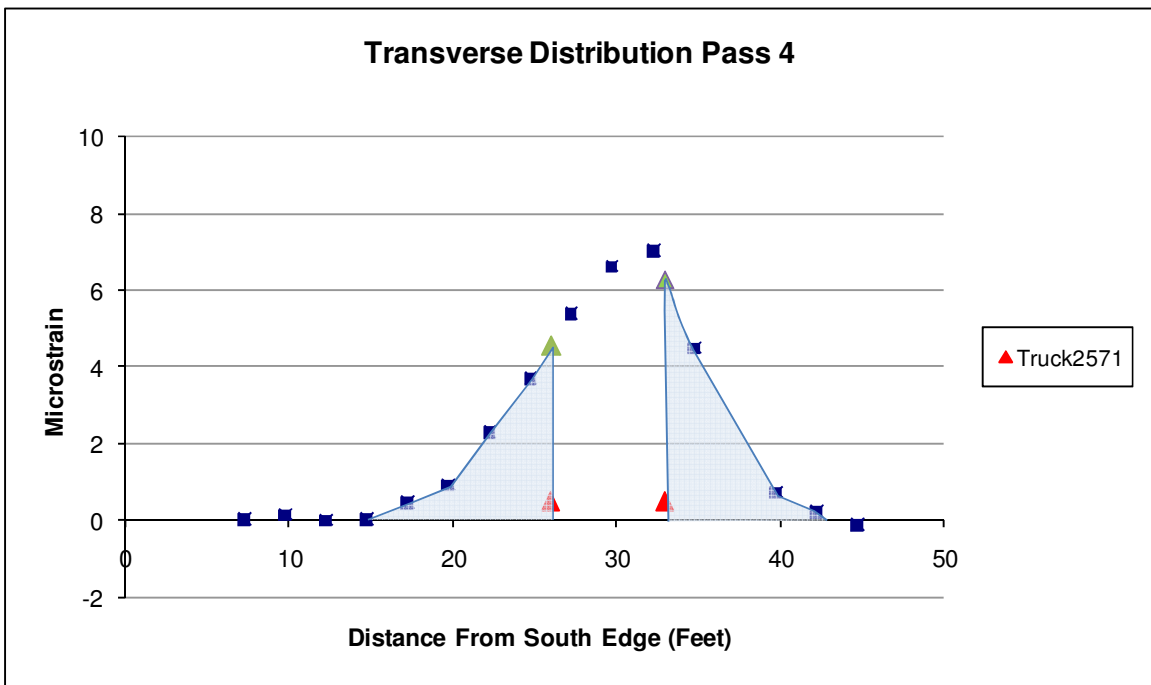


Figure 17. Determination of areas A1 and A3 for single truck

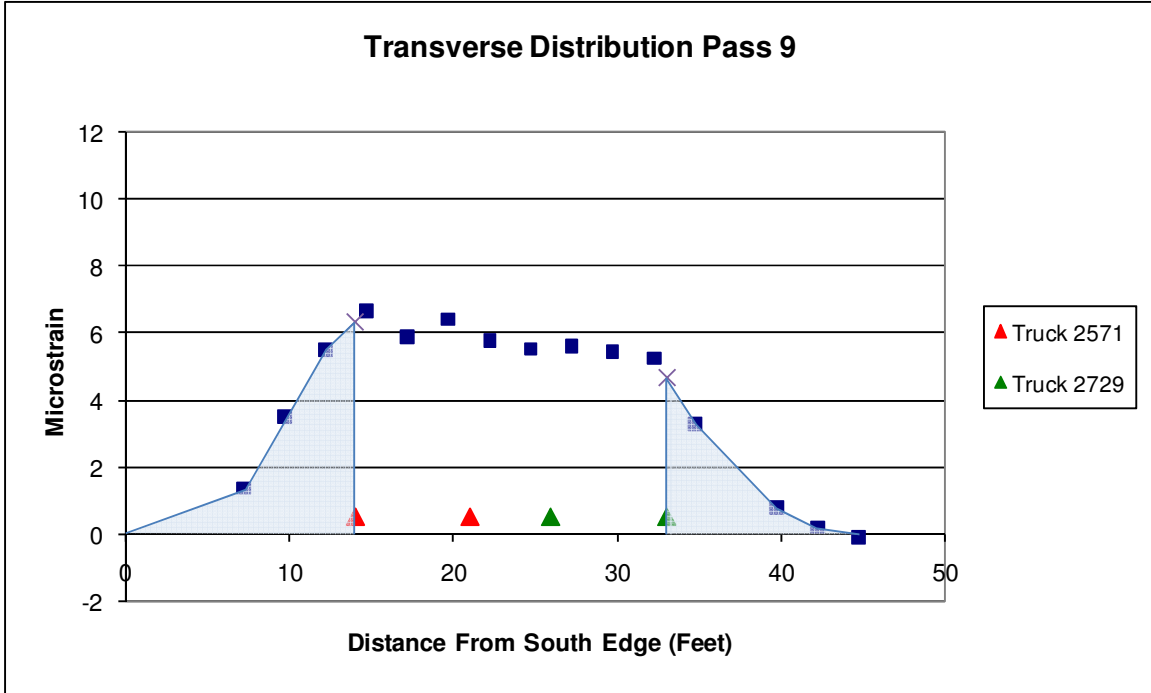


Figure 18. Determination of areas A1 and A3 for side-by-side trucks

Appendix D

BRIDGE TEST REPORT 1-384

FIELD TEST OF BRIDGE 1-384

by

Harry W Shenton III, Ph.D., Professor and Chair
&
Brian P Jones, Graduate Research Assistant

*Department of Civil and Environmental Engineering
Center for Innovative Bridge Engineering
University of Delaware
Newark, Delaware 19716*



August 4, 2009

Project:

Bridge 1-384 on Dutch Neck Road
New Castle County, Delaware

Client:

Delaware Department of Transportation
P.O. Box 778
Dover, DE 19903

Executive Summary

The University of Delaware conducted a load test of Bridge 1-384 on Dutch Neck Road northwest of Port Penn, Delaware on December 22, 2008, to evaluate its transverse load distribution. The slab bridge was originally constructed in 1931. The slab was instrumented with twelve strain transducers placed on the underside of the concrete slab. Two fully loaded 6-wheel dump trucks and a utility vehicle were used as a controlled live load for the test. The gross weight of truck #2729 was 37.5 kips, with a combined rear axle weight of 26.4 kips. The gross weight of truck #2741 was 34.2 kips, with a combined rear axle weight of 23.8 kips. The gross weight of truck #2719 was 15.8 kips. The test utilized 14 load passes in which the truck(s) moved across the bridge at a slow crawl. The maximum recorded concrete tensile stain at any time during the test was 26 $\mu\epsilon$. Based on evaluation of the observed transverse load distribution, a conservative estimate for the effective slab width of the bridge for two vehicles is 11.1 ft. This is 22% greater than the AASHTO LRFD width of 9.1 ft for multi-lane loading. For a single truck a conservative effective width is 13.2 ft, which is 61% greater than the AASHTO LRFD width of 8.2 ft for single lane loading. The test also provided a “proof” safe load limit relative to the current 7 ton load posting: a total of 36 tons was placed on the bridge without any measurable or visual distress to the bridge.

Description of the Bridge

Bridge 1-384 is located on Dutch Neck Road, northwest of Port Penn, New Castle County, Delaware. It is a concrete slab bridge/culvert with a 12 foot span and an out-to-out deck width of 26 foot. The bridge crosses a small creek and was originally constructed in 1931. A location map of the bridge is shown in Figure 1; pictures of the bridge are shown in Figure 2.

The bridge has an ADT of 351 vehicles (as of 2007) with 4% being trucks. It was last inspected on August 20, 2008 and is currently posted for 7 tons.

Test Purpose

The load test was performed at the request of DelDOT’s Bridge Management section in order to assess the transverse load distribution, i.e., effective width, of the slab. The reinforcement details at the ends of the slab do not appear to be sufficient to transfer negative bending into the abutment walls. As such, the bridge must be rated as a slab as opposed to a rigid frame. It was determined that a load test would allow a more accurate assessment of the bridge’s transverse load distribution characteristics. The remainder of this report discusses how the bridge was tested and how the effective slab width was computed using load test data, and provides a comparison to the AASHTO effective width.

AASHTO Effective Width

The equation for effective width of a slab, per AASHTO LRFD, is

$$E = 10.0 + 5.0\sqrt{L_1 W_1} \quad (1)$$

for a single lane loaded, and

$$E = 84.0 + 1.44\sqrt{L_1 W_1} \leq \frac{12.0W}{N_L} \quad (2)$$

for multilane loading, where:

- E = Equivalent width (in.)
- L_1 = Modified span length taken equal to the lesser of the actual span or 60.0 (ft.)
- W_1 = Modified edge-to-edge width of bridge taken to be equal to the lesser of the actual width or 60.0 for multilane loading, or 30.0 for single-lane loading (ft.)
- W = Physical edge-to-edge width of bridge (ft.)
- N_L = Number of design lanes

For bridge 1-384

- L_1 = 12 ft
- W_1 = 26 ft for single lane
26 ft for multilane loading
- W = 26 ft
- N_L = 2

Substituting these values into the expressions above yields $E = 98.3 \text{ in.} = 8.2 \text{ ft.}$ for single lane loading and $E = 109.4 \text{ in.} = 9.1 \text{ ft.}$ for multilane loading.

For comparison, the formula for effective width per the AASHTO Standard Specification is

$$b_{eff} = 4.0 + 0.06S \quad (3)$$

where S is the span (in ft.). The effective width per the Standard Specification is $b_{eff} = 4.72 \text{ ft.}$ Note that b_{eff} is for a single wheel line and must be multiplied by 2 for direct comparison with E , which is for two wheel lines.

Test Setup

The bridge load test was conducted on December 22, 2008 using the Bridge Diagnostics Inc, Structural Testing System (STS) and three 6-wheel trucks. Twelve strain transducers with 12 inch extensions were mounted to the underside of the concrete slab. All transducers were mounted at the midspan of

the 12 foot clear span. The transducers were mounted with a transverse spacing of 2 feet per transducer. The transducers were mounted to the slab using a quick setting two-part epoxy manufactured by Loctite. No special equipment or ladders were needed to access the bottom of the slab. Figure 3 shows one of the crew mounting gages to the bottom of the slab. Figure 4 shows the transducer layout with the associated three-digit transducer identification number. All of the strain transducers were connected to the STS data acquisition system and were read simultaneously, at an appropriate sampling rate during the test.

During the installation it was noted that a crack exists in the bottom of the slab, that runs longitudinally from one abutment to the other. It is to the west of the centerline of the bridge. It appears to have been filled as sometime with a type of polymer material. Strain gage 314 was located to the east of the crack and gage 302 was located to the west of the crack. The crack is indicated in Figure 4.

Two loaded dump trucks and one smaller utility truck were used as controlled live loads for the test. The truck axles were weighed at the site using Intercomp portable truck scales which are accurate to within ± 10 lbs. The gross weight of truck #2729 was 37.5 kips, with a combined rear axle weight of 26.4 kips. The gross weight of truck #2741 was 34.2 kips, with a combined rear axle weight of 23.8 kips. The spacing between the front and rear axle was 13'-6". The gross weight of truck #2719 was 15.8 kips, with a combined rear axle weight of 7.8 kips. The spacing between the front and rear axle was 15'-7". As a result, for each truck, when the rear axle was at midspan the front axle was off of the bridge. Figures 5 through 7 show the measured wheel spacings and wheel loads of the three vehicles.

A total of 16 truck passes were completed and are listed in Table 1. In all cases the truck or trucks crossed the bridge in a northeast direction (toward Delaware City). All passes were conducted at a "crawl" speed, i.e., between 5 and 10 mph. The transverse position of the truck on the bridge is defined by "right lane", "center", and "left lane" when looking in a northeasterly direction. Passes 1 through 3a involved only a single truck (#2729). Passes 4 and 5 were side-by-side truck passes with truck #2729 on the right and truck #2741 on the left. Passes 6 through 8a involved only a single truck (#2719).

Photos of the various truck passes are shown in Figures 8 through 12.

Results

Peak Strains and Transverse Strain Distribution

The strains induced in the slab by the load vehicles were very small: the absolute maximum recorded concrete tensile stain at any time during the test was 26 $\mu\epsilon$. This occurred at gage 535, which was located very near the center of the bridge and occurred for pass 4 (both vehicles on the bridge at the same time). The

absolute maximum strain recorded for a single truck pass was $19 \mu\epsilon$. This occurred at gage 314, also near the center of the bridge, for pass 2a (truck in the center). The absolute maximum recorded strains are listed for all gages in Table 2.

Although these strains are very low, good resolution was achieved in the measurements by using the concrete extensions. It should be noted, however, that these are average strains over the measurement range; the peak strain may be somewhat underestimated because of that.

The very low strains can be attributed to two factors. First is possible frame action provided by the abutments. Although the bridge was not designed as a rigid frame, there is some continuity between the slab and walls which will tend to reduce the strain at mid-span. Second, the concrete strength may be greater than the design specified strength, which will also tend to reduce the strain at mid-span.

Plots of the transverse distribution of strain for the single truck passes are shown in Figures 13 through 15, and for the side-by-side truck passes in Figure 16. Clearly the strains are largest underneath the vehicle and tend to get smaller as you move away from the vehicle.

Computation of Effective Slab Width

Figure 17 shows an idealized transverse strain distribution that might result if a rear axle were sitting on an infinitely wide slab. The strain would have a relatively constant peak value (strain max.) between the truck wheels, and would decrease to zero as one moves away from the wheels. This non-uniform strain (or stress) is a result of shear-lag. In order to simplify the evaluation of slabs that exhibit shear lag, the concept of effective width was developed. The effective width section has a constant strain (or stress) across its width. The widely accepted definition of the effective width is the width that would have a uniform strain equal to the maximum strain but creates the same total effect as that caused by the actual strain distribution (Chiewanichakorn et al., 2004). To turn the plot having a varying strain into one having a uniform strain, one must keep the areas A_1 and A_3 for the two distributions equal (see Figure 17).

Figures 18 and 19 show examples of the areas used in calculating the effective width for the single truck passes. Note that because the bridge is relatively narrow the strain at the edge of the bridge has been assumed to be equal to the measured strain of the gage closest to the edge (gage 298 on the east side and gage 337 on the west side, each are about 2 ft from the edge). A conservative approach would be to assume the strain at the edge is zero; engineering judgment tells us that the strain on the edge would not be zero. Assuming the strain is constant to the edge amounts to only a few percent increase in the

effective width. Effective widths have been calculated for all of the single truck passes and are summarized in Table 3.

The single truck effective widths vary from a low of 13.2 ft to a high of 21.2 ft. The average is 16.3 ft. The conservative value is the lowest, 13.2 ft, which is still 61% greater than the AASHTO LRFD value (8.2 ft.). The average value is 99% higher than the AASHTO LRFD width.

Referring to Table 3, the effective widths for passes 1 through 3a, obtained using truck 2729 (37.5 kips) and passes 6 through 8a, obtained using truck 2719 (15.8 kips) are very consistent (most corresponding values are within 5% of each other). This demonstrates the linearity of the bridge behavior, and that the calculation of the effective width is independent of the magnitude of the load.

What is interesting is that the effective widths for passes 1 and 1a are significantly higher than the corresponding values for passes 2, 2a, 3, and 3a, for truck #2729. Likewise, the effective widths for passes 6 and 6a are significantly higher than the corresponding values for passes 7, 7a, 8, and 8a, for truck #2719. This is most likely due to the longitudinal crack in the bottom of the slab. When the vehicle is on the right side, furthest from the crack, the effect of the crack is felt less and the load can be distributed more effectively, resulting in a larger effective width. This can be seen in passes 1 and 1a, and 6 and 6a. When the vehicle is in the center or left side of the bridge, i.e., very close to the crack, the load cannot be distributed transversely as effectively, resulting in a lower effective width. This can be seen in passes 2 through 3a and 7 through 8a. Nevertheless, even with the crack, the measured effective width is still significantly greater than the AASHTO LRFD value.

One will notice that the strain is not constant beneath the truck (as it is in the idealized depiction). While it may be acceptable to use the average value from this region as opposed to the peak value, effective width calculations found using the peak value will be conservative.

Consideration of Multiple Presence in the Effective Slab Width Calculation

The above calculated widths do not incorporate the effect of side-by-side trucks. In essence, the above values are the effective width resulting from a single vehicle load. If we want to account for side-by-side trucks in the effective width computation, we should place two trucks on the bridge with their wheels as close together as permitted by the code (this would be 4 feet; 2 feet from the edge of each 12 foot lane). These correspond to the results for passes 4 and 5.

Figure 20 shows an example of the areas used in calculating the effective width for the side-by-side trucks. The results are shown in Table 4.

The lowest effective width for the two side-by-side truck runs is 11.1 ft. This is 22% greater than the AASHTO LRFD multi-lane value (9.1 ft.). The average effective width for the two side-by-side trucks is 11.3 ft, which is 24% greater than the AASHTO LRFD multi-lane value.

Presented in Table 5 is a summary of the key results. Also presented in the table is the equivalent effective width for the vehicle based on the AASHTO Standard Specification. As mentioned, the measured values are all greater than the code specified values.

Although it is very unlikely to have side-by-side heavy vehicles on such a narrow bridge, a conservative value for the multi-lane effective width for bridge 1-384 would be 11.1 ft.

Finally, it should be noted that while this test was not designed to be a “proof” test, it did in fact provide proof of a safe load limit, relative to the current load posting. The bridge is currently posted for 7 tons. The side-by-side passes (4 and 5) amounted to 72 kips, or 36 tons being placed on the bridge, without any perceivable distress to the bridge (either measured or observed). This is shown in Figure 12. These results suggest that the posting on the bridge could be safely increased.

References

Chiewanichakorn, M, Aref, A.J., Chen, S.S., and Ahn, I-S, (2004). *Effective Flange Width Definition for Steel-Concrete Composite Bridge Girder*, Journal of Structural Engineering, ASCE, Volume 130, Number 12, P. 2016-2031.

Table 1. Truck passes

Pass #	Description (All trucks moving towards Elkton, West)
1	Truck 2729 Right Lane
1a	Truck 2729 Right Lane
2	Truck 2729 Center
2a	Truck 2729 Center
3	Truck 2729 Left Lane
3a	Truck 2729 Left Lane
4	Truck 2741 Left Lane / Truck 2729 Right Lane
5	Truck 2741 Left Lane / Truck 2729 Right Lane
6	Truck 2719 Right Lane
6a	Truck 2719 Right Lane
7	Truck 2719 Center
7a	Truck 2719 Center
8	Truck 2719 Left Lane
8a	Truck 2719 Left Lane

Table 2. Absolute maximum recorded strain

Absolute max microstrain measured for given gage ID												
Pass #	337	355	348	302	314	299	535	306	338	346	318	298
1	2.1	2.7	3.6	5.9	7.9	12.1	16.4	16.0	16.5	17.0	12.1	7.6
1a	2.3	3.0	4.0	6.5	8.5	12.5	15.4	15.3	16.1	15.0	10.8	6.9
2	4.1	5.6	8.3	13.9	17.2	13.2	13.6	15.8	10.0	5.8	4.4	3.2
2a	4.4	6.0	8.7	14.7	18.8	14.7	15.0	17.9	11.6	6.8	5.1	3.9
3	9.0	13.5	17.4	15.5	15.0	16.0	10.1	7.3	4.8	2.9	2.2	1.8
3a	9.3	14.6	17.5	15.4	14.5	14.6	9.1	6.5	4.1	2.4	1.7	1.3
4	10.5	13.5	16.1	18.6	20.4	22.1	25.6	23.6	20.9	21.1	16.9	10.6
5	10.9	17.2	18.3	18.5	21.4	22.7	24.0	24.0	20.5	21.1	17.4	10.8
6	0.7	0.9	1.0	1.8	2.1	3.2	4.5	4.2	4.3	5.0	3.9	2.3
6a	0.8	1.0	1.3	2.0	2.5	3.7	4.7	4.6	4.8	5.4	3.9	2.4
7	1.2	1.8	2.5	4.3	5.7	4.1	3.8	5.7	4.0	2.3	1.7	1.3
7a	1.5	2.0	2.7	4.7	4.6	3.9	3.8	5.5	3.4	1.9	1.5	1.2
8	3.3	5.4	5.1	4.8	4.5	4.2	2.4	1.8	1.0	0.7	0.6	0.5
8a	2.8	4.9	4.2	4.3	4.3	4.2	2.2	1.7	1.0	0.6	0.4	0.4

Table 3. Measured Effective width based on single truck passes

Pass	E_m (ft)
1	20.11
1a	21.24
2	14.86
2a	14.95
3	14.85
3a	13.73
6	19.27
6a	19.87
7	15.07
7a	15.32
8	13.19
8a	13.19
Average	16.30
St. Dev.	2.94

Table 4. Measured Effective width based on side-by-side truck passes

Pass	E_m (ft)
4	11.14
5	11.45
Average	11.29
St. Dev.	0.22

Table 5. Comparison of AASHTO and measured effective width (ft)

Lane loading	AASHTO LRFD (E)	AASHTO Standard Specification ($2b_{eff}$)	Measured E_m	
			Min	Average
Single	8.2	9.44	13.2	16.3
Multilane	9.1	9.44	11.1	11.3

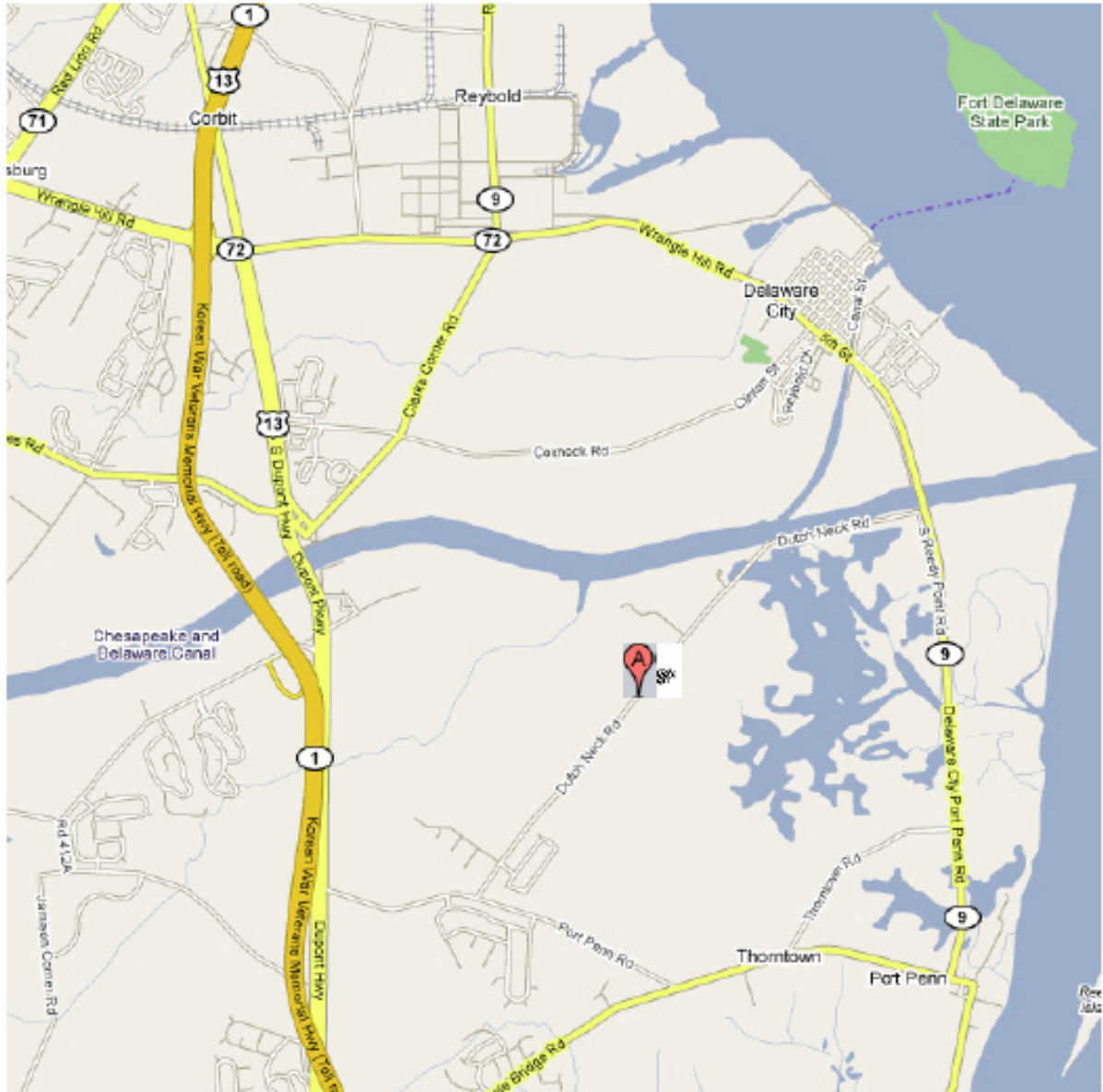


Figure 1. Map showing location of Bridge 1-384 (courtesy DeIDOT Bridge Management)



Figure 2 (a) Bridge 1-384 looking south west



Figure 2 (b) Bridge 1-384 looking south



Figure 3. Mounting transducers

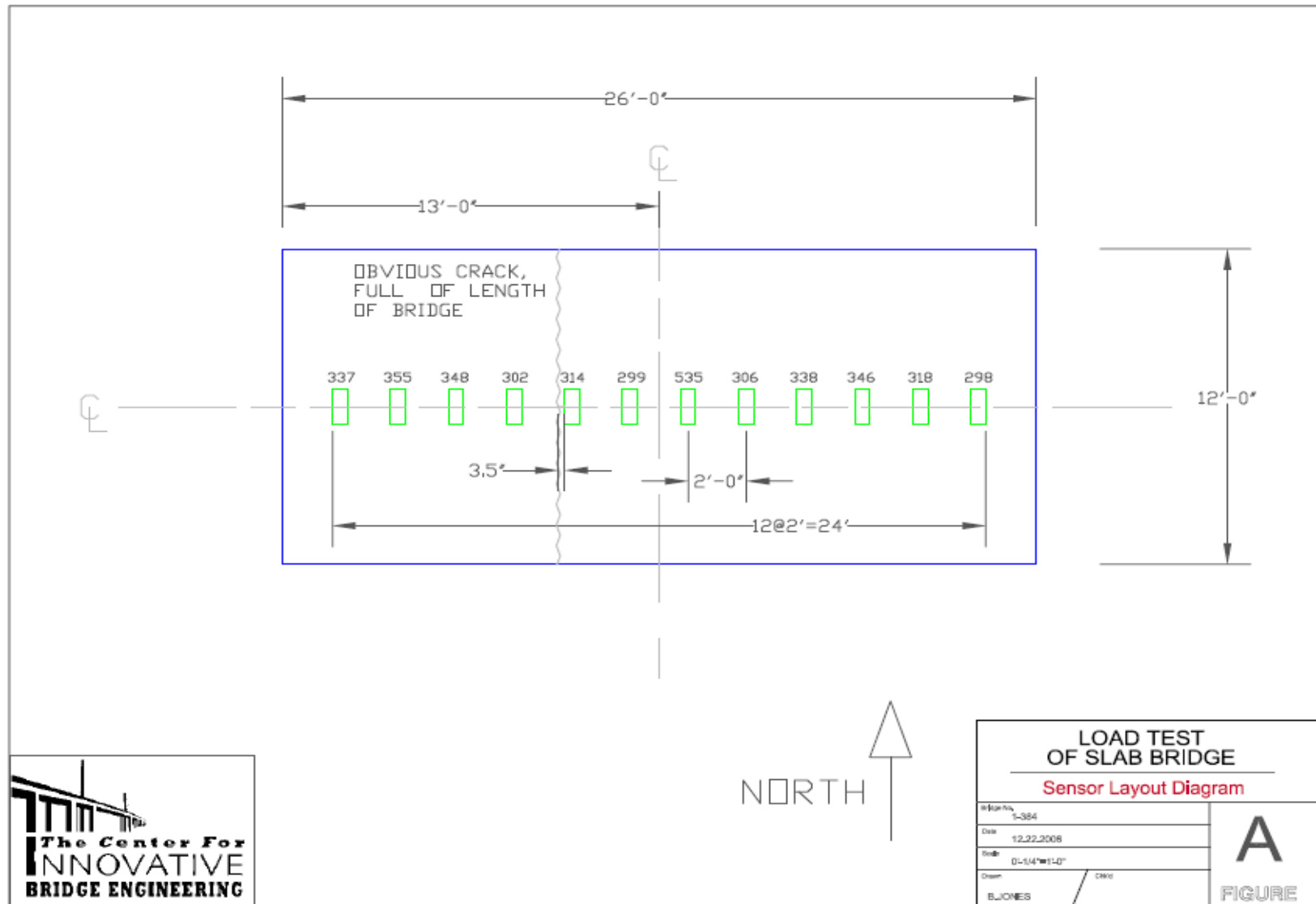


Figure 4. Sensor layout

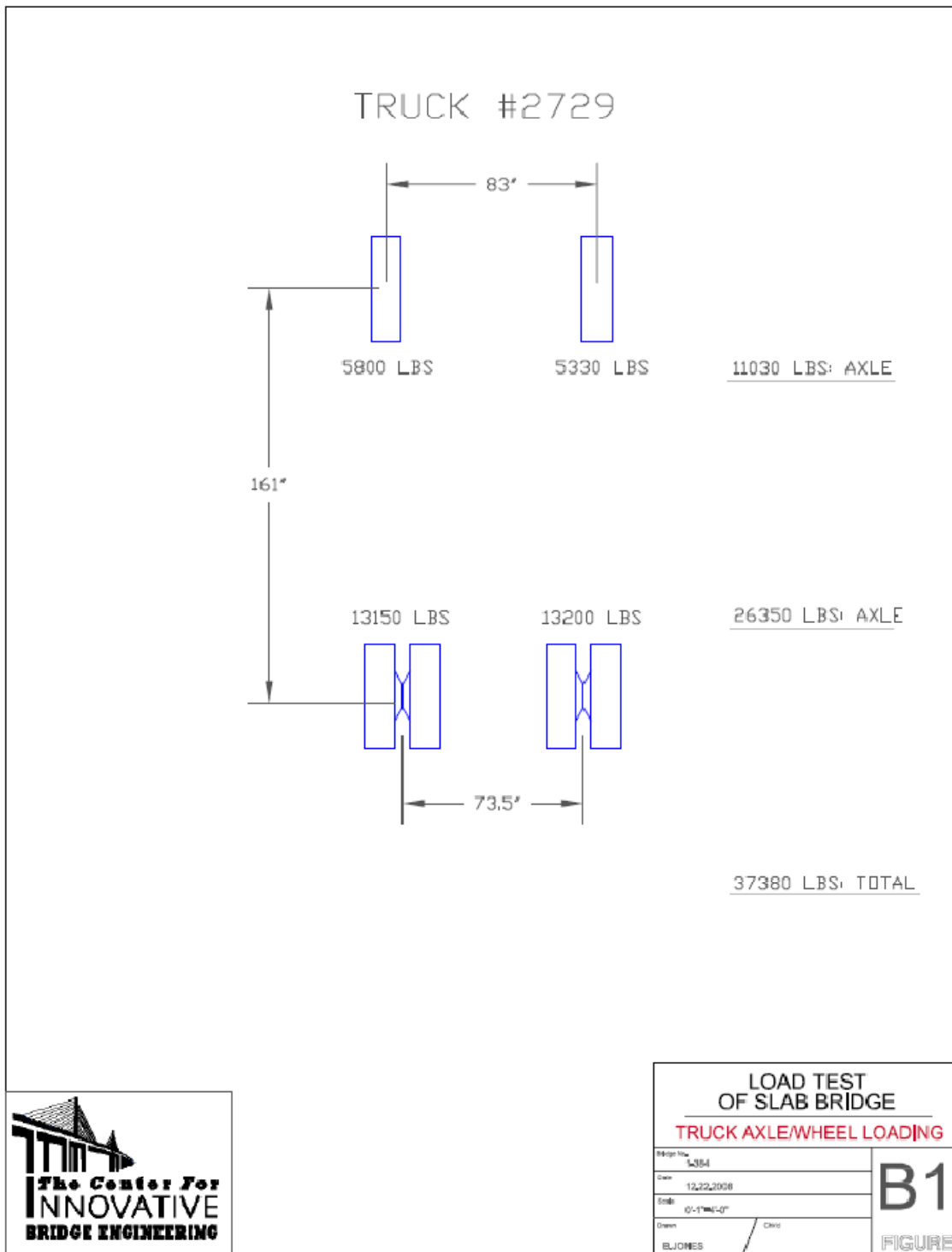


Figure 5. Wheel weights of truck #2729

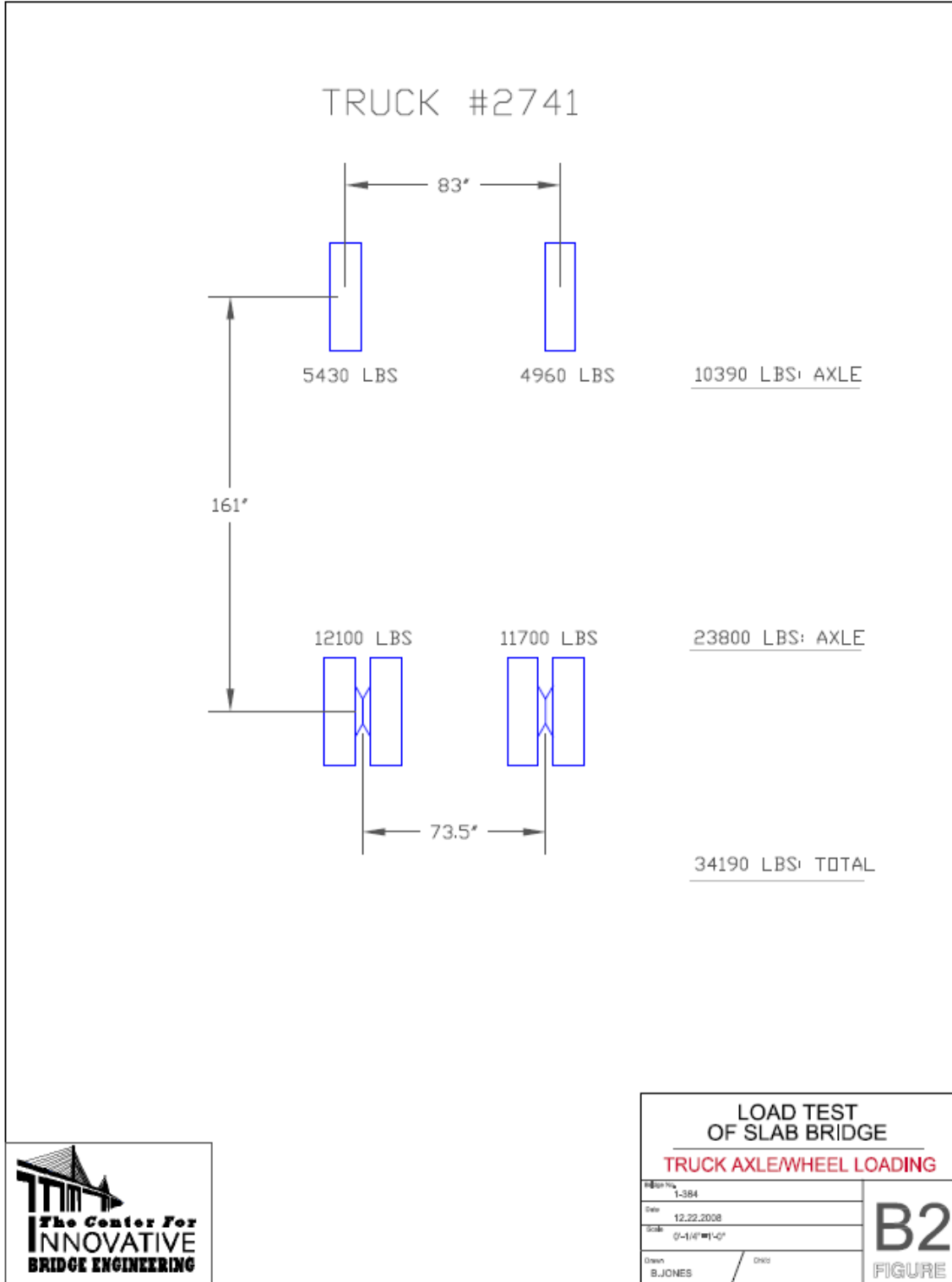


Figure 6. Wheel weights of truck #2741

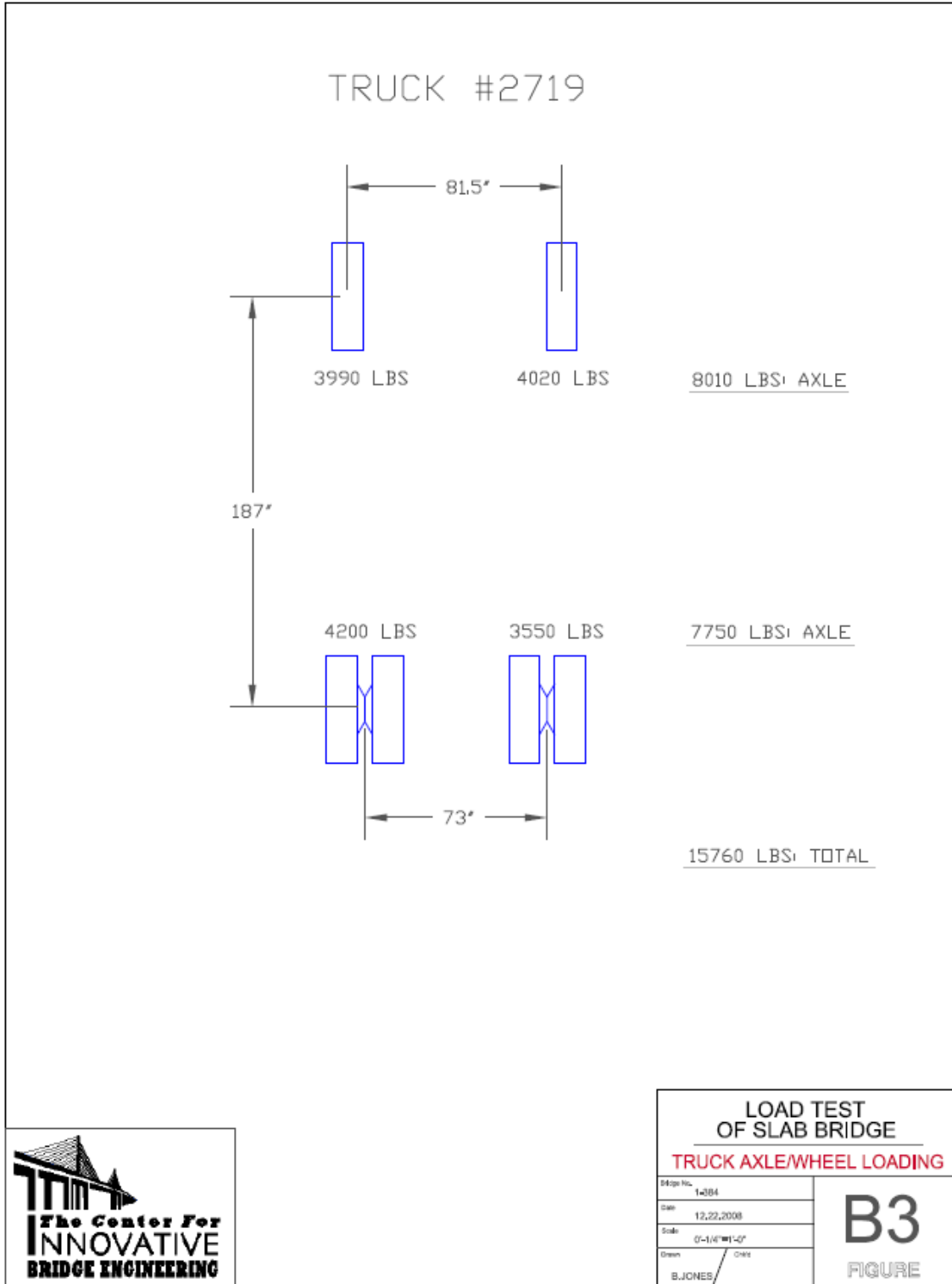


Figure 7. Wheel weights of truck #2719



Figure 8. Truck #2729 – right lane



Figure 9. Truck #2729 – center



Figure 10. Truck #2729 – left lane



Figure 11. Side-by-side truck (trucks #2729 and #2741) passes



Figure 12. Trucks #2729 and #2741 (36 ton combined load) on 7 ton posted bridge

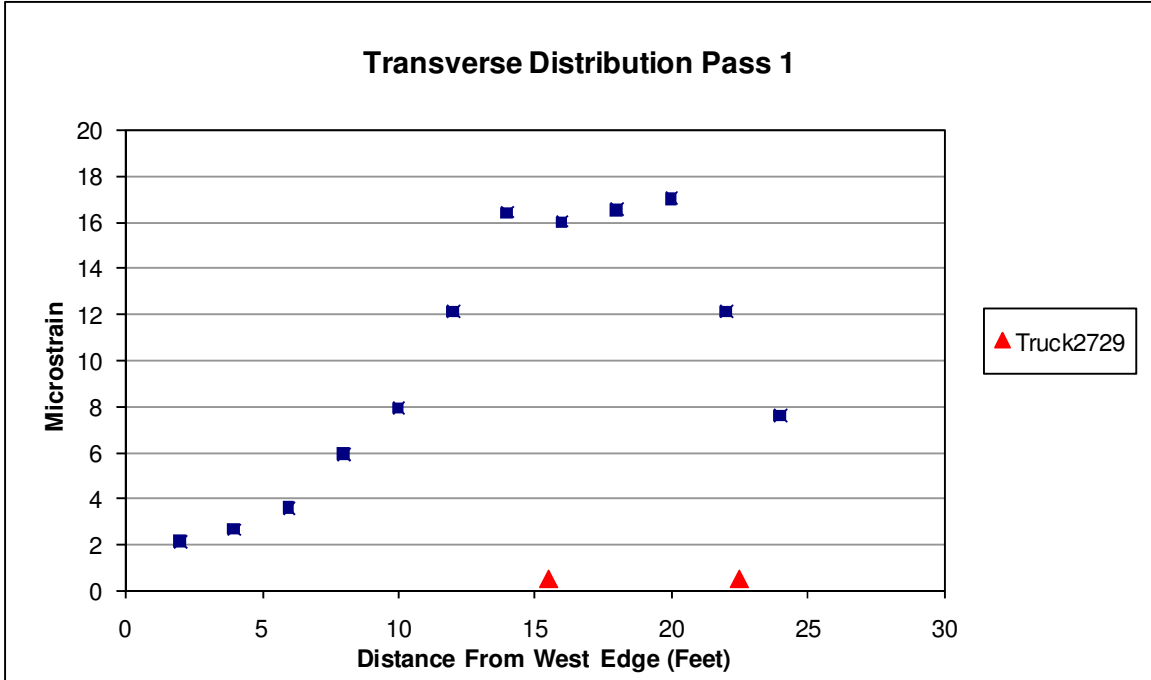


Figure 13. Transverse strain distribution Pass 1

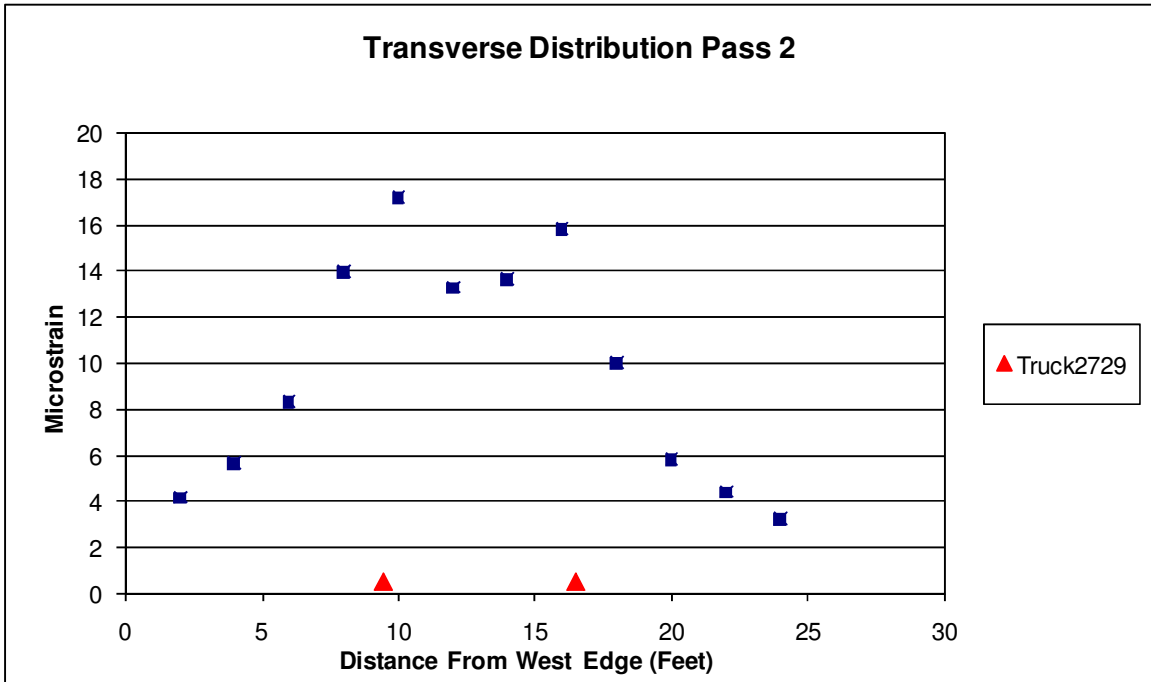


Figure 14. Transverse strain distribution Pass 2

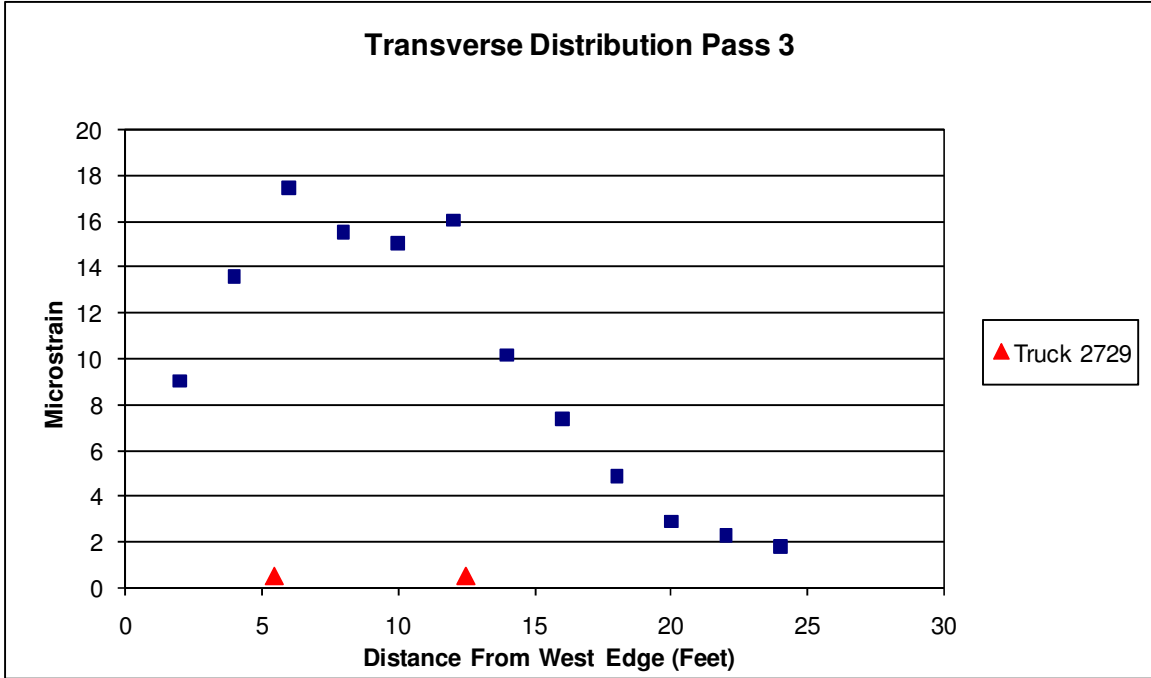


Figure 15. Transverse distribution of strain Pass 3

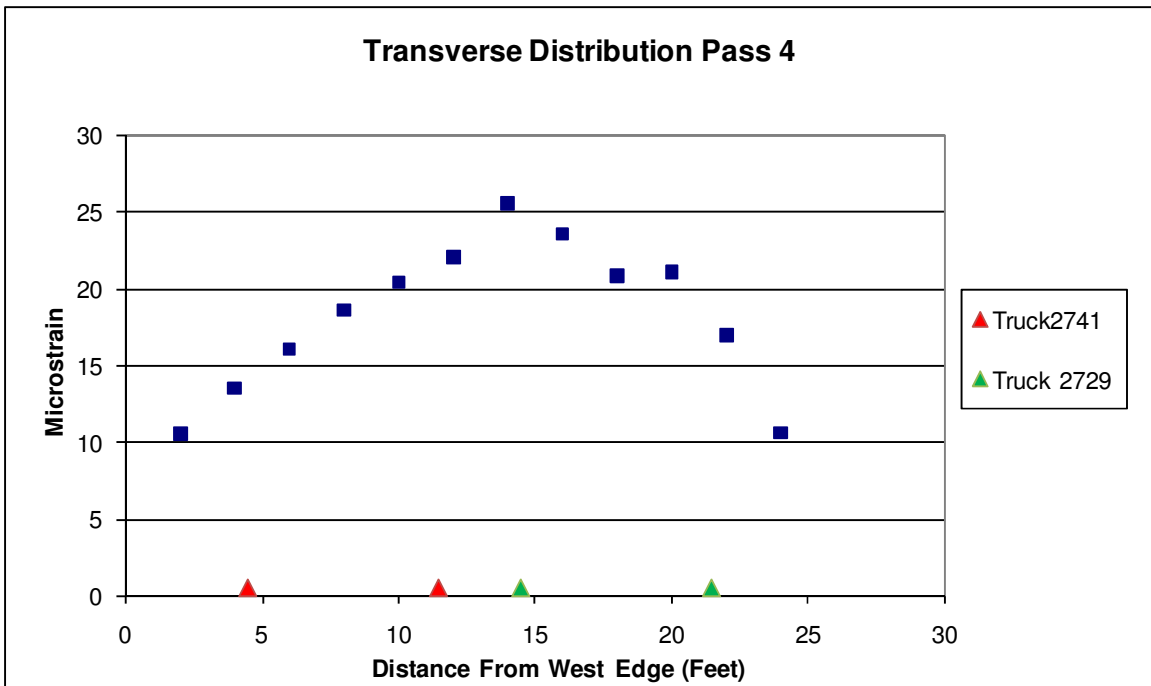


Figure 16. Transverse distribution of strain Pass 4 (two trucks side-by-side)

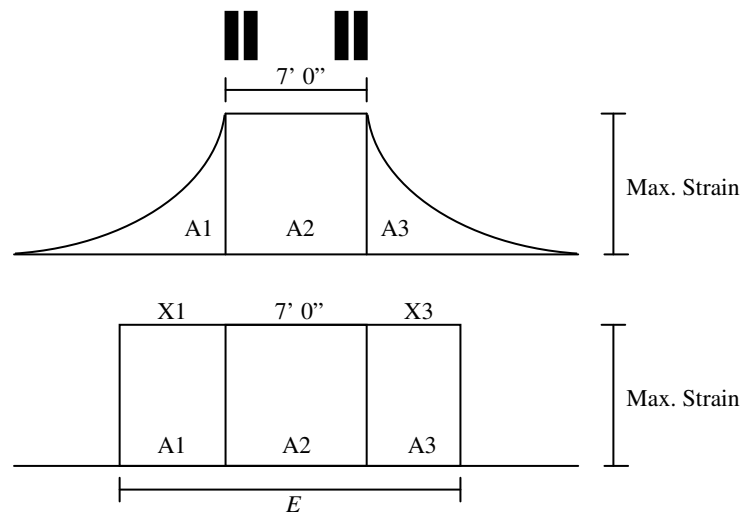


Figure 17. Idealized strain distribution and effective width representation

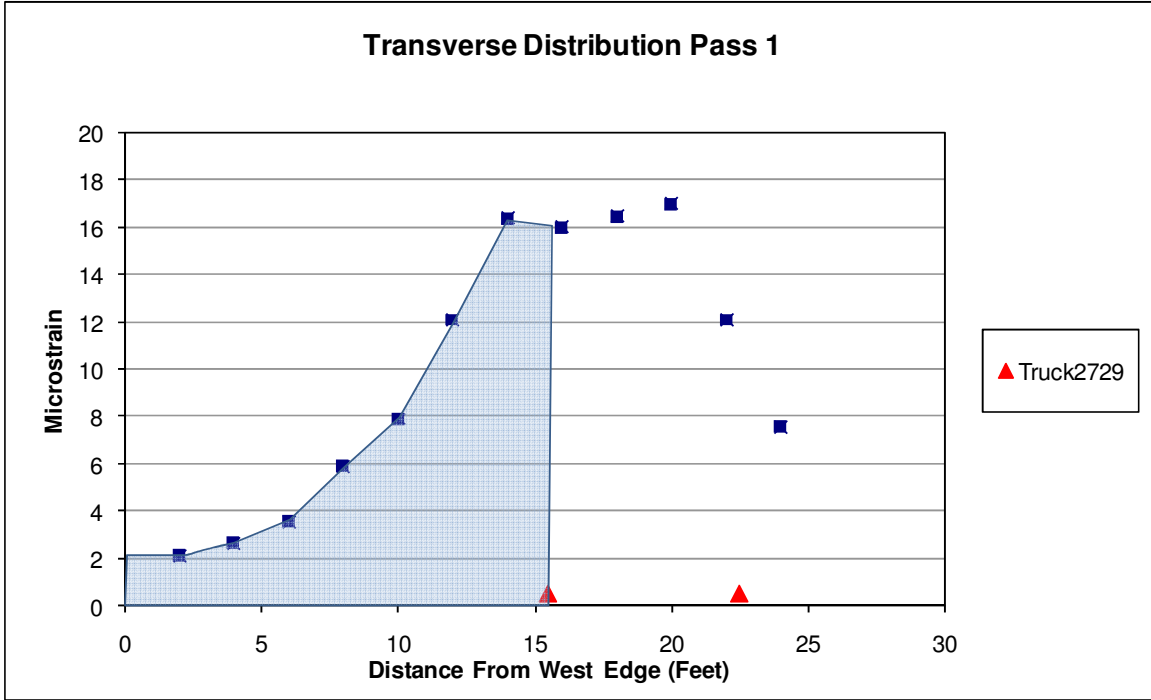


Figure 18. Determination of area A1 for single truck

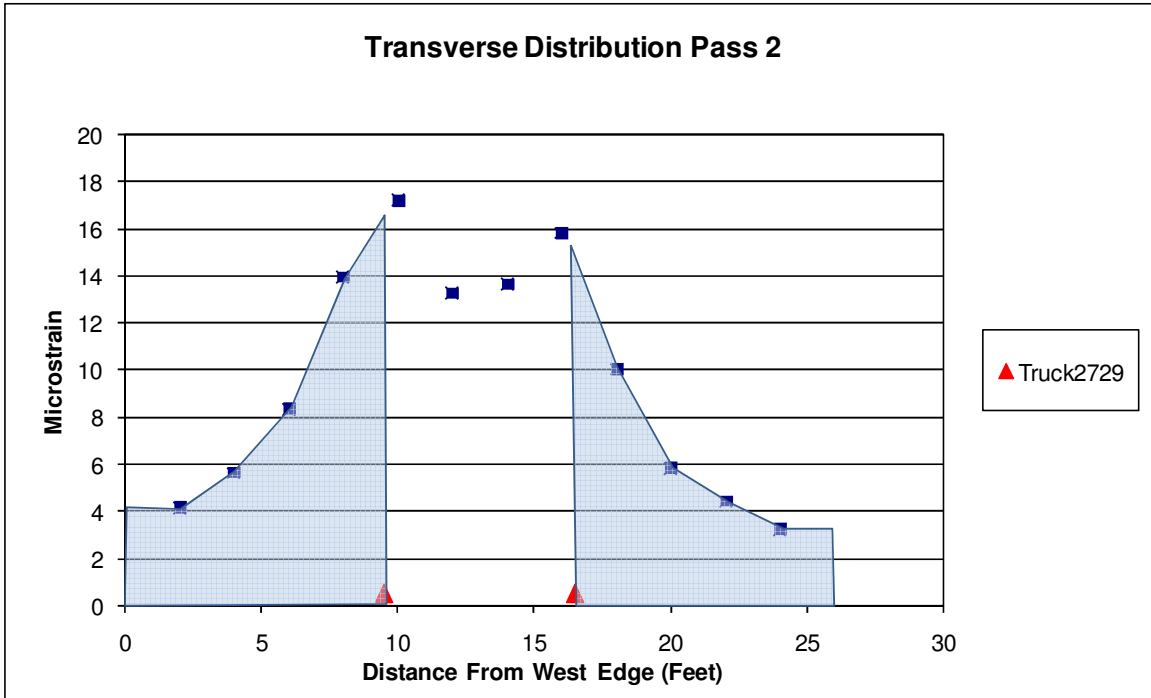


Figure 19. Determination of areas A1 and A3 for single truck

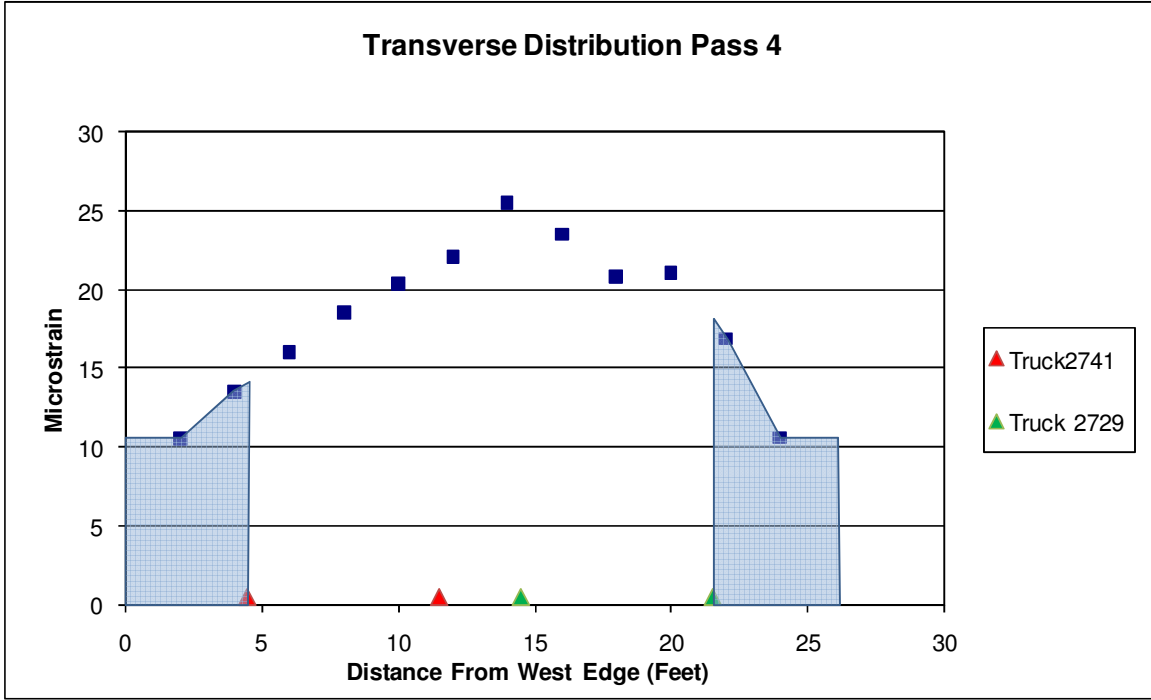


Figure 20. Determination of areas A1 and A3 for side-by-side trucks

Appendix E

BRIDGE TEST REPORT 3-318

FIELD TEST OF BRIDGE 3-318

by

Harry W Shenton III, Ph.D., Professor and Chair
&
Brian P Jones, Graduate Research Assistant

*Department of Civil and Environmental Engineering
Center for Innovative Bridge Engineering
University of Delaware
Newark, Delaware 19716*



January 11, 2010

Project:

Bridge 3-318 on Laurel Road
Sussex County, Delaware

Client:

Delaware Department of Transportation
P.O. Box 778
Dover, DE 19903

Executive Summary

The University of Delaware conducted a load test of Bridge 3-318 on Laurel Road, Sussex County, Delaware on October 29, 2009 to evaluate its transverse load distribution. The slab bridge was originally constructed in 1924; an additional 6 ft of roadway was added in 1949. The slab was instrumented with nineteen strain transducers placed on the underside of the concrete slab. Two fully loaded 10-wheel dump trucks were used as a controlled live load for the test. The gross weight of truck #2826 was 59.7 kips, with a combined rear axle weight of 45.2 kips. The gross weight of truck #2939 was 62.1 kips, with a combined rear axle weight of 45.7 kips. The test utilized 12 load passes in which the truck(s) moved across the bridge at a slow crawl. The maximum recorded concrete tensile stain at any time during the test was $14 \mu\epsilon$. Based on evaluation of the observed transverse load distribution, a conservative estimate for the effective slab width of the bridge for two vehicles is 9.0 ft. This is approximately equal to the AASHTO LRFD width of 9.1 ft for multi-lane loading. For a single truck a conservative effective width is 9.9 ft, which is 36% greater than the AASHTO LRFD width of 7.29 ft for single lane loading.

Description of the Bridge

Bridge 3-318 is located on Laurel Road, west of Bethany Beach, Sussex County, Delaware. It is a concrete slab bridge/culvert with an 8 foot span and an out-to-out deck width of 37.8 foot. The bridge was originally constructed in 1924 and renovated in 1949 when an additional 6 foot 6 inches of roadway were added. A location map of the bridge is shown in Figure 1; pictures of the bridge are shown in Figures 2 through 4.

The bridge has an ADT of 3219 vehicles (as of 2008) with 3% being trucks. It was last inspected on May 27, 2009.

Test Purpose

The load test was performed at the request of DelDOT's Bridge Management section in order to assess the transverse load distribution, i.e., effective width, of the slab. The reinforcement details at the ends of the slab do not appear to be sufficient to transfer negative bending into the abutment walls. As such, the bridge must be rated as a slab as opposed to a rigid frame. It was determined that a load test would allow a more accurate assessment of the bridge's transverse load distribution characteristics. The remainder of this report discusses how the bridge was tested and how the effective slab width was computed using load test data, and provides a comparison to the AASHTO effective width.

AASHTO Effective Width

The equation for effective width of a slab, per AASHTO LRFD, is

$$E = 10.0 + 5.0\sqrt{L_1 W_1} \quad (1)$$

for a single lane loaded, and

$$E = 84.0 + 1.44\sqrt{L_1 W_1} \leq \frac{12.0W}{N_L} \quad (2)$$

for multilane loading, where:

- E = Equivalent width (in.)
- L_1 = Modified span length taken equal to the lesser of the actual span or 60.0 (ft.)
- W_1 = Modified edge-to-edge width of bridge taken to be equal to the lesser of the actual width or 60.0 for multilane loading, or 30.0 for single-lane loading (ft.)
- W = Physical edge-to-edge width of bridge (ft.)
- N_L = Number of design lanes

For bridge 3-318

- L_1 = 8 ft
- W_1 = 30 ft for single lane
37.8 ft for multilane loading
- W = 37.8 ft
- N_L = 2

Substituting these values into the expressions above yields $E = 87.46$ in. = 7.29 ft. for single lane loading and $E = 109.0$ in. = 9.09 ft. for multilane loading.

For comparison, the formula for effective width per the AASHTO Standard Specification is

$$b_{eff} = 4.0 + 0.06S \quad (3)$$

where S is the span in ft. The effective width per the Standard Specification is $b_{eff} = 4.48$ ft. Note that b_{eff} is for a single wheel line and must be multiplied by 2 for direct comparison with E , which is for two wheel lines.

Test Setup

The bridge load test was conducted on October 29, 2009 using the Bridge Diagnostics Inc, Structural Testing System (STS) and two 10-wheel trucks. Nineteen strain transducers were mounted to the underside of the concrete slab.

Each transducer was equipped with 12 inch extensions and were mounted at the midspan of the 8 foot clear span. The transducers were mounted with a transverse spacing of 2 feet per transducer. The transducers were mounted to the slab using a quick setting two-part epoxy manufactured by Loctite. Four transducers were also mounted to the vertical walls (abutments) of the bridge; however, the data from these sensors was not used in analysis of the results and are not reported here. No special equipment or ladders were needed to access the bottom of the slab. Figure 5 shows the transducer layout with the associated three-digit transducer identification number. All of the strain transducers were connected to the STS data acquisition system and were read simultaneously, at an appropriate sampling rate during the test.

Along the bottom of the slab the construction joint was noted by the crew and can be seen in Figure 4. The joint is north of the centerline of the bridge and runs longitudinally from one abutment to the other. Transducers were mounted 6 inches to each side of the joint. Strain gage 1476 was located to the south of the joint and gage 1477 was located to the north of the joint.

Two loaded dump trucks were used as controlled live loads for the test. The truck axles were weighed at the site using Intercomp portable truck scales which are accurate to within ± 10 lbs. The gross weight of truck #2826 was 59.7 kips, with a combined rear axle weight of 45.2 kips. The spacing between the front and rear axle was 15'-5". The spacing between the first rear axle and the second rear axle was 4'6". The gross weight of truck #2939 was 62.1 kips, with a combined rear axle weight of 45.7 kips. The spacing between the front and rear axle was 15'-2". The spacing between the first rear axle and the second rear axle was 4'6". As a result, for each truck, when the rear axle was at midspan the front axle was off of the bridge. Figures 6 and 7 show the measured wheel spacings and wheel loads of the two vehicles.

A total of 12 truck passes were completed and are listed in Table 1. In all cases the truck or trucks crossed the bridge in a westward direction (toward Laurel). All passes were conducted at a "crawl" speed, i.e., between 5 and 10 mph. The transverse position of the truck on the bridge is defined by "right shoulder", "right lane", "center", and "left lane" when looking in a westward direction. Passes 1 through 8 involved only a single truck (#2826 and #2939). Passes 8 through 12 were side-by-side truck passes with truck #2826 on the right and truck #2939 on the left.

Photos of the various truck passes are shown in Figures 8 through 11.

Results

Peak Strains and Transverse Strain Distribution

The strains induced in the slab by the load vehicles were very small: the absolute maximum recorded concrete tensile stain at any time during the test was 14 $\mu\epsilon$. This occurred at gage 298, which was located very near the center of the bridge and occurred for pass 12 (both vehicles on the bridge at the same time). The absolute maximum strain recorded for a single truck pass was 11 $\mu\epsilon$. This occurred at gage 306, also near the center of the bridge, for pass 7 (truck in the left lane). The absolute maximum recorded strains are listed for all gages in Table 2.

Although these strains are very low, good resolution was achieved in the measurements by using the concrete extensions. It should be noted, however, that these are average strains over the measurement range; the peak strain may be somewhat underestimated because of that.

The very low strains can be attributed to two factors. First is possible frame action provided by the abutments. Although the bridge was not designed as a rigid frame, there is some continuity between the slab and walls which will tend to reduce the strain at mid-span. Second, the concrete strength may be greater than the design specified strength, which will also tend to reduce the strain at mid-span.

A few comments are in order regarding some of the sensors before discussing the results. Sensors 350 and 1478 did not function and thus there was no data read for those two sensors. Sensor 1478 was 3 ft north of the centerline and sensor 350 was 7 ft north of the centerline. Sensor 298 had a large amount of “noise” in the data. The readings appeared to follow a typical strain graph over time, but with a high amount of variation in the strain reading for a particular instant. This data was smoothed using a ten point moving average. Figures 12 and 13 show the strain over time of sensor 298, both raw data and smoothed.

Sensor 339 showed a large amount of “drift” in the data. Although most of the data from each run appears to follow a typical strain path, there is a certain positive or negative “drift” of the data during the reading. This was partially corrected by fitting a straight line to the linear trend and then subtracting that from the raw data. For instance, the data for Run 3 was an extreme outlier and calculated a large negative strain (See Table 2). Sample strain time histories for gage 339 are shown in Figures 14 and 15.

Finally, the data for sensor 346 was on average about 30% larger than what might be expected data, based on the transverse distribution plot. This value was calculated as a percent difference of what strain is expected on a typical distribution graph based on its two adjacent sensor’s data and what data was

actually read. Sensor 346 is located 2' 6" north of the joint. While it appeared to be consistently higher, no adjustments were made to the data from this sensor.

Plots of the transverse distribution of strain for sample single truck passes are shown in Figures 16 through 18, and for one side-by-side truck pass in Figure 19. Clearly the strains are largest underneath the vehicle and tend to get smaller as you move away from the vehicle.

Computation of Effective Slab Width

Figure 20 shows an idealized transverse strain distribution that might result if a rear axle were sitting on an infinitely wide slab. The strain would have a relatively constant peak value (strain max.) between the truck wheels, and would decrease to zero as one moves away from the wheels. This non-uniform strain (or stress) is a result of shear-lag. In order to simplify the evaluation of slabs that exhibit shear lag, the concept of effective width was developed. The effective width section has a constant strain (or stress) across its width. The widely accepted definition of the effective width is the width that would have a uniform strain equal to the maximum strain but creates the same total effect as that caused by the actual strain distribution (Chiewanichakorn et al., 2004). To turn the plot having a varying strain into one having a uniform strain, one must keep the areas A_1 and A_3 for the two distributions equal (see Figure 20).

Figures 21 and 22 show examples of the areas used in calculating the effective width for the single truck passes. Effective widths have been calculated for all of the single truck passes and are summarized in Table 3.

The single truck effective widths vary from a low of 9.9 ft to a high of 16.4 ft. The average is 13.2 ft. The conservative value is the lowest, 9.9 ft. which is 36% higher than the AASHTO LRFD value (7.29 ft.). The average value is 81% higher than the AASHTO LRFD width.

Referring to Table 3, the effective widths for the passes obtained using truck 2826 (59.7 kips) and truck 2939 (62.1 kips) are very consistent. (most corresponding values are within 10 to 15% of each other). This demonstrates the linearity of the bridge behavior, and that the calculation of the effective width is independent of the magnitude of the load.

The effective width calculations for the single truck do show a trend of being higher when the truck is on the north end (traveling westbound) than when it is on the south end. This could be due to the additional width of roadway that was added in 1949 and the construction joint. Two factors could be coming into play with this behavior (1) the concrete strengths in the original and newer section are not the same, and (2) the joint may not be transferring load as effectively as it should be.

One will notice that the strain is not constant beneath the truck (as it is in the idealized depiction). While it may be acceptable to use the average value from this region as opposed to the peak value, effective width calculations found using the peak value will be conservative.

Consideration of Multiple Presence in the Effective Slab Width Calculation

The above calculated widths do not incorporate the effect of side-by-side trucks. In essence, the above values are the effective width resulting from a single vehicle load. If we want to account for side-by-side trucks in the effective width computation, we should place two trucks on the bridge with their wheels as close together as permitted by the code (this would be 4 feet; 2 feet from the edge of each 12 foot lane). These correspond to the results for passes 9 through 12.

Figure 23 shows an example of the areas used in calculating the effective width for the side-by-side trucks. The results are shown in Table 4.

The lowest effective width for the two side-by-side truck runs is 9.0 ft. This is approximately equal to the AASHTO LRFD multi-lane value (9.1 ft.). The average effective width for the two side-by-side trucks is 10.1 ft, which is 11% greater than the AASHTO LRFD multi-lane value.

Presented in Table 5 is a summary of the key results. Also presented in the table is the equivalent effective width for the vehicle based on the AASHTO Standard Specification.

Although it is very unlikely to have side-by-side heavy vehicles on such a narrow bridge, a conservative value for the multi-lane effective width for bridge 3-318 would be 9.0 ft.

References

Chiewanichakorn, M, Aref, A.J., Chen, S.S., and Ahn, I-S, (2004). *Effective Flange Width Definition for Steel-Concrete Composite Bridge Girder*, Journal of Structural Engineering, ASCE, Volume 130, Number 12, P. 2016-2031.

Table 1. Truck passes

Pass #	Description (All trucks moving West towards Laurel)
1	Truck 2826 Right Shoulder
2	Truck 2939 Right Shoulder
3	Truck 2826 Right Lane
4	Truck 2939 Right Lane
5	Truck 2826 Center of Roadway
6	Truck 2939 Center of Roadway
7	Truck 2826 Left Lane
8	Truck 2939 Left Lane
9	Truck 2826 Right Shoulder, Truck 2939 Right Lane
10	Truck 2826 Right Shoulder, Truck 2939 Right Lane
11	Truck 2826 Right Lane, Truck 2939 Left Lane
12	Truck 2826 Right Lane, Truck 2939 Left Lane

Table 2. Absolute maximum recorded slab strain

Absolute max microstrain measured for given gage ID																	
Single Lane Truck Passes																	
Pass #	314	295	356	303	344	306	339	292	533	298	355	337	1476	1477	346	318	294
1	-0.1	0.0	0.2	0.3	0.2	0.2	0.4	0.8	1.1	2.4	4.1	7.2	6.0	5.7	8.5	4.8	2.7
2	0.0	0.0	0.0	0.1	0.3	0.3	0.0	0.7	1.2	3.4	4.2	6.8	5.8	5.7	8.4	4.8	2.4
3	0.2	0.3	0.5	0.6	0.8	1.4	-12.9	4.2	6.4	6.5	7.9	6.0	4.4	3.1	2.8	1.3	0.6
4	0.2	0.2	0.3	0.5	0.6	0.9	3.8	3.3	5.5	6.1	8.0	6.5	4.7	3.3	3.1	1.4	0.6
5	0.6	0.8	1.6	2.4	4.3	6.5	9.5	10.0	10.2	7.2	4.8	1.6	1.0	0.6	0.7	0.2	0.3
6	0.4	0.5	1.0	1.5	2.7	4.7	9.6	9.1	9.7	8.3	6.1	2.5	1.5	0.9	0.9	0.3	0.2
7	1.3	2.7	6.1	8.4	10.3	10.9	10.6	9.6	7.0	2.3	1.2	0.5	0.5	0.3	0.4	0.1	0.1
8	1.5	2.8	6.3	8.4	10.3	10.9	10.1	9.0	6.7	4.3	1.1	0.4	0.4	0.2	0.3	0.2	0.1
Max	1.5	2.8	6.3	8.4	10.3	10.9	10.6	10.0	10.2	8.3	8.0	7.2	6.0	5.7	8.5	4.8	2.7
Multi Lane Truck Passes																	
Pass #	314	295	356	303	344	306	339	292	533	298	355	337	1476	1477	346	318	294
9	0.3	0.5	0.9	1.4	2.3	4.1	5.8	9.2	10.2	12.2	10.2	9.5	7.5	6.4	9.3	5.6	3.1
10	0.3	0.5	1.1	1.7	3.0	5.2	9.8	10.3	11.0	13.4	10.7	9.7	7.8	6.8	9.2	5.3	3.1
11	1.6	3.0	6.6	8.9	11.1	12.3	12.7	13.5	13.3	8.5	9.2	6.6	4.8	3.4	3.3	1.3	0.9
12	1.5	2.9	6.5	8.8	10.7	11.7	13.3	12.6	12.5	14.0	9.0	6.7	4.9	3.6	3.4	1.3	0.8
Max	1.6	3.0	6.6	8.9	11.1	12.3	13.3	13.5	13.3	14.0	10.7	9.7	7.8	6.8	9.3	5.6	3.1

Table 3. Measured Effective width based on single truck passes

Pass	E_m
1	15.9
2	16.4
3	14.1
4	14.6
5	9.9
6	11.4
7	11.0
8	12.0
Average	13.2
SD	2.4

Table 4. Measured Effective width based on side-by-side truck passes

Pass	E_m
9	9.0
10	9.1
11	11.2
12	11.1
Average	10.1
SD	1.2

Table 5. Comparison of AASHTO and measured effective width (ft)

Lane loading	AASHTO LRFD (E)	AASHTO Standard Specification ($2b_{eff}$)	Measured E_m	
			Min	Average
Single	7.29	8.96	9.9	13.2
Multilane	9.09	8.96	9.0	10.1

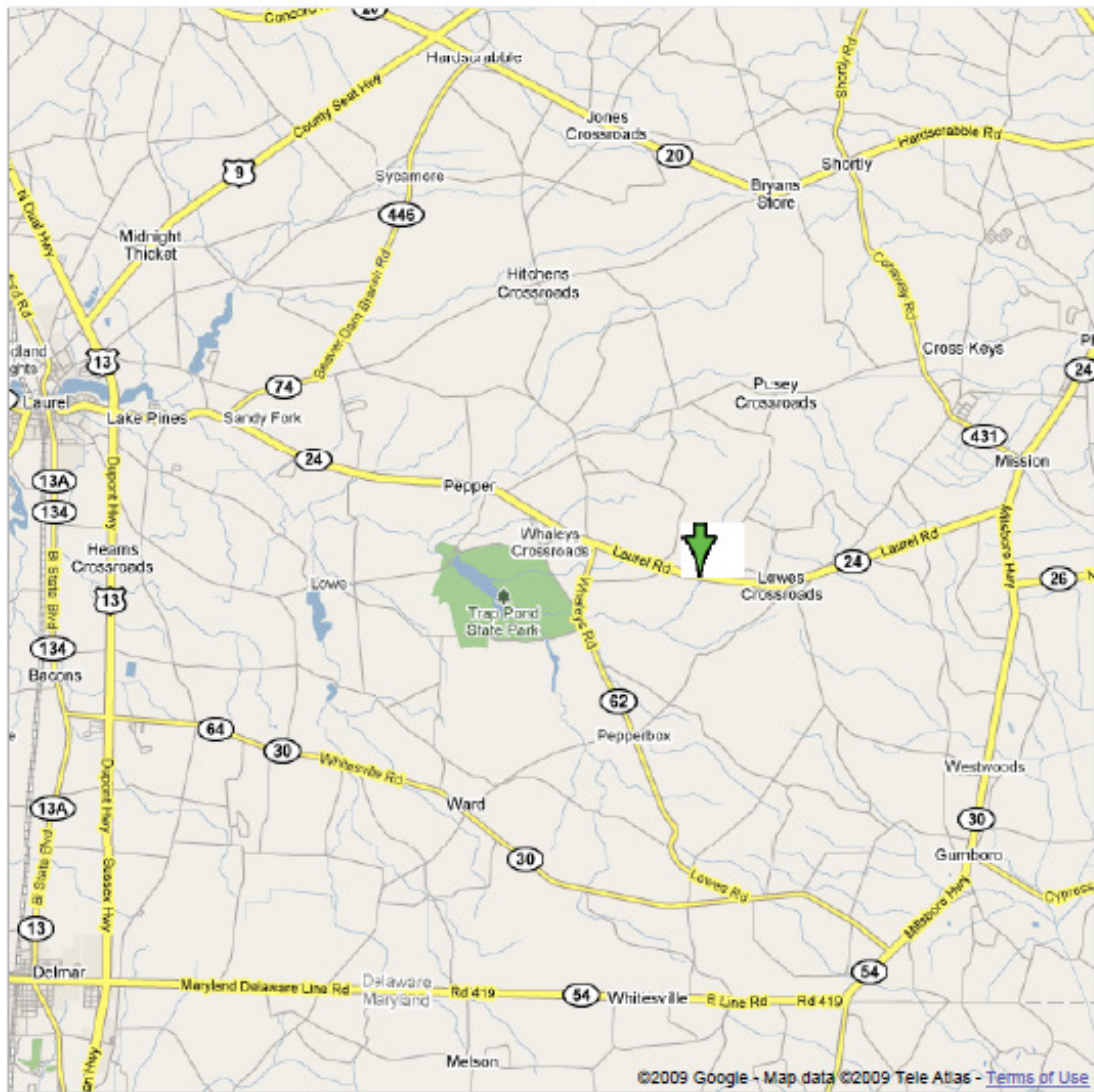


Figure 1. Map showing location of Bridge 3-318 (courtesy DeIDOT Bridge Management)



Figure 2 (a) Bridge 3-318 looking southeast



Figure 2 (b) Bridge 3-318 looking south



Figure 3. Mounted transducers



Figure 4. Longitudinal joint and adjacent sensors

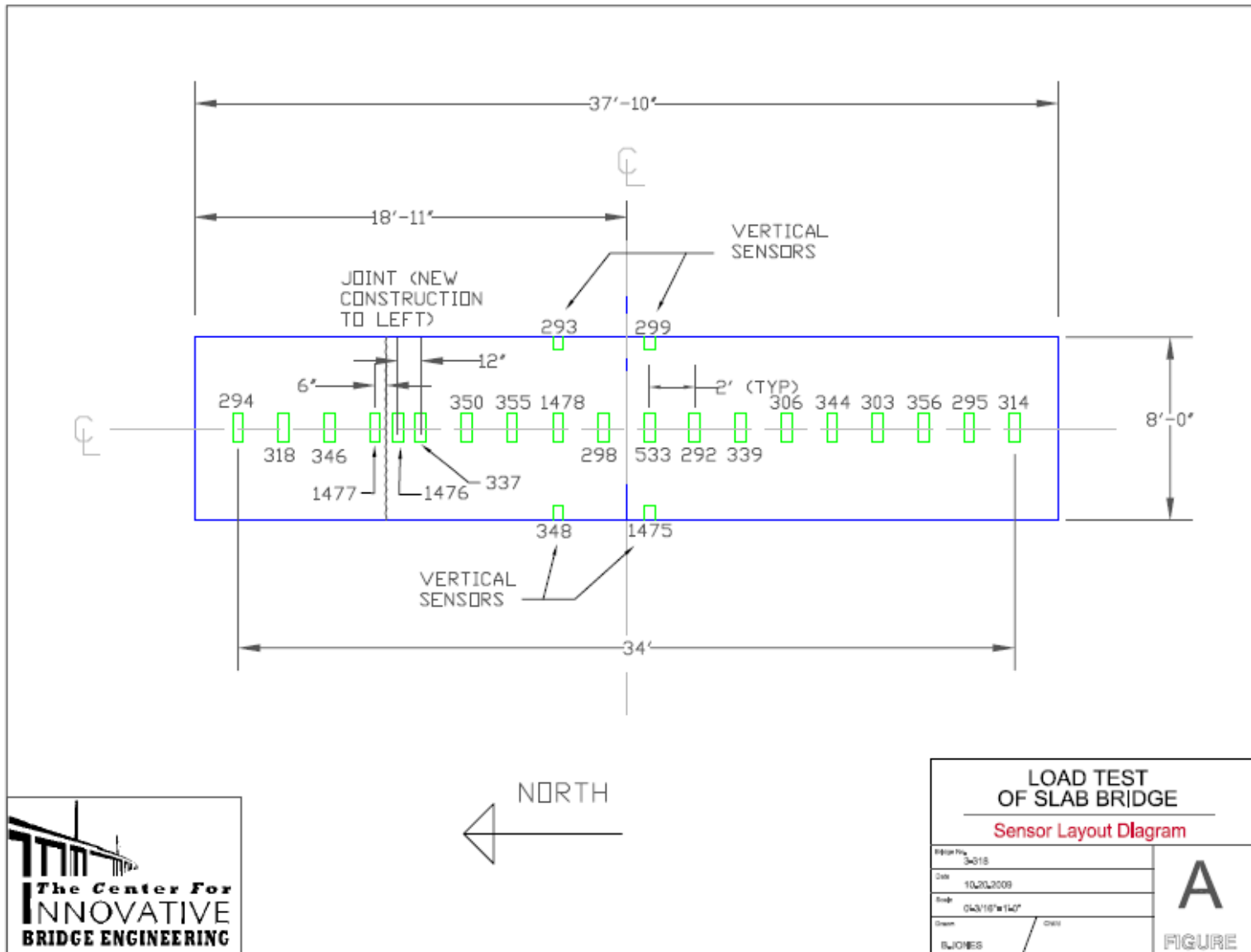


Figure 5. Sensor layout

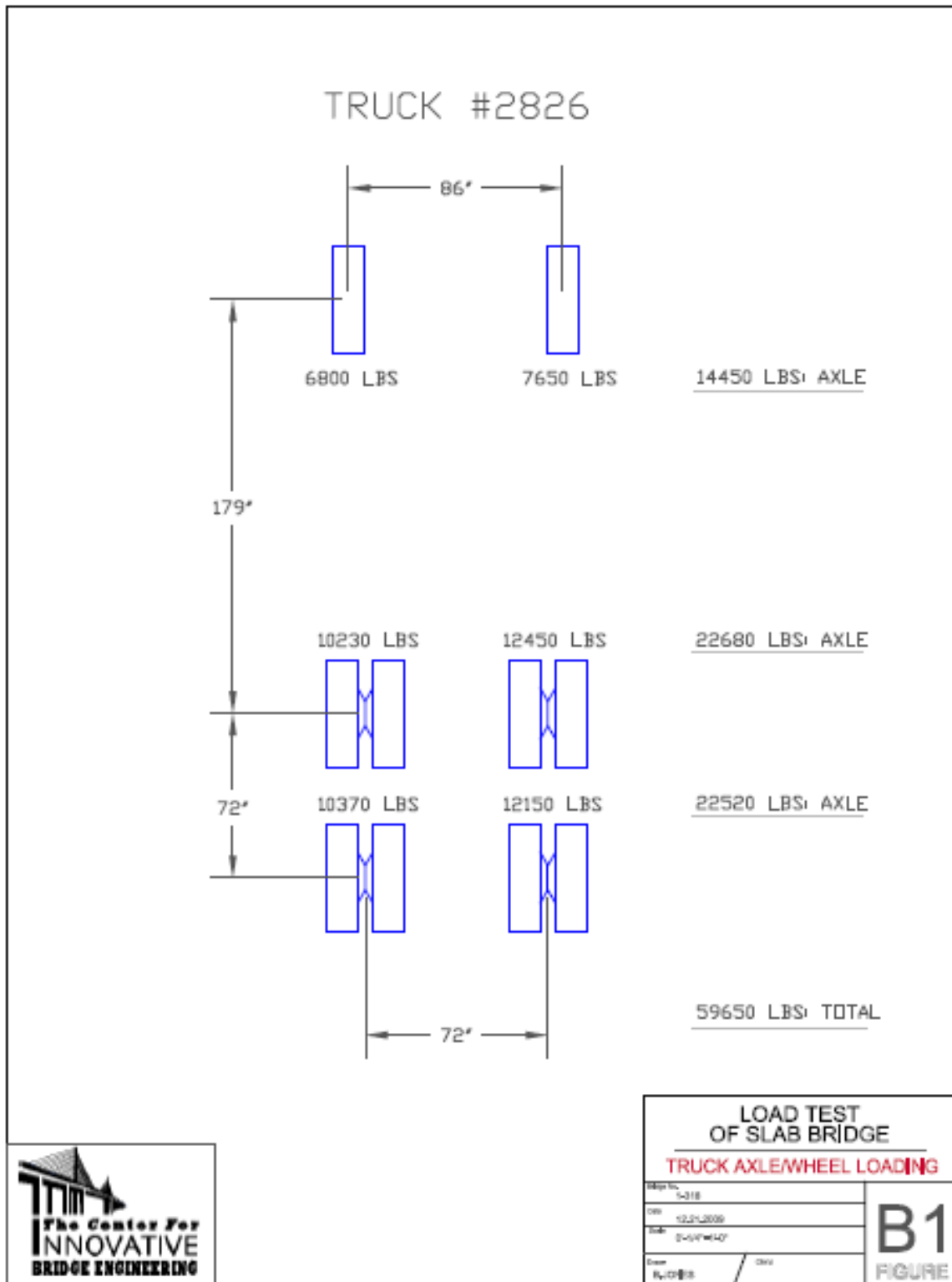


Figure 6. Wheel weights of truck #2826

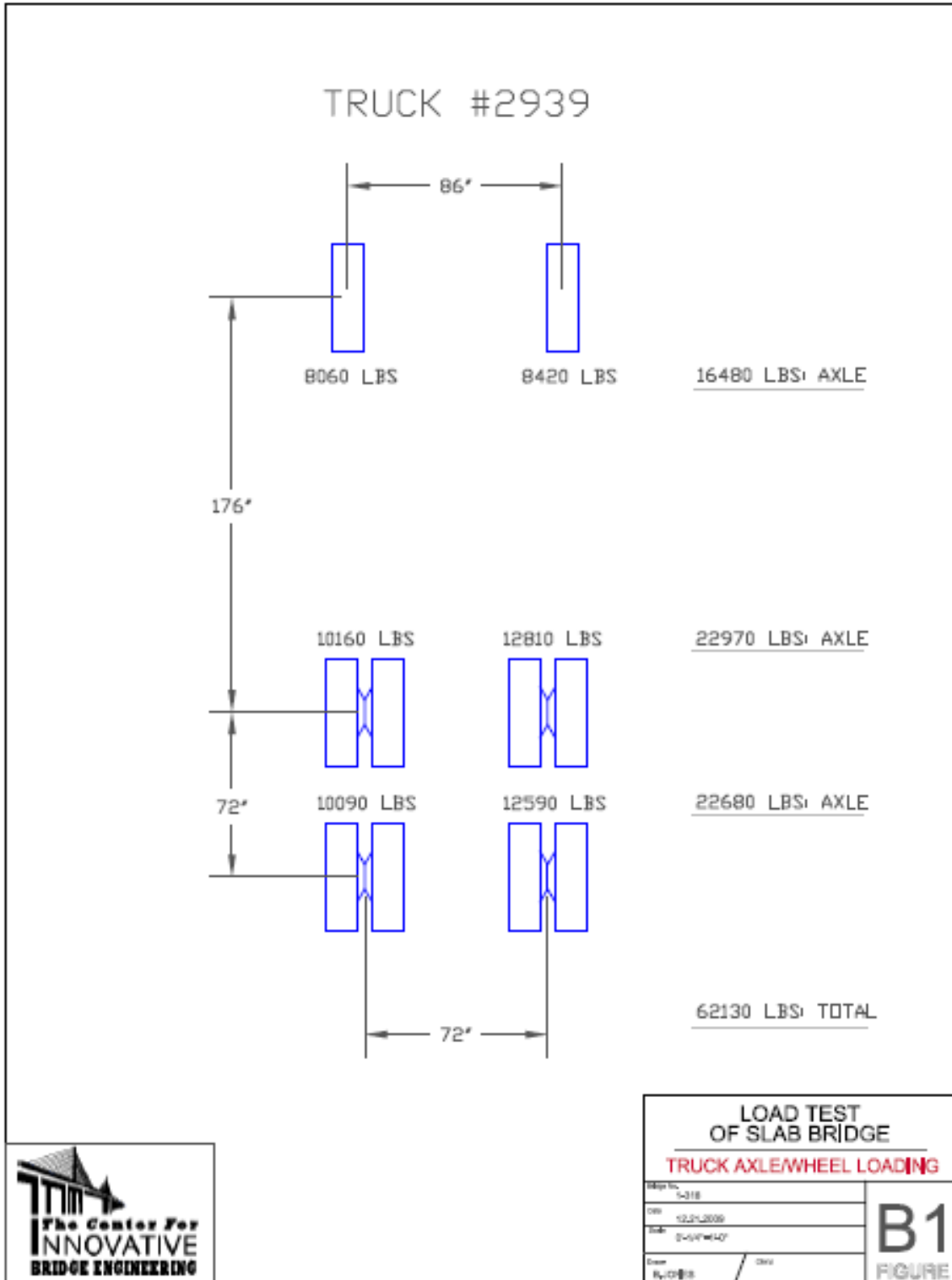


Figure 7. Wheel weights of truck #2939



Figure 8. Truck #2939 – right shoulder



Figure 9. Truck #2939 – center of roadway



Figure 10. Truck #2826 – left lane



Figure 11. Side-by-side truck (trucks #2826 and #2939) passes

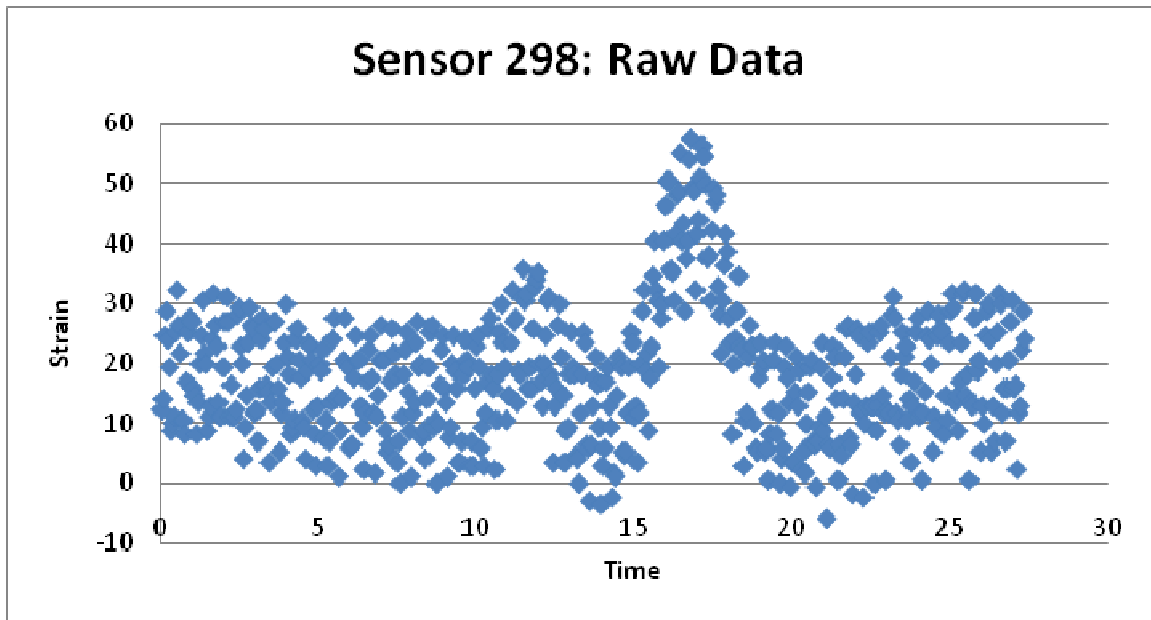


Figure 12: Raw data - sensor 298

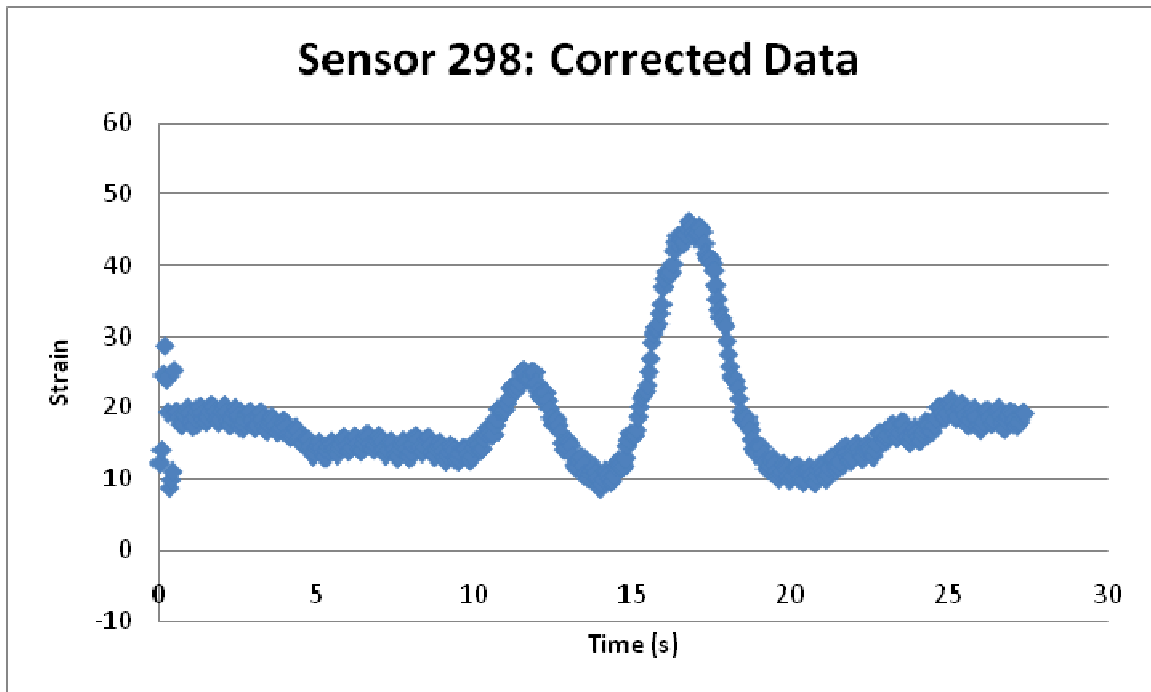


Figure 13: Sensor 298 after 10 point moving average

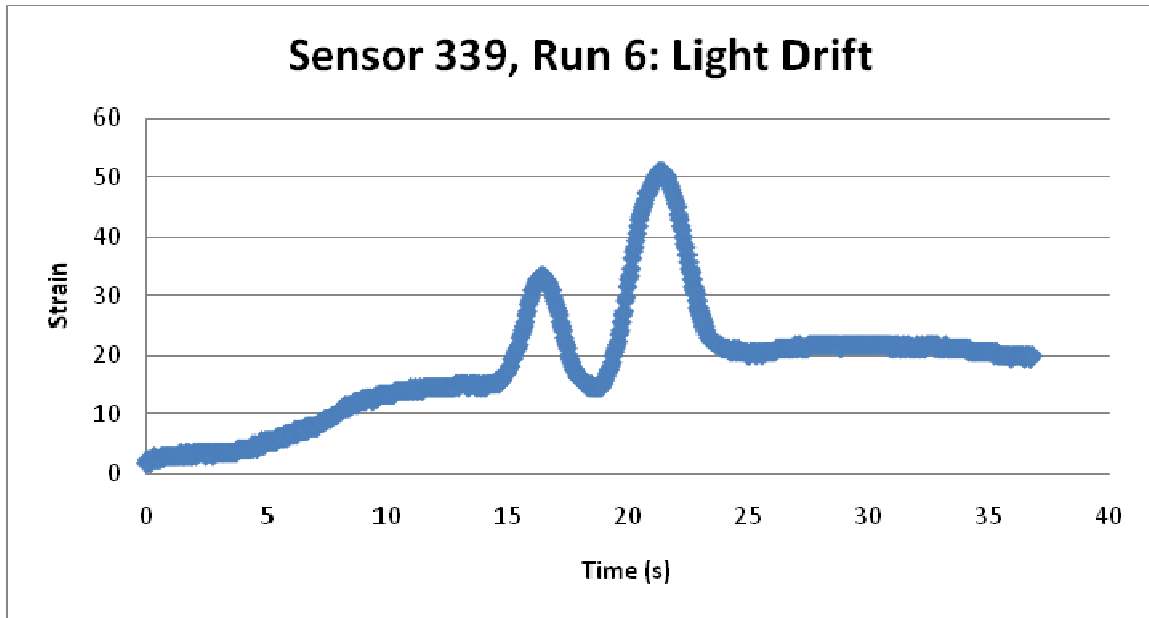


Figure 14: Sensor 339 strain over time, light drift

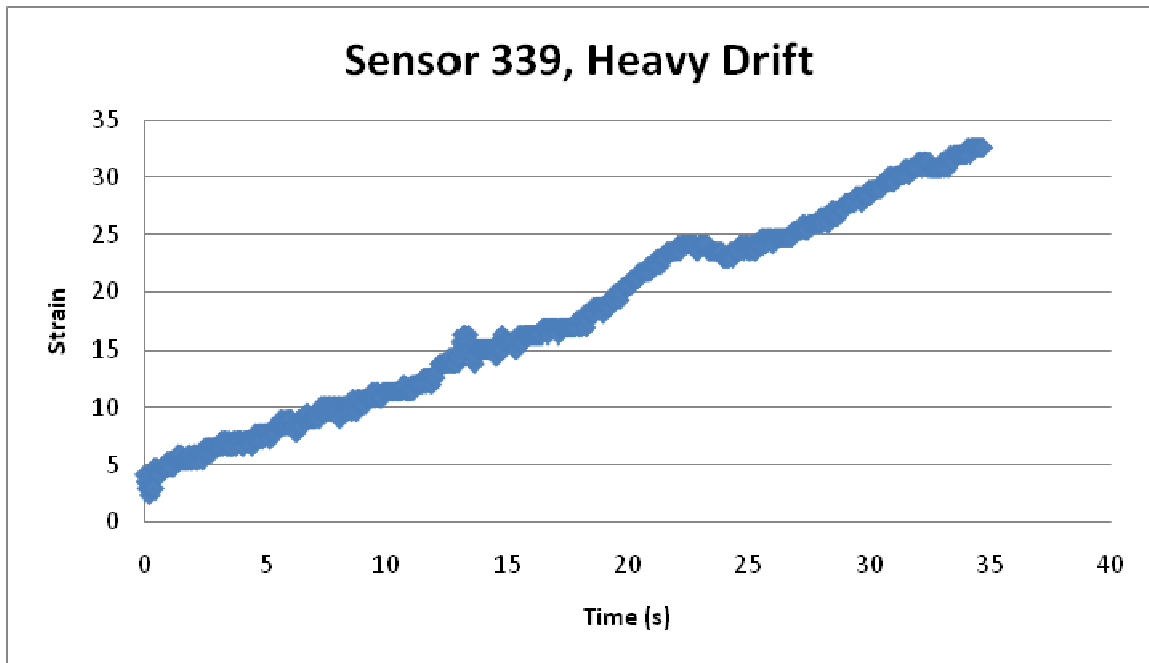


Figure 15: Sensor 339 strain over time, heavy drift

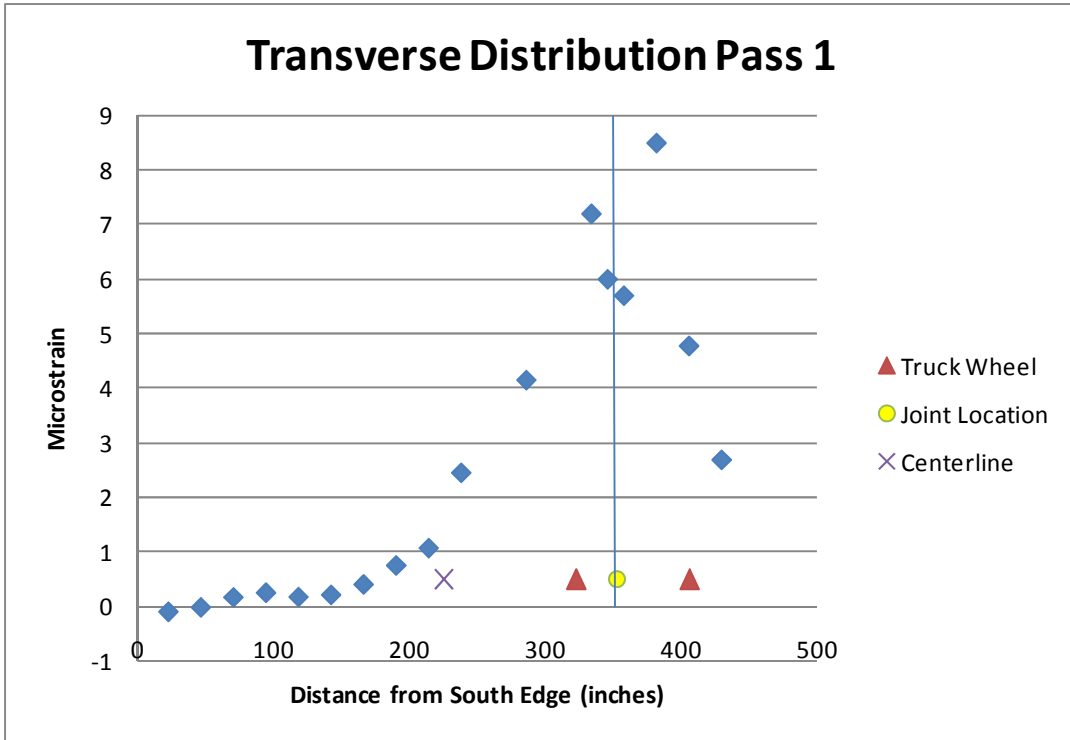


Figure 16. Transverse strain distribution Pass 1

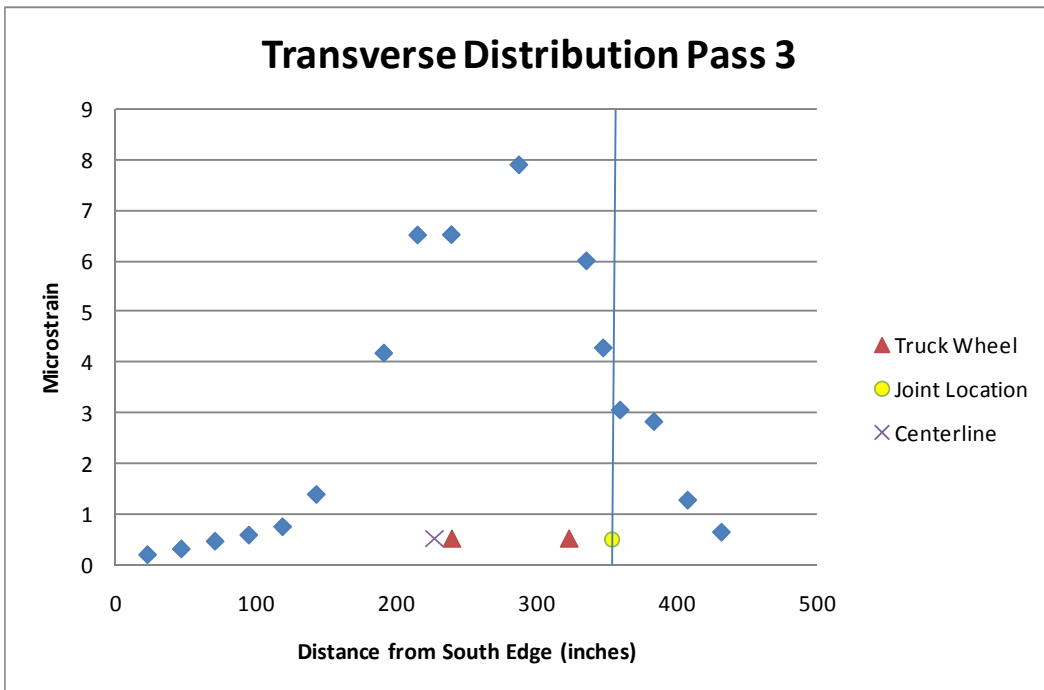


Figure 17. Transverse strain distribution Pass 3

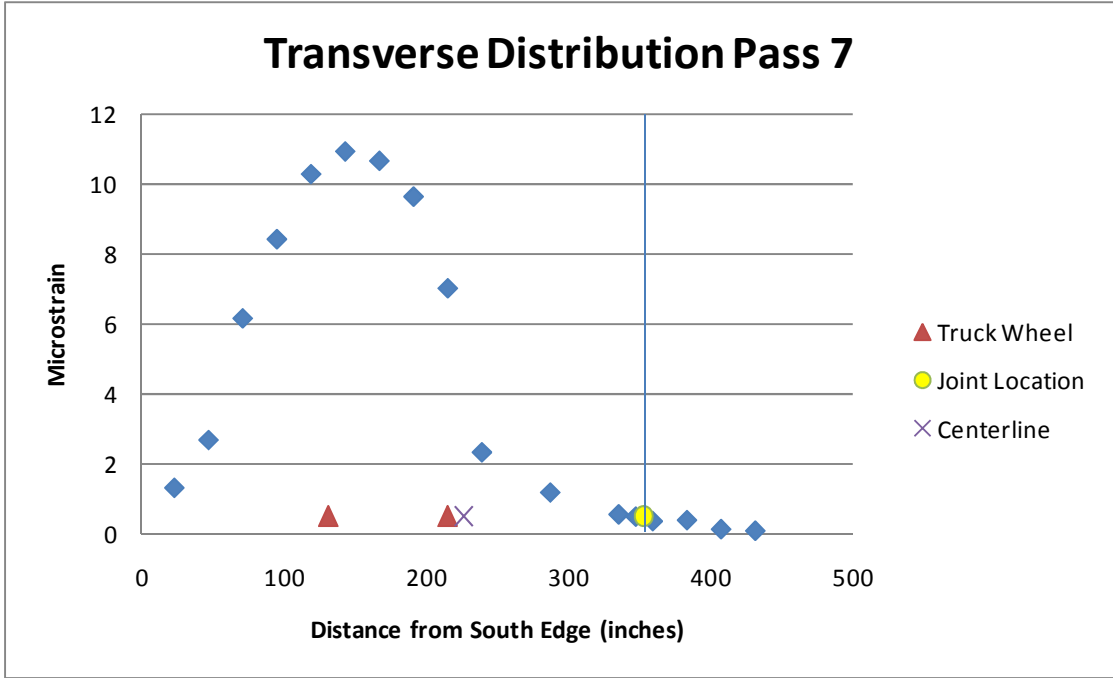


Figure 18. Transverse distribution of strain Pass 7

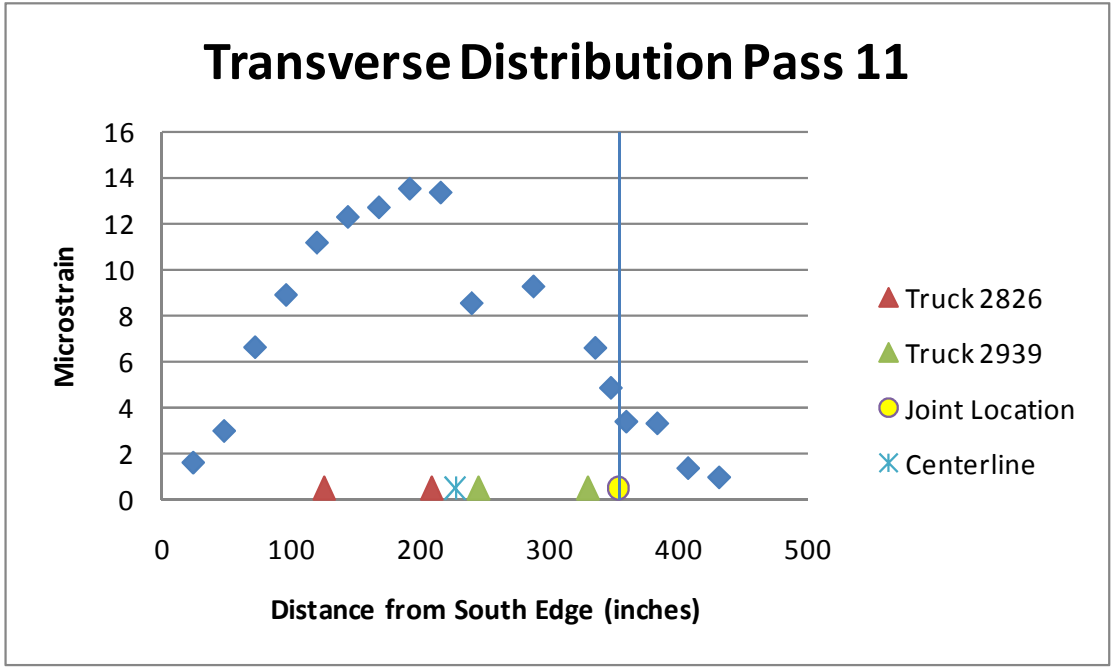


Figure 19. Transverse distribution of strain Pass 11 (two trucks side-by-side)

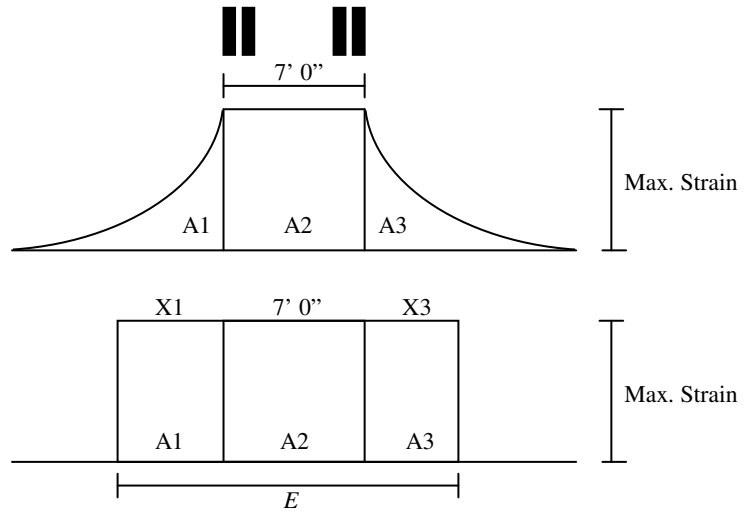


Figure 20. Idealized strain distribution and effective width representation

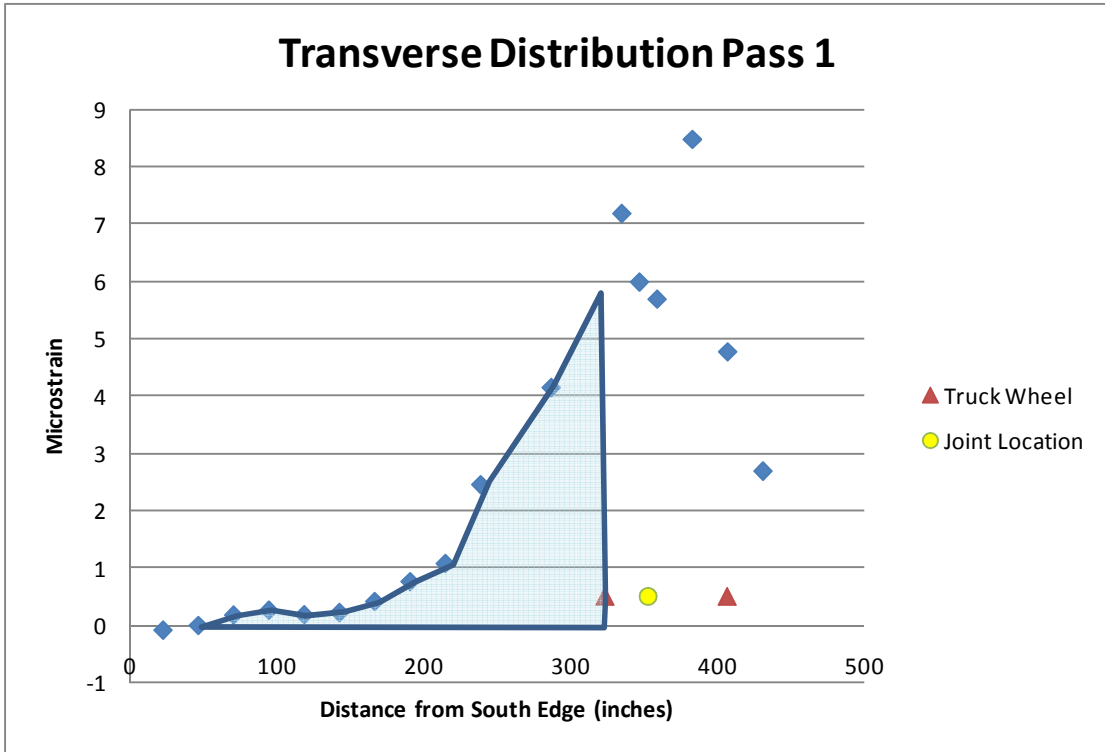


Figure 21. Determination of area A1 for single truck

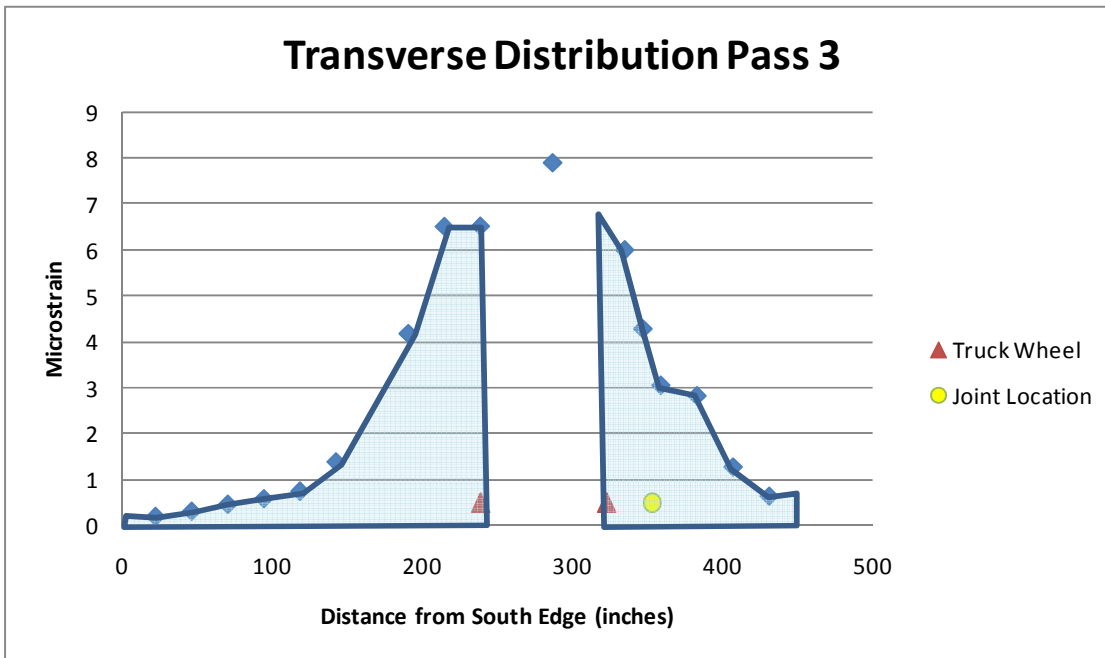


Figure 22. Determination of areas A1 and A3 for single truck

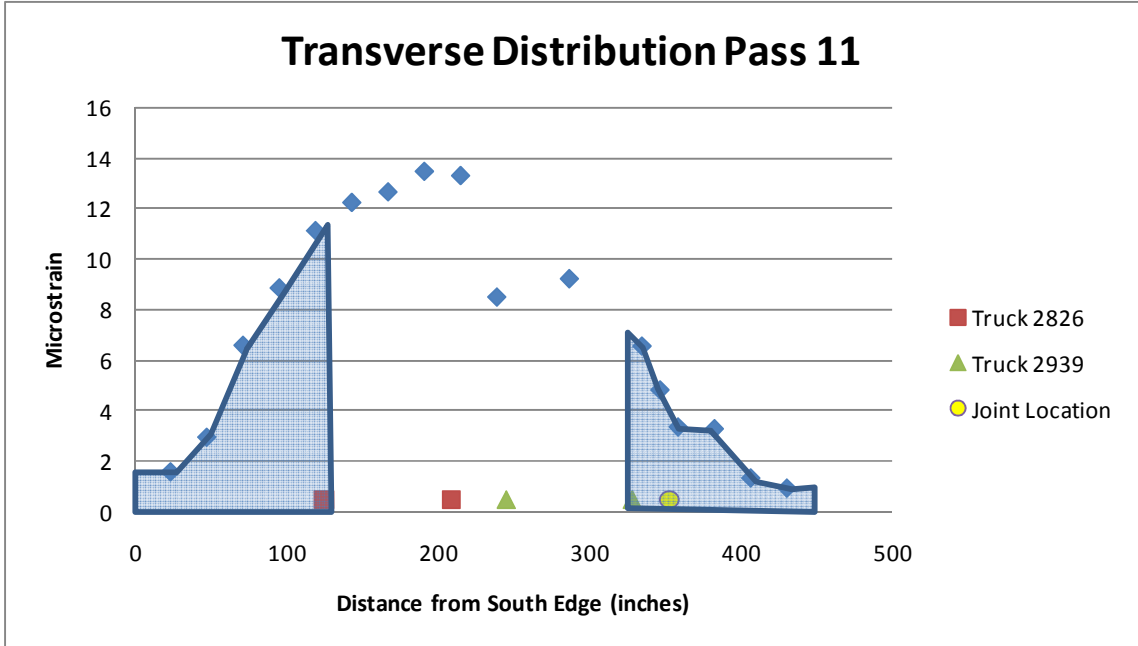


Figure 23. Determination of areas A1 and A3 for side-by-side trucks

Appendix F

BRIDGE TEST REPORT 3-316

FIELD TEST OF BRIDGE 3-316

by

Harry W Shenton III, Ph.D., Professor and Chair
&
Brian P Jones, Graduate Research Assistant

*Department of Civil and Environmental Engineering
Center for Innovative Bridge Engineering
University of Delaware
Newark, Delaware 19716*



June 25, 2010

Project:

Bridge 3-316 on Laurel Road
Sussex County, Delaware

Client:

Delaware Department of Transportation
P.O. Box 778
Dover, DE 19903

Executive Summary

The University of Delaware conducted a load test of Bridge 3-316 on Laurel Road, Sussex County, Delaware on April 19, 2010 to evaluate its transverse load distribution. The slab bridge was originally constructed in 1924; an additional 9 ft 6 in. of roadway was added in 1949. The slab was instrumented with eighteen strain transducers placed on the underside of the concrete slab. Two fully loaded 10-wheel dump trucks were used as a controlled live load for the test. The gross weight of truck #2818 was 59.7 kips, with a combined rear axle weight of 44.9 kips. The gross weight of truck #2939 was 65.1 kips, with a combined rear axle weight of 50.8 kips. The test utilized 13 load passes in which the truck(s) moved across the bridge at a slow crawl. The maximum recorded concrete tensile stain at any time during the test was 17.4 $\mu\epsilon$. Based on evaluation of the observed transverse load distribution, a conservative estimate for the effective slab width of the bridge for two vehicles is 11.7 ft. This is 18% greater than the AASHTO LRFD width of 9.91 ft for multi-lane loading. For a single truck a conservative effective width is 14.5 ft, which is 48% greater than the AASHTO LRFD width of 9.77 ft for single lane loading.

Description of the Bridge

Bridge 3-316 is located on Laurel Road, southwest of Millsboro, Sussex County, Delaware. It is a concrete slab bridge/culvert with a 14 foot span and an out-to-out deck width of 38.3 feet. When originally built in 1924 the bridge was 29 feet wide. It was widened in 1949 to its present width. A location map of the bridge is shown in Figure 1; pictures of the bridge are shown in Figure 2.

The bridge has an ADT of 3655 vehicles (as of 2006) with 7% being trucks. It was last inspected on May 30, 2007.

Test Purpose

The load test was performed at the request of DelDOT's Bridge Management section in order to assess the transverse load distribution, i.e., effective width, of the slab. The reinforcement details at the ends of the slab do not appear to be sufficient to transfer negative bending into the abutment walls. As such, the bridge must be rated as a slab as opposed to a rigid frame. It was determined that a load test would allow a more accurate assessment of the bridge's transverse load distribution characteristics. The remainder of this report discusses how the bridge was tested and how the effective slab width was computed using load test data, and provides a comparison to the AASHTO effective width.

AASHTO Effective Width

The equation for effective width of a slab, per AASHTO LRFD, is

$$E = 10.0 + 5.0\sqrt{L_1 W_1} \quad (1)$$

for a single lane loaded, and

$$E = 84.0 + 1.44\sqrt{L_1 W_1} \leq \frac{12.0W}{N_L} \quad (2)$$

for multilane loading, where:

- E = Equivalent width (in.)
- L_1 = Modified span length taken equal to the lesser of the actual span or 60.0 (ft.)
- W_1 = Modified edge-to-edge width of bridge taken to be equal to the lesser of the actual width or 60.0 for multilane loading, or 30.0 for single-lane loading (ft.)
- W = Physical edge-to-edge width of bridge (ft.)
- N_L = Number of design lanes

For bridge 3-316

- L_1 = 15.33 ft (center-to-center of abutment walls)
- W_1 = 30 ft for single lane
38.3 ft for multilane loading
- W = 38.3 ft
- N_L = 2

Substituting these values into the expressions above yields $E = 117.2$ in. = 9.77 ft. for single lane loading and $E = 118.9$ in. = 9.91 ft. for multilane loading.

For comparison, the formula for effective width per the AASHTO Standard Specification is

$$b_{eff} = 4.0 + 0.06S \quad (3)$$

where S is the span in ft. The effective width per the Standard Specification is $b_{eff} = 4.92$ ft. Note that b_{eff} is for a single wheel line and must be multiplied by 2 for direct comparison with E which is for two wheel lines, i.e., $2b_{eff} = 9.84$ ft.

Test Setup

The bridge load test was conducted on April 19, 2010 using the Bridge Diagnostics Inc, Structural Testing System (STS) and two 10-wheel trucks. Eighteen transducers were mounted to the underside of the concrete slab. Each

transducer was equipped with 12 inch extensions and were mounted at the midspan of the 14 foot clear span. The transducers were mounted with a transverse spacing of 2 feet. The transducers were mounted to the slab using a quick setting two-part epoxy manufactured by Loctite. Access to the bottom of the slab was from a boat (provided by DelDOT). Figure 3 shows a transducer being mounted to the slab; Figure 4 shows all of the transducers mounted. Figure 5 shows the transducer layout with the associated three-digit transducer identification number. All of the strain transducers were connected to the STS data acquisition system and were read simultaneously, at an appropriate sample rate during the test.

A construction joint exists in the slab where it was widened in 1949. The joint is 9 ft 6 in from the south edge of the slab. Strain gage 295 was located to the north of the joint and gage 355 was located to the south of the joint.

Two loaded dump trucks were used as controlled live loads for the test. The truck axles were weighed at the site using Intercomp portable truck scales which are accurate to within ± 10 lbs. The gross weight of truck #2818 was 59.7 kips, with a combined rear axle weight of 44.9 kips. The spacing between the front and rear axle was 15'-6". The spacing between the first rear axle and the second rear axle was 4'-6". The gross weight of truck #2939 was 65.1 kips, with a combined rear axle weight of 50.8 kips. The spacing between the front and rear axle was 15'-1". The spacing between the first rear axle and the second rear axle was 4'-6". As a result, for each truck, when the rear axle was at midspan the front axle was off of the bridge. Figure 6 and Figure 7 show the measured wheel spacings and wheel loads of the two vehicles.

A total of 13 truck passes were completed and are listed in Table 1. In all cases the truck or trucks crossed the bridge in an eastward direction (toward Millsboro). All passes were conducted at a "crawl" speed, i.e., between 5 and 10 mph. The transverse position of the truck on the bridge is defined by "right shoulder", "right lane", "center", "left lane," and "left shoulder" when looking in a eastward direction. Passes 1 through 10 involved only a single truck (#2818 or #2939). Passes 11 through 13 were side-by-side truck passes with truck #2818 on the right and truck #2939 on the left.

Photos of the various truck passes are shown in Figures 8 through 11.

Results

Peak Strains and Transverse Strain Distribution

The strains induced in the slab by the load vehicles were very small: the absolute maximum recorded concrete tensile stain at any time during the test was $17.5 \mu\epsilon$. This occurred at gage 356, which was located a few feet south of the centerline of the bridge and occurred for pass 11 (both vehicles on the bridge at the same time). The absolute maximum strain recorded for a single truck pass was $13.4 \mu\epsilon$. This occurred at gage 294, which was located approximately in the center of the westbound lane, for pass 8 (truck in the left lane). The absolute maximum recorded strains are listed for all gages in Table 2.

Although these strains are very low, good resolution was achieved in the measurements by using the concrete extensions. It should be noted, however, that these are average strains over the measurement range; the peak strain may be somewhat underestimated because of that.

The very low strains can be attributed to two factors. First is possible frame action provided by the abutments. Although the bridge was not designed as a rigid frame, there is some continuity between the slab and walls which will tend to reduce the strain at mid-span. Second, the concrete strength may be greater than the design specified strength, which will also tend to reduce the strain at mid-span (the strength of two cores taken from the slab and tested by DeIDOT were 11.9 ksi and 9.4 ksi respectively).

Plots of the transverse distribution of strain for sample single truck passes are shown in Figures 12 through 16, and for one side-by-side truck pass in Figure 17. These plots are created by first locating the absolute maximum strain recorded among all sensors for a given pass. The distribution plot shows the strain recorded by all sensors for that position of the vehicle (time), versus the sensor location on the slab. Clearly the strains are largest underneath the vehicle and tend to get smaller as you move away from the vehicle.

Computation of Effective Slab Width

Figure 18 shows an idealized transverse strain distribution that might result if a rear axle were sitting on an infinitely wide slab. The strain would have a relatively constant peak value (strain max.) between the truck wheels, and would decrease to zero as one moves away from the wheels. This non-uniform strain (or stress) is a result of shear-lag. In order to simplify the evaluation of slabs that exhibit shear lag, the concept of effective width was developed. The effective width section has a constant strain (or stress) across its width. The widely accepted definition of the effective width is the width that would have a uniform strain equal to the maximum strain but creates the same total effect as that caused by the actual strain distribution (Chiewanichakorn et al., 2004). To turn the plot having a

varying strain into one having a uniform strain, one must keep the areas A_1 and A_3 for the two distributions equal (see Figure 18).

Figures 19 and 20 show examples of the areas used in calculating the effective width for the single truck passes. Effective widths have been calculated for all of the single truck passes and are summarized in Table 3.

The single truck effective widths vary from a low of 14.5 ft to a high of 20.6 ft. The average is 17.4 ft. The conservative value is the lowest, 14.5 ft. which is 48% higher than the AASHTO LRFD value (9.77 ft.). The average value is 78% higher than the AASHTO LRFD width.

Referring to Table 3, the effective widths for the passes obtained using truck 2826 (59.7 kips) and truck 2939 (62.1 kips) are very consistent (most corresponding values are within 5 to 15% of each other). This demonstrates the linearity of the bridge behavior, and that the calculation of the effective width is independent of the magnitude of the load.

The effective width calculations for the single truck seem to be the highest near the edges of the slab and lowest when the truck is in the center of the travel lanes. There does not appear to be any distinguishable effect or difference between the older section of slab and the new section.

One will notice that the strain is not constant beneath the truck (as it is in the idealized depiction (Figure 18)). While it may be acceptable to use the average value from this region as opposed to the peak value, effective width calculations found using the peak value will be conservative.

Consideration of Multiple Presence in the Effective Slab Width Calculation

The above calculated widths do not incorporate the effect of side-by-side trucks. In essence, the above values are the effective width resulting from a single vehicle load. If we want to account for side-by-side trucks in the effective width computation, we should place two trucks on the bridge with their wheels as close together as permitted by the code (this would be 4 feet; 2 feet from the edge of each 12 foot lane). These correspond to the results for passes 11 through 13.

Figure 21 shows an example of the areas used in calculating the effective width for the side-by-side trucks. The results are shown in Table 4.

The lowest effective width for the two side-by-side truck runs is 11.7 ft. This is 18% greater than the AASHTO LRFD multi-lane value (9.91 ft.). The average effective width for the two side-by-side trucks is 12.0 ft, which is 21% greater than the AASHTO LRFD multi-lane value.

Presented in Table 5 is a summary of the key results. Also presented in the table is the equivalent effective width for the vehicle based on the AASHTO Standard Specification.

Although it is very unlikely to have side-by-side heavy vehicles on such a narrow bridge, a conservative value for the multi-lane effective width for bridge 3-316 would be 11.7 ft.

References

Chiewanichakorn, M, Aref, A.J., Chen, S.S., and Ahn, I-S, (2004). *Effective Flange Width Definition for Steel-Concrete Composite Bridge Girder*, Journal of Structural Engineering, ASCE, Volume 130, Number 12, P. 2016-2031.

Table 1. Truck passes

Pass #	Description (All trucks moving East towards Millsboro)
1	Truck 2818 Right Shoulder
2	Truck 2939 Right Shoulder
3	Truck 2818 Right Lane
4	Truck 2939 Right Lane
5	Truck 2818 Center of Roadway
6	Truck 2939 Center of Roadway
7	Truck 2818 Left Lane
8	Truck 2939 Left Lane
9	Truck 2818 Left Shoulder
10	Truck 2939 Left Shoulder
11	Truck 2818 Right Shoulder, Truck 2939 Right Lane
12	Truck 2818 Right Lane, Truck 2939 Left Lane
13	Truck 2818 Left Lane, Truck 2939 Left Shoulder

Table 2. Absolute maximum recorded slab strain

Absolute max microstrain measured for given gage ID																	
Single Lane Truck Passes																	
Pass #	306	317	314	344	294	337	293	348	1476	299	303	356	292	295	355	318	535
1	0.2	0.2	0.2	0.4	0.5	0.7	3.0	1.2	1.7	3.2	4.7	6.4	7.3	9.0	7.4	6.6	5.4
2	0.2	0.3	0.3	0.5	0.6	1.0	2.6	1.8	2.3	4.2	5.8	7.8	8.8	10.4	8.5	7.4	5.7
3	0.6	0.8	1.2	1.6	2.4	3.4	4.1	6.5	7.6	11.1	11.1	10.7	8.9	7.6	4.4	3.1	1.8
4	0.7	1.0	1.2	1.9	2.7	4.0	5.8	7.3	8.5	12.3	12.5	11.8	10.0	8.6	5.1	3.5	2.1
5	1.5	2.2	3.2	4.8	7.1	8.8	11.1	8.9	7.8	8.9	6.7	5.1	3.5	2.6	1.3	0.7	0.4
6	1.8	2.7	4.0	5.9	8.6	10.7	12.2	11.6	10.5	12.2	9.7	7.4	5.0	3.7	1.8	1.3	0.9
7	3.6	5.3	7.0	9.3	11.7	11.6	12.0	8.9	6.1	5.3	3.5	2.4	1.6	1.1	0.6	0.4	0.2
8	3.9	5.9	8.1	10.5	13.4	13.3	12.9	10.3	7.2	6.4	4.1	3.0	1.9	1.3	0.6	0.4	0.3
9	5.7	6.9	7.6	8.7	9.6	8.3	6.2	4.7	3.1	2.6	1.6	1.1	0.9	0.6	0.3	0.2	0.1
10	6.4	8.1	8.6	9.5	10.7	8.8	7.6	5.2	3.4	2.9	1.8	1.4	0.9	0.8	0.4	0.2	0.2
Max	6.4	8.1	8.6	10.5	13.4	13.3	12.9	11.6	10.5	12.3	12.5	11.8	10.0	10.4	8.5	7.4	5.7
Multi Lane Truck Passes																	
Pass #	306	317	314	344	294	337	293	348	1476	299	303	356	292	295	355	318	535
11	0.7	1.2	1.9	2.8	4.2	6.3	9.1	10.5	11.1	15.7	16.6	17.5	16.1	15.7	11.5	8.9	6.3
12	4.0	6.2	8.5	11.2	14.7	15.9	17.0	16.0	14.4	17.2	15.2	13.7	11.0	9.2	5.5	3.7	2.2
13	7.9	10.4	11.5	13.6	16.6	16.8	16.7	14.7	12.3	13.6	10.4	7.9	5.5	4.2	2.1	1.6	0.8
Max	7.9	10.4	11.5	13.6	16.6	16.8	17.0	16.0	14.4	17.2	16.6	17.5	16.1	15.7	11.5	8.9	6.3

Table 3. Measured Effective width (ft) based on single truck passes

Pass	E_m
1	19.5
2	20.6
3	15.1
4	15.3
5	16.0
6	18.0
7	14.5
8	14.5
9	19.4
10	20.6
Average	17.4
SD	2.5

Table 4. Measured Effective width (ft) based on side-by-side truck passes

Pass	E_m
11	11.7
12	12.1
13	12.1
Average	12.0
SD	0.3

Table 5. Comparison of AASHTO and measured effective width (ft)

Lane loading	AASHTO LRFD (E)	AASHTO Standard Specification ($2b_{eff}$)	Measured E_m	
			Min	Average
Single	9.77	9.84	14.5	17.4
Multilane	9.91	9.84	11.7	12.0

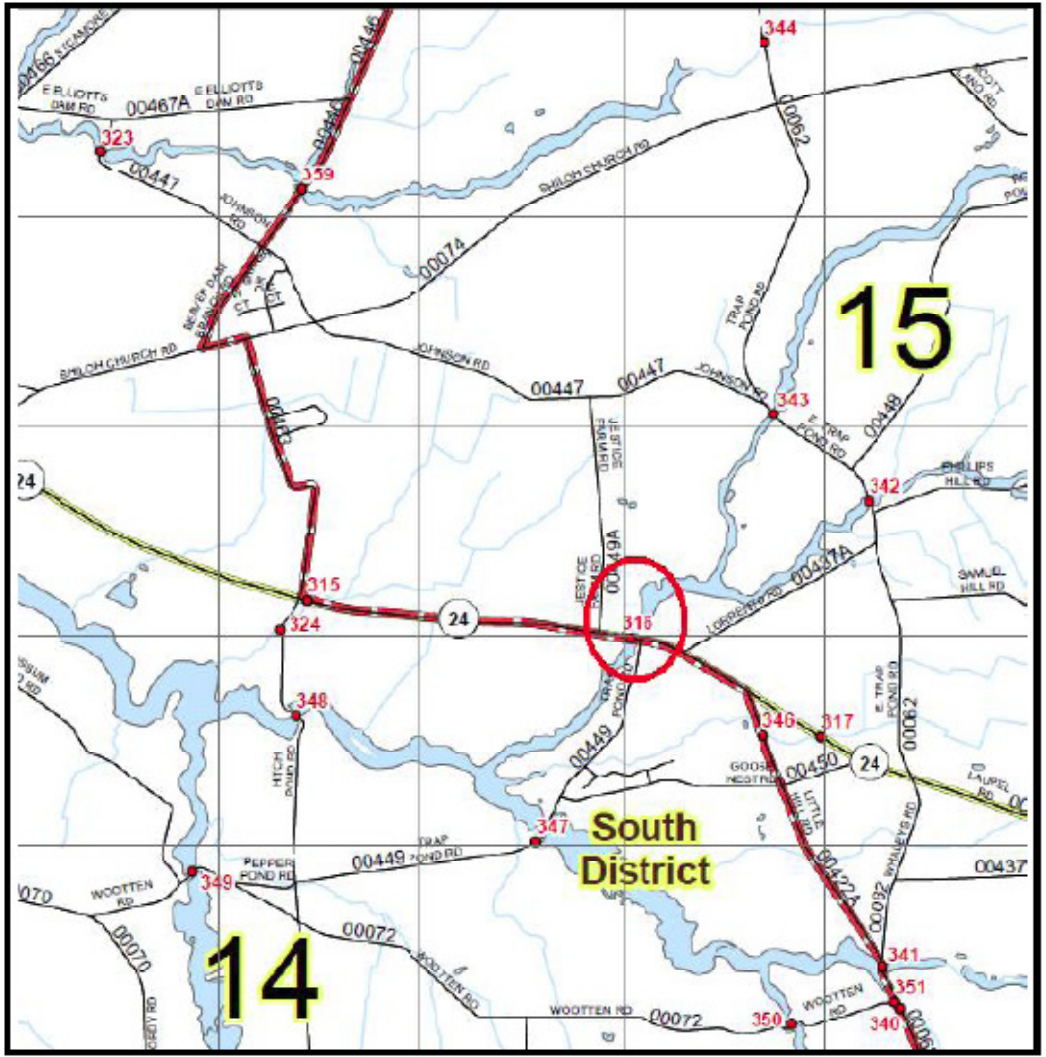


Figure 1. Map showing location of Bridge 3-316 (courtesy DeIDOT Bridge Management)



Figure 2 (a) Bridge 3-316 west approach (courtesy DelDOT Bridge Management)



Figure 2 (b) Bridge 3-316 south elevation (courtesy DelDOT Bridge Management)



Figure 3. Mounting transducers from boat



Figure 4. Mounted transducers

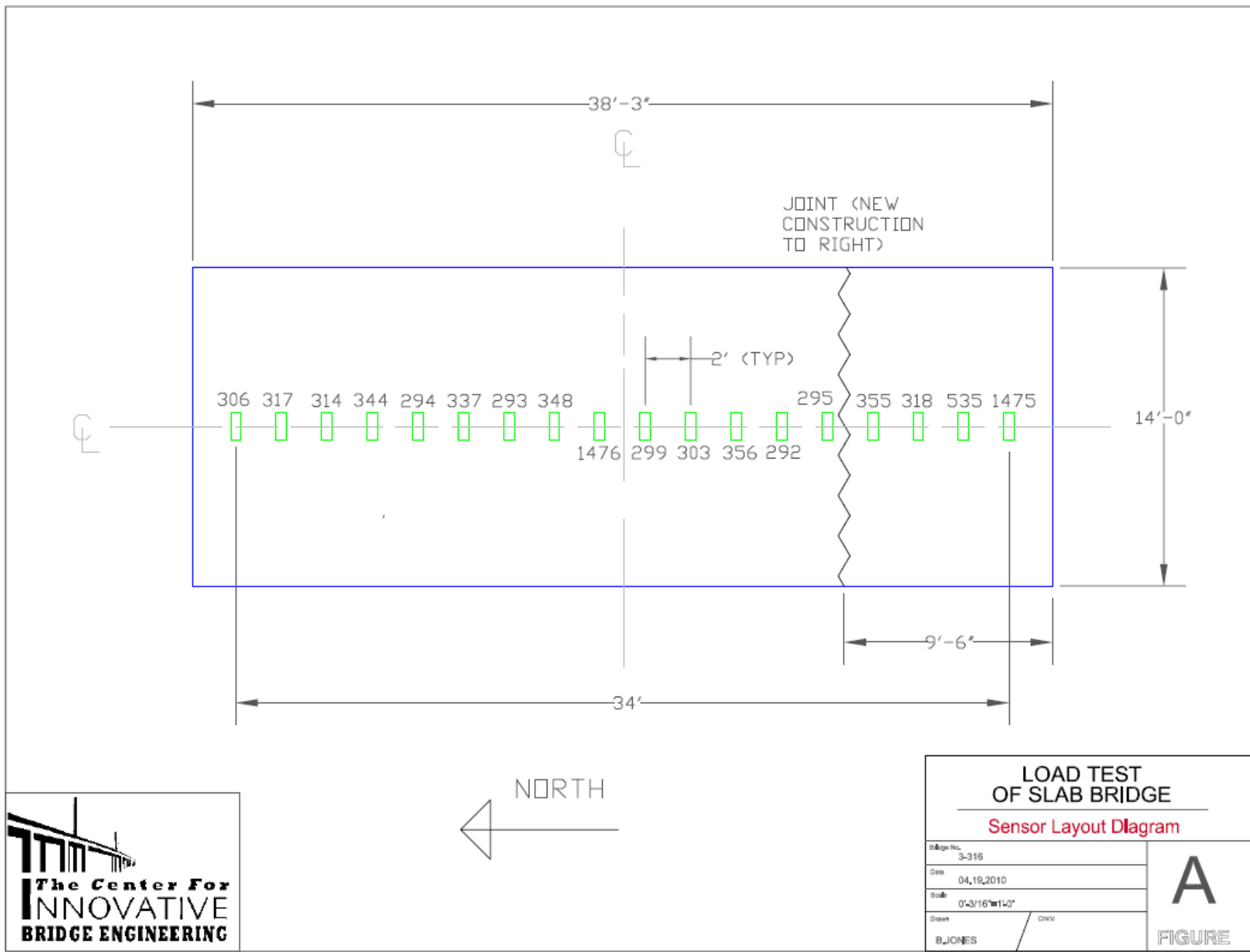


Figure 5. Sensor layout



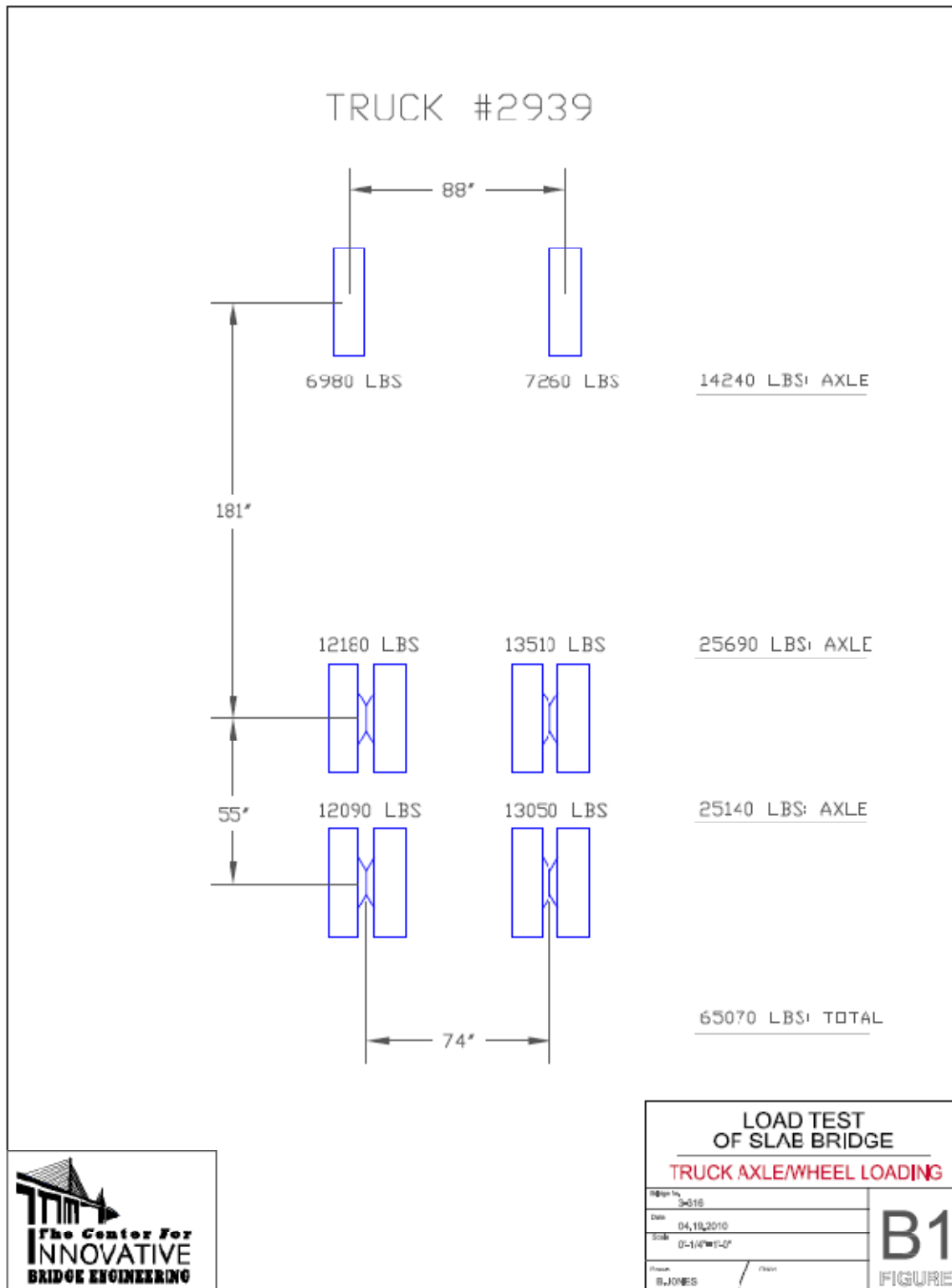


Figure 6. Wheel weights of truck #2939

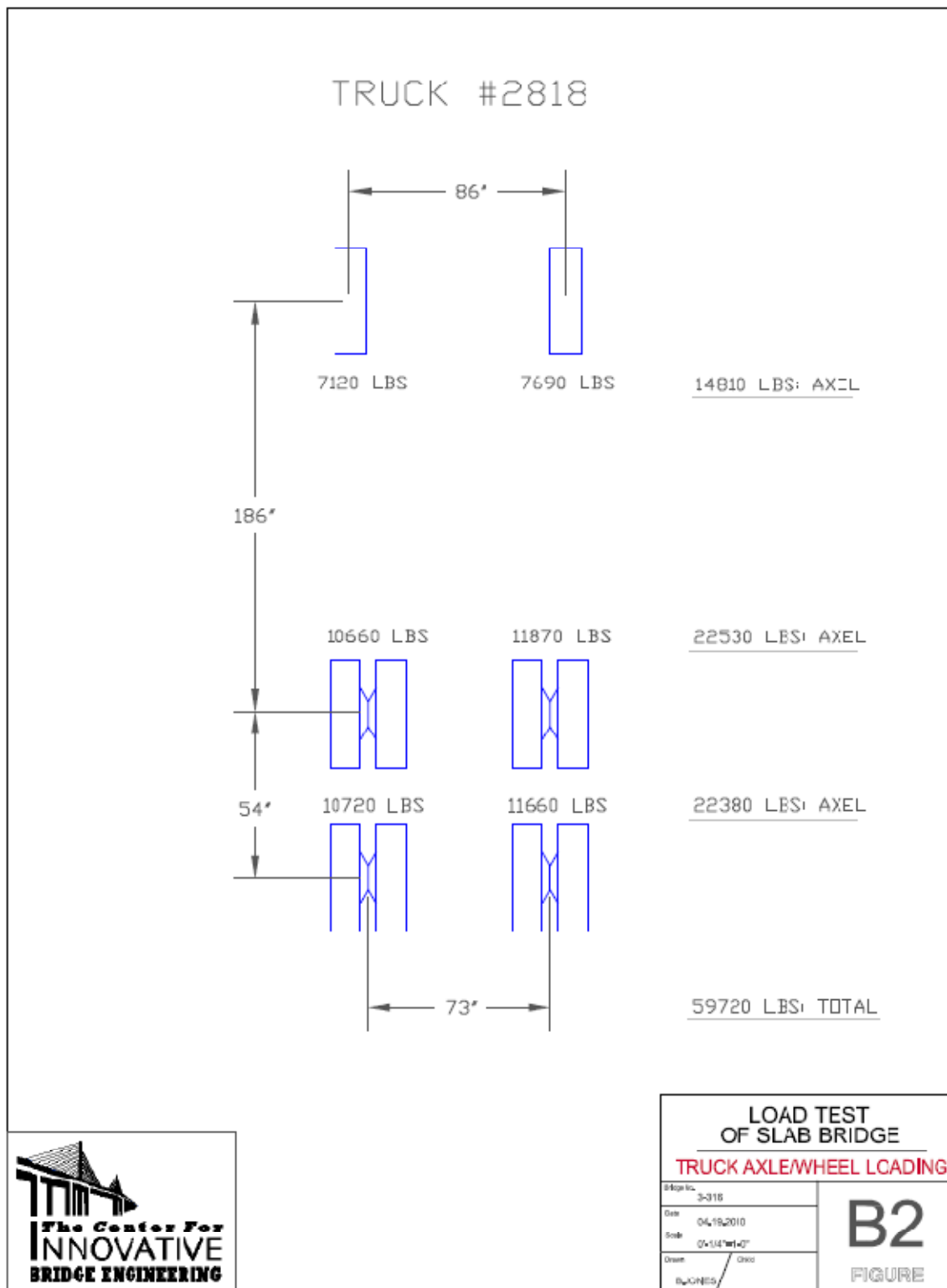


Figure 7. Wheel weights of truck #2818



Figure 8. Truck #2818 – right shoulder



Figure 9. Truck #2818 – center of roadway



Figure 10. Truck #2939 – left lane



Figure 11. Side-by-side truck (trucks #2818 and #2939) passes

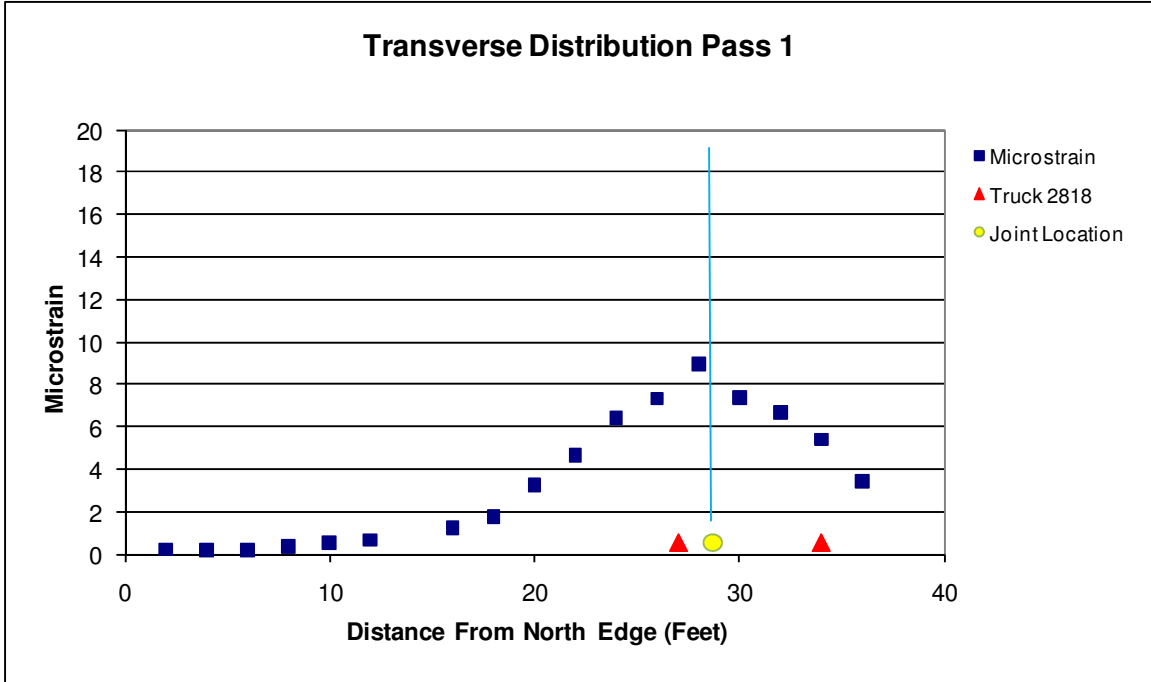


Figure 12. Transverse strain distribution Pass 1

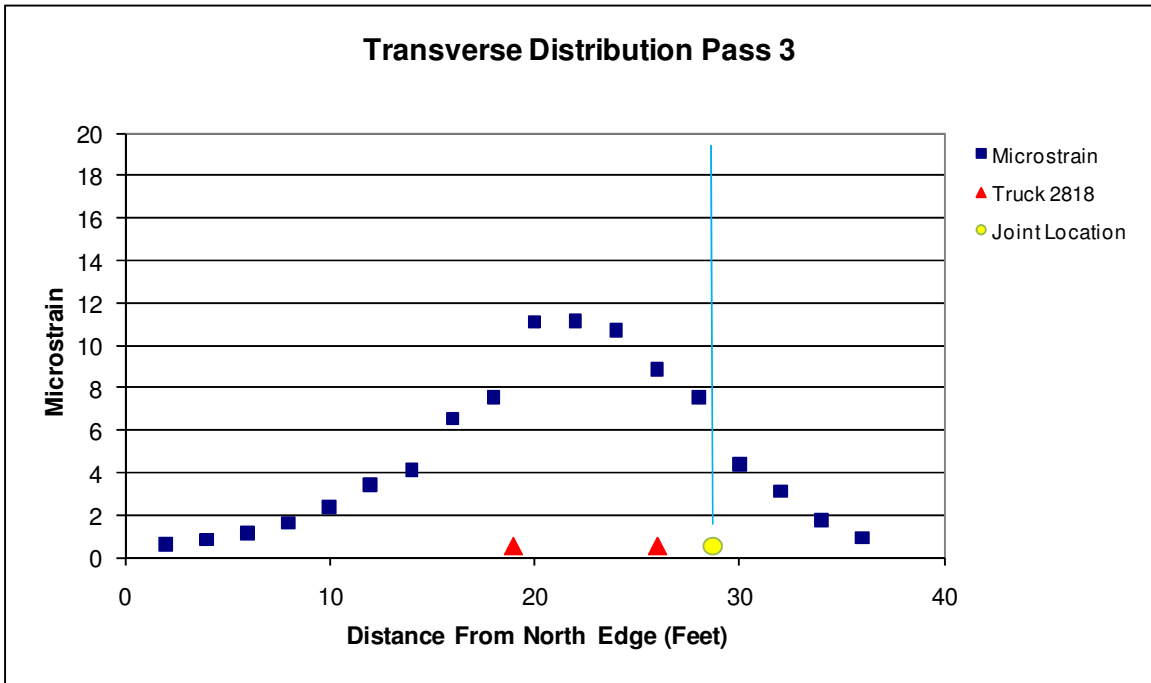


Figure 13. Transverse strain distribution Pass 3

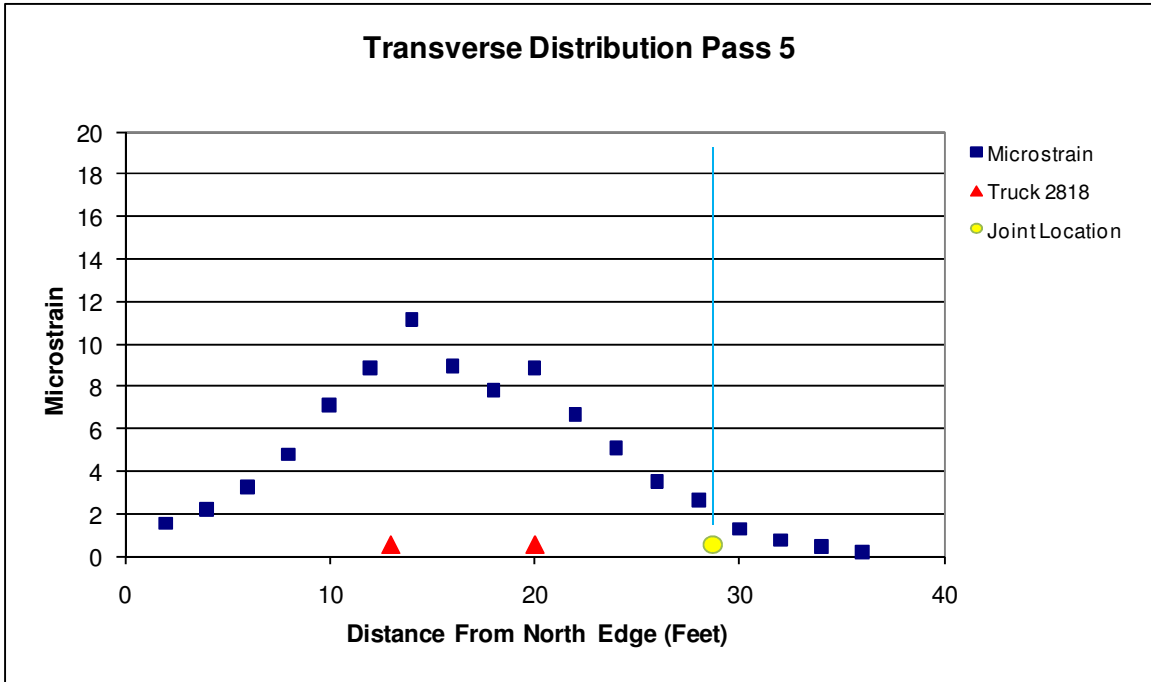


Figure 14. Transverse distribution of strain Pass 5

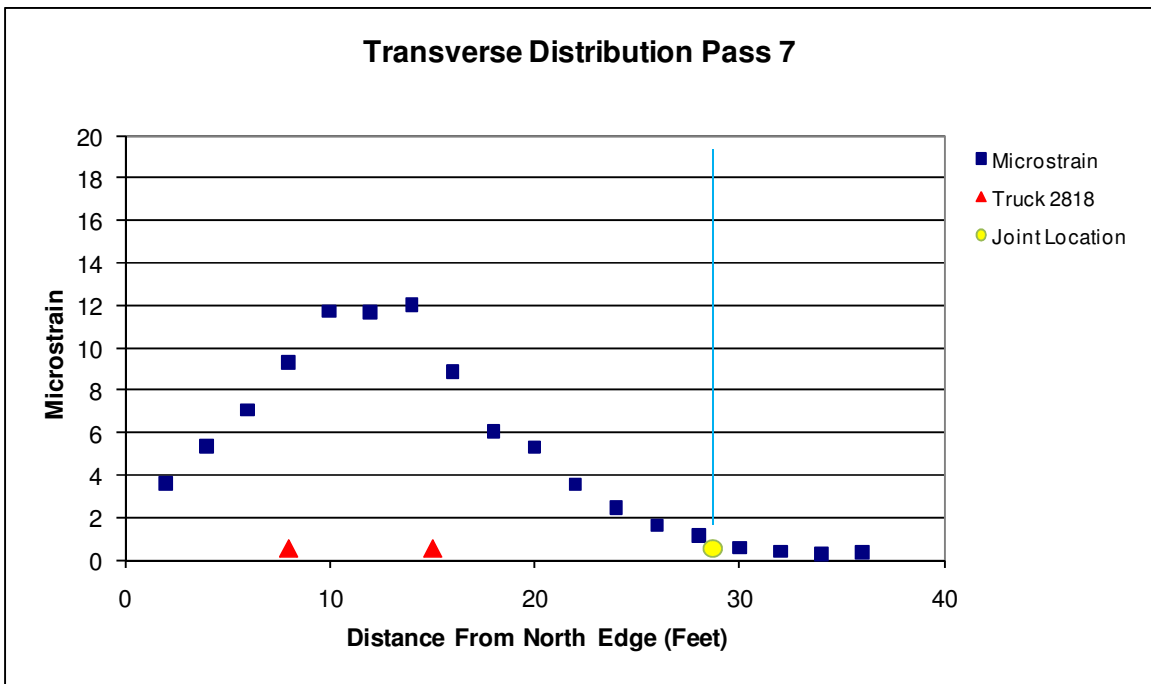


Figure 15. Transverse distribution of strain Pass 7

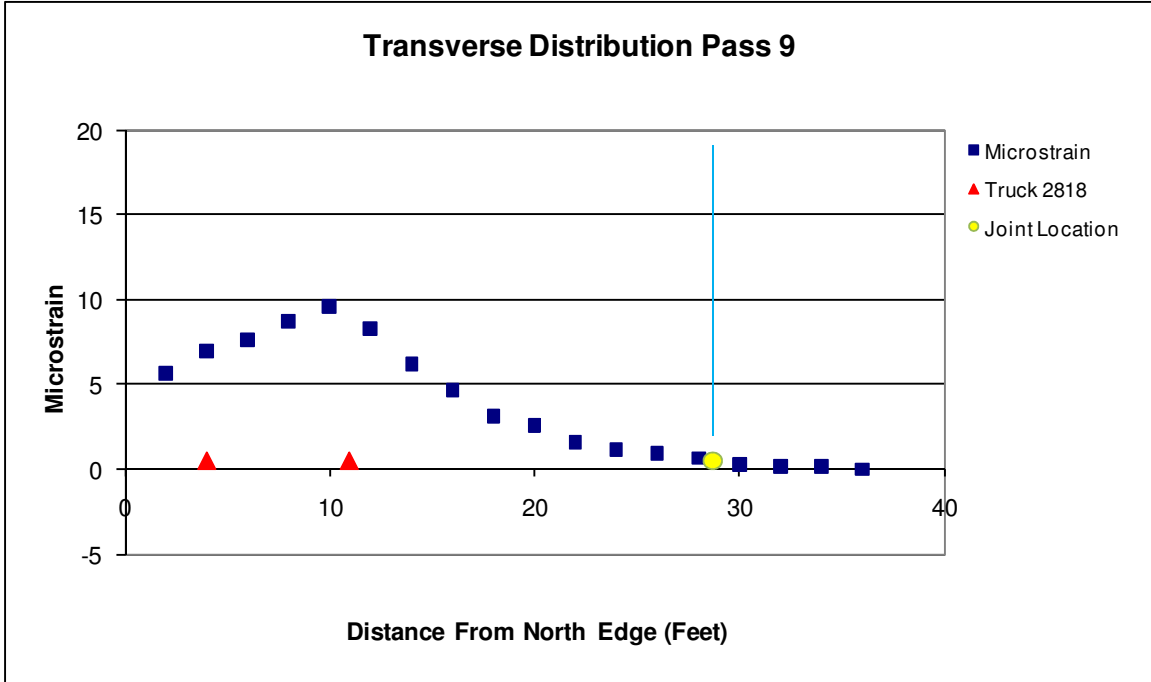


Figure 16. Transverse distribution of strain Pass 9

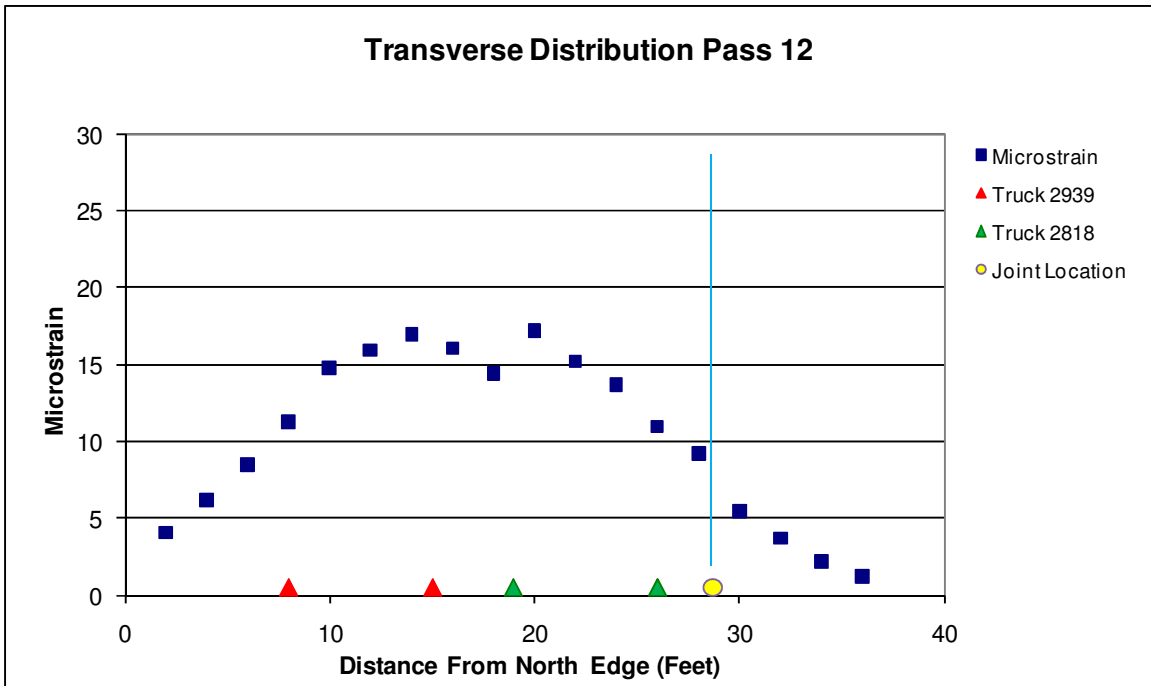


Figure 17. Transverse distribution of strain Pass 12 (two trucks side-by-side)

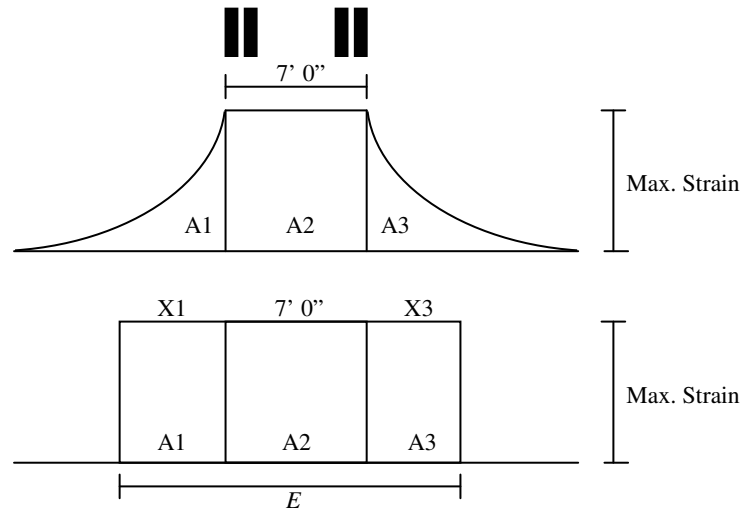


Figure 18. Idealized strain distribution and effective width representation

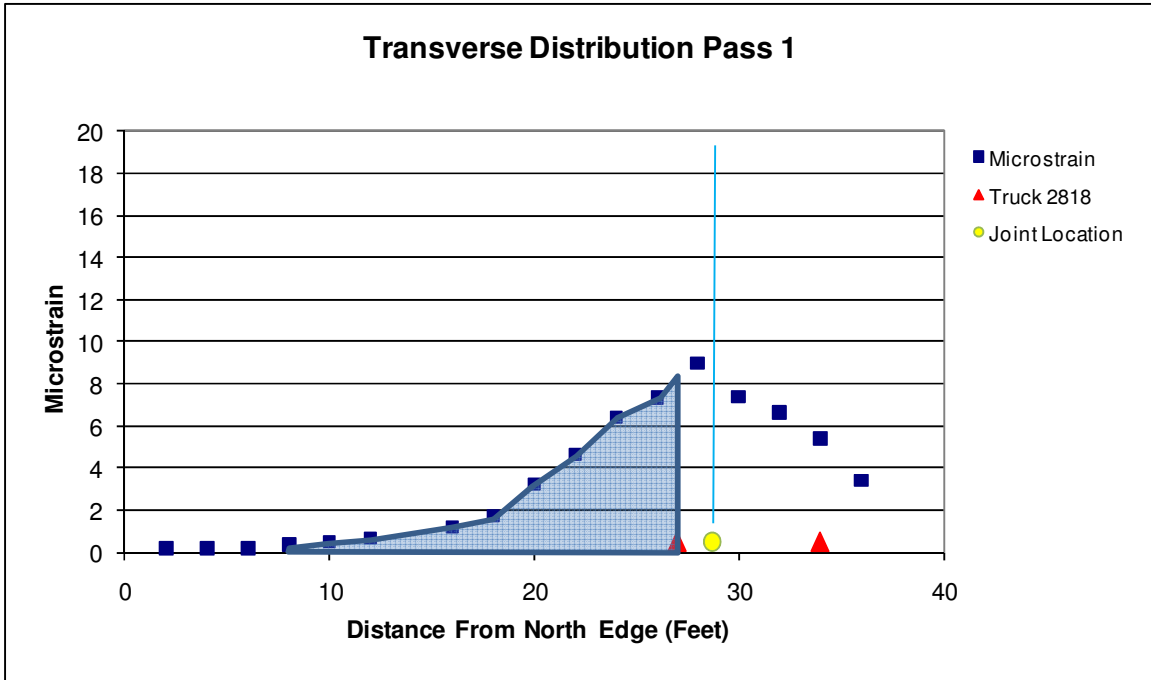


Figure 19. Determination of area A1 for single truck

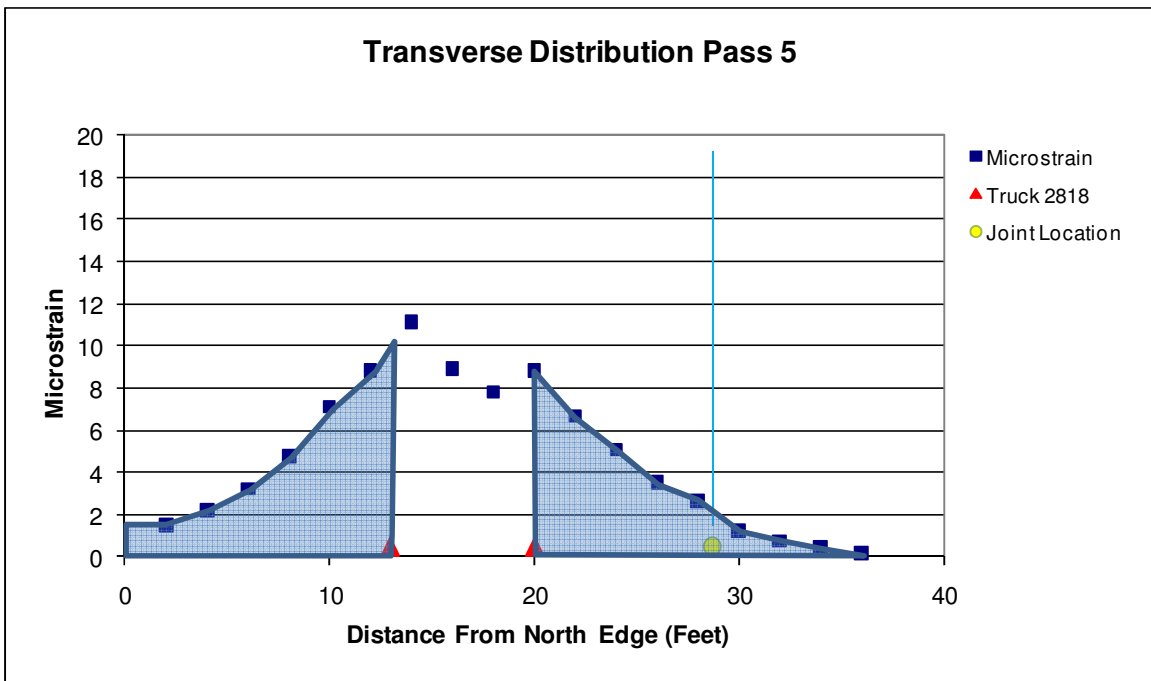


Figure 20. Determination of areas A1 and A3 for single truck

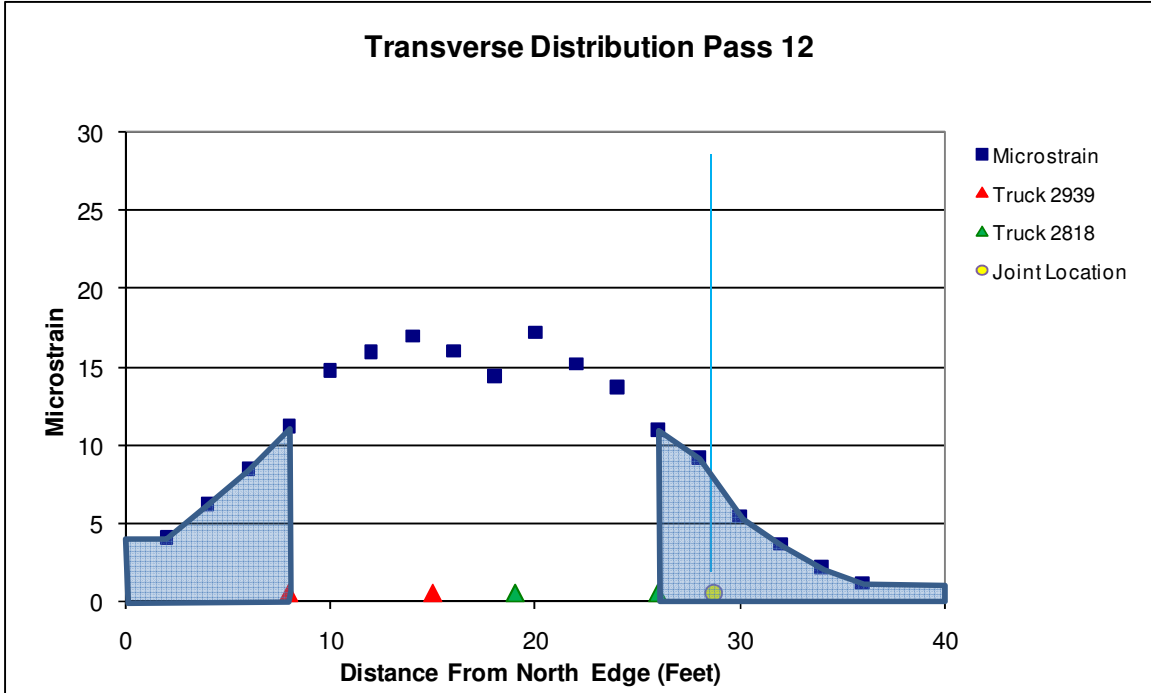


Figure 21. Determination of areas A1 and A3 for side-by-side trucks

Delaware Center for Transportation University of Delaware Newark, Delaware 19716

AN EQUAL OPPORTUNITY/AFFIRMATIVE ACTION EMPLOYER

To the extent permitted by applicable State and Federal laws, the University of Delaware is committed to assuring equal opportunity to all persons and does not discriminate on the basis of race, creed, color, sex, age, religion, national origin, veteran or handicapped status, or gender identity and expression, or sexual orientation in its educational programs, activities, admissions, or employment practices as required by Title IX of the Educational Amendments of 1972, Section 504 of the Rehabilitation Act of 1973, Title VII of the Civil Rights Act of 1964, and other applicable statutes. The University of Delaware has designated Karen Mancini, Director of the Office of Disabilities Support Services, as its ADA/Section 504 Coordinator under Federal law. Inquiries concerning Americans with Disabilities Act compliance, Section 504 compliance, campus accessibility, and related issues should be referred to Karen Mancini (302-831-4643) in the Office of Disabilities Support Services. Inquiries concerning Title VII and Title IX compliance and related issues should be referred to the Director of the Office of Equity and Inclusion, Becki Fogerty (302-831-8063).

